ABSTRACT

HOLMES, CHARISSE NICOLE. Influence of Environmental Chemicals on Regulatory Processes that Control Glucose and Lipid Homeostasis. (Under the direction of Gerald A. LeBlanc).

Metabolic syndrome is an escalating public-health challenge affecting over a quarter of adults worldwide. Metabolic syndrome is characterized by the co-occurrence of multiple health risk factors (e.g. obesity, type II diabetes) that may result from the disruption of lipid and glucose homeostasis. Lipid and glucose homeostasis is regulated by a group of nuclear receptors known as the peroxisome proliferator-activated receptors (PPARs) which dimerize with the retinoic X receptor (RXR). The PPAR signaling network has been recognized as potential targets of environmental chemicals, consequently, contributing to the high prevalence of metabolic disorders. The purpose of this research was to investigate the underlying mechanistic interactions of some environmental chemicals on the PPAR signaling network. The following hypothesis was tested: environmental chemicals can interact with multiple components of the PPAR signaling network in a manner that may lead to adipogenesis.

The main objective of the first study was to evaluate the effects of the organophosphate flame retardant, triphenyl phosphate, on the PPAR signaling network. Triphenyl phosphate inhibited transactivation of the PPARα:RXRα complex, as well as, the PPARα and RXRα subunits. Triphenyl phosphate activated the PPARγ:RXRα complex through the PPARγ subunit. Together, these results suggested that triphenyl phosphate may stimulate adipogenesis which was observed using mouse pre-adipocytes that differentiated into adipocytes with commensurate lipid accumulation.

Bioluminescence resonance energy transfer (BRET) assays revealed that triphenyl phosphate inhibited dimerization of PPARα and RXRα. Triphenyl phosphate had no measureable effect on the assembly/disassembly of the PPARγ:RXRα:SRC1 complex. Results from this study provided a mechanistic explanation for the observed adipogenic activity by triphenyl phosphate.

Next, we hypothesized that ligand-mediated receptor assembly (as measured using BRET) may be used as an informative endpoint for the screening of chemicals reducing both time and costs of traditional screening assays. Both reporter gene and BRET assays were utilized to assess the impact of known agonists along the PPARα signaling pathway. RXRα agonists stimulated PPARα:RXRα dimerization and the recruitment of SRC1 to this complex. While, no measurable effect on PPARα:RXRα:SRC1 complex assembly was observed with known PPARα agonists, suggesting that these ligands activated constitutively formed receptor complexes. We also evaluated whether the actions of triphenyl phosphate on PPARα signaling were common to other organophosphate flame retardants. 2-ethylhexyl diphenyl phosphate, tri-o-tolylphosphate, and tri-n-butyl phosphate inhibited PPARα:RXRα:SRC1 assembly and activity. Overall, the assessment of ligand-mediated receptor assembly/disassembly in conjunction with reporter gene assays provided greater mechanistic insight into the response of the receptor to ligand binding.

Finally, we hypothesized that some insect growth regulating insecticides (IGRs) may be adipogenic due to their structural similarity to some pharmacologic PPAR modulators. Pyriproxyfen, fenoxycarb, methoprene, and kinoprene activated the PPARγ:RXRα signaling pathway. Evaluation of the individual subunits revealed that pyriproxyfen activated the PPARγ subunit, but not RXRα. Fenoxycarb, methoprene, and kinoprene activated both the

PPARγ and RXRα subunits, but PPARγ:RXRα activation was specifically due to interaction with PPARγ. BRET assays supported the observation that the PPARγ subunit was the target of action by IGRs in the PPARγ signaling pathway. Finally, all of the IGRs stimulated pre-adipocytes to differentiate into adipocytes with commensurate lipid accumulation. Results revealed that the IGRs evaluated are PPARγ agonists and have the ability to stimulate adipogenesis *in vitro*.

This research supported our hypothesis that some commercial products have the potential to stimulate adipogenesis through interaction with the PPAR signaling network. While the potential for exposure to some of these compounds can be significant, additional research is warranted to establish whether such toxicological effects might be elicited at relevant exposure levels.

Influence of Environmental Chemicals on Regulatory Processes that Control Glucose and Lipid Homeostasis

by
Charisse Nicole Holmes

A dissertation submitted to the Graduate Faculty of
North Carolina State University
in partial fulfillment of the
requirements for the degree of
Doctor of Philosophy

Toxicology

Raleigh, North Carolina

2016

APPROVED BY:

Gerald A. LeBlanc Committee Chair	Yoshiaki Tsuji
Seth Kullman	Stuart E. Maxwell

DEDICATION

I dedicate this work to my parents Beverly and Ron Holmes.

BIOGRAPHY

Charisse Nicole Holmes was born on August 28, 1988 in Seaford, Delaware. She grew up with parents Beverly and Ron Holmes and her older brother, Ronnie. At a young age, Charisse had a passion for science. A few of her family members were diagnosed with cancer and type I diabetes, resulting in her dream to become an endocrinologist at the age of seven. Her parents encouraged her dreams by purchasing a little red microscope and this led her to develop an interest in research.

As an undergrad at Wake Forest University, Charisse was further inspired to pursue a career in research by her organic chemistry professor, Mark Welker. She joined the Welker lab in 2008 and was mentored by Tanya Pinder who eventually became one of her role models. In 2011, Charisse joined the Toxicology Department at North Carolina State University. Outside of research she spent the majority of her time relaxing with her wonderful dog Rudy.

ACKNOWLEDGMENTS

I would like to thank my advisor, Dr. Gerald LeBlanc, for his patience and guidance throughout the PhD process. I admire his passion for science and his determination to excel in every activity that he pursues. I am glad that I chose to work with him and hope I can use my degree to make him proud.

I would also like to thank my committee members: Dr. Yoshi Tsuji, Dr. Seth Kullman, and Dr. Stu Maxwell for their guidance throughout my PhD journey.

In addition, I would like to thank all of the past and present members of the LeBlanc lab for their constant encouragement and support. Special thanks are needed for Gwijun Kwon and Elizabeth Medlock Kakaley for everything that they have done for me these past few years. I would also like to thank others at North Carolina State University including: Melissa Pickett (my study-buddy), Janet Roe, Jeanne Burr, and Rob Smart.

Finally, I would like to thank my family for all of their love and encouragement. Any accomplishment I have made is due to their endless support and inspiration. I am truly grateful to have been blessed with such an amazing family.

TABLE OF CONTENTS

LIST OF TABLES

LIST OF FIGURES

CHAPTER ONE Page

APPENDIX

INTRODUCTION

The coordination of lipid and glucose metabolism is vital to energy homeostasis in vertebrates. Disruptions in this coordination can result in metabolic syndrome. Metabolic syndrome consists of the co-occurrence of multiple health risk factors including obesity, insulin resistance, dyslipidemia, and hypertension [1]. Approximately 24% of Americans are affected by metabolic syndrome leading to serious implications for health care cost and mortality as the current prevalence continues to rise [2]. Consequently, metabolic syndrome significantly increases the risk for two of the leading causes of deaths in the world, heart disease and diabetes mellitus [3, 4]. Ligand-activated transcription factors serve as major coordinators of lipid and glucose metabolism [5]. Included among these transcription factors are the peroxisome proliferator-activator receptors (PPARs). PPARs are members of the nuclear receptor superfamily, that include the estrogen, thyroid, glucocorticoid, retinoic acid, and vitamin D receptors among others [6]. Disruptions in PPAR signaling have been implicated in metabolic syndrome [7].

PPAR Structure

PPARs serve as transcription factors when heterodimerized with their partner nuclear receptor, the retinoid X receptor (RXR) [5, 8]. PPAR:RXR heterodimers bind to PPAR response elements (PPREs) which typically consist of two core recognition motifs, AGGTCA, spaced by one nucleotide. The PPRE 5' half-site is occupied by the PPAR subunit; while, the RXR subunit occupies the 3' half-site [9, 10]. Site-directed mutation of

PPAR and RXR revealed that the binding of RXR to the PPRE 3'half-site is more critical for PPAR:RXR transcriptional activation than the ability of PPAR to bind to the PPRE [9, 11]. Additionally, the PPAR amino-terminal region prohibits the subunit to bind as a monomer. Studies have shown that the full length PPAR subunit does not bind to the PPRE as a monomer, while deletion of the amino-terminal domain of the PPAR subunit allows the truncated protein to bind to DNA in the presence and absence of the RXR receptor [8].

Gene transcription can be mediated through ligand binding to either the PPAR or RXR subunit [12]. Additionally, co-treatment with both ligands has the potential to lead to additive or synergistic activation [13-15]. Ligand-mediated activated receptor complexes bound to the PPRE cause changes in the chromatin structure revealing new protein-protein interacting surfaces for coactivator recruitment. Coactivators acetylate histone tails to produce a transcriptionally competent structure with an accessible promoter. Basal transcriptional machinery is then recruited to the promoter and transcription is initiated [16].

PPAR Subtypes

Three PPAR subtypes exist in mammals PPAR alpha (PPARα), PPAR beta/delta (PPARβ/δ), and PPAR gamma (PPARγ) [17]. The mouse PPARα gene spans at least 30 kilobases of genomic DNA, while the PPARγ gene extends more than 100 kilobases and generates three mRNAs (PPARγ1, PPARγ2, and PPARγ3) that differ at their 5' end due to alternative splicing [18-20]. PPAR subtypes are expressed in a variety of tissues and some tissues express more than one isoform. PPARα is highly expressed in liver, cardiac, and kidney tissue, while PPARγ is highly expressed in adipose tissue and the immune system

[21]. PPARβ/δ is highly expressed in heart, colon, and skeletal tissue [22]. Studies evaluating PPARβ/δ have led to conflicting findings regarding its role in lipid and glucose processes thus, will not be discussed further [23].

RXR Subtypes

The RXR subunit is involved in a wide range of processes and consequently, found in a wide variety of tissues [24]. Three RXR subtypes exist in mammals; RXR alpha (RXRα), RXR beta (RXRβ), and RXR gamma (RXRγ) [24, 25]. Alternative splicing generates two different isoform for each subtype; RXRα (α1 and α2), RXRβ (β1 and β2), and RXRγ (γ1 and γ2). The role and function of each particular isoform remains unclear. RXRα is mainly expressed in the kidney, liver, intestine, and epidermal tissue. RXRβ is expressed in nearly all tissues. While, RXRγ is only expressed in muscle, brain, and pituitary tissue [24]. All three RXR subunits serve as heterodimerziation partners for other nuclear receptors (e.g. PPAR, farnesoid X, thyroid, and vitamin D receptors) and two members of the small nerve growth factor-induced clone B subfamily (i.e. NGFIB and NURR1) [24, 26-28]. In most cases, RXR dimerization partners do not prefer one RXR subtype over the others [24]. However, PPAR subunits typically dimerize with the RXRα subtype [29, 30].

PPAR Ligands

In contrast to many other nuclear receptors, PPARs accommodate a variety of ligands and these ligands typically bind with low affinity [16, 31, 32]. Some ligands are capable of binding to more than one PPAR subtype, but with differing affinities [32]. The ligand-

binding domain (LBD) consists of thirteen alpha helices arranged in three layers with a central hydrophobic pocket. The composition of thirteen alpha helices is unique from other nuclear receptors which have twelve alpha helices [31, 33]. At the entrance to the binding site between helices H2' and H3' exists a very flexible loop that allows the binding site entrance to adapt in order to accommodate large ligands without significantly altering the overall LBD structure [33].

In comparison to other nuclear receptors, PPARs have a very large binding cavity, which may explain the ability of PPARs to accommodate diverse ligands [31]. Within the cavity, hydrophobic regions interact with the ligand to form non-specific associations. These interactions lead to diverse binding conformations and various ligand-mediated activities [16].

Ligand-mediated activation occurs after a ligand interacts with helix 12 causing this helix to dock against helix 3 and helix 11. This conformational change permits helix 12 to form part of the coactivator site (AF-2) with helix 3 and helix 5 to allow coactivator recruitment. Binding of an antagonist physically restricts the movement of helix 12 and any helix 12-related conformational changes [34]. Furthermore, ligand bound to a specific PPAR subunit is attributed to the ligand's affinity for specific amino acids within helix 3 of that respective subunit [16, 34]. Replacement of these specific amino acids through site-directed mutagenesis resulted in a loss of transcriptional activity [16, 35].

The endogenous ligands for PPARs are fatty acids and fatty acid derivatives (e.g. eicosanoids) [36]. Numerous exogenous compounds activate the PPAR network as well. A well-known example are the fibrates which are a class of drugs designed to lower

cholesterol, triglyceride, and low-density lipoprotein levels [37]. Fibrates predominately activate the PPARα isoform and thus, regulate genes involved with lipid transport and metabolism [38, 39]. Thiazolidinediones are a class of antidiabetic drugs used to increase insulin sensitivity. Thiazolidinediones selectively activate PPARγ and also stimulate pre-adipocyte differentiation and lipid storage [40]. The PPARs also have been recognized as potential targets of environmental chemicals that may be contributing to the epidemic of obesity and other metabolic diseases. Such ligands include phthalates, organophosphates, and organotins [41].

Phthalates provide flexibility to plastics. The greatest potential for human exposure is through food and beverage containers [41, 42]. Other products composed of phthalates include detergents, children's toys, medical tubing, and soaps [42]. Phthalates (e.g diethylhexyl phthalate) and their metabolites (e.g monoethylhexyl phthalate, monobenzyl phthalate) were shown to activate the PPARγ receptor using luciferase reporter assays [42-44]. These compounds also stimulated adipocyte differentiation and lipid accumulation in cultured pre-adipocyte cells [43, 44]. Finally, a positive association exists between phthalate metabolites found in human urine and waist circumference thus providing, evidence to support the relationship between phthalate exposure and obesity [45, 46].

Organophosphate compounds are a diverse group of chemicals used in both industrial and domestic applications. They are most commonly used as flame-retardants, plasticizers, and insecticides [47, 48]. Some organophosphates (e.g. triphenyl phosphate, tributyl phosphate) activated the PPARγ receptor in reporter gene assays [49]. A rodent study

implicated triphenyl phosphate as an endocrine disruptor and environmentally relevant obesogen [50].

Organotins are largely used as heat stabilizers in plastic manufacturing, but they have also have been used as agricultural pesticides and in antifoulant paints [41, 51]. Organotins activated the PPARα, PPARγ, and RXRα receptors in transient transactivation assays. Affinities towards the PPARγ receptor were much greater in comparison to the PPARα receptor [52]. Tributyltin stimulated lipid accumulation in cultured pre-adipocyte cells and strongly induced adipogenesis in both *Xenopus laevis* and mice [53-55].

RXR Ligands

9-*cis* retinoic acid (vitamin A metabolite) binds and activates all RXR subtypes with high affinity [24, 56]. However, whether 9-*cis* retinoic acid is an endogenous ligand to the receptor is controversial [24]. A branched-chain fatty acid, phytanic acid, has been proposed to be an endogenous ligand for the RXR receptor [24]. Phytanic acid can be found in the plasma at micromolar concentrations and activated the RXR receptor in transcriptional activation assays [57]. Additionally, the *n*-3 polysaturated fatty acid, docosahexaenoic acid, has been proposed as an endogenous ligand for the RXR receptor. Docosahexanoic acid exists at high concentrations in the mammalian brain [58]. Nevertheless, a bona fide endogenous ligand for the RXR receptor has not been established. Conceivably, several fatty acids may serve as endogenous agonists to RXR with differing functions.

Role of PPARα in Lipid and Glucose Metabolism

PPARα regulates lipid and glucose metabolism in a manner that promotes lipid as a fuel for energy production. Ligand-mediated activation of PPARα directly regulates the transcription of key enzymes that stimulate fatty acid utilization as energetic substrates (e.g., CPT1, MCAD) [59]. The PPARα receptor is a major player in the reduction of intracellular fatty acid concentrations by stimulating β-oxidation of fatty acids; thus, PPARα activation leads to reduction in plasma triglyceride and lipoprotein levels. A major physiological outcome in response to PPARα activation in rodent models is weight-loss. Provision of a western-type high-fat diet combined with fibrate (PPARα agonist) treatment, significantly reduced adiposity in PPAR-competent mice through ligand-mediated PPARα activation in comparison to untreated mice [60].

PPARα is a key regulator of lipid metabolism, as well as, directly and indirectly influences glucose metabolism [61, 62]. PPARα upregulates TRB3 which disrupts insulin signaling and induces insulin resistance [63, 64]. However, other studies showed that activation of PPARα improved insulin sensitivity [65, 66]. Ligand-mediated activation of PPARα reduced plasma glucose levels in rodents [65, 67]. On the other hand, PPARα has been found to stimulate gluconeogenesis to maintain glucose levels [67]. PPARα may enhance glucose storage (e.g. glucose uptake and glycogen synthesis) during feeding and glucose production (e.g. glycogenolysis and gluconeogenesis) during fasting [62]. Thus, PPARα aids in adapting to glucose metabolism fluctuations during changes of energy states such as fed-to-fasted transitions [62]. Importantly, many of the genes modulating glucose processes are not direct target genes for PPARα (e.g. PDK4) resulting in the need for

clarification on the mechanisms of PPARα in glucose metabolism [62, 68]. Discordant results on the influence of PPARα on glucose metabolism is likely due to varying nutritional status and differing rodent models (e.g. transgenic animals) used in evaluations.

Role of PPARγ in Lipid and Glucose Metabolism

PPARγ regulates glucose metabolism in a manner that favors glucose as an energy substrate [16]. Regulation occurs through modulating the expression of key genes involved in glucose metabolism (e.g. c-Cbl-associated protein, glucose transporter 4) and the expression of several hormones secreted from adipose tissue which influence insulin sensitivity (e.g. leptin, tumor necrosis factor-α, adiponectin) [69-73]. Insulin sensitivity in humans can also be improved with treatment of thiazolidinediones, PPARγ agonists [74].

PPARγ also has a major role in lipid metabolism. PPARγ upregulates genes involved in lipid transport (i.e. FATP), fatty acid synthesis (i.e. the malic enzyme gene), and triglyceride synthesis (i.e. PECK) [75-77]. *In vitro* and *in vivo* studies have supported the critical role of PPARγ as the master regulator of adipogenesis. This adipogenic role can be observed *in vitro* using immortalized fibroblast cell lines (e.g. 3T3-F442A and 3T3-L1) that can be differentiated into adipocytes upon treatment with a hormone cocktail [78, 79]. The expression of PPARγ increases a few hours after treatment and is sustained to maintain the mature adipocyte [80, 81]. Immortalized fibroblast cell lines lacking PPARγ were incapable of promoting adipogenesis [82]. Numerous studies have shown that PPARγ agonists stimulate adipocyte differentiation and lipid accumulation in mouse fibroblast cells [83-86]. PPARγ agonists promoted the fibroblast-like pre-adipocytes to undergo a series of

biochemical and morphological changes leading to lipid accumulation which can then be visually observed and quantified [86].

PPARγ stimulated weight gain has been observed *in vivo.* Mice fed high-fat diets with an environmentally relevant PPARγ agonist (tributylin) experienced increased weight gain in comparison to mice that did not receive the agonist [54]. Additionally, excess weight gain from a high-fat diet was prevented when mice were treated with a PPARγ antagonist [87]. Weight gain was also evaded in PPARγ knockout mice. When fed a high-fat diet, these mice were incapable of gaining weight despite having increased appetites [88].

Weight gain is a common side effect of the anti-diabetic thiazolidinedione drugs which are PPARγ agonists. Type II diabetics given troglitazone for 6 months showed improvement in insulin-sensitivity, but increased body mass [89]. Rosiglitazone was administered to patients with high glucose levels in a 12-week, double-blind, multicenter study. Glycemic index levels improved as body weight increased [90].

High levels of circulating free fatty acids cause insulin resistance in insulin-sensitive tissues (i.e., liver and skeletal muscle) [91, 92]. The "fatty acid steal hypothesis" suggests that fatty acid-mediated insulin resistance can be improved with the treatment of thiazolidinediones [92]. Thiazolidinediones stimulate free fatty acid uptake and storage in adipose tissue without concomitant fatty acid uptake in liver and skeletal muscle tissues. Storage of fatty acids in adipose tissue decreases its systemic availability to other tissues leading to improvements in insulin sensitivity and insulin signaling [92, 93].

Consequences of Co-activation of PPARα and PPARγ

The ability to simultaneously activate both PPARα and PPARγ may prove to be the most efficacious means of treating metabolic diseases. PPARγ ligands improve insulin sensitivity but promote dyslipidemia; while, PPARα ligands improve dyslipidemia [94-97]. Many studies have investigated the effects of the simultaneous administration of PPARα and PPARγ agonists for the treatment of lipid and glucose disorders. Body weight of mice decreased when given fenofibrate alone (PPARα agonist) and increased when administered rosiglitazone (PPARγ agonist) alone [98]. In combination, fenofibrate prevented rosiglitazone induced body weight gain, and, improved other lipid and glucose dysfunctions (e.g. reduced plasma triglyceride, total cholesterol, and plasma glucose levels) in mice [98]. Unfortunately, fenofibrate did not prevent rosiglitazone induced body weight gain in a human clinical trial involving patients with Type II diabetes [99]. These compounds did however improve serum lipid levels (e.g. triglycerides, HDL cholesterol, LDL cholesterol levels) [99]. In another clinical trial, human glucose and lipid level effects by fenofibrate alone, pioglitazone (PPARγ agonist) alone, and fenofibrate in combination with pioglitazone were evaluated. Fenofibrate interacted with pioglitazone in an additive fashion to decrease triacylglycerol levels. However, there were no other beneficial effects of taking the two compounds together as opposed to individually [100].

Several glitazar class compounds have undergone clinical evaluation for efficacy as dual PPARα/PPARγ agonists. Compounds include: tesaglitazar, aleglitazar, saroglitazar, and muraglitzar. These compounds were more efficacious in improving lipid and glucose metabolism than individual selective PPAR agonists. For example, muraglitazar reduced

hyperlipidemia, prevented the development of diabetes, and abolished pre-existing diabetes [101]. Unfortunately, muraglitazar stimulated edema and adipogenesis [102]. The adverse toxicity profiles of muraglitazar and other glitazones is a major issue and the majority of these compounds have been discontinued [103].

Consequences of Co-activation of PPAR and RXR subunits

The permissive nature of the PPAR:RXR heterodimer has suggested that combined exposure to PPAR and RXR ligands may result in an additive or synergistic effect. For example, co-treatment of NIH 3T3 cells with a low concentration of BRL49653 (PPARγ agonist) combined with LG100268 (RXRα agonist), synergistically activated a PPAR-responsive reporter gene and synergistically increased lipid accumulation in the cells [15]. However, factors that dictate whether a PPAR ligand and a RXR ligand will interact in an additive or synergistic manner are unknown. Activation of some fraction of the PPAR:RXR population by a PPAR ligand with proportionate activation of another fraction of the population by a RXR ligand would result in gene transcription activation consistent with a model of additivity. Whereas, if both ligands are simultaneously bound to their respective subunits of the PPAR:RXR complex, then synergistic activation of the complex could occur. For example, RXR ligand binding may alter the conformation of the PPAR:RXR heterodimer in a manner that increases the dissociation of co-repressors, increases the affinity for PPAR ligands to their subunit, or enhances the recruitment of coactivators. Thus, allosteric communications may be responsible for PPAR:RXR ligand-mediated transcriptional activity [15, 104].

PPARs and Chemical Exposures

PPARs coordinate several biological processes involved in energy metabolism. Several studies have shown that disruption in PPAR signaling can contribute to etiology of metabolic syndrome, a combination of energy-source utilization and energy storage disorders [7]. Numerous studies support the biological plausibility that exposures to environmental chemicals disrupt the PPAR network in a manner that contributes to metabolic syndrome. Bisphenol A is a component of many plastics used in a variety of applications including food and beverage packaging and has been suggested to leach-out from these consumer products [41]. BPA weakly activated the PPARγ receptor in luciferase transactivation assays [86]. Additionally, halogenated BPA analogs (e.g. TBBPA, TCBPA) activated PPARγ in reporter assays and activation was dependent upon the degree of halogenation [105, 106]. BPA and its halogenated analogs were shown to stimulate adipocyte differentiation and lipid accumulation [107, 108] . Furthermore, epidemiological studies showed a positive association between urinary BPA concentration with both diabetes and coronary heart disease, two major risk factors for metabolic syndrome [109, 110].

The organotin, tributyltin (TBT), has been characterized as an obesogen. TBT potently activated both the PPARγ and RXRα receptors at nanomolar concentrations in transactivation assays [52]. Additionally, TBT increased adipocyte differentiation and lipid accumulation in mouse pre-adipocyte cells at concentrations as low as 10 nM [41, 111]. TBT-mediated activation was attenuated when TBT was combined with the PPARγ antagonist T007097 [55]. Furthermore, mice dosed with TBT *in utero* had more lipid

accumulation as neonates and larger adipose deposits as adults compared to unexposed mice [55].

Initial Objectives

Our lab was granted funding from the EPA to construct a high-throughput screening assay to evaluate endocrine signaling pathways. We proposed to create a multi-sensor cell-based assay that assessed individual chemicals and chemical mixtures in a single assay. This approach would save a considerable amount of time, money, and animals. We sought to combine a bioluminescence resonance energy transfer (BRET) assay with a standard luciferase reporter gene assay to evaluate the impact of chemicals on components within the PPAR signaling network. However, BRET and luciferase reporter gene assays were used separately in the research presented in the succeeding chapters.

Research Outline

Abundant evidence exists to support the hypothesis that some environmental chemicals are capable of modulating the PPAR signaling network in a manner that would contribute to conditions associated with metabolic syndrome. However, humans are typically exposed to environmental chemicals at levels significantly below those capable of triggering molecular initiating events that would lead to human disease. The PPAR signaling network provides for many opportunities whereby low levels of environmental chemicals may act together to elicit a significant initiating event. Such opportunities include the activation of PPARγ signaling by one chemical with a commensurate suppression of PPARα

signaling by another chemical. Alternatively, two chemicals may co-activate a PPAR:RXR complex through dual activation of the PPAR and RXR subunits resulting in additive or synergistic signaling.

We hypothesized that such combined actions of environmental chemicals may result in disruptions in PPAR signaling that could lead to physiologic dysfunction. We tested this hypothesis at the molecular level by generating the tools to measure the action of chemicals on PPAR receptor assembly and signaling. We evaluated the ability of several chemicals to perturb normal PPAR signaling. We sought to establish the mechanism of action by which active chemicals disrupted normal signaling. Finally, we inferred potential contributions of such disruptions on the etiology of metabolic syndrome.

Chapter one addresses the hypothesis that environmental chemicals may act on different targets of the PPAR network to perturb lipid signaling in a manner that would contribute to conditions associated with metabolic syndrome. The primary objective of the study was to elucidate the interactions of the organophosphate flame retardant, triphenyl phosphate, with the PPAR signaling network. Triphenyl phosphate inhibited PPARα signaling. Triphenyl phosphate disassembled constitutively formed PPARα:RXRα heterodimers and inhibited the activity of the PPARα subunit, the RXRα subunit, and the PPARα:RXRα receptor complex. In contrast, triphenyl phosphate activated the PPARγ signaling pathway. Triphenyl phosphate neither inhibited nor stimulated dimerization of the PPARγ:RXRα receptor complex. However, triphenyl phosphate was capable of activating the PPARγ:RXRα heterodimer through interaction with the PPARγ subunit. Inhibition of the

PPARα:RXRα signaling complex and activation of the PPARγ:RXRα signaling complex could lead to lipid disruption in a manner that promotes symptoms of metabolic syndrome.

Chapter two describes the development of tools for the evaluation of ligand-dependent PPARα receptor assembly and activation. The first objective of this study was to determine if ligand-dependent receptor assembly could be detected and used to discern specific interactions of some chemicals with the PPARα receptor complex. Protein-protein interactions within the PPARα:RXRα:SRC1 signaling pathway were analyzed using bioluminescence resonance energy transfer (BRET). The second objective was to use reporter gene transcription assays to evaluate the interactions of chemicals with the PPARα:RXRα receptor complex and define the subunit that the chemicals acts through. Results identified candidate disruptors of the PPARα signaling network including several organophosphate flame retardants. Results showed that some organophosphate compounds exhibited little impact on PPARα:RXRα receptor assembly or activity. Organophosphates that interacted with the PPARα signaling pathway dissociated PPARα:RXRα heterodimers and inhibited activity of the PPARα subunit, the RXRα subunit, and the PPARα:RXRα receptor complex. In conclusion, we found that other organophosphate flame retardants exhibited similar effects as triphenyl phosphate (Chapter 1) on the PPARα signaling pathway, and identified several additional inhibitors of the PPARα:RXRα receptor with the potential for human exposure.

Finally, Chapter three tested the hypothesis that insect growth regulating (IGR) insecticides would interact with the PPARγ signaling pathway in a manner that may favor adipogenesis. We evaluated four IGRs: pyriproxyfen, fenoxycarb, methoprene, and

kinoprene. The IGRs did not stimulate or inhibit assembly of PPARγ:RXRα:SRC1 complexes. However, all IGRs activated the PPARγ:RXRα receptor complex and the individual PPARγ subunit in luciferase reporter assays. Fenoxycarb, methoprene, and kinoprene also activated the individual RXRα subunit, however, activation of the PPARγ:RXRα complex was due to activation of the PPARγ subunit not the RXRα subunit. All of the IGRs promoted differentiation of cultured pre-adipocytes into adipocytes with excess lipid accumulation within these cells. Resultantly, we found a class of environmental chemicals that can interact with the PPARγ signaling pathway in a manner that could contribute to increased adiposity in humans.

Overall, the results from this research provided a mechanistic rationale that supports the hypothesis that exposure of certain chemicals or chemical combinations could cause disruption of the PPAR signaling network in a manner that can lead to symptoms of metabolic syndrome. These findings advance our understandings of the role of environmental chemicals in lipid metabolism and this research program will serve to advance our understanding of how environmental chemicals may contribute to the epidemic of metabolic syndrome.

References

1. Grundy, S.M., H.B. Brewer, J.I. Cleeman, S.C. Smith, C. Lenfant, and I.A.H, Definition of metabolic syndrome - report of the national heart, lung, and blood institute/american heart association conference on scientific issues related to definition. Arteriosclerosis Thrombosis and Vascular Biology, 2004. **24**(2): p. E13-E18.
2. Ford, E.S., W.H. Giles, and W.H. Dietz, Prevalence of the metabolic syndrome among us adults - findings from the third national health and nutrition examination survey. Journal of the American Medical Association, 2002. **287**(3): p. 356-359.
3. Scholze, J., E. Alegria, C. Ferri, S. Langham, W. Stevens, D. Jeffries, and K. Uhl-Hochgraeber, Epidemiological and economic burden of metabolic syndrome and its consequences in patients with hypertension in germany, spain and italy; a prevalence-based model. BMC Public Health, 2010. **10**.
4. WHO. The top 10 causes of death. Available from: http://www.who.int/mediacentre/factsheets/fs310/en/.
5. Shulman, A.I. and D.J. Mangelsdorf, Mechanisms of disease: Retinoid x receptor heterodimers in the metabolic syndrome. New England Journal of Medicine, 2005. **353**(6): p. 604-615.
6. Tyagi, S., P. Gupta, A.S. Saini, C. Kaushal, and S. Sharma, The peroxisome proliferator-activated receptor: A family of nuclear receptors role in various diseases. Journal of Advanced Pharmaceutical Technology & Research, 2011. **2**(4): p. 236-240.

7. Jia, F, PPAR: A pivotal regulator in metabolic syndromes. Journal of Endocrinology & Metabolic Syndrome, 2012.

8. Hsu, M.H., C.N.A. Palmer, W. Song, K.J. Griffin, and E.F. Johnson, A carboxyl-terminal extension of the zinc finger domain contributes to the specificity and polarity of peroxisome proliferator-activated receptor DNA binding. Journal of Biological Chemistry, 1998. **273**(43): p. 27988-27997.

9. Osada, S., T. Tsukamoto, M. Takiguchi, M. Mori, and T. Osumi, Identification of an extended half-site motif required for the function of peroxisome proliferator-activated receptor alpha. Genes to Cells, 1997. **2**(5): p. 315-327.

10. Ijpenberg, A., E. Jeannin, W. Wahli, and B. Desvergne, Polarity and specific sequence requirements of peroxisome proliferator-activated receptor (PPAR) retinoid x receptor heterodimer binding to DNA - a functional analysis of the malic enzyme gene PPAR response element. Journal of Biological Chemistry, 1997. **272**(32): p. 20108-20117.

11. Temple, K.A., R.N. Cohen, S.R. Wondisford, C. Yu, D. Deplewski, and F.E. Wondisford, An intact DNA-binding domain is not required for peroxisome proliferator-activated receptor gamma (PPAR gamma) binding and activation on some PPAR response elements. Journal of Biological Chemistry, 2005. **280**(5): p. 3529-3540.

12. Perez, E., W. Bourguet, H. Gronemeyer, and A.R. de Lera, Modulation of RXR function through ligand design. Biochimica Et Biophysica Acta-Molecular and Cell Biology of Lipids, 2012. **1821**(1): p. 57-69.

13. Mukherjee, R., L. Jow, D. Noonan, and D.P. McDonnell, Human and rat peroxisome proliferator activated receptors (PPARs) demonstrate similar tissue distribution but different responsiveness to ppar activators. Journal of Steroid Biochemistry and Molecular Biology, 1994. **51**(3-4): p. 157-166.
14. Mukherjee, R., J. Strasser, L. Jow, P. Hoener, J.R. Paterniti, and R.A. Heyman, RXR agonists activate PPAR alpha-inducible genes, lower triglycerides, and raise HDL levels in vivo. Arteriosclerosis Thrombosis and Vascular Biology, 1998. **18**(2): p. 272-276.
15. Schulman, I.G., G. Shao, and R.A. Heyman, Transactivation by retinoid x receptor peroxisome proliferator-activated receptor gamma (PPAR gamma) heterodimers: Intermolecular synergy requires only the PPAR gamma hormone-dependent activation function. Molecular and Cellular Biology, 1998. **18**(6): p. 3483-3494.
16. Desvergne, B. and W. Wahli, Peroxisome proliferator-activated receptors: Nuclear control of metabolism. Endocrine Reviews, 1999. **20**(5): p. 649-688.
17. Ahmadian, M., J.M. Suh, N. Hah, C. Liddle, A.R. Atkins, M. Downes, and R.M. Evans, PPAR gamma signaling and metabolism: The good, the bad and the future. Nature Medicine, 2013. **19**(5): p. 557-566.
18. Gearing, K.L., A. Crickmore, and J.A. Gustafsson, Structure of the mouse peroxisome proliferator activated receptor-alpha gene. Biochemical and Biophysical Research Communications, 1994. **199**(1): p. 255-263.

19. Fajas, L., J.C. Fruchart, and J. Auwerx, PPAR gamma 3 mrna: A distinct PPAR gamma mrna subtype transcribed from an independent promoter. Febs Letters, 1998. **438**(1-2): p. 55-60.

20. Fajas, L., D. Auboeuf, E. Raspe, K. Schoonjans, A.M. Lefebvre, R. Saladin, J. Najib, M. Laville, J.C. Fruchart, S. Deeb, A. VidalPuig, J. Flier, M.R. Briggs, B. Staels, H. Vidal, and J. Auwerx, The organization, promoter analysis, and expression of the human PPAR gamma gene. Journal of Biological Chemistry, 1997. **272**(30): p. 18779-18789.

21. Braissant, O., F. Foufelle, C. Scotto, M. Dauca, and W. Wahli, Differential expression of peroxisome proliferator-activated receptors (PPARs): Tissue distribution of PPAR-alpha, -beta, and -gamma in the adult rat. Endocrinology, 1996. **137**(1): p. 354-366.

22. Girroir, E.E., H.E. Hollingshead, P. He, B. Zhu, G.H. Perdew, and J.M. Peters, Quantitative expression patterns of peroxisome proliferator-activated receptor-beta/delta (PPAR beta/delta) protein in mice. Biochemical and Biophysical Research Communications, 2008. **371**(3): p. 456-461.

23. Karpe, F. and E.E. Ehrenborg, PPAR delta in humans: Genetic and pharmacological evidence for a significant metabolic function. Current Opinion in Lipidology, 2009. **20**(4): p. 333-336.

24. Germain, P., P. Chambon, G. Eichele, R.M. Evans, M.A. Lazar, M. Leid, A.R. De Lera, R. Lotan, D.J. Mangelsdorf, and H. Gronemeyer, International union of

pharmacology. Lxiii. Retinoid x receptors. Pharmacological Reviews, 2006. **58**(4): p. 760-772.

25. Shulman, A.I. and D.J. Mangelsdorf, Retinoid x receptor heterodimers in the metabolic syndrome. New England Journal of Medicine, 2005. **353**(6): p. 604-15.

26. Wallen-Mackenzie, A., A. Mata de Urquiza, S. Petersson, F.J. Rodriguez, S. Friling, J. Wagner, P. Ordentlich, J. Lengqvist, R.A. Heyman, E. Arenas, and T. Perlmann, Nurr1-RXR heterodimers mediate RXR ligand-induced signaling in neuronal cells. Genes & Development, 2003. **17**(24): p. 3036-3047.

27. Perlmann, T. and L. Jansson, A novel pathway for vitamin-a signaling mediated by RXR heterodimerization with ngfi-b and nurr1. Genes & Development, 1995. **9**(7): p. 769-782.

28. Evans, R.M. and D.J. Mangelsdorf, Nuclear receptors, RXR, and the big bang. Cell, 2014. **157**(1): p. 255-266.

29. Uniprotkb - p19793 (rxra_human). Available from: http://www.uniprot.org/uniprot/P19793.

30. Uniprotkb - p37231 (pparg_human). Available from: http://www.uniprot.org/uniprot/P37231.

31. Nolte, R.T., G.B. Wisely, S. Westin, J.E. Cobb, M.H. Lambert, R. Kurokawa, M.G. Rosenfeld, T.M. Willson, C.K. Glass, and M.V. Milburn, Ligand binding and co-activator assembly of the peroxisome proliferator-activated receptor-gamma. Nature, 1998. **395**(6698): p. 137-143.

32. Harmon, G.S., M.T. Lam, and C.K. Glass, PPARs and lipid ligands in inflammation and metabolism. Chemical Reviews, 2011. **111**(10): p. 6321-6340.

33. Vincent, Z.A., G.A. Aurelien, and O. Michielin, Peroxisome proliferator-activated receptor structures: Ligand specificity, molecular switch and interactions with regulators. Biochimica Et Biophysica Acta-Molecular and Cell Biology of Lipids, 2007. **1771**(8): p. 915-925.

34. Bruning, J.B., M.J. Chalmers, S. Prasad, S.A. Busby, T.M. Karnenecka, Y.J. He, K.W. Nettles, and P.R. Griffin, Partial agonists activate ppar gamma using a helix 12 independent mechanism. Structure, 2007. **15**(10): p. 1258-1271.

35. Hsu, M.H., C.N.A. Palmer, K.J. Griffin, and E.F. Johnson, A single amino-acid change in the mouse peroxisome proliferator-activated receptor-alpha alters transcriptional responses to peroxisome proliferators. Molecular Pharmacology, 1995. **48**(3): p. 559-567.

36. Kliewer, S.A., S.S. Sundseth, S.A. Jones, P.J. Brown, G.B. Wisely, C.S. Koble, P. Devchand, W. Wahli, T.M. Willson, J.M. Lenhard, and J.M. Lehmann, Fatty acids and eicosanoids regulate gene expression through direct interactions with peroxisome proliferator-activated receptors alpha and gamma. Proceedings of the National Academy of Sciences of the United States of America, 1997. **94**(9): p. 4318-4323.

37. National Institute of Diabetes and Digestive Kidney Diseases, Fibrates. Available from: http://livertox.nih.gov/Fibrates.htm.

38. Yu, K., W. Bayona, C.B. Kallen, H.P. Harding, C.P. Ravera, G. McMahon, M. Brown, and M.A. Lazar, Differential activation of peroxisome proliferator-activated

receptors by eicosanoids. Journal of Biological Chemistry, 1995. **270**(41): p. 23975-23983.

39. Luci, S., B. Giemsa, H. Kluge, and K. Eder, Clofibrate causes an upregulation of PPAR-alpha target genes but does not alter expression of srebp target genes in liver and adipose tissue of pigs. American Journal of Physiology-Regulatory Integrative and Comparative Physiology, 2007. **293**(1): p. R70-R77.

40. Lehmann, J.M., L.B. Moore, T.A. Smitholiver, W.O. Wilkison, T.M. Willson, and S.A. Kliewer, An antidiabetic thiazolidinedione is a high-affinity ligand for peroxisome proliferator-activated receptor gamma(PPAR-gamma). Journal of Biological Chemistry, 1995. **270**(22): p. 12953-12956.

41. National Toxicology Program workshop: Role of envrionmental chemicals in the development of diabetes and obesity. 2011. Raleigh, NC: National Toxicology Program.

42. Maloney, E.K. and D.J. Waxman, Trans-activation of PPAR alpha and PPAR gamma by structurally diverse environmental chemicals. Toxicology and Applied Pharmacology, 1999. **161**(2): p. 209-218.

43. Feige, J.N., L. Gelman, D. Rossi, V. Zoete, R. Metivier, C. Tudor, S.I. Anghel, A. Grosdidier, C. Lathion, Y. Engelborghs, O. Michielin, W. Wahli, and B. Desvergne, The endocrine disruptor monoethyl-hexyl-phthalate is a selective peroxisome proliferator-activated receptor gamma modulator that promotes adipogenesis. Journal of Biological Chemistry, 2007. **282**(26): p. 19152-19166.

44. Hurst, C.H. and D.J. Waxman, Activation of PPAR alpha and PPAR gamma by environmental phthalate monoesters. Toxicological Sciences, 2003. **74**(2): p. 297-308.

45. Hatch, E.E., J.W. Nelson, M.M. Qureshi, J. Weinberg, L.L. Moore, M. Singer, and T.F. Webster, Association of urinary phthalate metabolite concentrations with body mass index and waist circumference: A cross-sectional study of NHANES data, 1999-2002. Environmental Health, 2008. **7**: p. 27.

46. Stahlhut, R.W., E. van Wijngaarden, T.D. Dye, S. Cook, and S.H. Swan, Concentrations of urinary phthalate metabolites are associated with increased waist circumference and insulin resistance in adult U.S. Males. Environmental Health Perspectives, 2007. **115**(6): p. 876-882.

47. Mileson, B.E., J.E. Chambers, W.L. Chen, W. Dettbarn, M. Ehrich, A.T. Eldefrawi, D.W. Gaylor, K. Hamernik, E. Hodgson, A.G. Karczmar, S. Padilla, C.N. Pope, R.J. Richardson, D.R. Saunders, L.P. Sheets, L.G. Sultatos, and K.B. Wallace, Common mechanism of toxicity: A case study of organophosphorus pesticides. Toxicological Sciences, 1998. **41**(1): p. 8-20.

48. Fromme, H., T. Lahrz, M. Kraft, L. Fembacher, C. Mach, S. Dietrich, R. Burkardt, W. Volkel, and T. Goen, Organophosphate flame retardants and plasticizers in the air and dust in german daycare centers and human biomonitoring in visiting children (lupe 3). Environment International, 2014. **71**: p. 158-163.

49. Fang, M., T.F. Webster, and H.M. Stapleton, Activation of human peroxisome proliferator-activated nuclear receptors (ppargamma1) by semi-volatile compounds

(svocs) and chemical mixtures in indoor dust. Environmental Science and Technology, 2015. **49**(16): p. 10057-10064.

50. Patisaul, H.B., S.C. Roberts, N. Mabrey, K.A. McCaffrey, R.B. Gear, J. Braun, S.M. Belcher, and H.M. Stapleton, Accumulation and endocrine disrupting effects of the flame retardant mixture firemaster(r) 550 in rats: An exploratory assessment. Journal of Biochemical and Molecular Toxicology, 2013. **27**(2): p. 124-136.

51. National Toxicology Program. Organotin (methyl and butyl) toxicity. Available from: https://ntp.niehs.nih.gov/ntp/htdocs/chem_background/exsumpdf/organotins_508.pdf.

52. le Maire, A., M. Grimaldi, D. Roecklin, S. Dagnino, V. Vivat-Hannah, P. Balaguer, and W. Bourguet, Activation of RXR-PPAR heterodimers by organotin environmental endocrine disruptors. European Molecular Biology Organization Rep, 2009. **10**(4): p. 367-373.

53. Kanayama, T., N. Kobayashi, S. Mamiya, T. Nakanishi, and J. Nishikawa, Organotin compounds promote adipocyte differentiation as agonists of the peroxisome proliferator-activated receptor gamma/retinoid x receptor pathway. Molecular Pharmacolgy, 2005. **67**(3): p. 766-774.

54. Grun, F., H. Watanabe, Z. Zamanian, L. Maeda, K. Arima, R. Chubacha, D.M. Gardiner, J. Kanno, T. Iguchi, and B. Blumberg, Endocrine-disrupting organotin compounds are potent inducers of adipogenesis in vertebrates. Molecular Endocrinology, 2006. **20**(9): p. 2141-2155.

55. Kirchner, S., T. Kieu, C. Chow, S. Casey, and B. Blumberg, Prenatal exposure to the environmental obesogen tributyltin predisposes multipotent stem cells to become adipocytes. Molecular Endocrinology, 2010. **24**(3): p. 526-539.

56. Heyman, R.A., D.J. Mangelsdorf, J.A. Dyck, R.B. Stein, G. Eichele, R.M. Evans, and C. Thaller, 9-cis retinoic acid is a high affinity ligand for the retinoid x receptor. Cell, 1992. **68**(2): p. 397-406.

57. Kitareewan, S., L.T. Burka, K.B. Tomer, C.E. Parker, L.J. Deterding, R.D. Stevens, B.M. Forman, D.E. Mais, R.A. Heyman, T. McMorris, and C. Weinberger, Phytol metabolites are circulating dietary factors that activate the nuclear receptor RXR. Molecular Biology Cell, 1996. **7**(8): p. 1153-1166.

58. de Urquiza, A.M., S.Y. Liu, M. Sjoberg, R.H. Zetterstrom, W. Griffiths, J. Sjovall, and T. Perlmann, Docosahexaenoic acid, a ligand for the retinoid x receptor in mouse brain. Science, 2000. **290**(5499): p. 2140-2144.

59. Reddy, J.K. and T. Hashimoto, Peroxisomal beta-oxidation and peroxisome proliferator-activated receptor alpha: An adaptive metabolic system. Annual Review of Nutrition, 2001. **21**: p. 193-230.

60. Larsen, P.J., P.B. Jensen, R.V. Sorensen, L.K. Larsen, N. Vrang, E.M. Wulff, and K. Wassermann, Differential influences of peroxisome proliferator-activated receptors gamma and -alpha on food intake and energy homeostasis. Diabetes, 2003. **52**(9): p. 2249-2259.

61. Haluzik, M.M. and M. Haluzik, PPAR-alpha and insulin sensitivity. Physiological Research, 2006. **55**(2): p. 115-122.

62. Peeters, A. and M. Baes, Role of pparalpha in hepatic carbohydrate metabolism. PPAR Research, 2010. **2010**.

63. Du, K., S. Herzig, R.N. Kulkarni, and M. Montminy, Trb3: A tribbles homolog that inhibits akt/pkb activation by insulin in liver. Science, 2003. **300**(5625): p. 1574-1577.

64. Koo, S.H., H. Satoh, S. Herzig, C.H. Lee, S. Hedrick, R. Kulkarni, R.M. Evans, J. Olefsky, and M. Montminy, pgc-1 promotes insulin resistance in liver through PPAR-alpha-dependent induction of trb-3. Nature Medicine, 2004. **10**(5): p. 530-534.

65. Chou, C.J., M. Haluzik, C. Gregory, K.R. Dietz, C. Vinson, O. Gavrilova, and M.L. Reitman, Wy14,643, a peroxisome proliferator-activated receptor alpha (pparalpha) agonist, improves hepatic and muscle steatosis and reverses insulin resistance in lipoatrophic a-zip/f-1 mice. Journal of Biology and Chemistry, 2002. **277**(27): p. 24484-24489.

66. Schafer, S.A., B.C. Hansen, A. Volkl, H.D. Fahimi, and J. Pill, Biochemical and morphological effects of k-111, a peroxisome proliferator-activated receptor (ppar)alpha activator, in non-human primates. Biochemical Pharmacology, 2004. **68**(2): p. 239-251.

67. Kim, H., M. Haluzik, Z. Asghar, D. Yau, J.W. Joseph, A.M. Fernandez, M.L. Reitman, S. Yakar, B. Stannard, L. Heron-Milhavet, M.B. Wheeler, and D. LeRoith, Peroxisome proliferator-activated receptor-alpha agonist treatment in a transgenic model of type 2 diabetes reverses the lipotoxic state and improves glucose homeostasis. Diabetes, 2003. **52**(7): p. 1770-1778.

68. Sugden, M.C., K. Bulmer, G.F. Gibbons, B.L. Knight, and M.J. Holness, Peroxisome-proliferator-activated receptor-alpha (PPARalpha) deficiency leads to dysregulation of hepatic lipid and carbohydrate metabolism by fatty acids and insulin. Biochemical Journal, 2002. **364**(Pt 2): p. 361-368.

69. Hollenberg, A.N., V.S. Susulic, J.P. Madura, B. Zhang, D.E. Moller, P. Tontonoz, P. Sarraf, B.M. Spiegelman, and B.B. Lowell, Functional antagonism between ccaat/enhancer binding protein-alpha and peroxisome proliferator-activated receptor-gamma on the leptin promoter. Journal of Biological Chemistry, 1997. **272**(8): p. 5283-5290.

70. Iwaki, M., M. Matsuda, N. Maeda, T. Funahashi, Y. Matsuzawa, M. Makishima, and I. Shimomura, Induction of adiponectin, a fat-derived antidiabetic and antiatherogenic factor, by nuclear receptors. Diabetes, 2003. **52**(7): p. 1655-1663.

71. Hofmann, C., K. Lorenz, S.S. Braithwaite, J.R. Colca, B.J. Palazuk, G.S. Hotamisligil, and B.M. Spiegelman, Altered gene expression for tumor necrosis factor-alpha and its receptors during drug and dietary modulation of insulin resistance. Endocrinology, 1994. **134**(1): p. 264-270.

72. Ribon, V., J.H. Johnson, H.S. Camp, and A.R. Saltiel, Thiazolidinediones and insulin resistance: Peroxisome proliferatoractivated receptor gamma activation stimulates expression of the cap gene. Proceedings of the National Academy of Science, 1998. **95**(25): p. 14751-14756.

73. Armoni, M., C. Harel, and E. Karnieli, Transcriptional regulation of the glut4 gene: From PPAR-gamma and foxo1 to ffa and inflammation. Trends in Endocrinology and Metabolism, 2007. **18**(3): p. 100-107.

74. Sears, D.D., G. Hsiao, A. Hsiao, J.G. Yu, C.H. Courtney, J.M. Ofrecio, J. Chapman, and S. Subramaniam, Mechanisms of human insulin resistance and thiazolidinedione-mediated insulin sensitization. Proceedings of the National Academy of Science, 2009. **106**(44): p. 18745-18750.

75. Motojima, K., P. Passilly, J.M. Peters, F.J. Gonzalez, and N. Latruffe, Expression of putative fatty acid transporter genes are regulated by peroxisome proliferator-activated receptor alpha and gamma activators in a tissue- and inducer-specific manner. Journal of Biological Chemistry, 1998. **273**(27): p. 16710-16714.

76. Castelein, H., T. Gulick, P.E. Declercq, G.P. Mannaerts, D.D. Moore, and M.I. Baes, The peroxisome proliferator activated receptor regulates malic enzyme gene-expression. Journal of Biological Chemistry, 1994. **269**(43): p. 26754-26758.

77. Bogacka, I., H. Xie, G.A. Bray, and S.R. Smith, The effect of pioglitazone on peroxisome proliferator-activated receptor-gamma target genes related to lipid storage in vivo. Diabetes Care, 2004. **27**(7): p. 1660-1667.

78. Green, H. and M. Meuth, An established pre-adipose cell line and its differentiation in culture. Cell, 1974. **3**(2): p. 127-133.

79. Green, H. and O. Kehinde, Sublines of mouse 3t3 cells that accumulate lipid. Cell, 1974. **1**(3): p. 113-116.

80. Salma, N., H. Xiao, and A.N. Imbalzano, Temporal recruitment of ccaat/enhancer-binding proteins to early and late adipogenic promoters in vivo. Journal of Molecular Endocrinology, 2006. **36**(1): p. 139-151.

81. Wu, Z., E.D. Rosen, R. Brun, S. Hauser, G. Adelmant, A.E. Troy, C. McKeon, G.J. Darlington, and B.M. Spiegelman, Cross-regulation of c/ebp alpha and ppar gamma controls the transcriptional pathway of adipogenesis and insulin sensitivity. Molecular Cell, 1999. **3**(2): p. 151-158.

82. Rosen, E.D., C.H. Hsu, X. Wang, S. Sakai, M.W. Freeman, F.J. Gonzalez, and B.M. Spiegelman, C/ebpalpha induces adipogenesis through ppargamma: A unified pathway. Genes and Development, 2002. **16**(1): p. 22-26.

83. Lehmann, J.M., J.M. Lenhard, B.B. Oliver, G.M. Ringold, and S.A. Kliewer, Peroxisome proliferator-activated receptors alpha and gamma are activated by indomethacin and other non-steroidal anti-inflammatory drugs. Journal of Biological Chemistry, 1997. **272**(6): p. 3406-3410.

84. Albrektsen, T., K.S. Frederiksen, W.E. Holmes, E. Boel, K. Taylor, and J. Fleckner, Novel genes regulated by the insulin sensitizer rosiglitazone during adipocyte differentiation. Diabetes, 2002. **51**(4): p. 1042-1051.

85. Sandouk, T., D. Reda, and C. Hofmann, Antidiabetic agent pioglitazone enhances adipocyte differentiation of 3t3-f442a cells. American Journal of Physiology, 1993. **264**(6 Pt 1): p. C1600-1608.

86. Pereira-Fernandes, A., H. Demaegdt, K. Vandermeiren, T.L. Hectors, P.G. Jorens, R. Blust, and C. Vanparys, Evaluation of a screening system for obesogenic compounds:

Screening of endocrine disrupting compounds and evaluation of the ppar dependency of the effect. Public Library of Sciences One, 2013. **8**(10): p. e77481.

87. Nakano, R., E. Kurosaki, S. Yoshida, M. Yokono, A. Shimaya, T. Maruyama, and M. Shibasaki, Antagonism of peroxisome proliferator-activated receptor gamma prevents high-fat diet-induced obesity in vivo. Biochemical Pharmacology, 2006. **72**(1): p. 42-52.

88. Jones, J.R., C. Barrick, K.A. Kim, J. Lindner, B. Blondeau, Y. Fujimoto, M. Shiota, R.A. Kesterson, B.B. Kahn, and M.A. Magnuson, Deletion of ppar gamma in adipose tissues of mice protects against high fat diet-induced obesity and insulin resistance. Proceedings of the National Academy of Sciences of the United States of America, 2005. **102**(17): p. 6207-6212.

89. Mori, Y., Y. Murakawa, K. Okada, H. Horikoshi, J. Yokoyama, N. Tajima, and Y. Ikeda, Effect of troglitazone on body fat distribution in type 2 diabetic patients. Diabetes Care, 1999. **22**(6): p. 908-912.

90. Patel, J., R.J. Anderson, and E.B. Rappaport, Rosiglitazone monotherapy improves glycaemic control in patients with type 2 diabetes: A twelve-week, randomized, placebo-controlled study. Diabetes Obesity & Metabolism, 1999. **1**(3): p. 165-172.

91. Delarue, J. and C. Magnan, Free fatty acids and insulin resistance. Current Opinion in Clinical Nutrition & Metabolic Care, 2007. **10**(2): p. 142-148.

92. Yki-Jarvinen, H., Drug therapy: Thiazolidinediones. New England Journal of Medicine, 2004. **351**(11): p. 1106-1118.

93. Handbook of obesity: Etiology and pathophysiology. Vol. 1. 2003: CRC Press.

94. Caslake, M.J., C.J. Packard, A. Gaw, E. Murray, B.A. Griffin, B.D. Vallance, and J. Shepherd, Fenofibrate and LDL metabolic heterogeneity in hypercholesterolemia. Arteriosclerosis and Thrombosis, 1993. **13**(5): p. 702-711.

95. Goldberg, R.B., D.M. Kendall, M.A. Deeg, J.B. Buse, A.J. Zagar, J.A. Pinaire, M.H. Tan, M.A. Khan, A.T. Perez, S.J. Jacober, and G.S. Investigators, A comparison of lipid and glycemic effects of pioglitazone and rosiglitazone in patients with type 2 diabetes and dyslipidemia. Diabetes Care, 2005. **28**(7): p. 1547-1554.

96. Staels, B., J. Dallongeville, J. Auwerx, K. Schoonjans, E. Leitersdorf, and J.G. Fruchart, Mechanism of action of fibrates on lipid and lipoprotein metabolism. Circulation, 1998. **98**(19): p. 2088-2093.

97. Millar, J.S., K. Ikewaki, L.T. Bloedon, M.L. Wolfe, P.O. Szapary, and D.J. Rader, Effect of rosiglitazone on HDL metabolism in subjects with metabolic syndrome and low LDL. Journal of Lipid Research, 2011. **52**(1): p. 136-142.

98. Carmona, M.C., K. Louche, M. Nibbelink, B. Prunet, A. Bross, M. Desbazeille, C. Dacquet, P. Renard, L. Casteilla, and L. Penicaud, Fenofibrate prevents rosiglitazone-induced body weight gain in ob/ob mice. International Journal of Obesity, 2005. **29**(7): p. 864-871.

99. Seber, S., S. Ucak, O. Basat, and Y. Altuntas, The effect of dual ppar alpha/gamma stimulation with combination of rosiglitazone and fenofibrate on metabolic parameters in type 2 diabetic patients. Diabetes Research and Clinical Practice, 2006. **71**(1): p. 52-58.

100. Bajaj, M., S. Suraamornkul, L.J. Hardies, L. Glass, N. Musi, and R.A. DeFronzo, Effects of peroxisome proliferator-activated receptor (PPAR)-alpha and PPAR-gamma agonists on glucose and lipid metabolism in patients with type 2 diabetes mellitus. Diabetologia, 2007. **50**(8): p. 1723-1731.

101. Tozzo, E., R. Ponticiello, J. Swartz, D. Farrelly, R. Zebo, G. Welzel, D. Egan, L. Kunselman, A. Peters, L.Q. Gu, M. French, S. Chen, P. Devasthale, E. Janovitz, A. Staal, T. Harrity, R. Belder, P.T. Cheng, J. Whaley, S. Taylor, and N. Hariharan, The dual peroxisome proliferator-activated receptor alpha/gamma activator muraglitazar prevents the natural progression of diabetes in db/db mice. Journal of Pharmacology and Experimental Therapeutics, 2007. **321**(1): p. 107-115.

102. Mittra, S., G. Sangle, R. Tandon, S. Sharma, S. Roy, V. Khanna, A. Gupta, J. Sattigeri, L. Sharma, P. Priyadarsiny, S.K. Khattar, R.S. Bora, K.S. Saini, and V.S. Bansal, Increase in weight induced by muraglitazar, a dual ppar alpha/gamma agonist, in db/db mice: Adipogenesis/or oedema? British Journal of Pharmacology, 2007. **150**(4): p. 480-487.

103. Heald, M. and M.A. Cawthorne, Dual acting and pan-ppar activators as potential anti-diabetic therapies, in Diabetes - perspectives in drug therapy, M. Schwanstecher, Editor. 2011. p. 35-51.

104. Shulman, A.I., C. Larson, D.J. Mangelsdorf, and R. Ranganathan, Structural determinants of allosteric ligand activation in RXR heterodimers. Cell, 2004. **116**(3): p. 417-429.

105. Riu, A., C.W. McCollum, C.L. Pinto, M. Grimaldi, A. Hillenweck, E. Perdu, D. Zalko, L. Bernard, V. Laudet, P. Balaguer, M. Bondesson, and J.A. Gustafsson, Halogenated bisphenol-a analogs act as obesogens in zebrafish larvae (danio rerio). Toxicological Sciences, 2014. **139**(1): p. 48-58.

106. Riu, A., A. le Maire, M. Grimaldi, M. Audebert, A. Hillenweck, W. Bourguet, P. Balaguer, and D. Zalko, Characterization of novel ligands of eralpha, erbeta, and ppargamma: The case of halogenated bisphenol a and their conjugated metabolites. Toxicological Sciences, 2011. **122**(2): p. 372-382.

107. Riu, A., M. Grimaldi, A. le Maire, G. Bey, K. Phillips, A. Boulahtouf, E. Perdu, D. Zalko, W. Bourguet, and P. Balaguer, Peroxisome proliferator-activated receptor gamma is a target for halogenated analogs of bisphenol a. Environmental Health Perspectives, 2011. **119**(9): p. 1227-32.

108. Boucher, J.G., A. Boudreau, and E. Atlas, Bisphenol a induces differentiation of human preadipocytes in the absence of glucocorticoid and is inhibited by an estrogen-receptor antagonist. Nutrition & Diabetes, 2014. **4**: p. 8.

109. Ahmadkhaniha, R., M. Mansouri, M. Yunesian, K. Omidfar, M.Z. Jeddi, B. Larijani, A. Mesdaghinia, and N. Rastkari, Association of urinary bisphenol a concentration with type-2 diabetes mellitus. Journal of Environmental Health Sciences & Engineering, 2014. **12**(1): p. 64.

110. Melzer, D., N.E. Rice, C. Lewis, W.E. Henley, and T.S. Galloway, Association of urinary bisphenol a concentration with heart disease: Evidence from nhanes 2003/06. Public Library of Science One, 2010. **5**(1): p. e8673.

111. Pereira-Fernandes, A., C. Vanparys, T.L. Hectors, L. Vergauwen, D. Knapen, P.G. Jorens, and R. Blust, Unraveling the mode of action of an obesogen: Mechanistic analysis of the model obesogen tributyltin in the 3t3-l1 cell line. Molecular Cell Endocrinology, 2013. **370**(1-2): p. 52-64.

CHAPTER ONE: DIFFERENTIAL INTERACTIONS OF THE FLAME RETARDANT TRIPHENYL PHOSPHATE WITHINTHE PPAR SIGNALING NETWORK

Ying Wang[a], Gwijun Kwon[a], Lihui An[a,b], Charisse N. Holmes[a], Maher Haeba[a], and Gerald A. LeBlanc[a,c]

[a]Toxicology Program, Department of Biological Sciences, North Carolina State University, Raleigh, NC, USA
[b]State Key Laboratory of Environmental Criteria and Risk Assessment, Chinese Research Academy of Environment Sciences, Beijing 100012, China

Abstract

Triphenyl phosphate is an organophosphate flame retardant and plasticizer that has been detected in a variety of environmental media and shown to cause weight gain in rats. We hypothesized that triphenyl phosphate would modify the activity of the PPAR:RXR signaling network in a manner that would favor lipid accumulation. Gal4-driven luciferase-based transcription reporter gene assays were used to evaluate the responses of human PPARα:RXRα, PPARγ:RXRα, and the individual receptor subunits, to triphenyl phosphate. Triphenyl phosphate was a potent inhibitor of PPARα:RXRα signaling. The flame retardant interacted with both the PPARα and RXRα proteins to inhibit their respective activities at concentrations that were not overtly toxic to the cells. Bioluminescence resonance energy transfer experiments revealed that triphenyl phosphate actually inhibited the dimerization of PPARα and RXRα. In contrast, triphenyl phosphate modestly activated the PPARγ:RXRα receptor complex. This net activation of the complex was due to strong activation of the PPARγ receptor subunit and modest inhibition of the RXRα subunit. Further experiments revealed that triphenyl phosphate stimulated pre-adipocyte differentiation to lipid-laden adipocytes at a concentration that altered the PPAR signaling network. This dual activity of triphenyl phosphate, as an inhibitor of PPARα:RXRα signaling and an activator of PPARγ:RXRα signaling, provides a regulatory scenario that could lead to weight gain and other symptoms of metabolic syndrome.

Key words: triphenyl phosphate, diphenyl phosphate, PPAR, RXR, organotin, BRET, reporter gene assay, metabolic syndrome, weight gain

Introduction

Organophosphate flame retardants are increasing in commercial use with the banning of brominated flame retardants [1]. Some organophosphate flame retardants are also used as plasticizers [1]. Triphenyl phosphate is an organophosphate flame retardant that is used in applications such as polyurethane foams used in residential furniture [2]. Triphenyl phosphate has been detected in house dust ($\leq$1700 ug/g) [3,4], air ($\leq$200 ng/m^3) [5], and biota ($\leq$770 ng/g)[6]. Accordingly, the potential for human exposure to triphenyl phosphate is significant, and it has been detected in human milk ($\leq$11 ng/g) [6].

Triphenyl phosphate is considered to be of low concern with respect to reproductive, developmental, and systemic toxicity to mammals [7]. However, several studies have implicated this compound in interacting with nuclear receptors or steroidogenic enzymes [8-10]. Recently, triphenyl phosphate was reported to activate the peroxisome proliferator activated receptor gamma (PPARγ) [11]. PPARγ signaling stimulates pre-adipocyte differentiation and lipid accumulation [12,13]. Thus this molecular activity could be responsible for the observed obesogenic activity associated with feeding of a triphenyl phosphate-containing flame retardant to rats [14]. Indeed, triphenyl phosphate exposure stimulated lipid accumulation in cultured murine bone marrow stromally derived adipocytes (BMS2) [11].

The PPAR signaling network is comprised of several ligand-activated nuclear receptor proteins. Three isoforms of PPAR (α,β/δ,γ) contribute to the regulation of various aspects of energy homeostasis [15]. The PPAR proteins dimerize with the retinoid X receptors (RXRα,β,γ) to form active transcription factors [16]. The RXRs are also ligand-

activated and ligand occupancy on either the PPAR or the RXR subunit can result in activation of the complex [17]. Thus occupancy of the PPARγ protein by triphenyl phosphate would specifically activate PPARγ-regulated processes (e.g., increased insulin sensitivity, adipogenesis and lipid accumulation [17]). Whereas, activation of the PPARγ:RXR receptor complex by binding to the RXR subunit would likely result in the activation of all PPAR isoform receptor complexes, as well as other RXR-containing receptors resulting in pleiotropic consequences.

In the present study we tested the hypothesis that triphenyl phosphate elicits multiple effects on the PPAR signaling network through interactions with human PPARα, PPARγ, and RXRα. Further, we utilized bioluminescence resonance energy transfer (BRET) to decipher the impacts of triphenyl phosphate binding on subunit dimerization along with recruitment of the co-activator SRC1 to the receptor complex. Finally, we evaluated the ability of triphenyl phosphate to stimulate pre-adipocyte differentiation to adipocytes at levels that impacted the PPAR signaling network. Results revealed complex interactions of triphenyl phosphate on the PPAR signaling network which could be used to infer outcome of triphenyl phosphate exposure on lipid/glucose metabolism and other physiological processes.

Materials and Methods

Plasmids and Chemicals

The plasmids containing the human gal4-RXRα fusion construct (pBIND-gal4-hRXRα(DEF)) and the pG5-luc reporter gene under the control of the gal4 response element were previously described [18]. The pcDNA-RLuc2 plasmid was a gift from Dr. Sanjiv

Gambhir (Stanford University, Stanford, California). Plasmids containing human PPARα (pcDNA-hPPARα (ORF)) and PPARγ (pcDNA-hPPARγ (ORF) were generously provided by Dr. Jeffrey Peters (Pennsylvania State University, University Park, PA). pcDNA3.1(-) and pRL-CMV plasmids were provided by Dr. Seth Kullman (North Carolina State University, Raleigh, NC). Both pEBFP2-nuc and pBAD-mAmetrine1.1 were purchased from Addgene (www.addgene.org; Addgene plasmids 14893 and 18084). 9-*cis* retinoic acid, clofibrate, rosiglitazone, oleic acid, insulin, diphenyl phosphate and triphenyl phosphate were obtained from Sigma-Aldrich (www.sigmaaldrich.com).

RXRα-Rluc2 Construct

pBIND-gal4-hRXRα(DEF) was used as the source of RXRα fused to the gal4 DNA binding domain for use in transcription reporter gene assays as we have described previously [18]. This plasmid also was used as the source of RXRα for the preparation of fusions to *Renilla* luciferase 2 (Rluc2) for BRET assays. Rluc2 served as the photon source (emission: 410 nm) for the detection of fluorescent protein-fused PPARα, PPARγ, or SRC1 during BRET assays. Amplified gal4-hRXRα(DEF) fragments were digested with Nhe I and cloned into the pcDNA-RLuc2 plasmid. This plasmid contains *Renilla* luciferase (RLuc) with 2 mutations at C124A and M185V (RLuc2)[19]. A 21 base pair linker was added between gal4-RXRα(DEF) and RLuc2 to facilitate independent flexibility of the fused proteins. Antarctic Phosphatase (New England Biolabs, www.neb.com) was used to catalyze the removal of 5´ phosphate from the pcDNA-RLuc2 plasmid to decrease the possibility of

plasmid self-ligation. The chimeric construct was designated as pcDNA-gal4-hRXRα(DEF)-RLuc2. The final construct was verified by sequencing.

PPARα-EBFP2 and PPARγ-EBFP2 Constructs

PPAR was fused to the fluorophore Enhanced Blue Fluorescent Protein 2 (EBFP2; excitation: 410 nm, emission: 475 nm) to assess dimerization with RXRα-Rluc2 using BRET. PCR fragments of the PPARα and PPARγ open reading frame (ORF) without a stop codon were amplified from the parent plasmid using primers harboring ApaI/BamHI or NheI/XhoI restriction enzyme sites respectively, and subcloned into the pcDNA3.1(-) plasmid. EBFP2 was amplified out of its parent plasmid (pEBFP2-nuc) with a stop codon and a 30 base-pair linker at its 5' end. The EBFP2 was fused to the 3' end of PPARα or PPARγ at a BamHI or XhoI restriction enzyme fusion site, respectively. These constructs were named pcDNA-hPPARα-EBFP2 and pcDNA-hPPARγ-EBFP2. Linkers were placed between the PPAR and EBFP2 sequences to provide independent flexibility of the fused proteins. Final constructs were verified by sequencing. Preliminary experiments revealed that the fusion of EBFP2 to the 3' end of the PPARs provided the optimum BRET signal.

SRC1-mAmetrine Construct

The full frame of SRC1 isoform E used in this study was constructed from the 5' region of SRC1 derived from the pSG5-SRC1A-ORF plasmid (provided by Dr. Seth Kullman, North Carolina State University, Raleigh, NC) and the 3' portion of SRC1E (representing amino acids 381-1399) derived from pSG5-SRC1E (S. Kullman). Splice

variations at the 3' end of these mRNAs have been shown to render SRC1A much less effective than SRC1E as a co-activator [20,21]. Therefore, the 3' end of the SRC1A open reading frame was replaced with that derived from SRC1E. The SRC1E ORF was created by fusion PCR. The 5' portion of SRC1A was amplified using the primers: forward: 5'-CGTGCTGGTTATTGTGCTGT-3'; reverse : 5'-CTTCCGGGTGAGCATCCGAAACT TCCT-3'. The 3' portion of SRC1E was amplified using the primers: forward: 5'-AAGTTTCGG ATGCTCACCCGGAAGTCA-3'; reverse: 5'-ATTGATGAGTTTGGACAAACCAC-3'. A twenty four base pair overlap was used to conjoin the two PCR products. The resulting final PCR product was purified and amplified using the primers, forward: 5'-ATGAGTGGCCTTGGGGACAGTTC-3' and reverse: 5'-CTAGTCTGTAGTCACCACAGAGAAGAACTC-3' primers at 60.5˚C annealing temperature using the Advantage HF 2 PCR kit (Clontech) to give a 4kb PCR product. Restriction sites ApaI/AflII were added to the final PCR product for cloning by PCR using the 4kb product as template with the forward primer: 5'-TACTATGGGCCCACCATGAGTGGCCTTGGGGACAGTTC-3' and reverse primer: 5'-TACTATCTTAAGCTAGTCTGTAGTCACCACAGAG-3'. The amplified SRC1E ORF was subcloned into ApaI/AflII sites of pcDNA3.1(-) plasmid and named as pcDNA3.1-hSRC1E.

SRC1E was fused to the fluorescent protein mAmetrine (excitation: 410 nm, emission: 535 nm) to assess recruitment of SRC1 to the RXRα:PPAR dimers using BRET. The fusion construct of SRC1 and mAmetrine was created as described for the PPARs and EBFP2. SRC1 ORF fragments were amplified by PCR from the pcDNA3.1-hSRC1E plasmid

using primers with KpnI/AflII enzyme sites and then subcloned into the pcDNA3.1(-) plasmid. The mAmetrine PCR fragment without a stop codon but with a 30 base pair linker was ligated in-frame to the XhoI/KpnI sites at the 5' end of SRC1 to generate pcDNA-mAmetrine-SRC1. The final construct was verified by sequencing. Preliminary experiments revealed that the fusion of mAmetrine to the 5' end of SRC1 provided the optimum BRET signal.

PPARα -gal4 and PPARγ-gal4 Constructs

The human PPARα and PPARγ ligand binding domains with a stop codon was amplified from pcDNA-PPARα (ORF) or pcDNA-PPARγ (ORF) using the primers harboring SalI and KpnI restriction enzymes sites. Digested PCR product was then inserted at the 3' end of the gal4 DNA binding domain in the pBIND plasmid by SalI/KpnI restriction sites. The constructs were named pBIND-gal4-hPPARα and named pBIND-gal4-hPPARγ. The final construct was verified by sequencing.

Reporter Gene Transcription Assays

Reporter gene assays were used to evaluate the ability of triphenyl phosphate to modulate the PPAR signaling network. HepG2 cells (ATCC® ,www.ATCC.org) cultured in minimum essential medium (MEM) supplemented with 10% fetal bovine serum (FBS), were plated at a density of 25,000 cells per well in 96-well plates. The next day, 25 ng of the relevant plasmids containing the fusion constructs were co-transfected with 125 ng of pG5-luc, 6 ng of pRL-CMV, and 25 ng of pcDNA-mAmetrine-SRC1 using TransIT-LT1(Mirus,

www.mirusbio.com) reagent following the manufacturer's protocol. When assessing heterodimer activities, the transfected plasmids were pBIND-gal4-RXRα(DEF) along with pcDNA-PPARα-EBFP2 or pcDNA-PPARγ-EBFP2. When assessing reporter gene activation by individual receptor subunits, the plasmids transfected were either pBIND-gal4-hRXRα(DEF), pBIND-gal4-hPPARα, or pBIND-gal4-hPPARγ. Empty plasmid was transfected to keep the amount of plasmid transfected into the cells constant. The next day, the media in plates was replaced with serum-free media containing triphenyl phosphate or other ligands (i.e. positive controls) at the desired concentrations. DMSO was used as a solvent carrier for all ligands and kept constant among all treatments and controls (0.1%, v/v). After 24 hours of incubation, firefly and *Renilla* luciferase were measured using Dual-Glo luciferase assay system (Promega, www.promega.com) and a FLUOstar Omega microplate reader (BMG Labtech, www.bmglabtech.com). Firefly luciferase values were normalized to the *Renilla* luciferase values. Positive controls (9-*cis* retinoic acid for RXRα, clofibrate for PPARα, and rosiglitazone for PPARγ) were routinely evaluated to ensure proper assay function.

BRET Assays

Bioluminescence resonance energy transfer (BRET) assays were used to assess ligand-dependent dimerization of the PPAR subunits with RXRα and to assess recruitment of the co-activator SRC1 to the receptor complex. The fusion construct gal4-RXRα(DEF)-Rluc2 served as the photon donor during BRET assays. PPAR subunits (α and γ), fused to

EBFP2, and SRC1 fused to mAmetrine served as the fluorophore during BRET assays (Fig. 1).

BRET assays were performed in HepG2 cells and cultured in MEM supplemented with 10% FBS. Cells (650,000) were plated in each well in 6-well plates. The next day, the plasmids containing the gene constructs were transfected into the cells using TransIT-LT1 (Mirus) following manufacturer's protocol. 230 ng of plasmid containing the photon source and 1,380 ng of the plasmids containing the fluorophores were transfected. Cells were trypsinized after 24 hours and pelleted at 1,500g for 2 minutes. Cells were then suspended in phosphate-buffered saline (PBS) and transferred to 96-well plates where cells were incubated with triphenyl phosphate or other ligands for 20 minutes at 37C. Coelenterazine 400a (DeepBlueC, Biotium, www.biotium.com) in PBS was added at a final concentration of 5.0 μM to each wells which served as the luminescent substrate for the Rluc2. Photon emissions were measured immediately on a FLUOstar Omega microplate reader (BMG Labtech) with 3 filter settings (Rluc2, 410 ± 40nm; EBFP2 filter, 475 ± 15nm; mAmetrine filter, 535 ± 15nm).

Dimerization of RXRα and the PPARs was detected as the BRET ratio by measuring the light emitted by the fluorophore (475 nm) divided by the light emitted by the donor protein (410 nm) with corrections for background fluorescence (using cells that were not transfected with the fusion proteins) and contaminating emissions from the donor into the acceptor's emission wavelength (475nm). This latter correction factor was derived by measuring fluorescence at 475 nm in cells transfected with Rluc2-RXRα alone minus the fluorescence measured with untransfected cells at 475 nm divided by the fluorescence of

Rluc2-RXRα alone at 410 nm minus the fluorescence of untransfected cells at 410 nm. Recruitment of SRC1 was evaluated using this same procedure with BRET ratios determined using the fluorophore emission at 535 nm.

Cytotoxicity and Metabolic Viability

HepG2 cells were trypsinized and plated at a density of 10,000 cells per well in white opaque 96-well plates using MEM supplemented with 10% FBS. The next day, cells were treated with concentrations of triphenyl phosphate in serum free medium for 24 hours at 37C. Triphenyl phosphate was delivered to the wells dissolved in DMSO which was present in all wells, including controls, at a concentration of 0.1% v/v. Cellular toxicity (cell death) was measured using the CellTox™ Green Cytotoxicity Assay (Promega, www.promega.com) following manufacturer's protocol. This assay functions on the premise that living cells cannot take-up a cyanine dye; while, the dye traverses the compromised membrane of dead cells, binds to DNA, and fluoresces at 485 nm excitation/520 nm emission. Fluorescence was measured on a FLUOstar Omega microplate reader (BMG Labtech). Immediately following these assays, cells were evaluated for metabolic viability using the CellTiter-Glo® 2.0 Assay (Promega) following manufacturer's protocol. This assay is designed to measure cellular ATP levels by luminescence. Luminescence was measured on a FLUOstar Omega microplate reader (BMG Labtech).

Pre-adipocyte Differentiation Assays

Mouse 3T3-L1 cells (ATCC) were seeded at a density of 70,000 cells in 35 mm (diameter) petri dishes along with 2.0 ml of high glucose (4.5 g/l) Dulbecco's Modified Eagle Medium (DMEM) with 10% FBS and allowed to reach confluence. Two days after reaching confluence (day 0), cells were treated with either 10 μM triphenyl phosphate, 2.0 μM rosiglitazone (positive control), or 0.10% DMSO (negative control). On days 2 and 4, the media was renewed with the same concentrations of the test materials along with 10 μg/ml insulin (Sigma-Aldrich). On day 6, cells were rinsed twice with PBS, fixed with 3.7% formalin (Sigma-Aldrich) for 60 min at room temperature, and then rinsed twice with PBS. Next, 60% isopropanol (Fischer Scientific, www.fishersci.com) was added to each dish. After 5 min, the isopropanol was removed and cells were stained with freshly diluted Oil Red O solution (3 mg Oil Red O/ml isopropanol, diluted to 3 parts of Oil Red O stock solution to 2 parts deionized water and allowed to remain at room temperature for 10 min prior to use) for 60 min with gentle agitation. Excess stain was then removed with 60% ethanol (Sigma-Aldrich) and cells were rinsed three times with distilled water. Cells were imaged at 10X magnification using an Olympus microscope. Each treatment was replicated three times per experiment. Images presented are representative of the replicates.

Statistics

Significant ($p<0.05$) differences between treatments and controls were evaluated using One Way ANOVA accompanied by Tukey's test. Homogeneity of the variances were confirmed by Levenes's test. All assays were performed with three true replicates.

Results

Modulation of PPARα Signaling

Transcription reporter gene assays performed with the human PPARα:RXRα receptor complex revealed that triphenyl phosphate inhibited receptor signaling in a concentration-dependent manner with significant ($p<0.05$) inhibition occurring at 10 and 30 μM triphenyl phosphate (Fig. 2A). Evaluation of the individual receptor subunits revealed that triphenyl phosphate interacted with both the PPARα subunit and RXRα subunit in an inhibitory manner but with greater inhibitory potency towards PPARα (Figs, 2B, C).

The PPARα:RXRα gal reporter system used elicits a low level of constitutive receptor activation. Since no activating ligand was added to these assays, the inhibition caused by triphenyl phosphate reflected the loss of this constitutive activity. Therefore, the ability of triphenyl phosphate to inhibit PPARα:RXRα signaling following activation by the natural ligand oleic acid was evaluated. Oleic acid activated the PPARα:RXRα receptor (Fig. 3) and triphenyl phosphate inhibited oleic acid-activated PPARα:RXRα down to a residual level of activity consistent with that observed in the absence of ligand (Fig. 3). Thus, triphenyl phosphate can effectively suppress PPARα:RXRα responses to some activating ligands.

Suppression of the receptor activity suggested that triphenyl phosphate may be toxic to the HepG2 cells at these exposure concentrations. Cell toxicity and metabolic viability assays both established that triphenyl phosphate was not toxic to the cells at concentrations that inhibited receptor activation (30 μM; Fig. 4). Thus, triphenyl phosphate specifically suppressed the activation of PPARα:RXRα independent of overt adverse effects on the cells.

PPARα Receptor Assembly

We performed BRET assays with triphenyl phosphate to determine whether the inhibitory activity of this compound may be due to the prevention of subunit dimerization or the dissociation of constitutive dimers. The PPARα positive control ligand, clofibrate, did not stimulate dimerization of the PPARα and RXRα subunits (Fig.5A) nor did it stimulate SRC1 recruitment (Fig. 5D). While, the RXRα positive control ligand, 9-*cis* retinoic acid, stimulated subunit dimerization (Fig. 5B) and the recruitment of SRC1 to the dimer (Fig. 5E). In contrast, triphenyl phosphate caused dissociation of the PPARα:RXRα complex (Fig. 5C); while having no significant impact on the constitutive association of SRC1 with RXRα. Thus, the inhibitory activity of this compound is consistent with its negative effect on receptor dimerization.

Modulation of PPARγ Signaling

In contrast to the inhibitory effects of triphenyl phosphate on PPARα:RXRα signaling activity, this compound exhibited modest activation of the PPARγ:RXRα receptor (Fig. 6A). Evaluation of triphenyl phosphate with the PPARγ subunit established that this compound significantly activates this receptor (Fig. 6B). The dual interaction of triphenyl phosphate with the PPARγ subunit (activation, Fig. 6B) and the RXRα subunit (inhibition, Fig. 2C) appears to result in the net modest activation of the PPARγ:RXRα receptor complex (Fig. 6A).

PPARγ Receptor Assembly.

The PPARγ positive control ligand rosiglitazone had no effect on PPARγ receptor complex assembly (Figs. 7A,D) while the RXRα positive control ligand 9-*cis* retinoic acid stimulated PPARγ receptor complex assembly (Figs. 7B,E). Triphenyl phosphate had no effect on PPARγ receptor complex assembly (Figs. 7C,F). These results indicate that triphenyl phosphate likely activates constitutively present PPARγ:RXRα dimers.

Reporter Gene Activation by Diphenylphosphate

Diphenyl phosphate is the major hepatic metabolite of triphenyl phosphate. Therefore, the ability of this compound to modulate the PPAR signaling network was evaluated. Diphenyl phosphate had no effect on the activity of PPARα:RXRα or PPARγ:RXRα (Fig. 8).

Pre-adipocyte Differentiation

Results thus far would lead to the expectation of decreased lipid utilization and increased lipid storage by triphenyl phosphate. Indeed, exposure of mouse 3T3-L1 pre-adipocytes to 10 μM triphenyl phosphate or 2.0 μM rosiglitazone (positive control) resulted in increased differentiation of the cells from an elongated fibroblast-like appearance to globular, lipid-laden adipocytes (Fig. 9).

Discussion

The triphenyl phosphate-containing flame retardant Firemaster[r] has been implicated in metabolic dysfunction in a rodent model resulting in weight gain [14]. Results of the present study demonstrated that triphenyl phosphate interacts with several transcription factors that regulate lipid and glucose storage and metabolism. Further, the effects of this compound are differential, resulting in the activation of some regulatory processes and inhibition of others.

Notably, triphenyl phosphate is an inhibitor of RXRα regulatory activity. RXRα serves as a dimerization partner to several nuclear receptors that are involved in energy homeostasis; and, ligand-binding to the RXRα results in the activation of these dimeric nuclear receptors [16]. Responsive partners include the farnesoid X receptor (FXR), constitutive androstane receptor (CAR), the pregnane X receptor (PXR), the liver X receptor (LXR), and the focus of the present study, the peroxisome proliferator activated receptor (PPAR) [16]. Adverse outcomes from the inhibition of RXRα might include elevated bile acid levels [22] resulting in colon cancer [23] (FXR inhibition), increased cholesterol accumulation and associated risk of cardiovascular disease [24] (LXR inhibition), lipid accumulation and insulin resistance [25,26] (CAR, PPAR inhibition). Interestingly, these conditions are all associated with metabolic syndrome [17,27].

The effects of triphenyl phosphate on PPAR signaling are compounded by its ability to interact with both the RXRα subunit and the PPAR subunits. This dual activity is reminiscent of the activity of the obesogenic organotins [28,29]. However, unlike the organotins, which activate RXRα, PPARα, and PPARγ subunits, triphenyl phosphate only

activated the PPARγ subunit and inhibited the RXRα and PPARα subunits [28,30,31]. The net effect of these multiple interactions would be an enhancement of PPARγ-regulated processes and a suppression of PPARα regulated processes.

Evidence indicates that triphenyl phosphate-bound RXRα attenuates activation of the PPARγ subunit by this compound. In the present study, the PPARγ subunit was activated approximately 7-fold by triphenyl phosphate, but when associated with RXRα, activation was only ~2-fold. Belcher et al. observed a 20-fold activation of PPARγ using a commercial reporter assay that apparently does not include RXRα [9]. However, Pillai et al. observed a ~2-fold activation using a system that utilized both PPARγ and RXRα [11]. Taken together, results from these studies suggest that activity of the PPARγ:RXRα heterodimer is dominated by the compound's effects on the PPARγ subunit, while ligand interaction with the RXRα subunit can modify this activity.

Belcher et al. evaluated the toxicity of triphenyl phosphate in Chinese hamster ovary cells and D283 Med cells [9]. They observed evidence of toxicity, after 24-hours exposure, at concentrations as low as 3.0 μM with an IC50 in Hamster ovary cells of 37 μM. Cellular toxicity is normally evident in our BRET assays as a reduction in the signal associated with the Rluc2 fused to RXRα. These assays provided no evidence of toxicity to the HepG2 cells although exposure durations in this assay were short (20 min). Therefore, we performed two assays for cellular toxicity following exposure of HepG2 cells to triphenyl phosphate for 24 hours. These assays utilized the retention of membrane integrity and metabolic activity as indicators to cellular toxicity. These assays confirmed that, at concentrations as high as 30 μM, triphenyl phosphate elicited no discernible toxicity to the cells. Our results are

consistent with those of Pillai et al. who observed no toxicity to BMS2 cells following 24-hours exposure to triphenyl phosphate concentrations as high as 40 μM [11]. Thus, the modulation of PPAR signaling observed in our experiments was not an artifact of toxicity.

BRET analyses revealed that triphenyl phosphate stimulated the dissociation of the PPARα:RXRα dimer while having no effect on the dimerization on PPARγ and RXRα. Accordingly, this dissociative effect of triphenyl phosphate is not likely due to its demonstrated interaction with the RXRα subunit, but rather due to its interaction with the PPARα subunit. This inhibitory effect of triphenyl phosphate on PPARα:RXRα dimerization is not likely to be fully responsible for the observed inhibition of PPARα:RXRα activity since the compound also inhibited activity associated with the PPARα monomer. Thus, the binding of triphenyl phosphate to the PPARα subunit inhibited the ability of this protein to transactivate gene expression and crippled its ability to dimerize with its RXRα partner.

PPARα and PPARγ function coordinately in the allocation of fuel for the production of energy. PPARγ regulates the expression of genes that function in carbohydrate oxidation in the liver and other tissues while directing lipids towards their storage in adipocytes [32]. PPARα suppresses the cellular utilization of glucose as an energy source, and stimulates the liberation of stored lipids along with their oxidation [32,33]. Thus the simultaneous activation of PPARγ and the inhibition of PPARα would favor the utilization of glucose as an energy source while enhancing the storage and retention of lipids. Increased adiposity is a hallmark of both PPARα deficiency and PPARγ activation [34, 35]. We demonstrated in the

present study that triphenyl phosphate does indeed stimulate adipocyte differentiation and lipid storage.

Triphenyl phosphate undergoes hepatic hydrolysis to diphenyl phosphate [36]. Results from the present study indicated that this compound poses low risk of hazard as related to the modulation of the PPAR signaling network. Despite its metabolism, Jonsson, Dyremark, and Nilsson reported human plasma triphenyl phosphate concentrations ranged from 0.12 to 0.14 μg/g [37]. These analyses reflected levels in plasma samples from only three individuals and we are not aware of any other reports of triphenyl phosphate concentrations in human plasma or blood. Based upon these analyses, human plasma is estimated to contain approximately 0.4 μM triphenyl phosphate. The lowest triphenyl phosphate concentration that inhibited the PPARα signaling pathway and stimulated the PPARγ signaling pathway was 10 μM. Since we are presently unaware of the distribution of plasma triphenyl phosphate concentrations present in the human population and where 0.4 μM fits within this distribution, efforts to minimize exposure to this compound seem prudent.

Conclusion

The organophosphate flame retardant, triphenyl phosphate, both inhibits PPARα signaling and activates PPARγ signaling. This dual effect may be responsible for the observation that exposure to this compound causes weight gain in rodents.

References

[1] I. van der Veen and J. de Boer, Phosphorus flame retardants: Properties, production, environmental occurrence, toxicity and analysis, *Chemosphere*, 88, 1119, 2012.

[2] H.M. Stapleton, S. Sharma, G. Getzinger, P.L. Ferguson, M. Gabriel, T.F. Webster and A. Blum, Novel and high volume use flame retardants in US couches reflective of the 2005 pentaBDE phase out, *Environ. Sci. Technol.*, 46, 13432, 2012.

[3] S. Tajima, A. Araki, T. Dawai, T. Tsuboi, Y. Ait Bamai, E. Oshioka, A. Kanazawa, S. Cong and R. Kishi, Detection and intake assessment of organophosphate flame retardants in house dust in Japanese dwellings, *Sci. Total Environ.*, 478, 190, 2013.

[4] H.M. Stapleton, S. Klosterhaus, S. Eagle, J. Fuh, J.D. Meeker, A. Blum and T.F. Webster, Detection of organophosphate flame retardants in furniture foam and U.S. house dust, *Environ. Sci. Technol.*, 43, 7490, 2009.

[5] A. Salamova, Y. Ma, M. Venier and R.A. Hites, High levels of organophosphate flame retardants in the Great Lakes atmosphere, *Environ. Sci. Technol.*, 1, 8, 2014.

[6] A.M. Sundkvist, U. Olofsson and P. Haglund, Organophosporus flame retardants and plasticizers in marine and fresh water biota and in human milk, *J. Environ. Monit.*, 12, 943, 2010.

[7] IllinoisEPA, Report on Alternatives to the Flame Retardant DecaBDE: Evaluation of Toxicity, Availability, Affordability, and Fire Safety Issues. A Report to the Governor and the General Assembly. http://www.epa.state.il.us/reports/decabde-study/decabde-alternatives.pdf, 2007.

[8] H. Kojima, S. Takeuchi, T. Itoh, M. Iida, S. Kobayashi and T. Yoshida, In vitro endocrine disruption potential of organophosphate flame retardants via human nuclear receptors, *Toxicology*, 314, 76, 2013.

[9] S.M. Belcher, C.J. Cookman, H.B. Patisaul and H.M. Stapleton, In vitro assessment of human nuclear hormone receptor activity and cytotoxicity of the flame retardant mixture FM 550 and its triarylphosphate and brominated components, *Toxicology Letters*, 228, 93, 2014.

[10] X. Lui, K. Ji and K. Choi, Endocrine disruption potentials of organophosphate flame retardants and related mechanisms in H295R and MVLN cell lines and in zebrafish, *Aquatic Tox.*, 114-115, 173, 2012.

[11] H.K. Pillai, M. Fang, D. Beglov, D. Kozakov, S. Vajda, H.M. Stapleton, T.F. Webster and J.J. Schlezinger, Ligand Binding and activation of PPARγ by Firemaster^{R} 550: Effects on Adipogenesis and Osteogenesis In Vitro
Environ. Health Perspect., 122, 1225, 2014.

[12] J. Auwerx, PPARgamma, the ultimate thrifty gene, *Diabetologia*, 42, 1033, 1999.

[13] C. Christodoulides and A. Vidal-Puig, PPARs and adipocyte function, *Mol. Cell. Endocrin.*, 4, 61, 2010.

[14] H.B. Patisaul, S.C. Roberts, N. Mabrey, K.A. McCaffrey, R.B. Gear, J. Braun, S.M. Belcher and H.M. Stapleton, Accumulation and endocrine disrupting effects of the flame retardant mixture Firemaster^{R} 550 in rats: an exploratory assessment, *J. Biochem. Mol. Toxicol.*, 27, 124, 2013.

[15] Y.X. Wang, PPARs: diverse regulators in energy metabolism and metabolic diseases, *Cell Res.*, 20, 124, 2010.

[16] A. Chawla, J.J. Repa, R.M. Evans and D.J. Mangelsdorf, Nuclear receptors and lipid physiology: opening the X-files, *Science*, 294, 1866, 2001.

[17] A.I. Shulman and D.J. Mangelsdorf, Retinoid X receptor heterodimers in the metabolic syndrome, *New England J. Med.*, 353, 604, 2005.

[18] Y.H. Wang and G.A. LeBlanc, Interactions of methyl farnesoate and related compounds with a crustacean retinoid X receptor, *Mol. Cell. Endocrin.*, 309, 109, 2009.

[19] M. Kocan, H.B. See, R.M. Seeber, K.A. Eidne and K.D.G. Pfleger, Demonstration of improvements to the bioluminescence resonance energy transfer (BRET) technology for the monitoring of G protein-coupled receptors in live cells, *J. Biomol. Screening*, 13(888), DOI: 10.1177/1087057108324032, 2008.

[20] O.C. Maijer, E. Kalkhoven, S. van der Laan, P.J. Steenbergen, S.H. Houtman, T.F. Dijkmans, D. Pearce and E.R. de Kloet, Steroid receptor coactivator-1 splice variants differentially affect corticosteroid receptor signaling, *Endocrinology*, 146, 1438, 2005.

[21] E. Kalkhoven, J.E. Valentine, D.M. Heery and M.G. Parker, Isoforms of steroid receptor co-activator 1 differ in their ability to potentiate transcription by the oestogen receptor, *EMBO J.*, 17, 232, 1998.

[22] D.W. Russell, Nuclear orphan receptors control cholesterol catabolism, *Cell*, 97, 539, 1999.

[23] M.R.M. Rengasamy, A. Thomas, M. Roth, Z. Sheng, N. Eserly, D. Pinson, X. Gao, Y. Xhang, V. Ganapathy, F.J. Gonzalez and G.L. Guo, Farnesoid X receptor deficiency in mice leads to increased intestinal epithelial cell proliferation and tumor development, *Journ. Pharm. Exp. Ther.*, 328, 469, 2009.

[24] Y. Zhang, S.R. Breevoort, J. Angdisenm, M. Fu, D.R. Schmidt, S.R. Holmstromn, S.A. Kliewer, D.J. Mangelsdorf and I.G. Schulman, Liver LXRα expression is crucial for whole body cholesterol homeostasis and reverse cholesterol transport in mice, *J. Clin. Invest.*, 122, 1688, 2012.

[25] J. Gao, J. He, Y. Shai, T. Wada and W. Xie, The constitutive androstane receptor is an anti-obesity nuclear receptor that improves insulin sensitivity, *J. Biol. Chem.*, 284, 25984, 2009.

[26] S. Kersten, J. Seydoux, J.M. Peters, F. Gonzalez, B. Desvergne and W. Wahli, Peroxisome proliferator-activated receptor α mediates the adaptive response to fasting, *J. Clin. Invest.*, 103, 1489, 1999.

[27] E. Giovannucci, Metabolic syndrome, hyperinsulinemia, and colon cancer: a review, *Am. J. Clin. Nutr.*, 86(suppl), 836S, 2007.

[28] F. Grun, H. Watanabe, Z. Zamanian, L. Maeda, K. Arima, R. Cubacha, D.M. Gardiner, J. Kanno, T. Iguchi and B. Blumberg, Endocrine-disrupting organotin compounds are potent inducers of adipogenesis in vertebrates, *Mol. Endocrinol.*, 20, 2141, 2006.

[29] J. Brtko and Z. Dvorak, Triorganotin compounds - ligands for "rexinoid' inducible transcription factors: biological effects, *Toxicol. Lett.*, 234, 50, 2015.

[30] T. Kanayama, N. Kobayashi and S. Mamiya, Organotin compounds promote adipocyte differentiation as agonists of the peroxisome proliferator-activated receptor/retinoid X receptor pathway, *Mol. Pharmacol.*, 67, 766, 2005.

[31] A. le Maire, M. Grimaldi, D. Roecklin, S. Dagnino, V. Vivat-Hannah, P. Balaguer and W. Bourguet, Activation of RXR-PPAR heterodimers by organotin environmental endocrine disruptors, *EMBO reports*, 10, 367, 2009.

[32] P. Ferre, The biology of peroxisome proliferator-activated receptors, *Diabetes*, 3(Suppl. 1), S43, 2004.

[33] J. Berger and D.E. Moller, The mechanisms of action of PPARs, *Ann. Rev. Med.*, 53, 409, 2002.

[34] M. Guerre-Millo, C. Rouault, P. Poulain, J. Andre, V. Poitout, J.M. Peters, F.J. Gonzalez, J.-C. Fruchart, G. Reach and B. Staels, PPAR-α-null mice are protected from high-fat diet-induced insulin resistance, *Diabetes*, 50, 2809, 2001.

[35] W.W. Harrington, C.S. Britt, J.G. Wilson, M.O. Milliken, J.G. Binz, D.C. Lobe, W.R. Oliver, M.C. Lewis and D.M. Ignar, The effect of PPARalpha, PPARdelta, PPARgamma, and PPARpan agonists on body weight, body mass, and serum lipid profiles in diet-induced obese AKR/J mice, *PPAR Res.*, http://dx.doi.org/10.1155/2007/97125, 2007.

[36] OECD-SIDS, Triphenyl Phosphate, *http://www.inchem.org/documents/sids/sids/115866.pdf*, UNEP Publications 2002.

[37] O.B. Jonsson, E. Dyremark and U.L. Nilsson, Development of a microporous membrane liquid-liquid extractor for organophosphate esters in human blood plasma:

identification of triphenyl phosphate and octyl diphenyl phosphate in donor plasma., *J. Chromat. B*, 755, 157, 2001.

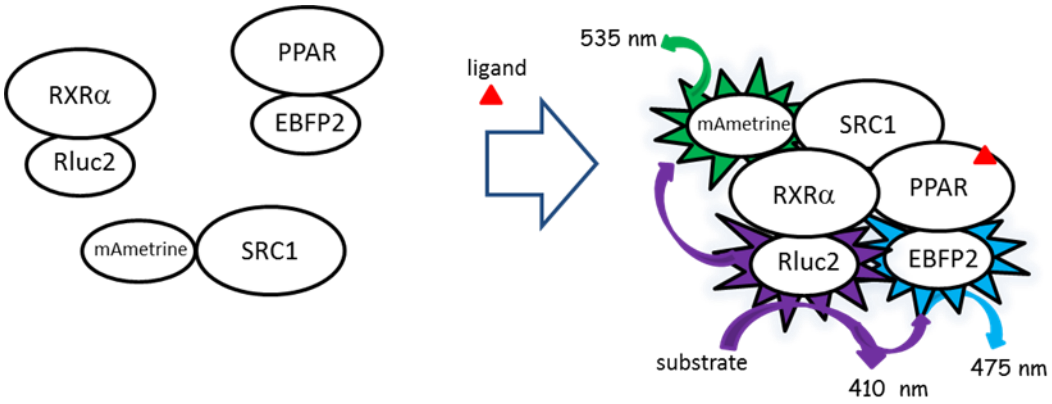

Figure 1 Diagrammatic representation of the BRET assay. RXRα was fused to the photon donor *Renilla* luciferase 2 (Rluc2, emission 410 nm). PPAR (α or γ) was fused to Enhanced Blue Fluorescent Protein 2 (EBFP2, emission 475 nm). SRC1 was fused to the fluorescent protein mAmetrine (emission 535 nm). Upon binding to RXRα-Rluc2 and the addition of substrate to the Rluc2, resulting fluorescence of the EBFP2 and mAmetrine was measured.

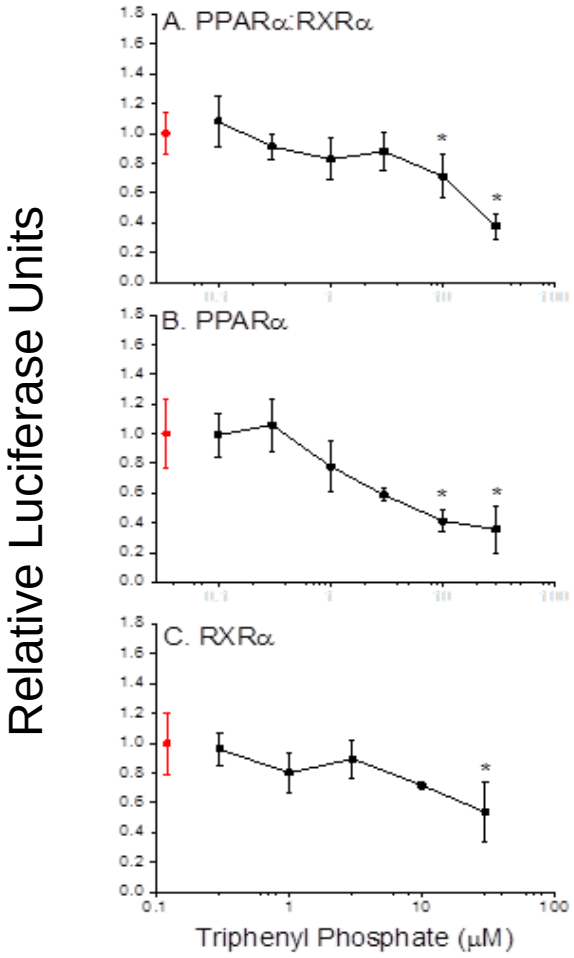

Figure 2. Gal4-driven luciferase reporter gene activity following treatment of cells with triphenyl phosphate. A. Activity associated with the PPARα:RXRα-Gal4 heterodimer. B. Activity associated with the PPARα-Gal4 subunit. C. Activity associated with the RXRα-Gal4 subunit. Control (0 μM triphenyl phosphate) values are presented in red. Data are presented as the mean and standard deviation (n=3) and are normalized to the control values. An asterisk denotes a significant ($p<0.05$) difference from the control.

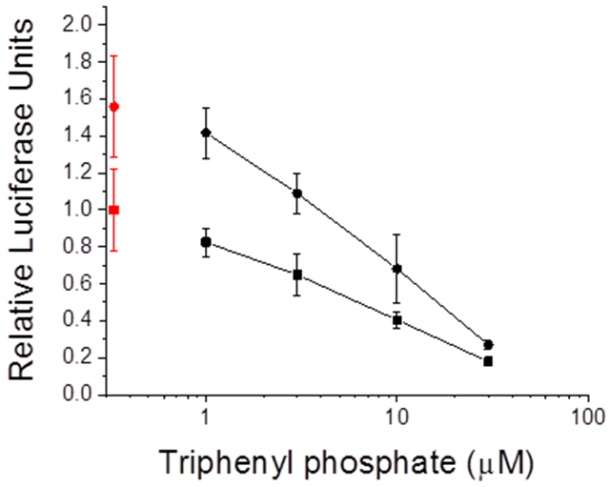

Figure 3. PPARα:RXRα-Gal4 driven reporter gene activity in cells treated with triphenyl phosphate alone (circles) or in combination with the PPARα ligand oleic acid (30 μM) (squares). Control (0 μM triphenyl phosphate) values are presented in red. Data are presented as the mean and standard deviation (n=3).

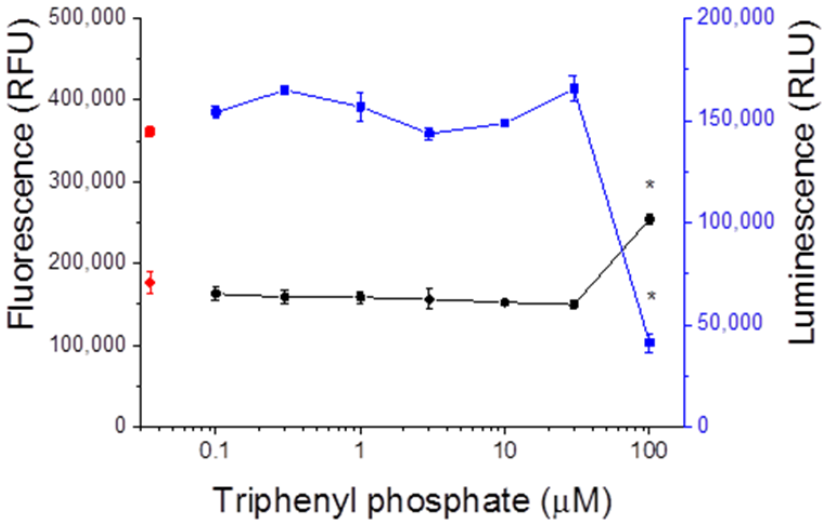

Figure 4. Viability of HepG2 cells following exposure to triphenyl phosphate. Cell membrane integrity was measured by the accumulation of a DNA-binding fluorescent substrate (black data points). Cellular metabolic activity was measured by the cellular conversion of a substrate to a luminescent product (blue data points). Each data point represents the means and standard deviation of three replicate treatments. An asterisk denotes a significant ($p \leq 0.05$) difference from the control (red data points).

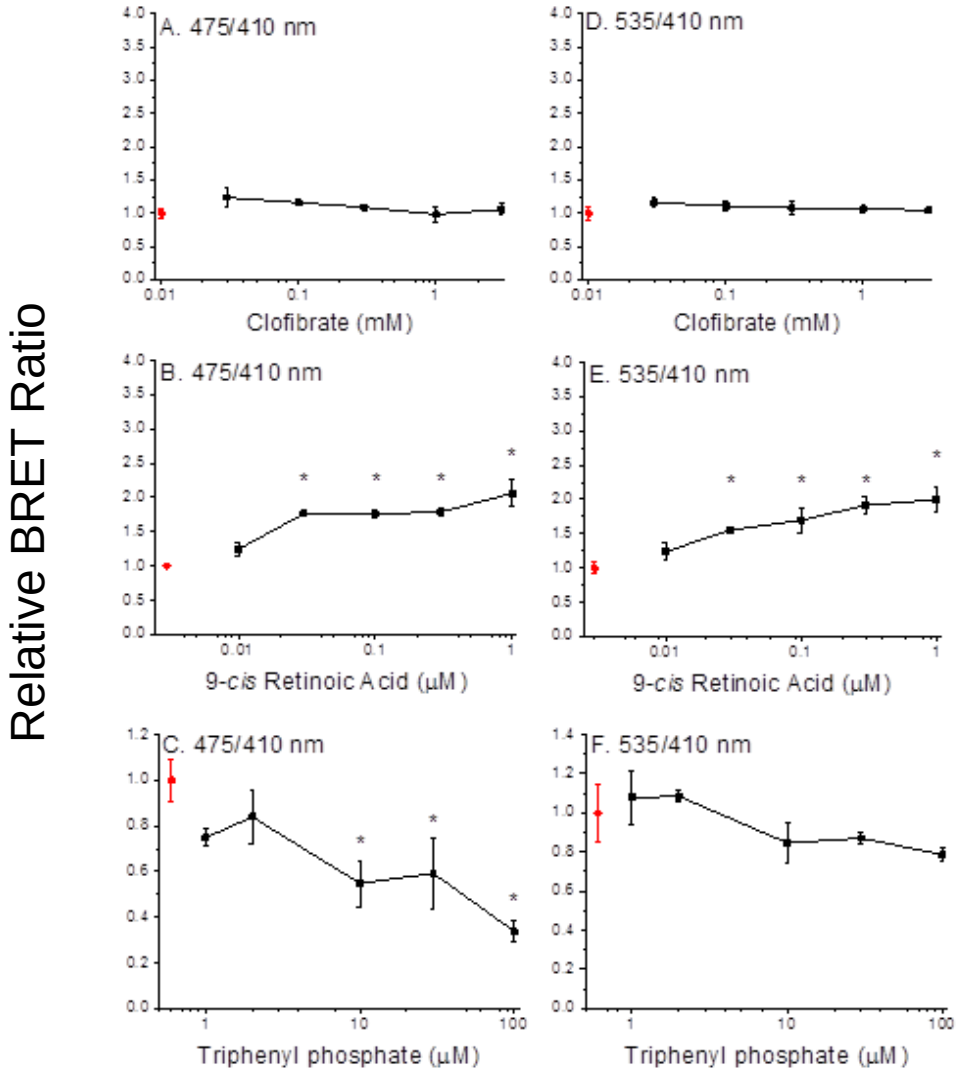

Figure 5. Dimerization of PPARα and RXRα (A-C) and recruitment of SRC1 (D-F) with increasing concentrations of clofibrate (A, D), 9-*cis* retinoic acid (B,E) and triphenyl phosphate (C,F). Data points and error bars represent the mean and standard deviation, respectively (n=3) and are normalized to the control BRET ratio. Control values (no ligand) are presented in red. An asterisk denotes a significant difference from the control value ($p \leq 0.05$).

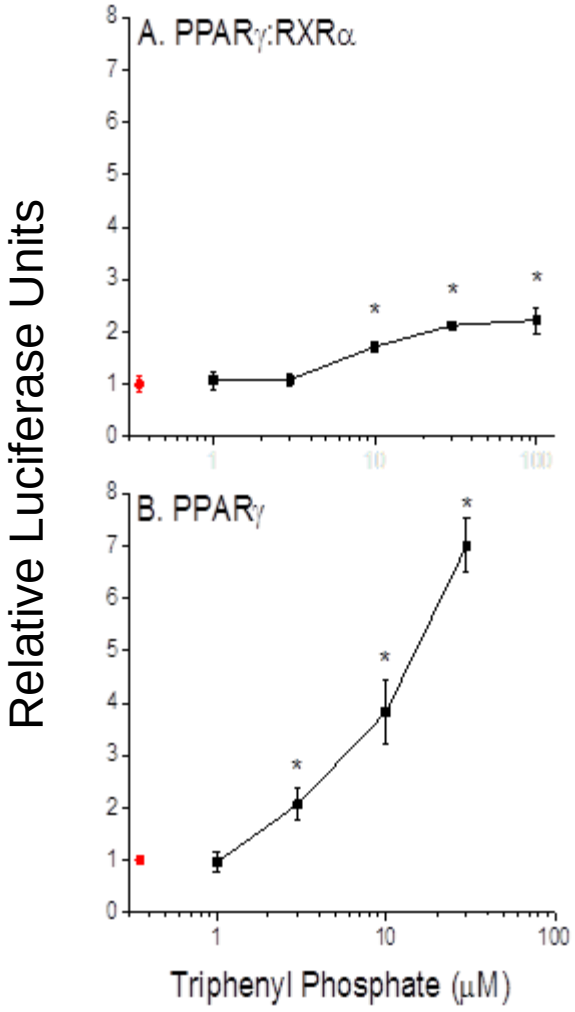

Figure 6. Gal4-driven luciferase reporter gene activity following treatment of cells with triphenyl phosphate. A. Activity associated with the PPARγ:RXRα-Gal4 heterodimer. B. Activity associated with the PPARγ-Gal4 subunit. Control (0 μM triphenyl phosphate) values are presented in red. Data are presented as the mean and standard deviation (n=3) and are normalized to the control values. An asterisk denotes a significant ($p<0.05$) difference from the control.

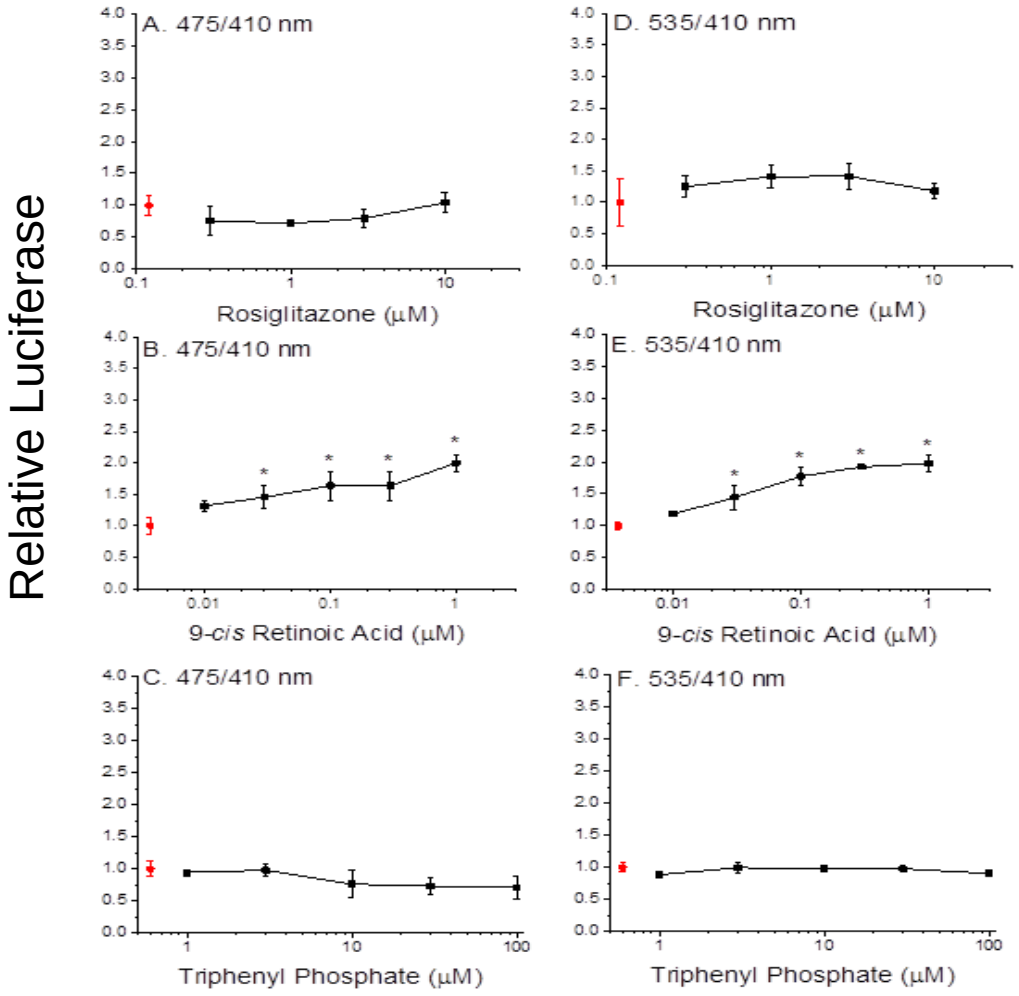

Figure 7. Dimerization of PPARγ and RXRα (A-C) and recruitment of SRC1 (D-F) with increasing concentrations of rosiglitazone (A, D), 9-*cis* retinoic acid (B,E) and triphenyl phosphate (C,F). Data points and error bars represent the mean and standard deviation, respectively (n=3) and are normalized to the control BRET ratio. Control values (no ligand) are presented in red. An asterisk denotes a significant difference from the control value ($p \leq 0.05$).

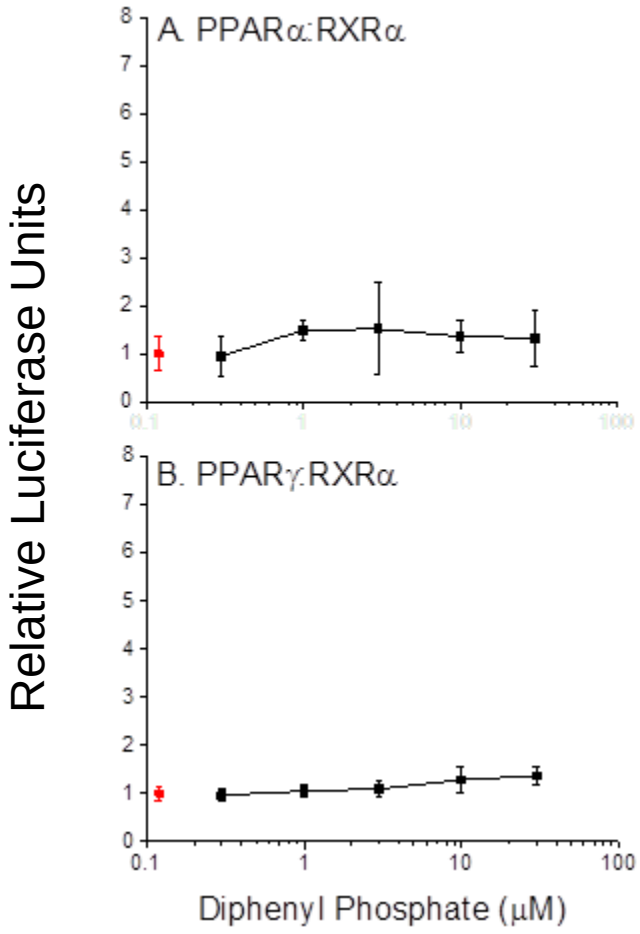

Figure 8. Gal4-driven luciferase reporter gene activity following treatment of cells with diphenyl phosphate. A. Activity associated with the PPARα:RXRα-Gal4 heterodimer. B. Activity associated with the PPARγ:RXRα-Gal4 heterodimer. Control (0 μM diphenyl phosphate) values are presented in red. Data are presented as the mean and standard deviation (n=3) and are normalized to the control values.

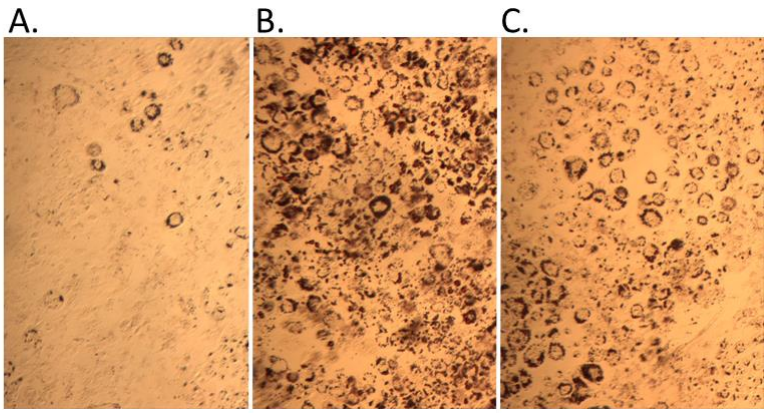

Fig. 9. Pre-adipocyte differentiation and lipid accumulation with triphenyl phosphate treatment. A. control, B. 2 μM rosiglitazone (positive control), C. 10 μM triphenyl phosphate.

CHAPTER TWO: LIGAND-DEPENDENT RECEPTOR ASSEMBLY AS AN ENDPOINT FOR THE HIGH-THROUGHPUT SCREENING OF CHEMICALS FOR ENDOCRINE ACTIVITY.

Charisse N. Holmes. Gwijun Kwon, Ying H. Wang, Lihui An[a], and Gerald A. LeBlanc[b]
Toxicology Program, Department of Biological Sciences, North Carolina State University, Raleigh NC 27605.

[a]Current address: State Key Laboratory of Environmental Criteria and Risk Assessment, Chinese Research Academy of Environment Sciences, Beijing 100012, China

Abstract

Reporter gene assays are commonly used to screen chemicals for interaction with nuclear receptors. We hypothesized that endpoints may exist earlier in the adverse outcome pathway that may preserve the advantages of reporter gene technology while reducing the time investment. We used bioluminescence resonance energy transfer (BRET) technology to investigate the utility of ligand-dependent receptor assembly as an endpoint for use in the screening of chemicals for interaction with the PPARα:RXRα:SRC1 nuclear receptor complex. The human retinoid X receptor α (RXRα) was fused to the *Renilla* luciferase 2 protein to serve as the photon donor. While, human PPARα and human co-activator SRC1 were fused to photon acceptor proteins that fluoresced upon excitation by the luciferase emission. Reporter gene transcription assays also were performed to evaluate ligand interactions with individual receptor subunits and the multimeric complex. Using known RXRα and PPARα agonists, we revealed that RXRα agonists stimulated receptor assembly and activation of the assembled transcription factors. While, PPARα agonists activated existing receptor complexes. We next evaluated a suite of flame-retarding organophosphate compounds. Three compounds (2-ethylhexyl diphenyl phosphate, tri-*o*-tolylphosphate, tri-*n*-butyl phosphate) inhibited activity of the PPARα receptor complex by interacting with both the PPARα and the RXRα subunits in a manner that caused dissociation of the receptor complex. Results demonstrate that monitoring the assembly of some nuclear receptors has the potential to discern agonist and antagonist activity along with identification of the specific subunit affected by the chemical all in a single assay and in a time conservative manner.

Keywords endocrine disruption, organophophates, endocrine receptor, alternatives to animal testing

Introduction

The publication of the National Research Council's *Toxicity Testing in the 21st Century: A Vision and a Strategy (NRC, 2007)* crystalized the need to advance the science of toxicology by emphasizing the elucidation of molecular targets and pathways that are impacted by chemicals rather than focusing exclusively on the description of apical outcomes associated with chemical exposure. This shift in emphasis would allow for the development and use of high-throughput approaches in toxicological evaluations, would reduce the number of animals used in toxicity testing, would reduce time and cost associated with the toxicological assessment of chemicals, and ultimately, would reduce the backlog of chemicals in use for which toxicological hazard assessments have not been performed.

Cell-based assays are being used with increasing frequency in the hazard characterization process. These assays are often used to screen chemicals for testing prioritization (Dix *et al.*, 2007) , and to identify putative mechanisms of toxicity (Barile, 2013). Cell-based assays will likely gain increasing prominence in the hazard assessment process as methods, applications, and approaches continue to expand (Hofer *et al.*, 2004).

The cell–based assay of choice for assessing the interaction of chemicals with nuclear receptors is the reporter gene assays (McLachlan, 1993). These assays utilize a reporter gene expressed in cells that is transcriptionally activated by a specific nuclear receptor, once bound by a chemical agonist. The product of the reporter gene is a protein that is easily detected and quantified, such as a luciferase or fluorescent protein (Daunert *et al.*, 2000). Batteries of reporter gene assays designed to detect interaction of chemicals with a variety of nuclear receptors are presently in use (Piersma *et al.*, 2013). Reporter gene assays are

proximal to the initiating event along the adverse outcome pathway relatively inexpensive, definitive, and conducive to high-throughput applications (Ankley *et al.*, 2010; Glass, 2013). As such, they serve as important tools for screening chemicals for the potential to elicit toxicity by activating or suppressing the transcription of genes that are regulated by the targeted receptor.

Gene transcription in response to receptor activation is an early event in the adverse outcome pathway but is not necessarily the initiating event. Most nuclear receptors function as homodimers or heterodimers (Glass, 2013). Many precedents exist for the concept that receptor subunit dimerization is ligand-stimulated (Depoix *et al.*, 2001; Kakizawa *et al.*, 1997; Wang *et al.*, 1995). Thus, in many instances, ligand dimerization or dissociation may be an early indicator of activity of a chemical with a nuclear receptor (Shanle and Xu, 2011). This early event in the adverse outcome pathway could provide added value over reporter gene assays as a screening tools as reporter gene assays require transcription/translation to generate sufficient quantity of the reporter protein for detection. This typically requires approximately 24 hours. Dimerization assays would make use of existing nuclear receptor proteins thus the response would occur immediately following treatment with the test chemical, greatly reducing the time requirement for the assay.

Bioluminescence resonance energy transfer (BRET) is a powerful technology for the assessment of protein:protein interactions in living cells (Pfleger *et al.*, 2006; Xu and Powell, 2008). The method involves fusing one protein of interest with a photon donor and fusing a putative dimerization partner protein with a fluorescent protein. Dimerization is measured by the light that is emitted at a defined wavelength when the fluorescent protein is

excited by photons generated from the photon donor-tagged protein. A stable association of the proteins resulting in a distance of less than 10 nm between the proton emitter protein and the photon acceptor protein results in energy transfer which can be measured by the fluorescent output of the photon acceptor protein (Borroto-Escuela *et al.*, 2013). The fundamental difference between BRET and fluorescence resonance energy transfer (FRET) is that the photon source in FRET is a fluorescent protein that is activated by an external light source while the photon source in BRET is a bioluminescent protein that generates photons upon addition of a suitable chemical substrate. BRET has advantages over FRET in that photobleaching and autofluorescence can limit the sensitivity of FRET (Piston and Kremers, 2007). Further, the external light required for FRET can damage some cellular components. We viewed BRET as an ideal technology for the rapid detection of ligand-mediated protein-protein interactions in living cells, in real time.

The overall goal of this study was to test the hypothesis that dimerization assays alone or in combination with reporter gene assays could provide a wealth of mechanistic information regarding the ability of chemicals to disrupt nuclear receptor signaling. We chose to evaluate the human peroxisome proliferator-activated receptor alpha (PPARα) signaling pathway to test this hypothesis. PPARα contributes to regulation of energy production by stimulating processes that contribute to the utilization of glucose as a fuel source (Lefebvre *et al.*, 2006). PPARα dimerizes with the retinoid X receptor alpha (RXRα) along with co-activators including steroid receptor co-activator 1 (SRC1) to form the active transcription factor. We used BRET to evaluate ligand-mediated PPARα:RXRα dimerization and SRC1 recruitment. We use reporter assays to assess the consequence of ligand binding

and to determine which subunit interacted with the test chemicals. Experiments were initially performed with known PPARα and RXRα agonists, then the methods were used to evaluate the interactions of several organophosphate flame retardants with this signaling pathway. The organophosphate flame retardant, triphenyl phosphate, inhibited the PPARα signaling pathway (Chapter One) and we predict that other organophosphate flame retardants will act similarly on this pathway.

Materials and Methods

The plasmids containing the human gal4-RXRα fusion construct (pBIND-gal4-hRXRα (DEF)) and the pG5-luc reporter gene under the control of the gal4 response element were previously described (Wang and LeBlanc, 2009). The pcDNA-RLuc2 plasmid was a gift from Dr. Sanjiv Gambhir (Stanford University, Stanford, California). Plasmid containing human PPARα (pcDNA-hPPARα (ORF)) was generously provided by Dr. Jeffrey Peters (Pennsylvania State University, University Park, PA). pcDNA3.1(-) and pRL-CMV plasmids were provided by Dr. Seth Kullman (North Carolina State University, Raleigh, NC). Both pEBFP2-nuc and pBAD-mAmetrine1.1 were purchased from Addgene (www.addgene.org; Addgene plasmids 14893 and 18084). 9-*cis* retinoic acid, clofibrate, Wy-14,643, 2-ethylhexyl diphenyl phosphate, tri-*n*-butyl phosphate, tris(2-butoxyethyl) phosphate, tris(2-chloroethyl) phosphate, and tris(2-ethylhexyl) phosphate were obtained from Sigma-Aldrich (www.sigmaaldrich.com). LGD1069 (Bexarotene) was purchased from LC Laboratories (www.lclabs.com). Tri-*o*-tolyl phosphate was purchased from Fisher Scientific (www.fishersci.com).

RXRα-Rluc2 construct

pBIND-gal4-hRXRα(DEF) was used as the source of RXRα fused to the gal4 DNA binding domain for use in transcription reporter assays as we have described previously (Wang and LeBlanc, 2009). This plasmid also was used as the source of RXRα for the preparation of fusions to *Renilla* luciferase 2 (Rluc2). Rluc2 served as the photon source (emission: 410 nm) for the detection of fluorescent protein-fused PPARα or SRC1 during BRET assays. Amplified gal4-hRXRα (DEF) fragments were digested with Nhe I and cloned into the pcDNA-RLuc2 plasmid. This plasmid contains *Renilla* luciferase (RLuc) with 2 mutations at C124A and M185V (RLuc2)(Kocan *et al.*, 2008). A 21 base pair linker was added between gal4-RXRα (DEF) and RLuc2 to facilitate independent flexibility of the fused proteins. Antarctic Phosphatase (New England Biolabs, www.neb.com) was used to catalyze the removal of 5´ phosphate from the pcDNA-RLuc2 plasmid to decrease the possibility of plasmid self-ligation. The chimeric construct was designated as pcDNA-gal4-hRXRα (DEF)-RLuc2. The final construct was verified by sequencing.

hPPARα-gal4 construct

The human PPARα ligand binding domain (amino acid 167-469) with a stop codon was amplified from pcDNA-PPARα using the primers harboring SalI and KpnI restriction enzymes sites. Digested PCR product was then inserted at the 3' end of the gal4 DNA binding domain in the pBIND plasmid by SalI/KpnI restriction sites. The construct was named pBIND-gal4-hPPARα. The final construct was verified by sequencing.

PPARα-EBFP2 constructs

PPARα was fused to the fluorescent protein Enhanced Blue Fluorescent Protein 2 (EBFP2; excitation 410 nm, emission: 475 nm) to assess dimerization with RXRα-Rluc2 using BRET. PCR fragments of the PPARα open reading frame (ORF) with and without a stop codon were amplified from a the parent plasmid using primers harboring KpnI/AflII or ApaI/BamHI restriction enzyme sites respectively, and subcloned into the pcDNA3.1(-) plasmid. EBFP2 was amplified out of its parent plasmid (pEBFP2-nuc) without its stop codon but with a 30 base pair linker ending with a KpnI restriction enzyme fusion site. This amplified sequence was fused with the amplified PPARα sequence via a BamHI/KpnI site at the 5' end of PPARα. This construct was named pcDNA-EBFP2-hPPARα. Amplified EBFP2, with stop codon, but containing the 30 base pair linker at its 5' end was prepared and fused to the BamHI/KpnI site at 3' end of PPARα and named pcDNA-hPPARα-EBFP2. Linkers were placed between the PPARα and EBFP2 sequences to provide independent flexibility of the fused proteins. Final constructs were verified by sequencing.

SRC1-mAmetrine constructs

The full frame of SRC1 isoform E used in this study was constructed from the 5' region of SRC1 derived from the pSG5-SRC1A-ORF plasmid (provided by Dr. Seth Kullman, North Carolina State University, Raleigh, NC) and the 3' portion of SRC1E (representing amino acids 381-1399) derived from pSG5-SRC1E (S. Kullman). Splice variations at the 3' end of these mRNAs have been shown to render SRC1A much less

effective than SRC1E as a co-activator (Kalkhoven *et al.*, 1998; Maijer *et al.*, 2005). Therefore, the 3' end of the SRC1A open reading frame was replaced with that derived from SRC1E. The SRC1E ORF was created by fusion PCR. The 5' portion of SRC1A was amplified using the primers: forward: 5'-CGTGCTGGTTATTGTGCTGT-3'; reverse : 5'-CTTCCGGGTGAGCATCCGAAACT TCCT-3'. The 3' portion of SRC1E was amplified using the primers: forward: 5'-AAGTTTCGG ATGCTCACCCGGAAGTCA-3'; reverse: 5'-ATTGATGAGTTTGGACAAACCAC-3'. A twenty four base pair overlap was used to conjoin the two PCR products. The resulting final PCR product was purified and amplified using the primers, forward: 5'-ATGAGTGGCCTTGGGGACAGTTC-3' and reverse: 5'-CTAGTCTGTAGTCACCACAGAGAAGAACTC-3' primers at 60.5˚C annealing temperature using the Advantage HF 2 PCR kit (Clontech) to give a 4kb PCR product. Restriction sites ApaI/AflII were added to the final PCR product for cloning by PCR using the 4kb product as template with the forward primer: 5'-TACTATGGGCCCACCATGAGTGGCCTTGGGGACAGTTC-3' and reverse primer: 5'-TACTATCTTAAGCTAGTCTGTAGTCACCACAGAG-3'. The amplified SRC1E ORF was subcloned into ApaI/AflII sites of pcDNA3.1(-) plasmid and named as pcDNA3.1-hSRC1E.

SRC1E was fused to the fluorescent protein mAmetrine (excitation: 410 nm, emission: 535 nm) to assess recruitment of SRC1 to the RXRα:PPARα dimer using BRET. The fusion construct of SRC1 and mAmetrine was created as described for PPARα and EBFP2. SRC1 ORF fragments were amplified by PCR from the pcDNA-hSRC1E plasmid using primers with KpnI/AflII and ApaI/XhoI enzyme sites and then subcloned into the

pcDNA3.1(-) plasmid. The mAmetrine PCR fragment without a stop codon but with a 30 base pair linker was ligated in-frame to the XhoI/KpnI sites at 5' end of SRC1 to generate pcDNA-mAmetrine-SRC1. Another mAmetrine PCR fragment with its stop codon and 30 base pair linker at its 5' end was subcloned in-frame to the XhoI/KpnI sites at the 3' end of SRC1 and designated as pcDNA-SRC1-mAmetrine. The final constructs were verified by sequencing.

BRET assays

Bioluminescence resonance energy transfer (BRET) assays were used to assess ligand-dependent dimerization of PPARα and RXRα along with recruitment of SRC1 to the receptor complex. BRET is used to assess protein-protein interactions by fusing a photon donor to one protein and a fluorescent photon acceptor to the other. Detectable energy transfer from the donor to the acceptor proteins requires a distance between the proteins of <10nm which effectively discerns donor-receptor protein complexes, but not free proteins.

HepG2 cells (ATCC®, www.ATCC.org) were cultured in MEM supplemented with 10% FBS. One day before transfection, approximately 650,000 cells were seeded into individual wells of 6-well plates. The next day, pcDNA-gal4-hRXRα(DEF)-Rluc2, PPARα-EBFP2, and SRC1-mAmetrine fusion constructs were transfected into the cells with TransIt–LT1 (Mirus,www.mirusbio.com) reagent according to manufacturer's protocol. Empty plasmid pcDNA3.1(-) was used to provide the same quantity of transfected DNA to each treatment. Cells were trypsinized twenty-four hours later and centrifuged at 1,500g for 2 minutes. Cells were resuspended in PBS (Sigma-Aldrich) and cells from one well of the 6-

well plate were divided into three wells in 96-well white bottom plates (PerkinElmer Life Sciences, MA, USA). Cells were incubated in the presence or absence of various test ligands for 1 hour. The amount of DMSO, used to deliver ligands, was kept constant in all wells (0.1% (v/v)). Rluc2 substrate coelenterazine 400a (DeepBlueC , Biotium, www.biotium.com) was added to the wells in PBS at a final concentration of 5.0 μM. Emission readings were performed immediately on a FLUOstar Omega microplate reader (BMG Labtech,www.bmglabtech.com) with 3 filter settings (Rluc2 filter, 410 ± 40nm; EBFP2 filter, 475 ± 15nm; mAmetrine filter, 535 ± 15nm). A conceptual diagram of the BRET assays used in this study is provided in Fig. 1A.

Dimerization of RXRα and PPARα was detected as the BRET ratio by measuring the light emitted by the acceptor protein (475 nm) divided by the light emitted by the donor protein (410 nm) with corrections for background fluorescence (using cells that were not transfected with the fusion proteins) and contaminating emissions from the donor into the acceptor's emission wavelength (475nm). This latter correction factor was derived by measuring fluorescence at 475 nm in cells transfected with Rluc2-RXRα alone minus the fluorescence measured with untransfected cells at 475 nm divided by the fluorescence of Rluc2-RXRα alone at 410 nm minus the fluorescence of untransfected cells at 410 nm.

Recruitment of SRC1 was determined using this same general procedure with BRET ratios determined using emissions detected at 535 nm.

Functional assessment of fusion proteins

Functional integrity of protein constructs was established using the dual (PPARα and RXRα) ligand tributyltin in both reporter gene and BRET assays. BRET assays were optimized for maximum signal (BRET ratio) with different ratios of photon donor molecules and photon acceptor molecules and with different positioning of the photon acceptor protein on the receptor protein (N-terminal fusion versus C-terminal fusion). Optimization results are depicted in Figs. 1B-C. Fusion of EBFP2 to the C-terminus of PPARα out-performed fusion to the N-terminus. Conversely, fusion of mAmetrine to the N-terminus of SRC1 out-performed fusion to the C-terminus.

Experiments were performed to establish whether the measured BRET signal generated from one fluorescent protein may reflect contaminating emissions from the other fluorescent protein or random transfer of photons to unbound photon acceptor proteins. The 475/410 nm BRET signal, which was indicative of PPARα:RXRα dimerization, increased with increasing 9-*cis* retinoic acid concentration when all assay components (RXRα-Rluc2, PPARα-EBFP2, SRC1-mAmetrine) were included in the assay but did not increase when PPARα was excluded from the assay (RXRα-Rluc2, EBFP2, SRC1-mAmetrine) (Fig. 1D). Similarly, the 535/410 nm BRET signal, which was indicative of SRC1 recruitment to the complex, increased with increasing 9-*cis* retinoic acid concentration when all assay components were included in the assay (RXRα-Rluc2, PPARα-EBFP2, SRC1-mAmetrine) but did not increase when SRC1 was excluded from the assay (RXRα-Rluc2, PPARα-EBFP2, mAmetrine) (Fig. 1E). These results established that the measured increases in BRET signals were due to targeted dimerization and not due to random energy transfer to

photon acceptors or contaminating emissions. Overall, results established that the fusion proteins exhibited ligand-dependent assembly that could be measured by the energy transferred.

Reporter gene transcription assays

HepG2 cells, cultured in MEM supplemented with 10% FBS, were plated at a density of 25,000 cells per well in 96-well white-bottom plates. The next day, 25 ng of plasmids containing the specific receptor proteins under evaluation were transfected into the cells along with 25ng of pcDNA-mAmetrine-SRC1, 125 ng of pG5-luc (firefly luciferase), and 6 ng of PRL-CMV (*Renilla* luciferase) using TransIT-LT1 (Mirus) reagent according to the manufacturer's protocol. Receptor plasmids that were transfected were either 25 ng of pBIND-gal4-hPPARα alone or pBIND-gal4-hRXRα (DEF) alone for assessment of ligand interaction with the individual receptor subunits, or 25 ng of pBIND-gal4-hRXRα (DEF) along with 25 ng of pcDNA-PPARα-EBFP2 for the assessment of heterodimer transactivation. Twenty-four hours later, media was replaced with serum-free media containing various ligands at the desired concentrations for another 24 hours. Ligands were delivered in DMSO and the concentration of DMSO was kept constant among all treatments, including controls (0.10%, v/v). After incubation, firefly and *Renilla* luciferase activities were measured using Dual-Glo luciferase assay system (Promega, www.promega.com) using the manufacturer's protocol. Luminescent signals were obtained using a FLUOstar Omega microplate reader (BMG Labtech) and firefly luciferase values were normalized to the *Renilla* luciferase values.

Cellular toxicity

Toxicity to HepG2 cells, caused by the organophosphate flame retardants, was evaluated. Cells were plated at a density of 10,000 cells per well in white opaque 96-well plates using MEM supplemented with 10% FBS. The next day, cells were treated with each organophosphate compound at the concentrations used in the reporter assays in serum free media for 24 hours at 37C. The organophosphates were delivered to the wells dissolved in DMSO which was present in all wells, including controls, at a concentration of 0.1% v/v. Cellular toxicity was measured using the CellTox™ Green Cytotoxicity Assay (Promega, www.promega.com) following manufacturer's protocol. This assay functions on the premise that living cells cannot take-up the cyanine dye; while, the dye traverses the compromised membrane of dead or moribund cells, binds to DNA, and fluoresces at 485 nm excitation/520 nm emission. Fluorescence was measured on a FLUOstar Omega microplate reader (BMG Labtech).

Statistics

Significant ($p \leq 0.05$) differences between treatments and control or among treatments were evaluated using One Way ANOVA accompanied by Tukey's test. Homogeneity of the variances was confirmed by Levenes's test.

Results

RXRα agonists

Comparative assays were performed to evaluate the activity of the known RXRα agonists 9-*cis* retinoic acid and LGD1069 in reporter gene assays and BRET assays. Both ligands activated gene transcription in the PPARα:RXRα reporter assay (Figs. 2A, 3A). Activity of both ligands was due to interaction with the RXRα subunit (Figs. 2C, 3C) and not the PPARα subunit (Figs. 2B, 3B). Both compounds also stimulate dimerization of PPARα and RXRα (Figs. 2D, 3D) and recruitment of SRC1 to the receptor complex (Figs. 2E, 3E) as measured in the BRET assays. Thus, these RXRα agonists stimulate the assembly of the PPARα:RXRα:SRC1 triplex to form an active transcription factor.

PPARα agonists

Next, we comparatively evaluated the activity of the known PPARα agonists clofibrate and Wy-14,643 in reporter gene assays and BRET assays. Both compounds activated gene transcription in our PPARα:RXRα reporter gene assay (Figs. 4A, 5A). Activity of both compounds was due to interaction with the PPARα subunit (Figs. 4B, 5B) and not the RXRα subunit (Figs. 4C, 5C). In contrast to results obtained with the RXRα agonists, both PPARα agonists failed to stimulate subunit dimerization (Figs. 4D, 5D) or SRC1 recruitment (Figs. 4E, 5E).

Activation of the PPARα:RXRα receptor by clofibrate and Wy-14,643 in the reporter gene assay had to involve assembled receptor complexes as the gal4 DNA-binding element was associated with the RXRα subunit and the ligand-binding element was associated with

the PPARα subunit. The lack of ligand-stimulated assembly of the transcription factor suggested that PPARα agonists activated constitutively assembled receptors. The presence of constitutively assembled receptor dimers was substantiated by the observation that ligand-independent (i.e., constitutive) reporter gene activity was low and comparable when only either PPARα-gal4 or RXRα-gal4 was transfected into the assay but significantly increased when both receptor subunits were expressed (Fig. 6). Taken together results with known RXRα and PPARα ligands indicated that the BRET assay would be informative in the detection of RXRα agonists but not in the detection of PPARα agonists. We next evaluated the relative performance of the BRET and reporter gene assays with several organophosphates that we viewed as candidate ligands to the PPARα:RXRα receptor based off of results reported in Chapter One.

2-Ethylhexyl diphenyl phosphate

2-Ethylhexyl diphenyl phosphate significantly ($p \leq 0.05$) inhibited PPARα:RXRα activity at concentrations as low as 3.0 μM (Fig. 7A). This compound interacted with both receptor subunits but was at least 10X more inhibitory towards the PPARα subunit (Figs. 7B, C). 2-Ethylhexyl diphenyl phosphate also inhibited dimerization of the PPARα and RXRα subunits albeit at concentrations appreciably higher than those that inhibited activity (Fig. 7D). This compound had no significant effect on the recruitment of SRC1; although empirically, a decline in SRC1 recruitment commensurate with the decline in subunit dimerization was observed (Fig. 7E).

Tri-o-tolyl phosphate

Tri-*o*-tolylphosphate significantly ($p \leq 0.05$) inhibited PPARα:RXRα activity at concentrations as low as 30 μM (Fig. 8A). This inhibitory effect was reflected when evaluating the PPARα receptor activity alone (Fig. 8B). In contrast, tri-*o*-tolylphosphate activated the RXRα receptor, with maximum activation occurring at 10 μM (Fig. 8C). At concentrations greater than 10 μM, this compound interacted with the RXRα subunit in an inhibitor manner (Fig. 8C). This decline in activity was significantly ($p \leq 0.05$) different at 100 μM tri-*o*-tolylphosphate as compared to the peak activity observed at 10 μM. Tri-*o*-tolylphosphate inhibited dimerization of the PPARα and RXRα subunits at concentrations as low as 30 μM (Fig. 8D) and inhibited recruitment of SRC1 at concentrations as low as 100 μM (Fig. 8E).

Tri-n-butyl phosphate

Tri-*n*-butyl phosphate inhibited the PPARα:RXRα at concentrations as low as 1.0 μM though the severity of the inhibition was less than the other organophosphate compounds evaluated (Fig. 9A). Similar to tri-*o*-tolylphosphate, tri-*n*-butyl phosphate inhibited the PPARα subunit (Fig. 9B) and elicited a biphasic effect on the RXRα subunit with activation followed by inhibition Fig. 9C). The decline in activity was significantly ($p \leq 0.05$) different at 30 and 100 μM tri-*n* -butyl phosphate as compared to the peak activity observed at 3.0 μM. Tri-*n*-butyl phosphate inhibited the dimerization of the PPARα and RXRα subunits although significant ($p \leq 0.05$) inhibition was evident only at the highest exposure concentration (300

μM) (Fig. 9D). This compound had no effect on SRC1 recruitment of SRC1 to the receptor complex (Fig. 9E).

Tris(2-butoxyethyl) phosphate

Tris(2-butoxyethyl) phosphate was weakly inhibitory towards the PPARα:RXRα receptor complex with significance ($p \leq 0.05$) only at 100 μM (Fig. 10A). This inhibitory effect was not evident when evaluating interaction specifically with the PPARα subunit (Fig. 10B). Tris(2-butoxyethyl) phosphate decreased activity associated with the RXRα subunit at concentrations greater than 3 μM with a significant reduction, as compared to activity at 3 μM, observed at 30 and 100 μM (Fig. 10C). This compound also had no effect on receptor subunit dimerization (Fig. 10D) or SRC1 recruitment (Fig. 10E).

Tris(2-chloroethyl) phosphate

Tris(2-chloroethyl) phosphate elicited no effect on PPARα:RXRα activity or the individual subunits (Figs. 11A-C). High concentrations of the compound did inhibit dimerization of the receptor subunits (Fig. 11D) but had no effect on SRC1 recruitment to the receptor (Fig. 11E).

Tris(2-ethylhexyl) phosphate

Tris (2-ethylhexyl) phosphate behave similarly to tris (2-chloroethyl) phosphate with no effect in the reporter gene assays (Figs. 12 A-C), inhibition of receptor dimerization (Fig. 12D), and no effect on SRC1 recruitment (Fig. 12E).

Cellular toxicity

None of the organophosphate compounds elicited toxicity to the HepG2 cells at concentrations as high as 100 μM. While BRET assays were performed at concentrations as high as 300 μM, this higher concentration was not evaluated for toxicity as cells were exposed to the organophosphates in the BRET assays for only 1 hour.

Discussion

The assessment of PPARα receptor assembly using BRET in conjunction with reporter gene assays provided mechanistic data that informed on the relationships between ligand-induced receptor assembly/disassembly and receptor activity. Results also identified ligand-types with which BRET assays could supplant reporter assays in toxicity screening programs (PPARα ligands) as well as ligand-types for which the BRET assay would not be as informative as the reporter assay (RXRα ligands). Finally, we determined that some organophosphate flame retardants act similarly on the PPARα signaling pathway as triphenyl phosphate (Chapter One).

BRET analyses revealed that provision of the RXRα ligands 9-*cis* retinoic acid or LGD1069 stimulated RXRα:PPARα dimerization. Provision of the PPARα ligands clofibrate or Wy-14,643 did not enhance dimer formation. This differential effect of RXRα and partner ligands on dimerization support the conclusions made by Dong and Noy (Dong and Noy, 1998) involving RXR:RAR and RXR:VDR heterodimerization. They and others (Gampe Jr. *et al.*, 2000; Kersten *et al.*, 1995) observed that ligand-free RXR exists in the cell predominantly as inactive homo-tetramers and to a lesser degree, hetero- or homo- dimers.

Dong and Noy (Dong and Noy, 1998) results suggested that binding of 9-*cis* retinoic acid caused dissociation of the tetramers with the commensurate accumulation of dimers and monomers. RAR or VDR ligands did not stimulate heterodimerization but rather these ligands were able to bind and stabilize pre-existing heterodimeric associations with RXR. Thus, ligand interactions resulting in RXRα:PPARα activation paralleled interaction observed with other RXR heterodimers, where RXR ligands serve to enhance the formation of active heterodimers; and, PPARα ligands serve to activate constitutively existing heterodimers. Thus BRET was informative of receptor activation by RXRα ligands, but not PPARα ligands.

Recruitment of the co-activator SRC1 tracked well with receptor dimerization in the present experiments with the RXRα and PPARα activating ligands. RXRα agonists enhanced recruitment of SRC1 to the PPARα:RXRα dimer; while, PPARα agonists did not enhance SRC1 recruitment to the receptor dimer. The RXRα ligand, concentration-dependent recruitment of SRC1 to RXRα is consistent with previous observations (DiRenzo *et al.*, 1997). RXR activators have been shown to promote recruitment of SRC1 to the RXR:PPARγ heterodimer; while, a PPARγ-specific ligand had no effect on SRC1 recruitment to the heterodimer (Schulman *et al.*, 1998; Yang *et al.*, 2000). In contrast, SRC1 also has been reported to be recruited to the ligand-occupied PPAR (DiRenzo, Soderstrom, Kurokawa, Ogliastro, Ricote, Ingrey, Horlein, Rosenfeld and Glass, 1997; Zhou *et al.*, 1998). However, these demonstrations of ligand-dependent recruitment of SRC1 to PPARs have used cell free experimental systems. Furthermore, PPARα remained ligand responsive in SRC1 knockout mice (Qi *et al.*, 1999), indicating that SRC1 is not obligatory for PPARα

activity. Taken together, previous and present observations indicate that SRC1 is recruited to the PPAR:RXR dimer in response to ligand-activation of the RXR subunit, with negligible recruitment in response to PPARα ligand-dependent activation in intact cells. Rather, PPAR agonists are known to selectively recruit other co-activators (e.g. DRIP) to the receptor complex (Yang, Rachez and Freedman, 2000).

Evaluation of the organophosphate flame retardants revealed several inhibitors of the PPARα:RXRα receptor. Typically, this inhibitory activity was elicited towards both the PPARα and RXRα receptor subunits (Table 1). Several of these inhibitors elicited a biphasic effect on the RXRα subunit with initial modest activation of the subunit followed by inhibition at higher exposure concentrations. For most of these inhibitors, receptor subunit dimerization also was reduced indicating that the compounds were binding and dissociating constitutively existing dimers. SRC1 association with the receptor was largely unaffected by these inhibitors, suggesting retention of the coactivator on the ligand-occupied RXRα subunits.

Two organophosphate compounds, tris(2-chloroethyl) phosphate and tris(2-ethylhexyl) phosphate, stimulated dissociation of the receptor subunits while having no discernible effect in the reporter gene assays. We speculate that these compounds did indeed cause dissociation of constitutively present dimers but that the RXRα subunit, which was capable of binding to the reporter gene via its gal4 DNA binding domain, maintained the constitutive level of reporter activity.

Receptor assembly assays may serve to complement or replace conventional reporter gene assays in toxicological screenings for chemical interaction with nuclear receptors.

Results from the present study revealed that BRET assays can discern receptor agonists and antagonists in a single assay. Both BRET and reporter gene assays can be performed in a multi-well plate format and are conducive to high-throughput screening. However, the time between chemical addition and output reading for the BRET is significantly less than that required for reporter gene assays as the BRET assay does not rely upon gene transcription and translation. However, the BRET assay could not universally replace the reporter gene assays as it was shown to be deficient in its ability to detect agonists that function through binding to the PPARα subunit.

In designing our BRET assay, we chose gal4-RXRα as the receptor subunit fused to the Rluc2 photon donor with PPARα and SRC1 fused to photon-accepting fluorescent proteins. This configuration allows for the use of the existing assay system with other RXR partners by simply replacing the PPARα-EBFP2 fusion construct with EBFP2 fusion constructs using other RXRα partners. For example, we have and are currently using this same assay system to evaluate the effects of chemical exposures on PPARγ:RXRα:SRC1 (Chapter One and Three) and VDR:RXRα:SRC1 assembly.

In combination, the BRET and reporter gene assays could provide a wealth of mechanistic information regarding the specific target of action of chemicals. These assays could also facilitate the identification of chemical combinations that may function synergistically with respect to either therapeutic efficacy or toxicity. Studies have suggested that combined exposure to RXR and PPAR agonists may result in either additive or synergistic activation (Mukherjee *et al.*, 1997; Mukherjee *et al.*, 1994; Mukherjee *et al.*, 2013; Schulman, Shao and Heyman, 1998; Tolon *et al.*, 1998). Factors that dictate whether

a RXR ligand and a PPAR ligand will function additively or synergistically are unknown. Conceivably, activation of some fraction of the RXR:PPAR population by an RXR ligand with commensurate activation of another fraction of the population by a PPAR ligand would result in the activation of gene transcription consistent with a model of additivity. Alternatively, if both ligands bind to their respective subunits of the RXR:PPAR complex, the outcome may be synergistic activation. For example, the RXR ligand binding might elicit allosteric conformational changes to the PPAR ligand binding domain (Schulman, Shao and Heyman, 1998; Shulman *et al.*, 2004) resulting in increased affinity of the domain for PPAR ligands, resulting in increased recruitment of co-activators, or increased dissociation of co-repressors. RXR ligands may also increase the pool of PPAR:RXR dimers that are available for activation by the PPAR receptor (Dong and Noy, 1998). BRET assays would inform on whether ligands are functioning as synergists by enhancing subunit dimerization or impacting co-activator/co-repressor interactions with the receptor.

PPARα and PPARγ cooperate in complementary roles to regulate the balance between lipid and glucose utilization for the production of energy (Desvergne and Wahli, 1999). PPARα activation favors the utilization of lipid as an energy source; while, activation of PPARγ favors the oxidation of glucose and the storage of lipid (Lefebvre, Chinetti, Fruchart and Staels, 2006; Shulman and Mangelsdorf, 2005). Thus the inhibition of PPARα or the activation of PPARγ could contribute to symptoms of metabolic syndrome (Grundy *et al.*, 2004). Epidemiological and toxicological studies have linked human exposure to several environmental chemicals to symptoms of metabolic syndrome. These include glucose intolerance with exposure to triphenyltin (Colosio *et al.*, 1991) and increased waist

circumference, insulin resistance with exposure to phthalate esters (Hatch *et al.*, 2008; Stahlhut *et al.*, 2007). Members of the organotins and phthalates have been shown to activate PPARγ and, in some cases, cause weight gain in animal experiments (Feige *et al.*, 2010; Feige *et al.*, 2007; Grun and Blumberg, 2006; Grun *et al.*, 2006; Hurst and Waxman, 2003). Conceivably, chemicals or chemical combinations that inhibit PPARα, as observed with many of the organophosphates, and activate PPARγ could result in synergistic outcomes with respect to metabolic syndrome. The relevance of high-dose animal toxicological studies to human risk is a challenge to the chemical risk assessment process. However, humans are exposed to multiple chemicals through normal daily activities and additive or synergistic effects of these chemicals on a common regulatory pathway, such as the PPAR signaling pathway, could have adverse consequences as observed in some epidemiologic studies. The utilization of BRET assays in toxicity screening programs could provide mechanistic data that would identify chemical combinations that should be earmarked for in vivo toxicological investigations of additive or synergistic toxicity.

References

Ankley, G. T., Bennett, R. S., Erickson, R. J., Hoff, D. J., Hornung, M. W., Johnson, R. D., Mount, D. M., Nichols, J. W., Russom, C. L., Schmieder, P. K., Serrano, J. A., Tietge, J. E. and Villeneuve, D. L. (2010). Adverse outcome pathways: a conceptual framework to support ecotoxicology research and risk assessment. *Environ. Toxcol. Chem.* **29**, 730-741.

Barile, F. A. (2013). Principles of Toxicology Testing, Second Edition. CRC Press, Boca Raton, FL.

Borroto-Escuela, D. O., Flajotel, M., Agnati, L. F., Greengard, P. and Fuxe, K. (2013). Bioluminiscence resonance energy transfer (BRET) methods to study G protein-coupled receptor tyrosine kinase heteroreceptor complexes. *Methods Cell. Biol.* **117**, 141-164.

Colosio, C., Tomasini, M., Cairoli, S., Foa, V., Minoia, C., Marinovich, M. and Galli, C. L. (1991). Occupational triphenyltin acetate poisoning: a case report. *Br. J. Ind. Med.* **48**, 136-139.

Daunert, S., Barrett, G., Feliciano, J. S., Shetty, R. K., Shrestha, S. and Smith-Spencer, W. (2000). Genetically engineered whole-cell sensing systems: coupling biological recognition with reporter genes. *Chem. Rev.* **100**, 2705-2738.

Depoix, C., Delmotte, M.-H., Formstecher, P. and Lefebvre, P. (2001). Control of retinoic acid receptor heterodimerization by ligand-induced structural transitions. *J. Biol. Chem.* **276**:9452-9459.

Desvergne, B. and Wahli, W. (1999). Peroxisome proliferator-activated receptors: Nuclear control of metabolism. *Endocrine Rev.* **20**, 649-688.

DiRenzo, J., Soderstrom, M., Kurokawa, R., Ogliastro, M. H., Ricote, M., Ingrey, S., Horlein, A., Rosenfeld, M. G. and Glass, C. K. (1997). Peroxisome proliferator-activated receptors and retinoic acid receptors differentially control the interactions of retinoid X receptor heterodimers with ligands, coactivators, and corepressors. *Mol. Cell. Biol.* **17**, 2166-2176.

Dix, D. J., Houck, K. A., Martin, M. T., Richard, A. M., R.W., S. and Kavlock, R. J. (2007). The ToxCast program for prioritizing toxicity testing of environmental chemicals. *Toxicol. Sciences* **95**, 5-12.

Dong, D. and Noy, N. (1998). Heterodimer formation by retinoid X receptor: regulation by ligands and by the receptor's self-association properties. *Biochemistry* **37**, 10691-10700.

Feige, J., Gerber, A., Casals-Casas, C., Yang, Q., Winkler, C., Bedu, E., Bueno, M., Gelman, L., Auwerx, J. and Gonzalez, F. (2010). The pollutant diethylhexyl phthalate regulates hepatic energy metabolism via species-specific PPARalpha-dependent mechanisms. *Environ. Health Perspect.* **118**, 234-241.

Feige, J. N., Gelman, L., Rossi, D., Zoete, V., Metivier, R., Tudor, C., Anghel, S. I., Grosdidier, A., Lathion, C., Engelborghs, Y., Michielin, O., Wahli, W. and Desvergne, B. (2007). The endocrine disruptor monoethyl-hexyl-phthalate is a selective peroxisome proliferator-activated receptor gamma modulator that promotes adipogenesis. *J. Biol. Chem.* **282**, 19152-19166.

Gampe Jr., R. T., Montana, V. G., Lambert, M. H., Wisely, G. B., Milburn, M. V. and Xu, H. E. (2000). Structural basis for autorepression of retinoid X receptor by tetramer formation and the AF-2 helix. *Genes Develop.* **14**, 2229-2241.

Glass, C. K. (2013). Differential recognition of target genes by nuclear receptor monomers, dimers, and heterodimers. *Endocrine Rev.* **15,** DOI: http://dx.doi.org/10.1210/edrv-15-3-391.

Grun, F. and Blumberg, B. (2006). Environmental obesogens: Organotins and endocrine disruption via nuclear receptor signaling. *Endocinology* **147**, S50-S55.

Grun, F., Watanabe, H., Zamanian, Z., Maeda, L., Arima, K., Cubacha, R., Gardiner, D. M., Kanno, J., Iguchi, T. and Blumberg, B. (2006). Endocrine-disrupting organotin compounds are potent inducers of adipogenesis in vertebrates. *Mol. Endocrinol.* **20**, 2141-2155.

Grundy, S. M., Brewer Jr., H. B., Cleeman, J. I., Smith Jr., S. C. and Lenfant, C. (2004). Definition of metabolic syndrome. *Circulation* **109**, 433-438.

Hatch, E. E., Nelson, J. W., Qureshi, M. M., Weinberg, J., Moore, L. L., Singer, M. and Webster, T. F. (2008). Association of urinary phthalate metabolite concentrations with body mass index and waist circumference: a cross-sectional study of NHANES data, 1999-2002. *Environ. Health* **7**, 27, 222.ehjournal.ent/content/7/1/27.

Hofer, T., Gerner, I., Gundert-Remy, U., Liebsch, M., Schulte, A., Spielmann, H., Vogel, R. and Wettig, K. (2004). Animal testing and alternative approaches for the human health risk assessment under the proposed new European chemicals regulation. *Arch. Toxicol.* **78**, 549-564.

Hurst, C. H. and Waxman, D. J. (2003). Activation of PPARα and PPARγ by environmental phthalate monoesters. *Toxicol. Sc i.* **74**, 297-308.

Kakizawa, T., Miyamoto, T., Kaneko, A., Yajima, H., Ichikawa, K. and Hashizume, K. (1997). Ligand-dependent heterodimerization of thyroid hormone receptor and retinoid X receptor. *J. Biol. Chem.* **272**, 23799-23804.

Kalkhoven, E., Valentine, J. E., Heery, D. M. and Parker, M. G. (1998). Isoforms of steroid receptor co-activator 1 differ in their ability to potentiate transcription by the oestrogen receptor. *EMBO J.* **17**, 232-243.

Kersten, S., Kelleher, D., Chambon, P., Gronemeyer, H. and Noy, N. (1995). Retinoid X receptor α forms tetramers in solution. *Proc. Nat. Acad. Sciences USA* **92**, 8645-8649.

Kocan, M., See, H. B., Seeber, R. M., Eidne, K. A. and Pfleger, K. D. G. (2008). Demonstration of improvements to the bioluminescence resonance energy transfer (BRET) technology for the monitoring of G protein-coupled receptors in live cells. *J. Biomol. Screening* **13**, DOI: 10.1177/1087057108324032.

Lefebvre, P., Chinetti, g., Fruchart, J. C. and Staels, B. (2006). Sorting out the roles of PPAR alpha in energy metabolism and vascular homeostasis. *J. Clin. Invest.* **116**, 571-580.

Maijer, O. C., Kalkhoven, E., van der Laan, S., Steenbergen, P. J., Houtman, S. H., Dijkmans, T. F., Pearce, D. and de Kloet, E. R. (2005). Steroid receptor coactivator-1 splice variants differentially affect corticosteroid receptor signaling. *Endocrinology* **146**, 1438-1448.

McLachlan, J. A. (1993). Functional toxicology: a new approach to detect biologically active xenobiotics. *Environ. Health Perspect.* **101**, 386-387.

Mukherjee, R., Davies, P. J. A., Crombie, D. L., Bischoff, E. D., Cesario, R. M., Jow, L., Hamann, L. G., Boehm, M. F., Mondon, C. E., Nadzan, A. M., Paterniti Jr., J. R. and Heyman, R. A. (1997). Sensitization of diabetic and obese mice to insulin by retinoid X receptor agonists. *Nature* **386**, 407-410.

Mukherjee, R., Jow, L., Noonan, D. J. and McDonnell, D. P. (1994). Human and rat peroxisome proliferator activated receptors (PPARs) demonstrate similar tissue distribution but different responsiveness to PPAR activators. *J. Steroid Biochem. Molec. Biol.* **51**, 157-166.

Mukherjee, R., Strasser, J., Jow, L., Hoener, P., Paterniti Jr., J. R. and Heyman, R. A. (2013). RXR agonists activate PPARα-inducible genes, lower triglycerides, and raise HDL levels in vivo. *Arterioscler. Thromb. Vasc. Biol.* **18**, 272-276.

NRC (2007). Toxicity Testing in the 21st Century: A Vision and a Strategy. The National Academies Press, Washington DC.

Pfleger, K. D. G., Seeber, R. M. and Eidne, K. A. (2006). Bioluminescence resonance energy transfer (BRET) for the real-time detection of protein-protein interactions. *Nature Prot.* **1**, 337-345.

Piersma, A. H., Bosgra, S., van Duursen, M. B., Hermsen, S. A., Jonker, L. R., Kroese, E. D., van der Linden, S. C., Man, H., Roelofs, M. J., Schulpen, S. H., Schwarz, M., Uibel, F., van Vugt-Lussenburg, B. M., Westerhout, J., Wolterbeek, A. P. and van der Burg, B. (2013). Evaluation of an alternative in vitro test battery for detecting reproductive toxicants. *Reprod. Toxicol.* **38**, 53-64.

Piston, D. W. and Kremers, G. J. (2007). Fluorescent protein FRET: the good, the bad and the ugly. *Trends Biochem. Sci.* **32**, 407-414.

Qi, C., Zhu, Y., Pan, J., Yeldandi, A. V., Rao, M. S., Maeda, N., Subbarao, V., Pulikuri, S., Hashimoto, T. and Reddy, J. K. (1999). Mouse steroid receptor coactivator-1 is not essential for peroxisome proliferator-activated receptor α-regulated gene expession. *Proc. Nat. Acad. Sciences USA* **96**, 1585-1590.

Schulman, I. G., Shao, G. and Heyman, R. A. (1998). Transactivation by retinoid X receptor-peroxisome proliferator-activated receptor γ (PPARγ) heterodimers: intermolecular synergy requires only the PPARγ hormone-dependent activation function. *Mol. Cell. Biol.* **18**, 3483-3494.

Shanle, E. K. and Xu, W. (2011). Endocrine disrupting chemicals targeting estrogen receptor signaling: identification and mechanisms of action. *Chem. Res. Toxicol.* **14**, 6-19.

Shulman, A. I., Larson, C., Mangelsdorf, D. J. and Ranganathan, R. (2004). Structural determinants of allosteric ligand activation in RXR heterodimers. *Cell* **116**, 417-429.

Shulman, A. I. and Mangelsdorf, D. J. (2005). Retinoid X receptor heterodimers in the metabolic syndrome. *New England J. Med.* **353**, 604-615.

Stahlhut, R. W., van Wijngaarden, E., Dye, T. D., Cook, W. and Swan, S. H. (2007). Concentrations of urinary phthalate metabolites are associated with increased waist circumference and insulin resistance in adult U.S. males. *Environ. Health Perspect.* **115**, 876-882.

Tolon, R. M., Castillo, A. I. and Aranda, A. (1998). Activation of the prolactin gene by peroxisome proliferator-activated receptor-α appears to be DNA binding-independent. *J. Biol. Chem.* **273**, 26652-26661.

Wang, H. Y., Peters, G.A., Zeng, X., Tang, M., Ip, W. and Khan, S. A. (1995). Yeast two-hybrid system demonstrates that estrogen receptor dimerization is ligand-dependent in vivo. *J. Biol. Chem.* **270**, 23322-23329.

Wang, Y. H. and LeBlanc, G. A. (2009). Interactions of methyl farnesoate and related compounds with a crustacean retinoid X receptor. *Mol. Cell. Endocrin.* **309**, 109-116.

Xu, W. and Powell, E. (2008). Intermolecular interactions identify ligand-selective activity of estrogen receptor α/β dimers. *Proc. Nat. Acad. Sciences USA* **105**, 19012-19017.

Yang, W., Rachez, C. and Freedman, L. P. (2000). Discrete roles for peroxisome proliferator-activated reeptor γ and retinoid X receptor in recruiting nuclear receptor coactivators. *Mol. Cell. Biol.* **20**, 8008-8017.

Zhou, G., Cummings, R., Li, Y., Mitra, S., Wilkinson, H. A., Elbrecht, A., Hermes, J. D., Schaeffer, J. M., Smith, R. G. and Moller, D. E. (1998). Nuclear receptors have distinct affinities for coactivators: characterization by fluorescence resonance energy transfer. *Mol. Endocrin.* **12**, 1594-1604.

Table 1. Summary[a] of the impacts of the evaluated compounds on PPARα, RXRα, and PPARα:RXRα mediated activation/suppression of the transcription reporter gene; ligand-mediated dimerization of PPARα and RXRα; and, recruitment of SRC1 to the complex.

Compound	Reporter Gene Activation			Complex Assembly	
	PPARα	RXRα	PPARα:RXRα	PPARα:RXRα	SRC1 recruitment
9-*cis* retinoic acid	ne	+	+	+	+
LGD1069	ne	+	+	+	+
Clofibrate	+	ne	+	ne	ne
Wy-14,643	+	ne	+	ne	ne
2-Ethylhexyl diphenyl phosphate	-	-	-	-	ne
Tri-*o*-tolyl phosphate	-	+/-	-	-	-
Tri-*n*-butyl phosphate	-	+/-	-	-	ne
Tris(2-butoxyethyl) phosphate	ne	+/-	-	ne	ne
Tris(2-chloroethyl) phosphate	ne	ne	ne	-	ne
Tris(2-ethylhexyl) phosphate	ne	ne	ne	-	ne

[a] + = activation (reporter gene assays) or assembly (BRET assays); - = inhibition (reporter gene assays) or dissociation (BRET assays); +/- non-monotonic-concentration response; ne = no effect.

FIGURE 1. Conceptual diagram of the BRET assay (A); the effect of construct orientation on BRET activity (B,C); and specificity of the BRET signals (D, E). A. I. Fusion proteins expressed in the cell-based assay are indicated. II. Ligand binding stimulates dimerization of PPARα and RXRα. This dimerization is detected upon addition of Rluc2 substrate which, upon metabolism, produces a 410 nm emission (purple) that excites the EBFP2 resulting in an emission at 475 nm (blue). SRC1 also is recruited to the complex and the Rluc2 emission excites the mAmetrine resulting in an emission at 535 nm (green). B. BRET ratios with EBFP2 fused to either the N-terminus or C-terminus of PPARα. C. BRET ratios with mAmetrine fused to either the N-terminus or C-terminus of SRC1. Assays were performed at mass ratios of the photon donor:photon acceptor of 1:2 and 1:6, as indicated. Black bars: no ligand provided. Red bars: the dual PPARα/RXRα ligand tributyltin (0.1 μM) was provided. Error bars represent the standard deviation (n=3). An asterisk denotes a significant difference ($p \leq 0.05$) between assays performed in the presence and absence of ligand. D. BRET ratio (475/410 nm) in the presence of all components (RXRα-Rluc2, PPARα-EBFP2, SRC1-mAmetrine) (red) and all components (RXRα-Rluc2, EBFP2, SRC1-mAmetrine) except PPARα (black). E. BRET ratio (535/410 nm) in the presence of all components (RXRα-Rluc2, PPARα-EBFP2, SRC1-mAmetrine) (red) and all components (RXRα-Rluc2, PPARα-EBFP2, mAmetrine) except SRC1 (black). Data depicts the mean and standard deviations (n=3). An asterisk denotes a significant ($p \leq 0.05$) difference from the control (0 μM 9-*cis* retinoic acid).

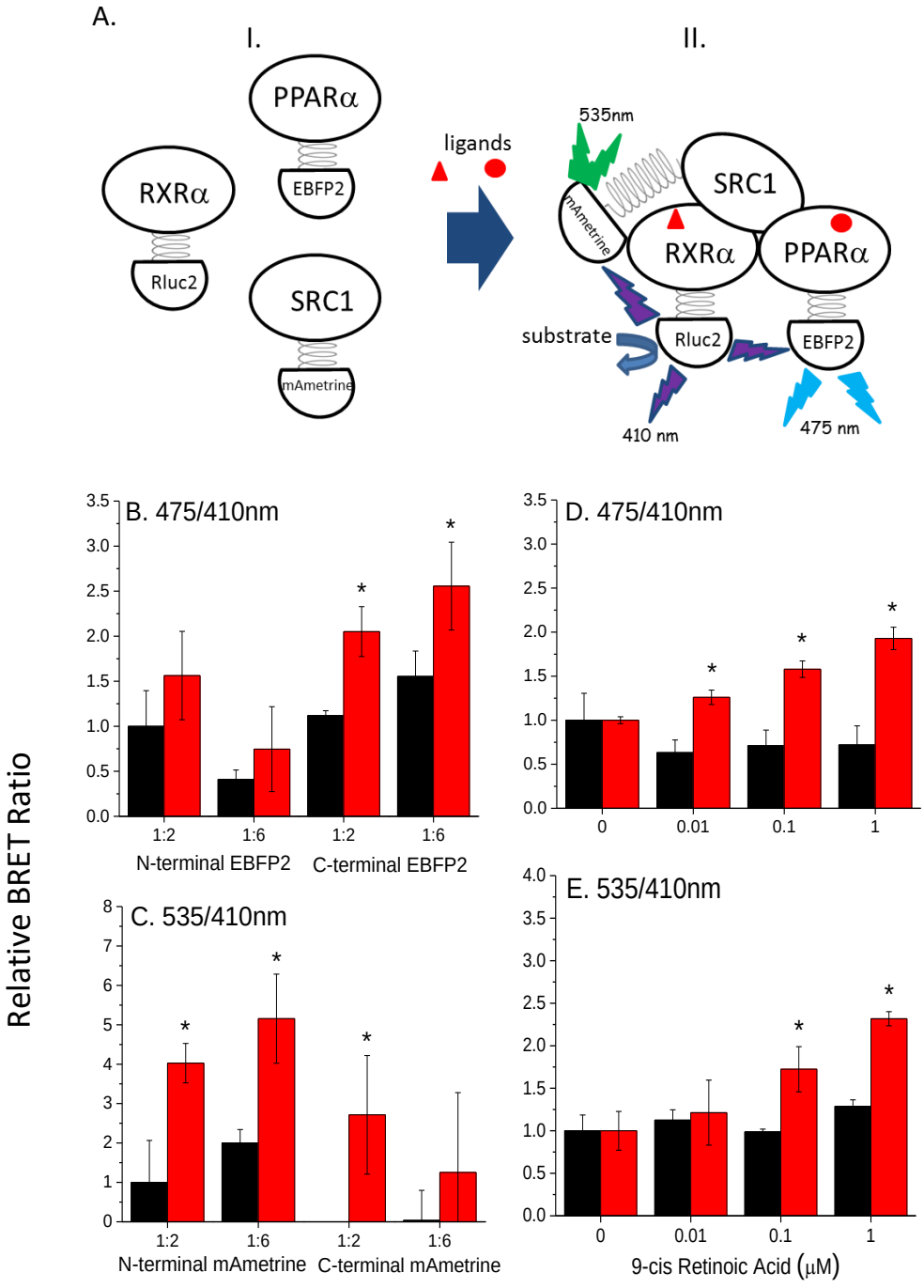
A.
I.
II.
PPARα
EBFP2
RXRα
Rluc2
SRC1
mAmetrine
ligands
535nm
substrate
410 nm
475 nm
Relative BRET Ratio
B. 475/410nm
N-terminal EBFP2
C-terminal EBFP2
C. 535/410nm
N-terminal mAmetrine
C-terminal mAmetrine
D. 475/410nm
E. 535/410nm
9-cis Retinoic Acid (μM)

FIGURE 2. The impact of 9-*cis* retinoic acid on reporter gene transcriptional activity driven by PPARα:RXRα (A), PPARα, (B) and RXRα (C) and dimerization of PPARα and RXRα (D) with recruitment of SRC1 (E). Data are presented as mean and standard deviation (n=3). An asterisk denotes a significant ($p<0.05$, One-Way ANOVA, Tukey's Multiple Comparison Test) difference from the control (red data point).

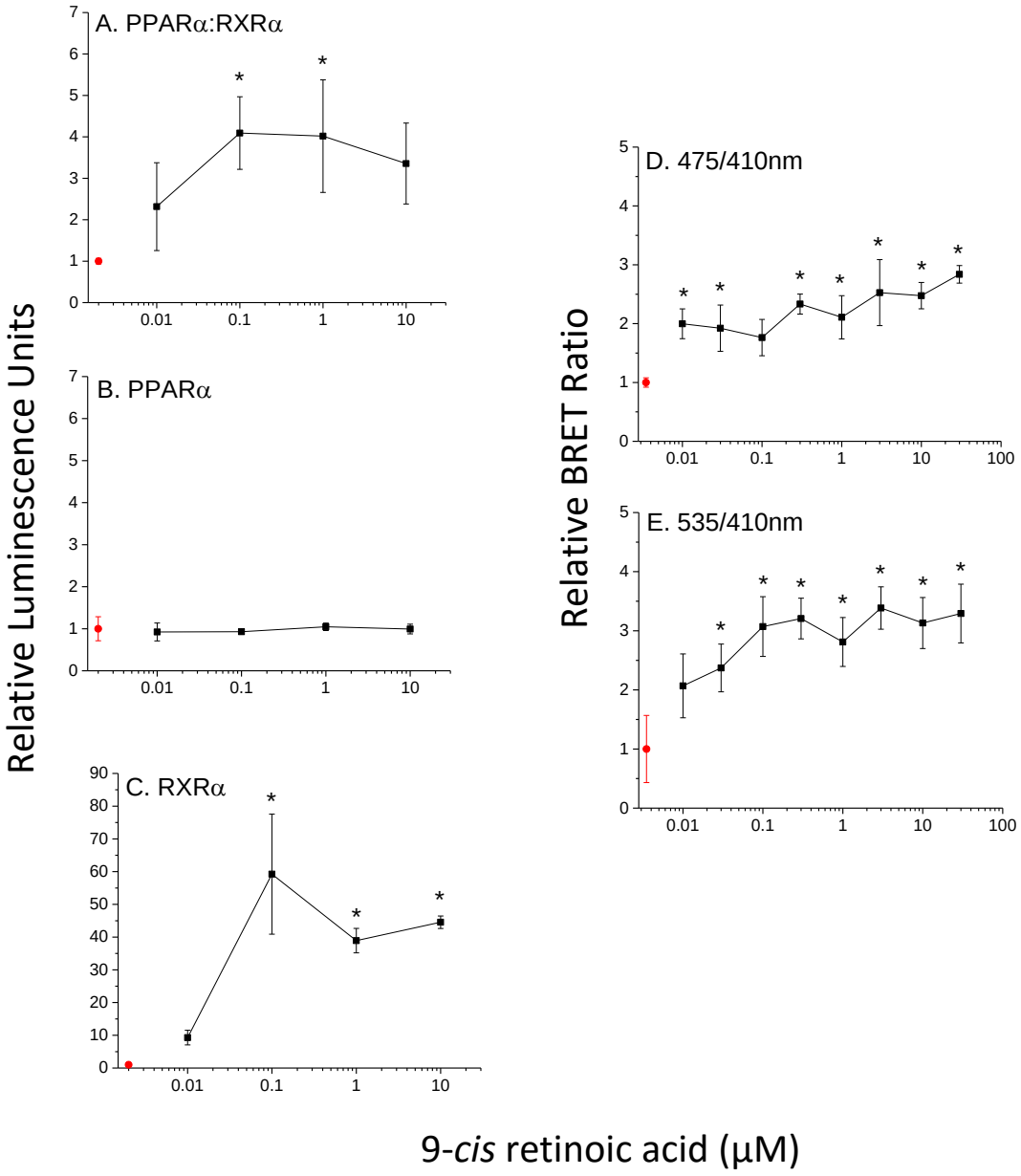
A. PPARα:RXRα
B. PPARα
C. RXRα
D. 475/410nm
E. 535/410nm
Relative Luminescence Units
Relative BRET Ratio
9-cis retinoic acid (μM)

FIGURE 3. The impact of LGD1069 on reporter gene transcriptional activity driven by PPARα:RXRα (A), PPARα, (B) and RXRα (C) and dimerization of PPARα and RXRα (D) with recruitment of SRC1 (E). Data are presented as mean and standard deviation (n=3). An asterisk denotes a significant ($p<0.05$, One-Way ANOVA, Tukey's Multiple Comparison Test) difference from the control (red data point).

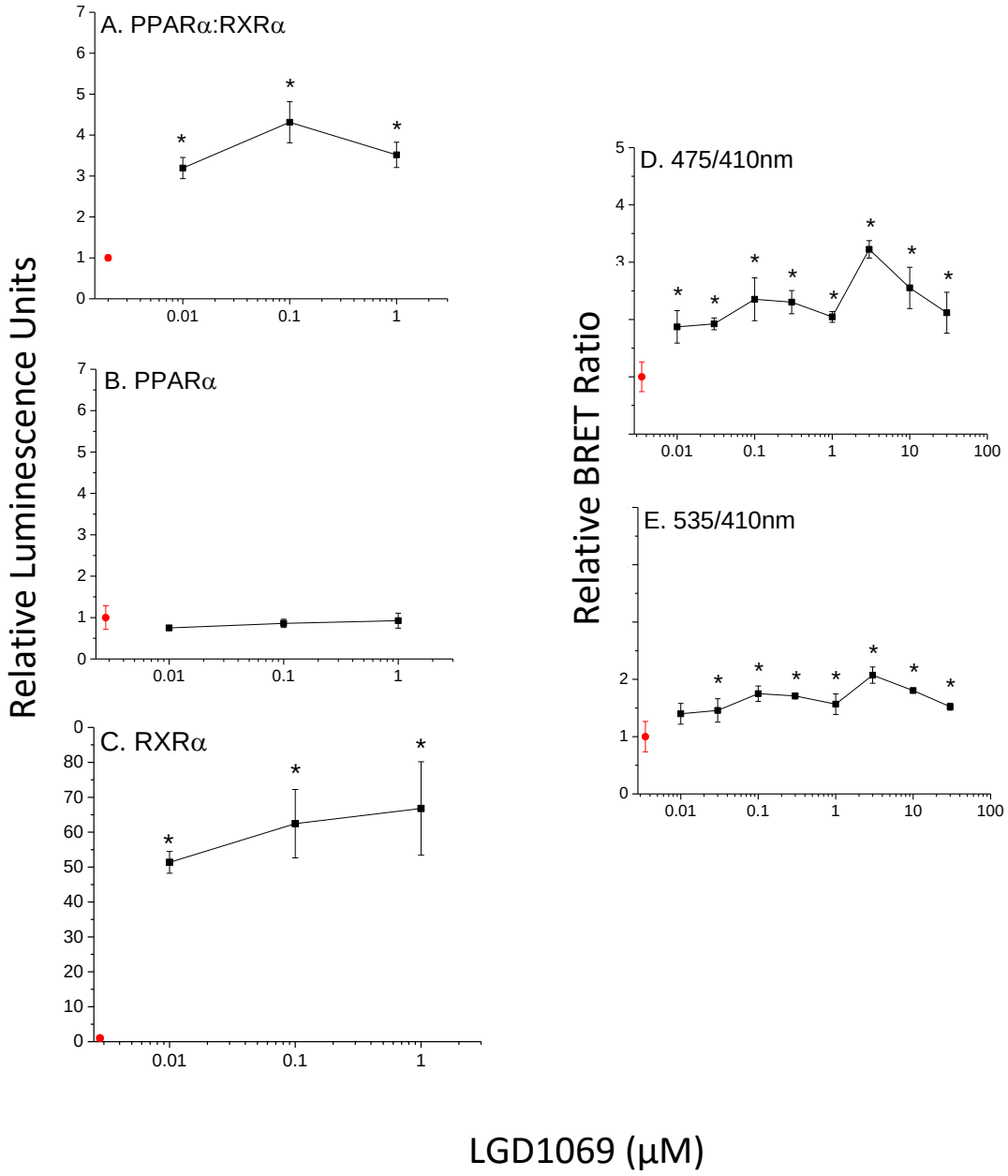
A. PPARα:RXRα
B. PPARα
C. RXRα
D. 475/410nm
E. 535/410nm
Relative Luminescence Units
Relative BRET Ratio
LGD1069 (µM)

FIGURE 4. The impact of clofibrate on reporter gene transcriptional activity driven by PPARα:RXRα (A), PPARα, (B) and RXRα (C) and dimerization of PPARα and RXRα (D) with recruitment of SRC1 (E). Data are presented as mean and standard deviation (n=3). An asterisk denotes a significant ($p<0.05$, One-Way ANOVA, Tukey's Multiple Comparison Test) difference from the control (red data point).

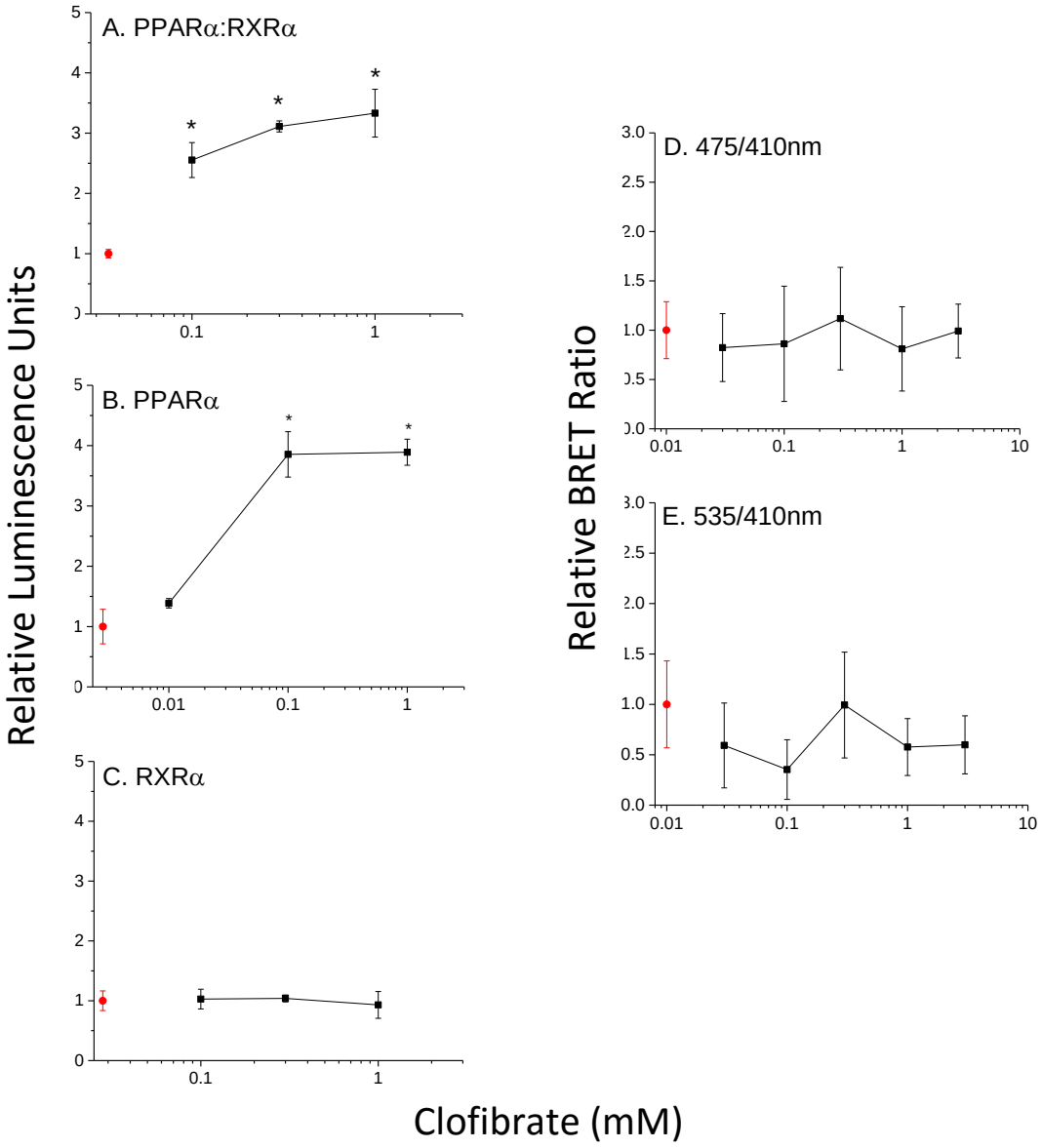
A. PPARα:RXRα
B. PPARα
C. RXRα
D. 475/410nm
E. 535/410nm
Relative Luminescence Units
Relative BRET Ratio
Clofibrate (mM)

FIGURE 5. The impact of Wy-14,643 on reporter gene transcriptional activity driven by PPARα:RXRα (A), PPARα, (B) and RXRα (C) and dimerization of PPARα and RXRα (D) with recruitment of SRC1 (E). Data are presented as mean and standard deviation (n=3). An asterisk denotes a significant ($p<0.05$, One-Way ANOVA, Tukey's Multiple Comparison Test) difference from the control (red data point).

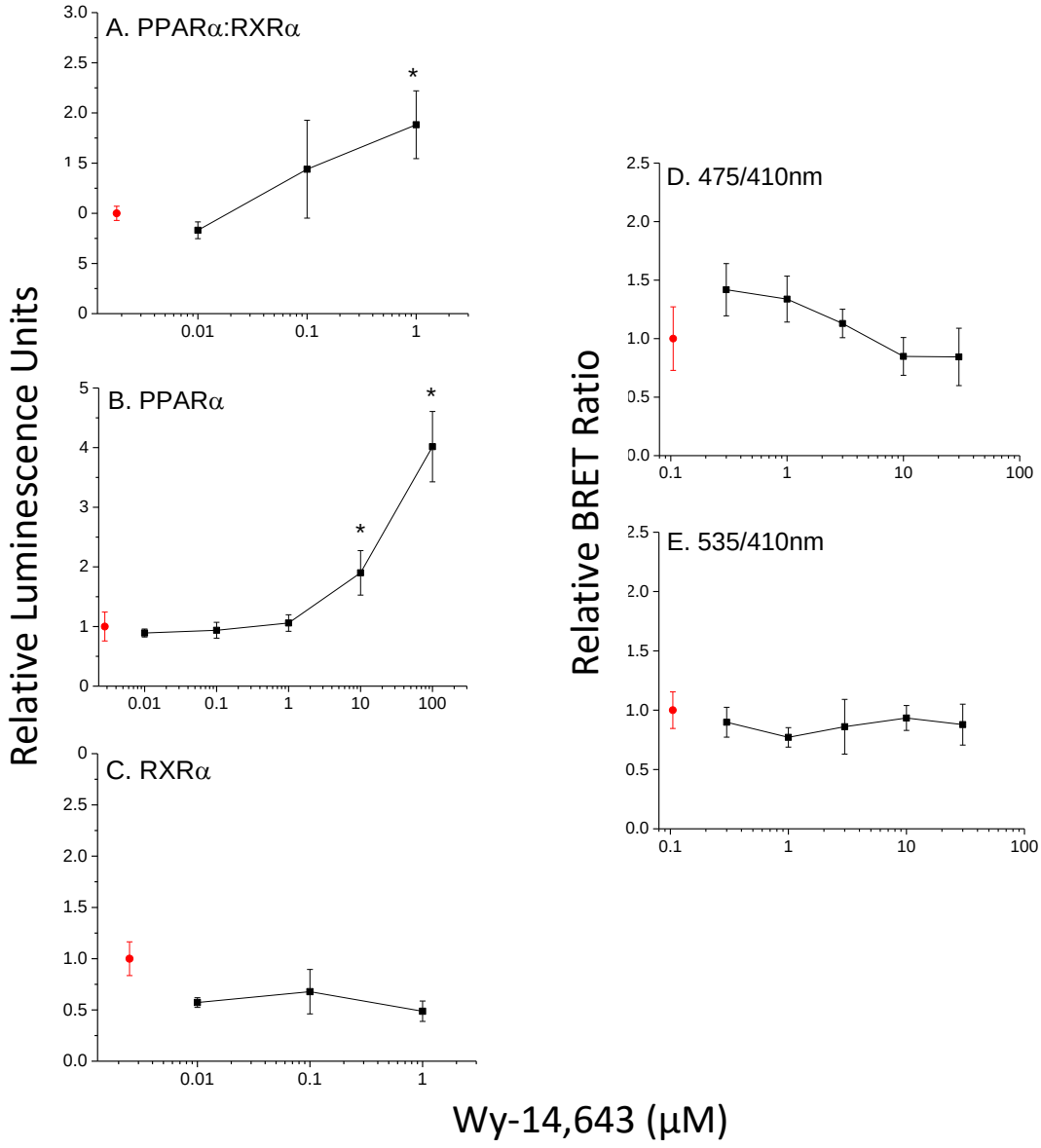
A. PPARα:RXRα
B. PPARα
C. RXRα
D. 475/410nm
E. 535/410nm
Relative Luminescence Units
Relative BRET Ratio
Wy-14,643 (μM)

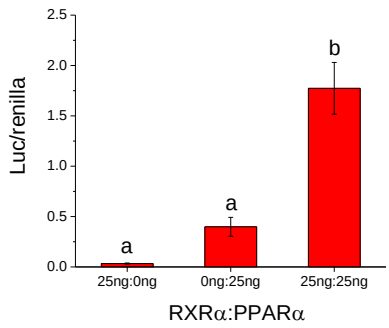

FIGURE 6. Ligand-independent gene transcription in cells expressing RXRα, PPARα, or RXRα and PPARα. Treatments having the same letter assignment are not significantly different. Treatments having different letter assignments are significantly different ($p \leq 0.05$).

FIGURE 7. The impact of 2-ethylhexyl diphenyl phosphate on reporter gene transcriptional activity driven by PPARα:RXRα (A), PPARα, (B) and RXRα (C) and dimerization of PPARα and RXRα (D) with recruitment of SRC1 (E). Data are presented as mean and standard deviation (n=3). An asterisk denotes a significant ($p<0.05$, One-Way ANOVA, Tukey's Multiple Comparison Test) difference from the control (red data point).

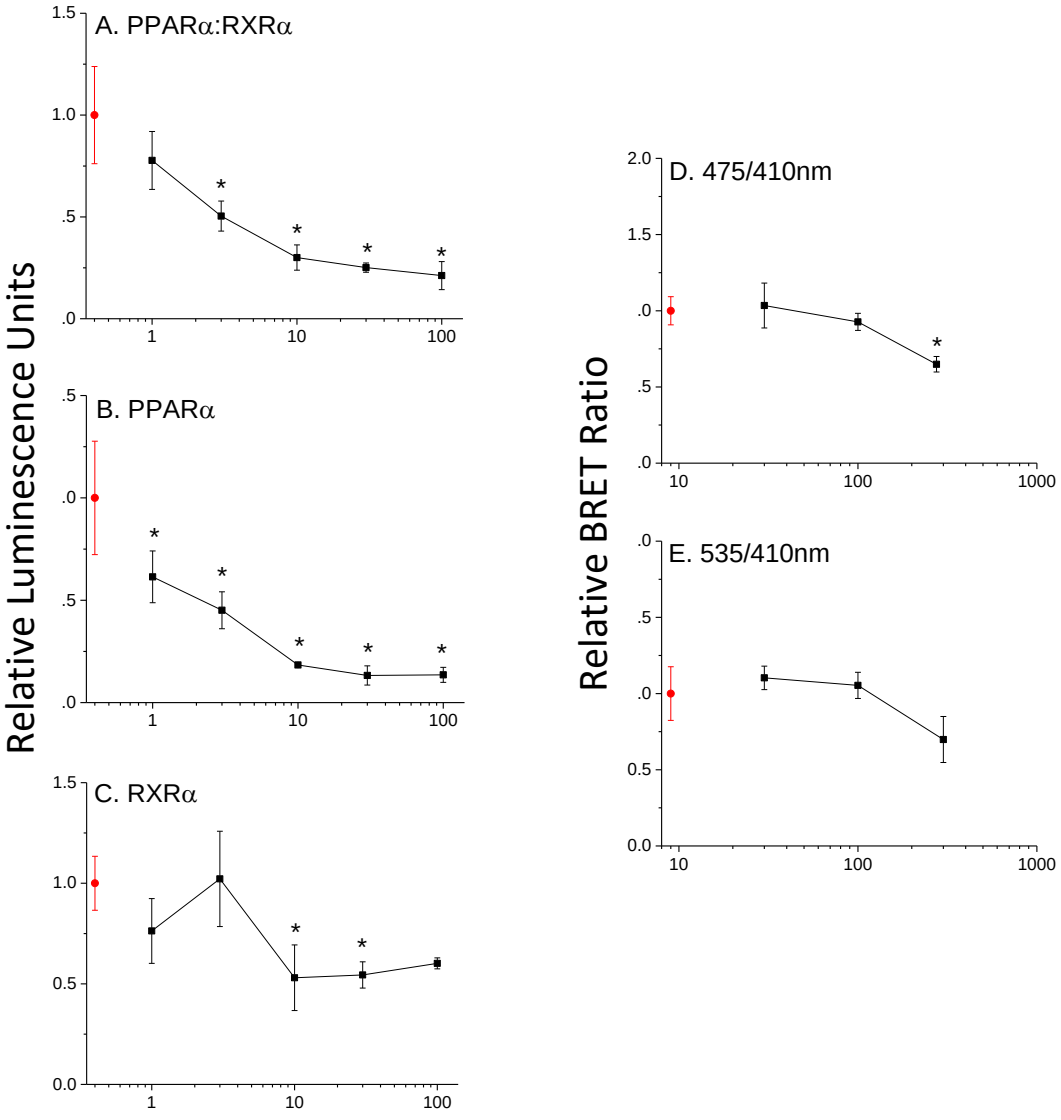
A. PPARα:RXRα
B. PPARα
C. RXRα
D. 475/410nm
E. 535/410nm
Relative Luminescence Units
Relative BRET Ratio
2-Ethylhexyl diphenyl phosphate (µM)

FIGURE 8. The impact of tri-*o*-tolyl phosphate on reporter gene transcriptional activity driven by PPARα:RXRα (A), PPARα, (B) and RXRα (C) and dimerization of PPARα and RXRα (D) with recruitment of SRC1 (E). Data are presented as mean and standard deviation (n=3). An asterisk denotes a significant ($p \leq 0.05$) difference from the control (red data point). A plus sign denotes a significant ($p \leq 0.05$) difference from the peak activity at 10 μM.

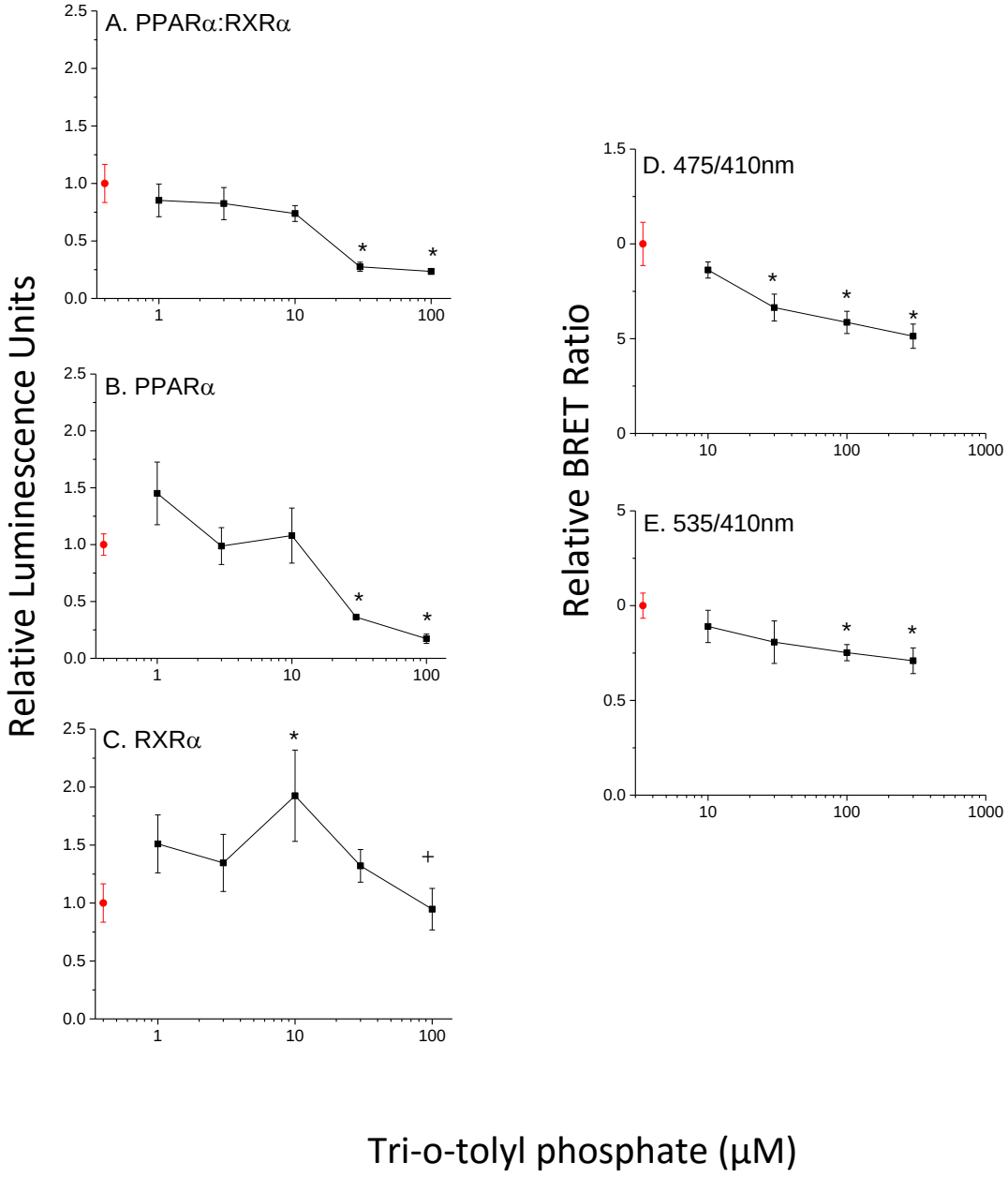
A. PPARα:RXRα
B. PPARα
C. RXRα
D. 475/410nm
E. 535/410nm
Relative Luminescence Units
Relative BRET Ratio
Tri-o-tolyl phosphate (μM)

FIGURE 9. The impact of tri-*n*-butyl phosphate on reporter gene transcriptional activity driven by PPARα:RXRα (A), PPARα, (B) and RXRα (C) and dimerization of PPARα and RXRα (D) with recruitment of SRC1 (E). Data are presented as mean and standard deviation (n=3). An asterisk denotes a significant ($p \leq 0.05$) difference from the control (red data point). A plus sign denotes a significant ($p \leq 0.05$) difference from the peak activity at 3.0 μM.

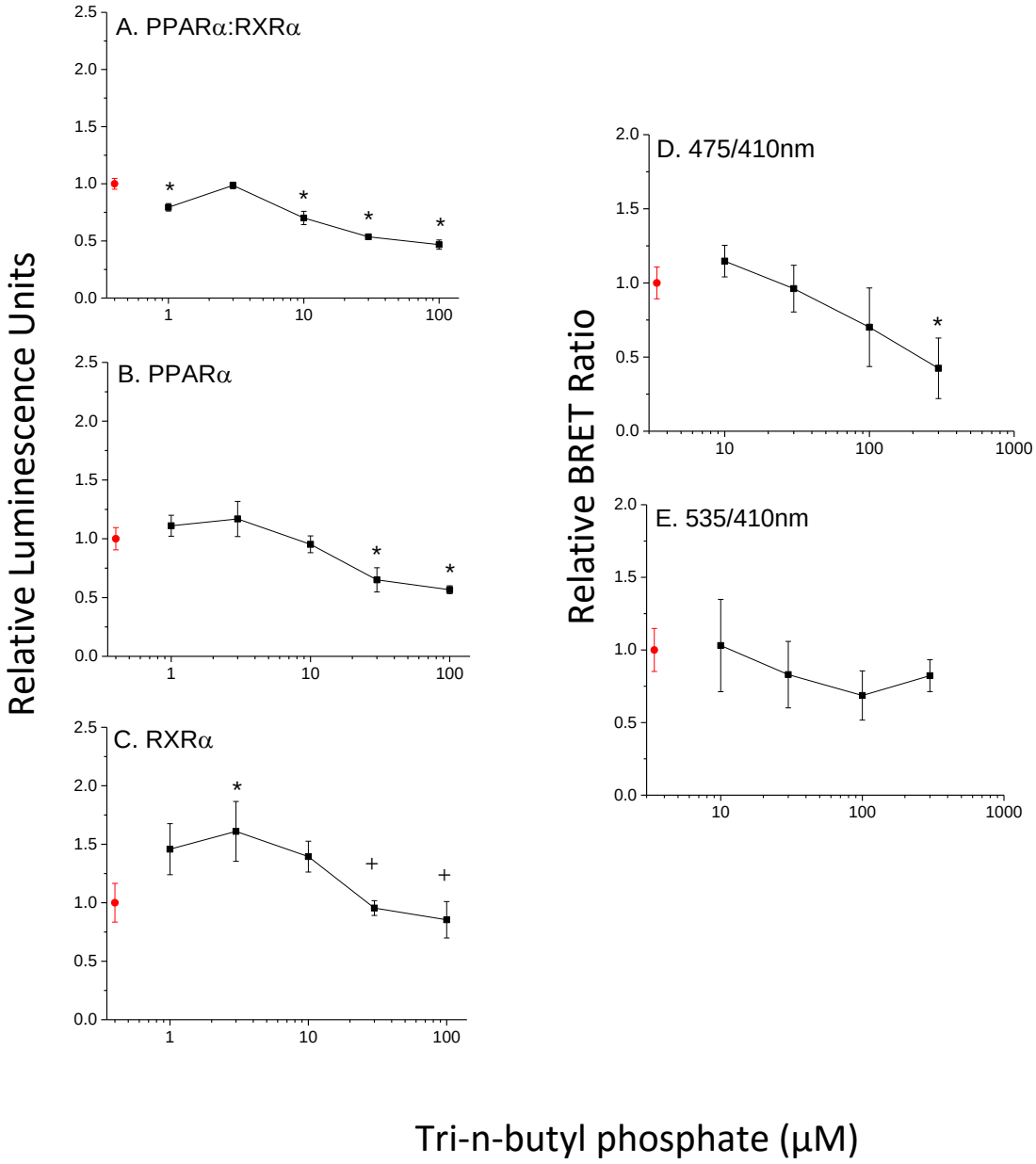
A. PPARα:RXRα
B. PPARα
C. RXRα
D. 475/410nm
E. 535/410nm
Relative Luminescence Units
Relative BRET Ratio
Tri-n-butyl phosphate (µM)

FIGURE 10. The impact of tri (2-butoxyethyl) phosphate on reporter gene transcriptional activity driven by PPARα:RXRα (A), PPARα, (B) and RXRα (C) and dimerization of PPARα and RXRα (D) with recruitment of SRC1 (E). Data are presented as mean and standard deviation (n=3). An asterisk denotes a significant ($p \leq 0.05$) difference from the control (red data point). A plus sign denotes a significant ($p \leq 0.05$) difference from the peak activity at 3.0 μM.

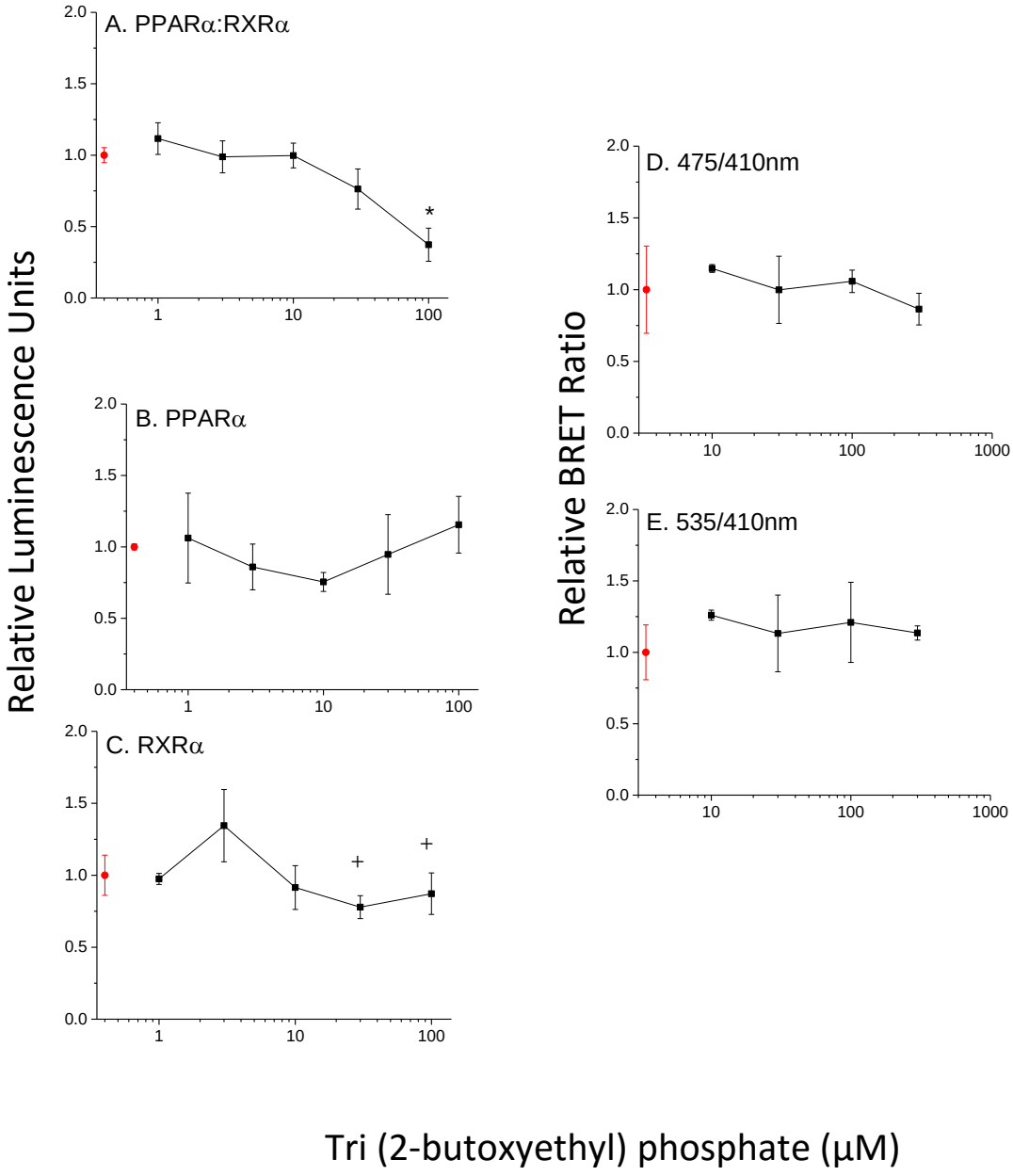
A. PPARα:RXRα
B. PPARα
C. RXRα
D. 475/410nm
E. 535/410nm
Relative Luminescence Units
Relative BRET Ratio
Tri (2-butoxyethyl) phosphate (µM)

FIGURE 11. The impact of tris (2-chloroethyl) phosphate on reporter gene transcriptional activity driven by PPARα:RXRα (A), PPARα, (B) and RXRα (C) and dimerization of PPARα and RXRα (D) with recruitment of SRC1 (E). Data are presented as mean and standard deviation (n=3). An asterisk denotes a significant ($p \leq 0.05$) difference from the control (red data point).

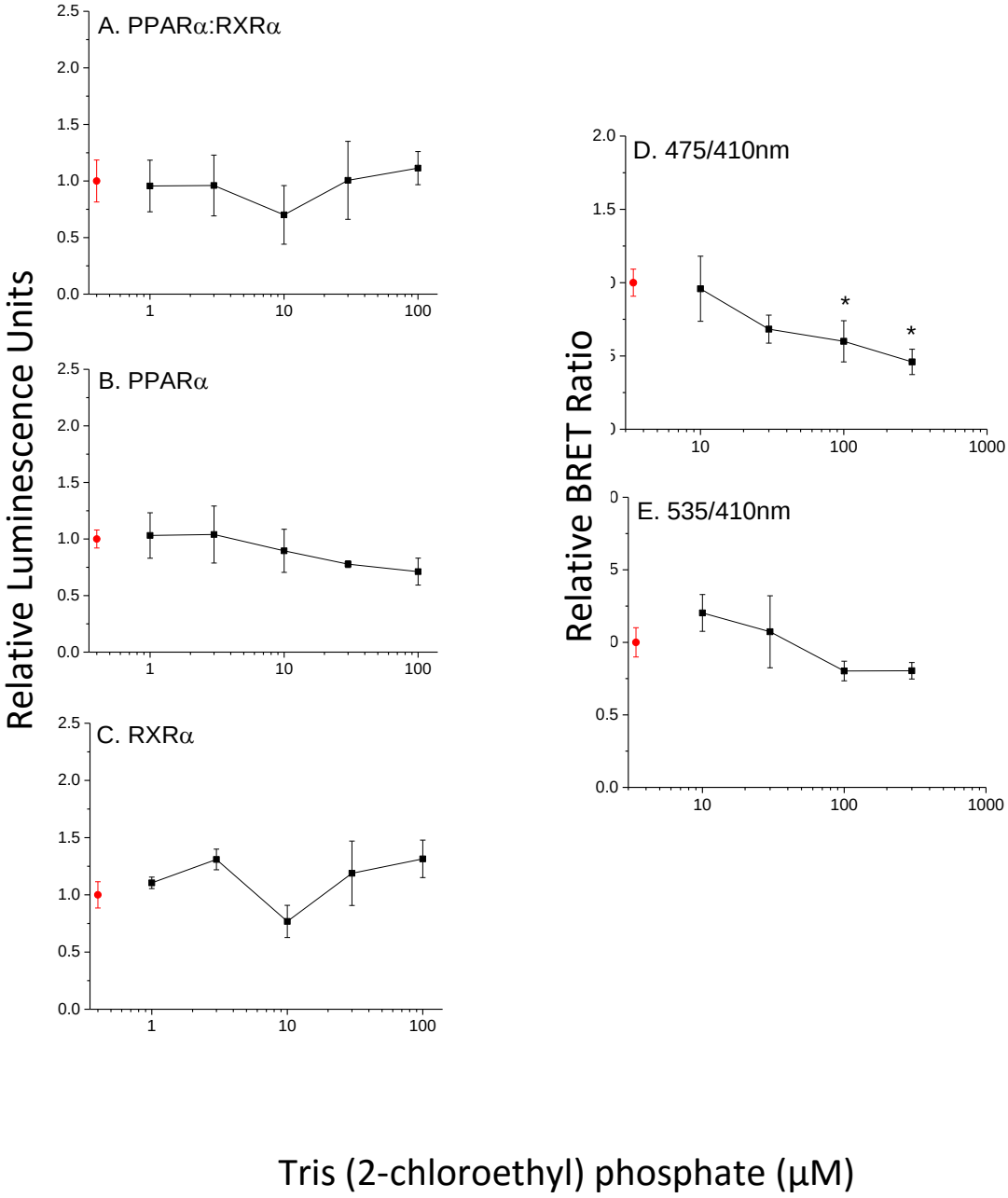
A. PPARα:RXRα
B. PPARα
C. RXRα
D. 475/410nm
E. 535/410nm
Relative Luminescence Units
Relative BRET Ratio
Tris (2-chloroethyl) phosphate (µM)

FIGURE 12. The impact of tris (2-ethylhexyl) phosphate on reporter gene transcriptional activity driven by PPARα:RXRα (A), PPARα, (B) and RXRα (C) and dimerization of PPARα and RXRα (D) with recruitment of SRC1 (E). Data are presented as mean and standard deviation (n=3). An asterisk denotes a significant ($p \leq 0.05$) difference from the control (red data point).

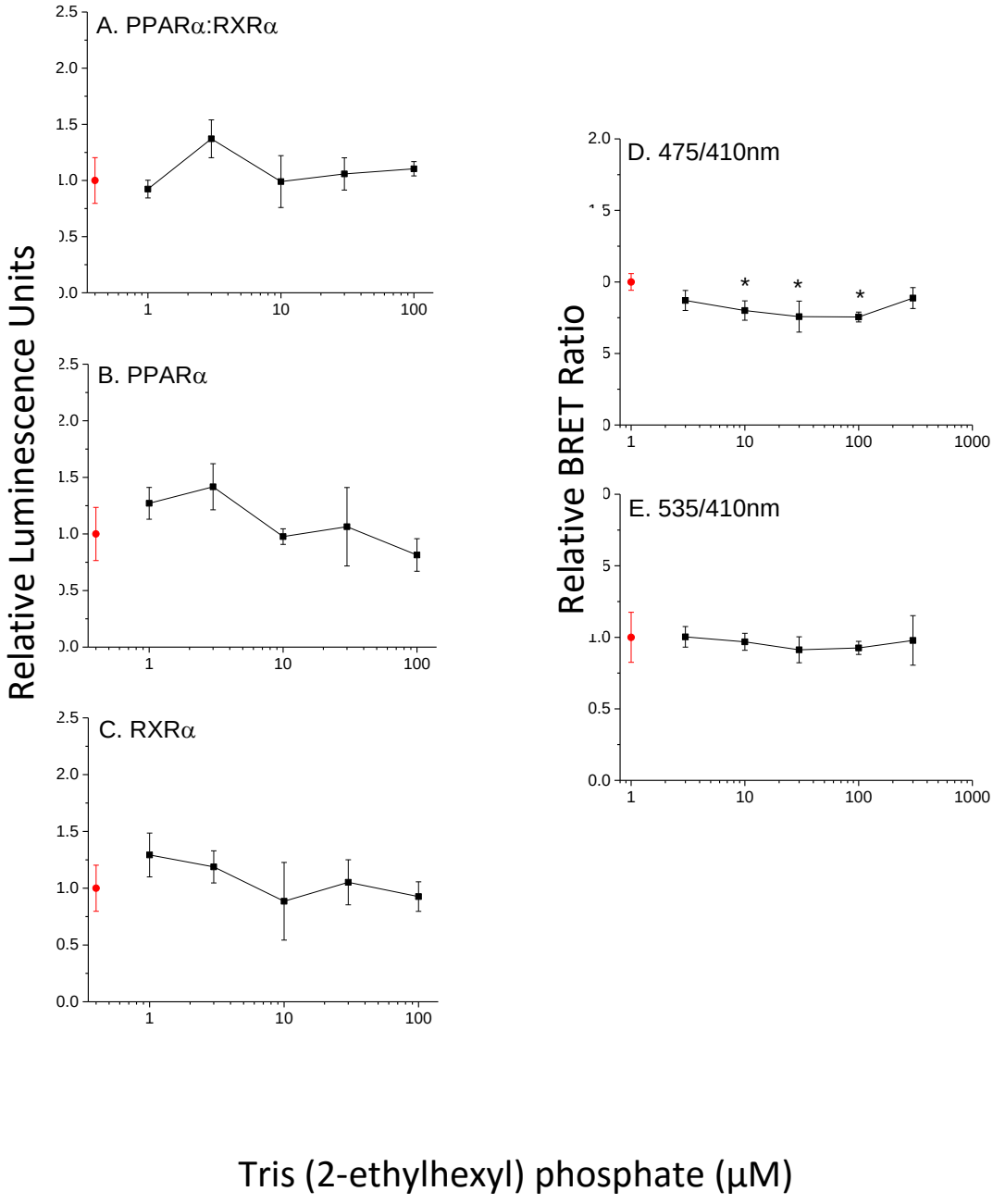
A. PPARα:RXRα
B. PPARα
C. RXRα
D. 475/410nm
E. 535/410nm
Relative Luminescence Units
Relative BRET Ratio
Tris (2-ethylhexyl) phosphate (µM)

CHAPTER THREE: INSECT GROWTH REGULATING INSECTICIDES TRANSACTIVATE THE PPAR GAMMA SIGNALING NETWORK

Charisse N. Holmes, Gwijun Kwon, Huahong Shi, and Gerald A. LeBlanc
Toxicology Program
Department of Biological Sciences
North Carolina State University
Raleigh, NC 27695

Abstract

Metabolic syndrome (i.e., obesity, diabetes, etc.) is endemic in some human populations. The involvement of environmental chemicals in this condition remains speculative. Insect growth regulating insecticides (IGRs) are used in a variety of indoor and outdoor applications including pest control on household pets. These compounds are considered to be relatively non-toxic to mammals; however, the potential for prolonged exposure to pets and their owners is significant. We evaluated the ability of the IGRs pyriproxyfen, fenoxycarb, methoprene, and kinoprene to interact with the peroxisome proliferator-activated receptor (PPAR) gamma signaling pathway which contributes to the regulation of lipid and glucose metabolism and whose perturbation could contribute to the etiology of metabolic syndrome. Transactivation reporter gene assays were used to evaluate the ability of IGRs to activate the human PPARγ:RXRα receptor complex. All of the IGRs activated the human PPARγ:RXRα receptor complex. Evaluation of the individual receptor subunits revealed that all of the IGRs activated the PPARγ receptor subunit; while, fenoxycarb, methoprene, and kinoprene also activated the RXRα receptor subunit. UVI 3003, an RXRα inhibitor, had no effect on PPARγ:RXRα transactivation indicating that interaction of the IGRs with the PPARγ subunit was responsible for activating the receptor complex. Bioluminescence resonance energy transfer (BRET) assays were used to evaluate the ability of the IGRs to stimulate dimerization of PPARγ and RXRα along with the recruitment of the coactivator SRC1 to the complex. Known RXRα agonist stimulated receptor assembly as measured by BRET; while, PPARγ agonist had no measurable effect on receptor assembly. The IGRs also had no effect on receptor assembly, further implicating the

PPARγ subunit as the target of IGR action. PPARγ:RXRα activation typically results in differentiation of pre-adipocytes into adipocytes and lipid accumulation within the differentiated adipocytes. Therefore, the ability of the IGRs to stimulate differentiation and lipid accumulation in mouse 3T3-L1 pre-adipocytes was evaluated. The IGRs stimulated differentiation and significantly elevated lipid accumulation within these cells. In conclusion, the IGRs evaluated are PPARγ agonists to which sufficient exposure could lead to weight gain and other symptoms of metabolic syndrome.

Keywords: pesticides, nuclear receptors, obesity, metabolic syndrome, hazard assessment

Introduction

Over the past two decades, metabolic syndrome has become endemic in some human populations [1, 2]. Metabolic syndrome refers to the co-occurrence of multiple health risk-factors including obesity, insulin resistance, dyslipidemia, and hypertension [3]. Approximately 24% of Americans are affected by metabolic syndrome leading to serious implications for health care cost and mortality [4]. While the causes of metabolic syndrome are multifactorial, toxicological studies suggest that environmental chemicals may contribute by disrupting lipid metabolism through interaction with the peroxisome proliferator-activated receptor (PPAR) signaling network.

In mammals, there are three members of the PPAR family: PPARα, PPARβ/δ and, PPARγ [5]. Through heterodimeric binding with the retinoid X receptor (RXR α,β,γ), PPARs regulate lipid and glucose metabolism. Ligand-mediated activation of the PPARα:RXRα heterodimer promotes glucose retention and fatty acid oxidation, while activation of the PPARγ:RXRα heterodimer promotes glucose utilization and fatty acid storage [6, 8-12]. Activation of the PPAR:RXR heterodimers can be enhanced by the recruitment of coactivators including PPAR gamma coactivator 1, PPAR-binding protein, and steroid receptor coactivator-1 (SRC1) [13, 14].

PPAR:RXR heterodimers are considered to be permissive; thus, ligands can interact with either subunit to cause transcriptional activation [15]. This ligand-mediated activation can be stimulated by endogenous fatty acids as well as, a variety of exogenous compounds [16, 17]. However, many exogenous chemicals for which human exposure can be significant have not undergone evaluation with respect to activation of the PPAR signaling network.

Insect growth regulators (IGRs) are commonly used in a variety of agricultural and domestic applications including pest control on fruit and tobacco, carpet cleaning powders, and pest control on household pets [18-21]. IGRs are popular due to their specificity towards insects making them less hazardous to humans, pets, and wildlife at concentrations typically used. Nonetheless, the potential for prolonged exposure to humans and pets is significant. For example, ectoparasiticides used to control fleas and ticks on cats and dogs (e.g., Certifect®, Avantage II®, Frontline Plus®) contain the IGRs pyriproxyfen or methoprene. These treatments are applied to the pet's coat and are typically considered to provide pest control for a month. During this time, pets are groomed and petted by children with potential for oral uptake from hand to mouth [22].

We noted some basic structural similarities between the IGR pyriproxyfen and the antidiabetic drug rosiglitazone (Avandia®; Fig. 1). Rosiglitazone is a potent activator of the PPARγ:RXRα receptor complex [23, 24]. This observation led us to hypothesize that some IGRs might activate the PPARγ signaling pathway and accordingly might pose risk of disrupting lipid homeostasis, causing or exacerbating symptoms of metabolic syndrome. In the present study, we tested the hypothesis that the IGRs pyriproxyfen, fenoxycarb, methoprene, and kinoprene have the ability to activate the human PPARγ:RXRα receptor complex. Mechanistic evaluations into the transactivation of the signaling pathway provided insight into the molecular target of the IRGs. Finally, we sought to link the observed molecular effects of the IGRs to an apical outcome: pre-adipocyte differentiation into adipocytes with commensurate lipid accumulation.

Materials and Methods

The plasmids containing the human RXRα-gal4 fusion construct (pBIND-gal4-hRXRα (DEF)) and the pG5-luc reporter gene under the control of the gal4 response element were previously described [25]. Dr. Sanjiv Gambhir (Stanford University, Stanford, California) provided the pcDNA3.1-Rluc2 plasmid containing *Renilla* luciferase (Rluc) with two mutations at M185V and C124A (Rluc2) as a gift [26]. Plasmids containing human PPARγ (pcDNA3.1-hPPARγ(ORF) were generously provided by Dr. Jeffrey Peters (Pennsylvania State University, University Park, PA). pcDNA3.1(-) and pRL-CMV plasmids were provided by Dr. Seth Kullman (North Carolina State University, Raleigh, NC). The PPRE-X3-TK-luc plasmid (Addgene plasmid #1015) was created by Dr. Bruce Spiegelman (Harvard Medical School, Boston, MA) [27].

HepG2 cells (ATCC, www.ATCC.org) were cultured in Modified Eagle's Media (MEM; Cellgro, www.cellgro.com) supplemented with 10% fetal bovine serum (FBS; Atlanta Biologicals, www.atlantabio.com) at 5% CO_2 and 37°C. 3T3-L1 cells (ATCC®) were cultured in Dulbecco's Modified Eagle's Media (DMEM) supplemented with 10% newborn calf serum (NCS; Sigma-Aldrich, www.sigmaaldrich.com) at 5% CO_2 and 37°C. Pyriproxyfen, methoprene, 9-*cis* retinoic acid, and rosiglitazone were purchased from Sigma-Aldrich. Fenoxycarb and kinoprene were supplied from Chem Service (www.chemservice.com) and UVI 3003 was purchased from Tocris Bioscience (www.tocris.com).

PPARγ-gal4 construct

The human PPARγ DEF domain with a stop codon was amplified from pcDNA3.1-hPPARγ(ORF) using the primers harboring SalI and KpnI restriction enzymes sites. Digested PCR product was then inserted at the 3' end of the gal4 DNA binding domain in the pBIND plasmid (*Promega, www.promega.com*) by SalI/KpnI restriction sites. The final pBIND-gal4-hPPARγ(DEF) construct was verified by sequencing and named PPARγ-gal4 (Table 1).

RXRα-ORF construct

Human RXRα was amplified from pBIND-gal4-hRXRα(ORF) (provided by Dr. Andrew Wallace, North Carolina State University, Raleigh, NC) using the primers harboring Xbal and HindIII enzyme sites. Digested PCR product was then inserted in pcDNA3.1(-) plasmid by Xbal/HindIII restriction sites. The final pcDNA3.1-hRXRα-(ORF) construct was verified by sequencing and named RXRα-ORF (Table 1).

SRC1 construct

The full frame of SRC1 isoform E used in this study was constructed from the 5' region of SRC1 derived from the pSG5-SRC1A-ORF plasmid (provided by Dr. Seth Kullman, North Carolina State University, Raleigh, NC) and the 3' portion of SRC1E (representing amino acids 381-1399) derived from pSG5-SRC1E (S. Kullman). Splice variations at the 3' end of these mRNAs have been shown to render SRC1A much less effective than SRC1E as a coactivator [28, 29]. Therefore, the 3' end of the SRC1A open reading frame was replaced with that derived from SRC1E. The SRC1E ORF was created by

fusion PCR [30, 31]. The 5' portion of SRC1A was amplified using the primers: forward: 5'-CGTGCTGGTTATTGTGCTGT-3'; reverse : 5'-CTTCCGGGTGAGCATCCGAAACTTCCT-3'. The 3' portion of SRC1E was amplified using the primers: forward: 5'-AAGTTTCGGATGCTCACCCGGAAGTCA-3'; reverse: 5'-ATTGATGAGTTTGGACAAACCAC-3'. A twenty four base pair overlap was used to conjoin the two PCR products. The resulting final PCR product was purified and amplified using the primers, forward: 5'-ATGAGTGGCCTTGGGGACAGTTC-3' and reverse: 5'-CTAGTCTGTAGTCACCACAGAGAAGAACTC-3' primers at 60.5˚C annealing temperature using the Advantage HF 2 PCR kit (Clontech, www.clontech.com) to give a 4kb PCR product. Restriction sites ApaI/AflII were added to the final PCR product for cloning by PCR using the 4kb product as template with the forward primer: 5'-TACTATGGGCCCACCATGAGTGGCCTTGGGGACAGTTC-3' and reverse primer: 5'-TACTATCTTAAGCTAGTCTGTAGTCACCACAGAG-3'. The amplified SRC1E ORF was subcloned into ApaI/AflII sites of pcDNA3.1(-) plasmid and named SRC1 (Table 1).

Toxicity assessment

The IGRs were evaluated for their toxicity towards HepG2 cells. Cells were plated in a white bottom 96-well plate at a density of 10,000 cells/well in MEM supplemented with 10% FBS. One day later, cells were treated with an IGR at the concentrations used in the reporter gene assays in serum free media and incubated at 37°C for 24 hours. All treatments, including controls, contained the same concentration of DMSO (0.1%) used to deliver the IGRs. Cellular toxicity was measured using the CellToxTM Green Cytoxicity Assay

(Promega) following manufacturer's protocol. This assay functions on the principal that living cells cannot accumulate the cyanine dye provided in the assay; however the dye crosses compromised membranes of dead cells, binds to DNA, and fluoresces at 485 nm excitation/ 520 nm emission. Fluorescence was measured using a FLUOstar Omega microplate reader (BMG LabTech, www.bmglabtech.com).

PPARγ:RXRα complex activation

The human PPAR response element (PPRE) luciferase reporter gene transactivation system was used to assess the ability of the IGRs to activate the PPARγ:RXRα heterodimer complex. HepG2 cells were plated at a density of 25,000 cells per well in 96-well plates. The next day, 10 ng of RXRα-ORF, 10 ng of PPARγ-ORF, 10 ng of SRC1, 100 ng of PPRE-tk-luc (Table 1) firefly luciferase, and 6 ng of pRL-CMV *Renilla* luciferase control reporter vector (Table 1) were transfected using TransIT-LT1 transfection reagent (Mirus, www.mirusbio.com). Twenty-four hours later, the media in plates was replaced with serum-free media containing the candidate ligands (IGRs, positive controls) at the desired concentrations. DMSO was used as a solvent carrier for all ligands and kept constant among all treatments and controls ($\leq$0.2%, v/v). In some experiments, the RXRα antagonist (UVI 3003) also was included in the assay. After 24 hours or 48 hours of incubation, firefly and *Renilla* luciferase were measured using a Dual-Glo luciferase assay system (Promega) and a FLUOstar Omega microplate reader. Firefly luciferase values were normalized to the *Renilla* luciferase values. Positive controls (9-*cis* retinoic acid for RXRα and rosiglitazone for PPARγ) were evaluated to ensure proper assay function.

Individual subunit evaluation

Assays were performed using a luciferase reporter gene driven by a gal4 response element to evaluate activation of the individual receptor subunits by the IGRs. HepG2 cells were plated in 96-well plates at a density of 25,000 cells/well in DMEM supplemented with 10% FBS. The next day, 25 ng of PPARγ-gal4 or 50 ng of RXRα-gal4, 25 ng of SRC1, 6 ng of the pRL-CMV, and 125 ng of the reporter vector pG5 firefly luciferase were transfected using TransIT-LT1 transfection reagent to evaluate the individual receptor subunit. Twenty-four hours later, the media in plates was replaced with serum-free media containing the candidate ligands (IGRs, positive controls) at the desired concentrations. DMSO was used as a solvent carrier for all ligands and kept constant among all treatments and controls (0.1%, v/v). After 24 hours of incubation, firefly and *Renilla* luciferase were measured and firefly luciferase was normalized to the *Renilla* luciferase values.

BRET constructs

Human RXRα was amplified from pBIND-gal4-hRXRα(DEF) and digested with NheI then cloned into the pcDNA3.1-Rluc2 plasmid. We added a 21 base pair linker between gal4-RXRα(DEF) and Rluc2 to provide independent flexibility for the fused proteins. The 5' phosphate from the pcDNA3.1-Rluc2 plasmid was removed using Antarctic Phosphatase (New England Biolabs, www.neb.com) to limit the possibility of plasmid self-ligation. Final constructs were confirmed by sequencing and named RXRα-Rluc2 (Table 1).

Human PPARγ was fused to the fluorescent protein, Enhanced Blue Fluorescent Protein 2 (EBFP2; excitation 410 nm, emission: 475 nm), to evaluate dimerization with

RXRα-Rluc2. PCR fragments of the PPARγ open reading frame without a stop codon was amplified from pcDNA3.1-hPPARγ(ORF) using primers harboring a Nhe1/Xho1 restriction enzyme site and subcloned into the pcDNA3.1(-) plasmid. EBFP2 (Addgene, www.addgene.org) was amplified out of its parent plasmid with a stop codon containing a 30 base-pair linker at its 5'end. This construct was fused to the Xho1/Kpn1site at the 3' end of PPARγ to generate pcDNA3.1-hPPARγ-EBFP2. Linkers were placed between the PPARγ and EBFP2 sequences to supply independent flexibility for the fused proteins. The final construct was verified by sequencing and named PPARγ-EBFP2 (Table 1).

Human SRC1 was amplified from pcDNA3.1-hSRC1E using primers with KpnI/AfIII and ApaI/XhoI restriction enzyme sites then subcloned into pcDNA3.1(-). mAmetrine PCR fragments with a 30 base pair linker and without a stop codon were ligated in-frame to the Xhol/KpnI sites at the SRC1 5' end to create pcDNA3.1-mAmetrine-hSRC1E. Final constructs were confirmed by sequencing and named mAmetrine-SRC1 (Table 1). Arrangement of the fluorescent tags that were used for all BRET constructs provided the strongest BRET signal in preliminary experiments.

BRET assays

BRET assays were performed to gain further mechanistic insight regarding the interactions between the IGRs and the PPARγ:RXRα receptors. IGRs were evaluated for their ability to stimulate PPARγ:RXRα dimerization and the recruitment of SRC1 to the receptor complex. We previously observed that RXRα agonists stimulated receptor assembly, while PPARγ agonists did not stimulate assembly (Chapter 2). Thus, BRET assays

would assist in identifying the subunit responsible for activation of the receptor complex by the IGRs.

HepG2 cells were plated in 6-well plates at a density of 650,000 cells/well in MEM supplemented with 10% FBS. Fusion proteins were transfected into the cells 24 hours later using TransIT-LT1 transfection reagent, according to the manufacture's protocol. Each well was transfected with RXRα-Rluc2 (230 ng), PPARγ-EBFP2 (1380 ng), and mAmetrine-SRC1 (1380 ng). Twenty-four hours after transfection, cells were trypsinized, centrifuged for 2 minutes at 1500 g, and resuspended in PBS (Sigma-Aldrich). Cells originating from one well of the 6-well plate were divided into three wells of a white bottom 96-well plate. Cells were treated for 10 minutes with candidate agonists at the desired concentrations. DMSO was used as a solvent carrier for all ligands and kept constant among all treatments and controls (0.1%, v/v). Rluc2 substrate, DeepBlueC (Biotium, www. biotium.com), was added to each well at a final concentration of 5.0 μM, and fluorescence was immediately measured using a FLUOstar Omega microplate reader. The filter settings for the microplate reader were as followed: Rluc2 filter, 410 ± 40 nm; EBFP2 filter, 475 ± 15 nm; and mAmetrine filter, 535 ± 15 nm.

Dimerization of PPARγ and RXRα was detected as the BRET ratio by measuring the light emitted by the fluorophore (475 nm; PPARγ-EBFP2) divided by the light emitted by the photon donor protein (410 nm; RXRα-Rluc2) with corrections for both background fluorescence (using cells that were not transfected with the fusion proteins) and residual fluorescence from the donor into the fluorophore emission wavelength. The following formula was used to calculate the BRET ratio:

$$\text{Emission} \left(\frac{\text{Treated cells at 475 nm – untransfected cells at 475 nm}}{\text{Treated cells at 410 nm – untransfected cells at 410 nm}} \right) - \text{CF}$$

where CF (correction factor) equals the emission measured at 475 nm in cells transfected with Rluc2-RXRα alone minus the emission of untransfected cells at 475 nm divided by the emission of Rluc2-RXRα alone at 410 nm minus the emission of untransfected cells at 410 nm. The CF corrects for residual fluorescence from the donor into the emission reading of the fluorophore. Recruitment of SRC1 was determined using this same general procedure with BRET ratios determined using emissions detected at 535 nm instead of 475 nm.

Pre-adipocyte differentiation and lipid accumulation

The ability of the IGRs to stimulate lipid accumulation was assessed using mouse 3T3-L1 pre-adipocytes. Cells were plated in clear bottom 96-well plates at a density of 6,500 cells/well in high glucose DMEM (ATCC®) supplemented with 10% NCS. All treatments, including controls, were replicated three times. Once cells reached 100% confluence, media was replaced with fresh media and the cells were incubated for an additional 2 days. The media was then replaced with differentiation media: high glucose DMEM supplemented with 10% FBS and the PPARγ agonist. Two days later (day 0), media was replaced with adipocyte maintenance media: high glucose DMEM supplemented with 10% FBS, 10 μg/ml insulin (Sigma-Aldrich) and the PPARγ agonist. All treatments, including controls contained 0.1% DMSO which was used to deliver the PPARγ agonists. Treatment media was renewed on days 2 and 4. On day 6, cells were washed with 200 μL of PBS and then incubated for 10

minutes with 200 μL of PBS and 5 μL of AdipoRed reagent, (Lonza, www.lonza.com) which fluoresces upon partitioning into lipid droplets [32]. Lipid accumulation was quantified as the fluorescence measured at an excitation of 485 nm and an emission of 572 nm using a FLUOstar Omega microplate. Fluorescence values were normalized to the mean fluorescence measured in the negative controls.

The ability of IGRs to stimulate differentiation of mouse 3T3-L1 cells with accompanying lipid accumulation was assessed by staining cells with Oil Red O [33]. These assays were performed under the same conditions as described using AdipoRed reagent. On day 6, cells were washed twice with PBS and fixed with 3.7% formalin (Sigma-Aldrich) for 30-60 minutes at room temperature. Cells were then washed twice with distilled water and rinsed in 60% isopropanol (Fischer Scientific, www.fishersci.com) for 5 minutes. Cells were stained with Oil-Red-O for 60 minutes. The excess stain was removed by washing the cells with 60% ethanol and three times with distilled water. Cells were inspected for differentiation and lipid accumulation using a Nikon Eclipse microscope and imaged using a MicroPublisher 3.3 RTV (QImaging) camera affixed to the microscope at 100X and 400X.

Statistics

Significant ($p<0.05$) differences between treatments and controls were evaluated using One Way Analysis of Variance (ANOVA) accompanied by Tukeys Multiple Comparison Test for reporter gene and BRET assays. Homogeneity of the variances was confirmed by Levene's test. Two-tailed Student's t-tests were used to evaluate significant ($p<0.05$) differences between treatments and controls for lipid accumulation assays.

Results

Toxicity assessment

Pyriproxyfen and methoprene evoked no discernible toxicity to the HepG2 cells at concentrations as high as 100 μM (Fig. 2A,C). Fenoxycarb and kinoprene elicited toxicity towards HepG2 cells at 100 μM (Fig. 2B,D). The highest concentration used for all IGRs in subsequent assays was 30 μM. BRET assays were performed at concentrations as high as 300 μM; however, HepG2 cells were exposed to IGRs in the BRET assay for only 10 minutes. Therefore, toxicity was not a concern due to a short exposure window.

PPARγ:RXRα complex activation

Experiments were performed to determine whether the IGRs pyriproxyfen, fenoxycarb, methoprene, and kinoprene activate the human PPARγ signaling pathway. Exposure to pyriproxyfen, fenoxycarb, methoprene, or kinoprene for 24 (Fig. 3A-D) or 48 (Fig. 3E-H) hours activated the PPARγ:RXRα receptor complex. Fenoxycarb did not activate PPARγ:RXRα after 24 hour exposure, but significantly suppressed basal activity at 30 μM. (Fig. 3B). After 48 hour exposure, fenoxycarb significantly activated the receptor complex at 10 μM with continued suppression at 30 μM. (Fig. 3F).

Individual subunit evaluation

The PPARγ:RXRα complex is reportedly subject to activation by ligands to either subunit [15]. We investigated whether the IGRs interacted with the PPARγ or the RXRα subunit using gal4 fused receptor subunits and a luciferase reporter gene driven by the gal4

response element. All of the IGRs activated the PPARγ receptor subunit (Fig. 4A-D). Fenoxycarb, methoprene, and kinoprene also activated RXRα (Fig. 4F-H); while, pyriproxyfen had no effect with this receptor subunit (Fig. 4E). Heterodimerization with putative endogenous receptor subunits did not confound interpretation of these assays as activation was observed only with substrates specific to the transfected receptor subunit (Fig. 5).

RXRα inhibition

Fenoxycarb, methoprene, and kinoprene activated both the PPARγ and RXRα receptor subunits. Reporter gene transcription assays were performed with UVI 3003, a specific RXRα inhibitor, to determine the relative contribution of RXRα to the activation of the PPARγ:RXRα receptor complex. Experiments performed with the known RXRα agonist 9-*cis* retinoic acid and the known PPARγ agonist rosiglitazone demonstrated that UVI 3003 inhibited receptor activity due to antagonistic interaction with the RXRα subunit and had no inhibitory effects on the PPARγ subunit (Fig. 6A, B). UVI 3003 did not inhibit PPARγ:RXRα activation by fenoxycarb, methoprene, or kinoprene (Fig. 6D-F). Therefore, although these IGRs interacted with both receptor subunits, activation of the receptor complex was specifically due to interaction with the PPARγ subunit.

BRET

Results generated thus far indicated that all of the IGRs activated the PPARγ:RXRα complex through their interaction with the PPARγ subunit. Consistent with previous

observations (Chapter 2), protein dimerization assays performed using BRET and known PPARγ or RXRα agonists revealed that RXRα ligands stimulated PPARγ:RXRα:SRC1 assembly; while PPARγ ligands had no effect on receptor complex assembly (Fig. 7). None of the IGRs stimulated receptor assembly (Fig. 8) supporting the finding that the PPARγ subunit and not the RXRα subunit is the target of IGR action.

Adipocyte differentiation/ lipid accumulation

PPARγ is recognized as a master regulator of pre-adipocyte differentiation into adipocytes and lipid accumulation within the differentiated adipocytes [34, 35]. The IGRs stimulated PPARγ:RXRα receptor activation; therefore, these compounds were evaluated for their ability to stimulate pre-adipocyte differentiation into adipocytes with lipid accumulation. All of the IGRs (30 μM) increased the proportion of pre-adipocytes that underwent differentiation and significantly increased lipid accumulation associated with the cells (Fig. 9).

Discussion

Metabolic syndrome is a global health crisis with a steadily rising prevalence due to increasing obesity rates [36]. Imbalance of food intake and energy expended is recognized as a major cause of this condition [37]. More current studies suggested that exposure to environmental chemicals may be contributing to lipid disorders [38, 39]. There are tens of thousands of chemicals in use and hundreds more are created each year [40]. Only a small portion of these chemicals have been evaluated for hazard. An even smaller portion have

been evaluated for potential to disrupt lipid and glucose signaling [41]. The National Pesticide Information Center could not find any studies which evaluated the ability of methoprene to cause endocrine disruption in humans and long-term studies investigating pyriproxyfen only examined the estrogen, androgen, and thyroid hormone signaling pathways [42, 43]. Results of the present study demonstrated that IGRs interact with the PPARγ signaling pathway in a manner that promotes adipogenesis.

Our major goal was to evaluate if the IGRs had the ability to activate the PPARγ:RXRα heterodimer and determine the mechanistic contributions of each subunit towards activation of the receptor complex. All of the IGRs activated the PPARγ:RXRα receptor complex and activation was due to interactions with the PPARγ receptor subunit. An important regulatory characteristic of PPARγ:RXRα heterodimers is that activation occurs due to ligand-mediated interactions with PPARγ, RXRα, or both as a consequence of being a permissive heterodimer [44-47]. Whereas, RXRα subunits are silent in non-permissive heterodimers and heterodimer activation can only occur through ligand-mediated interactions with the partner subunit [48]. Although fenoxycarb, methoprene, and kinoprene were capable of activating both the PPARγ and RXRα subunits, RXRα appeared to act as a silent partner incapable of contributing to the overall activation of the PPARγ:RXRα receptor complex. Studies have reported that RXRα could act as a silent partner with PPARγ; consequently, this along with other increasing evidence has led others to question the concepts of permissivity [49-51].

Conflicting findings have reported thyroid hormone receptor:RXR and retinoic acid receptor:RXR complexes as both non-permissive and permissive heterodimers [52-55].

Dawson and Xia have raised the notion that RXR heterodimers are conditionally permissive [51]. RXRα activity depends upon cellular environment, tissue specificity, and the ability of RXRα ligands to recruit specific corepressors/coactivators to the complex [51, 56]. Our experiments demonstrated that the permissive nature of the PPARγ:RXRα complex could be conditional.

Methoprene and kinoprene's ability to strongly activate the RXRα subunit, as well as, the PPARγ subunit would lead one to predict that transactivation by these IGRs would be greater than the transactivation by pyriproxyfen or fenoxycarb. Yet, we did not observe two activated subunits leading to an additive or synergistic response due to methoprene or kinoprene. Reports of dual ligand occupancy of permissive heterodimers resulting in additive or synergistic activation are limited. Additive or synergistic outcomes due to dual subunit ligands are more commonly observed when the measured endpoints are more apical (e.g., cellular proliferation and death) and this may be due to the ligand's ability to activate other RXRα signaling pathways [52, 57, 58]. Alternatively, the lack of observable additivity or synergy could be due to the silencing of RXRα.

Permissive partners of RXR have greater functional dominance than their RXR partner; thus, partner subunits have the ability to modulate RXRα responses [51]. In this study, the PPARγ subunit dominated the PPARγ:RXRα transactivation response, as well as, BRET dimerization responses. As PPARγ agonists, the IGRs had no effect on dimerization of PPARγ and RXRα consistent with the findings in Chapter 2. Vitamin D and retinoic acid receptor agonists had no effect on the formation of their respective complexes with RXRα; instead, these ligands stabilized and activated constitutively formed receptor complexes [59,

60]. Fluorescence resonance energy transfer assays showed that PPAR:RXR dimerization occurred prior to ligand or DNA binding, and ligand-binding stabilized existing PPAR:RXR complexes to DNA [61]. This study further supports the existence of constitutively formed PPARγ:RXRα receptor complexes with the ability to be activated by PPARγ agonists. Additionally, RXRα ligands stimulated dimerization of PPARγ and RXRα in this study and in previous chapters. This is consistent with studies showing that RXR ligands enhance the formation of RXR heterodimers [60, 62-64].

The IGR's inability to recruit SRC1 paralleled their inability to stimulate dimerization. Recruitment of SRC1 to ligand-occupied PPAR has been reported; however, these studies used cell free experimental systems [65, 66]. RXR agonists were reported to recruit SRC1 to the PPARγ:RXRα complex, and our study further demonstrated the critical role of these ligands and their subunit (RXRα) in PPARγ:RXRα:SRC1 complex assembly [47, 67, 68].

Methoprene is readily metabolized by vertebrates into methoprene acid, 7-methoxy-citronellal, and its corresponding acid [69, 70]. Methoprene acid activated mammalian RXRα, thus exposure to methoprene poses high risk of hazard to humans due to its ability to be biotransformed into a potentially harmful metabolite [70]. Concentrations of IGRs in human plasma have not been reported and additional studies are warranted to determine whether humans are subjected to sufficient IGR exposure with the potential to contribute to metabolic syndrome.

A positive correlation exists between the prevalence of metabolic syndrome in humans and among companion animals (i.e. household dogs and cats) [71]. Environmental chemical exposure has been suggested to play a role in human metabolic syndrome and obesity [39,

72]. However, toxicological studies evaluating the effects of environmental chemical exposure on companion pets often investigate the impact of these chemicals on the development of reproductive toxicities and cancers [73-77]. Obesogenic studies for companion pets primarily focus on the role of diet [78-80]. Additional studies are warranted to determine whether pets are subjected to sufficient IGR exposure with the potential to contribute to metabolic syndrome.

References

1. Batsis, J.A., R.E. Nieto-Martinez, and F. Lopez-Jimenez, Metabolic syndrome: From global epidemiology to individualized medicine. Clin Pharmacol Ther, 2007. **82**(5): p. 509-524.
2. Spalding, A., J. Kernan, and W. Lockette, The metabolic syndrome: A modern plague spread by modern technology. J Clin Hypertens (Greenwich), 2009. **11**(12): p. 755-760.
3. Grundy, S.M., H.B. Brewer, J.I. Cleeman, S.C. Smith, C. Lenfant, and C. Participants, Definition of metabolic syndrome - report of the national heart, lung, and blood institute/american heart association conference on scientific issues related to definition. Circulation, 2004. **109**(3): p. 433-438.
4. Ford, E.S., W.H. Giles, and W.H. Dietz, Prevalence of the metabolic syndrome among us adults - findings from the third national health and nutrition examination survey. Jama-Journal of the American Medical Association, 2002. **287**(3): p. 356-359.
5. Ahmadian, M., J.M. Suh, N. Hah, C. Liddle, A.R. Atkins, M. Downes, and R.M. Evans, PPPAR gamma signaling and metabolism: The good, the bad and the future. Nature Medicine, 2013. **19**(5): p. 557-566.
6. http://themedicalbiochemistrypage.org/fatty-acid-oxidation.php#ketogenesis, 2004
7. Chakravarthy, M.V., I.J. Lodhi, L. Yin, R.R.V. Malapaka, H.E. Xu, J. Turk, and C.F. Semenkovich, Identification of a physiologically relevant endogenous ligand for PPAR alpha in liver. Cell, 2009. **138**(3): p. 476-488.

8. Peeters, A. and M. Baes, Role of PPAR alpha in hepatic carbohydrate metabolism. PPAR Research, 2010.

9. Desvergne, B. and W. Wahli, Peroxisome proliferator-activated receptors: Nuclear control of metabolism. Endocrine Reviews, 1999. **20**(5): p. 649-688.

10. Pyper, S.R., N. Viswakarma, S. Yu, and J.K. Reddy, PPPARalpha: Energy combustion, hypolipidemia, inflammation and cancer. Nucl Recept Signal. **8**: p. e002.

11. Puigserver, P., G. Adelmant, Z. Wu, M. Fan, J. Xu, B. O'Malley, and B.M. Spiegelman, Activation of ppargamma coactivator-1 through transcription factor docking. Science, 1999. **286**(5443): p. 1368-1371.

12. Wang, Y.X., PPARs: Diverse regulators in energy metabolism and metabolic diseases. Cell Research, 2010. **20**(2): p. 124-137.

13. Vega, R.B., J.M. Huss, and D.P. Kelly, The coactivator pgc-1 cooperates with peroxisome proliferator-activated receptor alpha in transcriptional control of nuclear genes encoding mitochondrial fatty acid oxidation enzymes. Mol Cell Biol, 2000. **20**(5): p. 1868-1876.

14. Jain, S., S. Pulikuri, Y. Zhu, C. Qi, Y.S. Kanwar, A.V. Yeldandi, M.S. Rao, and J.K. Reddy, Differential expression of the peroxisome proliferator-activated receptor gamma (ppargamma) and its coactivators steroid receptor coactivator-1 and PPAR-binding protein pbp in the brown fat, urinary bladder, colon, and breast of the mouse. Am J Pathol, 1998. **153**(2): p. 349-354.

15. Perez, E., W. Bourguet, H. Gronemeyer, and A.R. de Lera, Modulation of RXR function through ligand design. Biochimica Et Biophysica Acta-Molecular and Cell Biology of Lipids, 2012. **1821**(1): p. 57-69.

16. Larsen, T.M., S. Toubro, and A. Astrup, Ppargamma agonists in the treatment of type ii diabetes: Is increased fatness commensurate with long-term efficacy? Int J Obes Relat Metab Disord, 2003. **27**(2): p. 147-161.

17. Peraza, M.A., A.D. Burdick, H.E. Marin, F.J. Gonzalez, and J.M. Peters, The toxicology of ligands for peroxisome proliferator-activated receptors (PPAR). Toxicol Sci, 2006. **90**(2): p. 269-295.

18. Staal, G.B., Insect growth-regulators with juvenile-hormone activity. Annual Review of Entomology, 1975. **20**: p. 417-460.

19. Stephen Saul, J.S., Methoprene on papayas-persistence and toxicity to different developmental stages on fruit-flies (diptera, tephritidae. J Econ Entomol, 1990. **83**(3): p. 901-904.

20. EPA. Available from: http://www.epa.gov/oppsrrd1/REDs/factsheets/0030fact.pdf.

21. Mike Merchant, J.R. Controlling fleas. http://theurbanrancher.tamu.edu/retiredsite/bugs/l1738.pdf

22. Gupta R., N.H., Doss R., Bland S., Canerdy T., J. Zieren, Toxicity and safety assessment of fipronil, s-methoprene, and amitraz in dogs following topical certifect(r) application. 2015.

23. Edvardsson, U., M. Bergstrom, M. Alexandersson, K. Bamberg, B. Ljung, and B. Dahllof, Rosiglitazone (brl49653), a ppargamma-selective agonist, causes peroxisome proliferator-like liver effects in obese mice. J Lipid Res, 1999. **40**(7): p. 1177-1184.

24. Carmona, M.C., K. Louche, B. Lefebvre, A. Pilon, N. Hennuyer, V. Audinot-Bouchez, C. Fievet, G. Torpier, P. Formstecher, P. Renard, P. Lefebvre, C. Dacquet, B. Staels, L. Casteilla, and L. Penicaud, S 26948: A new specific peroxisome proliferator activated receptor gamma modulator with potent antidiabetes and antiatherogenic effects. Diabetes, 2007. **56**(11): p. 2797-2808.

25. Wang, Y.H. and G.A. LeBlanc, Interactions of methyl farnesoate and related compounds with a crustacean retinoid x receptor. Mol. Cell. Endocrin., 2009. **309**: p. 109-116.

26. Kocan, M., H.B. See, R.M. Seeber, K.A. Eidne, and K.D.G. Pfleger, Demonstration of improvements to the bioluminescence resonance energy transfer (bret) technology for the monitoring of g protein-coupled receptors in live cells. J. Biomol. Screening, 2008. **13**(888): p. DOI: 10.1177/1087057108324032.

27. Kim, J.B., H.M. Wright, M. Wright, and B.M. Spiegelman, Add1/srebp1 activates ppargamma through the production of endogenous ligand. Proc Natl Acad Sci U S A, 1998. **95**(8): p. 4333-4337.

28. Maijer, O.C., E. Kalkhoven, S. van der Laan, P.J. Steenbergen, S.H. Houtman, T.F. Dijkmans, D. Pearce, and E.R. de Kloet, Steroid receptor coactivator-1 splice variants differentially affect corticosteroid receptor signaling. Endocrinology, 2005. **146**: p. 1438-1448.

29. Kalkhoven, E., J.E. Valentine, D.M. Heery, and M.G. Parker, Isoforms of steroid receptor co-activator 1 differ in their ability to potentiate transcription by the oestogen receptor. EMBO J., 1998. **17**: p. 232-243.

30. Kalkhoven, E., J.E. Valentine, D.M. Heery, and M.G. Parker, Isoforms of steroid receptor co-activator 1 differ in their ability to potentiate transcription by the oestrogen receptor. Embo j, 1998. **17**(1): p. 232-243.

31. Meijer, O.C., E. Kalkhoven, S. van der Laan, P.J. Steenbergen, S.H. Houtman, T.F. Dijkmans, D. Pearce, and E.R. de Kloet, Steroid receptor coactivator-1 splice variants differentially affect corticosteroid receptor signaling. Endocrinology, 2005. **146**(3): p. 1438-1448.

32. Lonza. Adipored (tm) assay reagent. 2010; Available from: http://bio.lonza.com/uploads/tx_mwaxmarketingmaterial/Lonza_ManualsProductInstructions_AdipoRed_Assay_Reagent.pdf.

33. Rizzatti, V., F. Boschi, M. Pedrotti, E. Zoico, A. Sbarbati, and M. Zamboni, Lipid droplets characterization in adipocyte differentiated 3t3-l1 cells: Size and optical density distribution. Eur J Histochem, 2013. **57**(3).

34. Rosen, E.D., C.H. Hsu, X. Wang, S. Sakai, M.W. Freeman, F.J. Gonzalez, and B.M. Spiegelman, C/ebpalpha induces adipogenesis through ppargamma: A unified pathway. Genes Dev, 2002. **16**(1): p. 22-26.

35. Moseti, D., A. Regassa, and W.K. Kim, Molecular regulation of adipogenesis and potential anti-adipogenic bioactive molecules. Int J Mol Sci, 2016. **17**(1).

36. Kaur, J., A comprehensive review on metabolic syndrome. Cardiology research and practice, 2014. **2014**: p. 943162-943162.

37. Hill, J.O., H.R. Wyatt, and J.C. Peters, Energy balance and obesity. Circulation, 2012. **126**(1): p. 126-132.

38. Tuma, R.S., Environmental chemicals - not just overeating - may cause obesity. Journal of the National Cancer Institute, 2007. **99**(11): p. 835-835.

39. Ntp workshop: Role of envrionmental chemicals in the development of diabetes and obesity. 2011, Raleigh, NC: National Toxicology Program.

40. Agency, E.P. Chemical safety for sustainability strategic research action plan 2016-2019. 2015; Available from: http://www.epa.gov/sites/production/files/2015-10/documents/strap_2016_css_508.pdf.

41. Janesick, A.S. and B. Blumberg, Obesogens: An emerging threat to public health. Am J Obstet Gynecol, 2016.

42. Wick, K.B., C.; Buhl, K.; Stone, D. Methoprene general fact sheet. 2012; Available from: http://npic.orst.edu/factsheets/methogen.html.

43. Hallman, A.B., C.; Buhl, K.; Stone, D. Pyriproxyfen general fact sheet. 2015; Available from: http://npic.orst.edu/factsheets/pyriprogen.html.

44. Leblanc, B.P. and H.G. Stunnenberg, 9-cis retinoic acid signaling: Changing partners causes some excitement. Genes Dev, 1995. **9**(15): p. 1811-1816.

45. Mukherjee, R., L. Jow, D. Noonan, and D.P. McDonnell, Human and rat peroxisome proliferator activated receptors (PPARs) demonstrate similar tissue distribution but

different responsiveness to PPAR activators. Journal of Steroid Biochemistry and Molecular Biology, 1994. **51**(3-4): p. 157-166.

46. Mukherjee, R., J. Strasser, L. Jow, P. Hoener, J.R. Paterniti, and R.A. Heyman, RXR agonists activate PPAR alpha-inducible genes, lower triglycerides, and raise HDl levels in vivo. Arteriosclerosis Thrombosis and Vascular Biology, 1998. **18**(2): p. 272-276.

47. Schulman, I.G., G. Shao, and R.A. Heyman, Transactivation by retinoid x receptor peroxisome proliferator-activated receptor gamma (PPARgamma) heterodimers: Intermolecular synergy requires only the PPAR gamma hormone-dependent activation function. Molecular and Cellular Biology, 1998. **18**(6): p. 3483-3494.

48. Evans, R.M. and D.J. Mangelsdorf, Nuclear receptors, rxr, and the big bang. Cell, 2014. **157**(1): p. 255-266.

49. Mascrez, B., N.B. Ghyselinck, P. Chambon, and M. Mark, A transcriptionally silent rxralpha supports early embryonic morphogenesis and heart development. Proc Natl Acad Sci U S A, 2009. **106**(11): p. 4272-4277.

50. Mascrez, B., M. Mark, W. Krezel, V. Dupe, M. LeMeur, N.B. Ghyselinck, and P. Chambon, Differential contributions of af-1 and af-2 activities to the developmental functions of RXR alpha. Development, 2001. **128**(11): p. 2049-2062.

51. Dawson, M.I. and Z. Xia, The retinoid x receptors and their ligands. Biochim Biophys Acta, 2012. **1821**(1): p. 21-56.

52. Botling, J., D.S. Castro, F. Oberg, K. Nilsson, and T. Perlmann, Retinoic acid receptor/retinoid x receptor heterodimers can be activated through both subunits

providing a basis for synergistic transactivation and cellular differentiation. J Biol Chem, 1997. **272**(14): p. 9443-9449.

53. Castillo, A.I., R. Sanchez-Martinez, J.L. Moreno, O.A. Martinez-Iglesias, D. Palacios, and A. Aranda, A permissive retinoid x receptor/thyroid hormone receptor heterodimer allows stimulation of prolactin gene transcription by thyroid hormone and 9-cis-retinoic acid. Mol Cell Biol, 2004. **24**(2): p. 502-513.

54. Kojetin, D.J., E. Matta-Camacho, T.S. Hughes, S. Srinivasan, J.C. Nwachukwu, V. Cavett, J. Nowak, M.J. Chalmers, D.P. Marciano, T.M. Kamenecka, A.I. Shulman, M. Rance, P.R. Griffin, J.B. Bruning, and K.W. Nettles, Structural mechanism for signal transduction in rxr nuclear receptor heterodimers. Nat Commun, 2015. **6**.

55. Lammi, J., T. Perlmann, and P. Aarnisalo, Corepressor interaction differentiates the permissive and non-permissive retinoid x receptor heterodimers. Arch Biochem Biophys, 2008. **472**(2): p. 105-114.

56. Roszer, T., M.P. Menendez-Gutierrez, M. Cedenilla, and M. Ricote, Retinoid x receptors in macrophage biology. Trends in Endocrinology and Metabolism, 2013. **24**(9): p. 460-468.

57. Shimizu, M. and H. Moriwaki, Synergistic effects of ppargamma ligands and retinoids in cancer treatment. PPAR Res, 2008. **2008**: p. 181047.

58. Garcia-Bates, T.M., C.J. Baglole, M.P. Bernard, T.I. Murant, P.J. Simpson-Haidaris, and R.P. Phipps, Peroxisome proliferator-activated receptor gamma ligands enhance human b cell antibody production and differentiation. J Immunol, 2009. **183**(11): p. 6903-6912.

59. Prufer, K., A. Racz, G.C. Lin, and J. Barsony, Dimerization with retinoid x receptors promotes nuclear localization and subnuclear targeting of vitamin d receptors. Journal of Biological Chemistry, 2000. **275**(52): p. 41114-41123.

60. Dong, D. and N. Noy, Heterodimer formation by retinoid x receptor: Regulation by ligands and by the receptor's self-association properties. Biochemistry, 1998. **37**(30): p. 10691-10700.

61. Feige, J.N., L. Gelman, C. Tudor, Y. Engelborghs, W. Wahli, and B. Desvergne, Fluorescence imaging reveals the nuclear behavior of peroxisome proliferator-activated receptor/retinoid x receptor heterodimers in the absence and presence of ligand. J Biol Chem, 2005. **280**(18): p. 17880-17890.

62. Kersten, S., L. Pan, and N. Noy, On the role of ligand in retinoid signaling: Positive cooperativity in the interactions of 9-cis retinoic acid with tetramers of the retinoid x receptor. Biochemistry, 1995. **34**(43): p. 14263-14269.

63. Kersten, S., D. Kelleher, P. Chambon, H. Gronemeyer, and N. Noy, Retinoid x receptor alpha forms tetramers in solution. Proc Natl Acad Sci U S A, 1995. **92**(19): p. 8645-8649.

64. Kersten, S., L. Pan, P. Chambon, H. Gronemeyer, and N. Noy, Role of ligand in retinoid signaling. 9-cis-retinoic acid modulates the oligomeric state of the retinoid x receptor. Biochemistry, 1995. **34**(42): p. 13717-13721.

65. DiRenzo, J., M. Soderstrom, R. Kurokawa, M.H. Ogliastro, M. Ricote, S. Ingrey, A. Horlein, M.G. Rosenfeld, and C.K. Glass, Peroxisome proliferator-activated receptors and retinoic acid receptors differentially control the interactions of retinoid x receptor

heterodimers with ligands, coactivators, and corepressors. Mol Cell Biol, 1997. **17**(4): p. 2166-2176.

66. Zhou, G., R. Cummings, Y. Li, S. Mitra, H.A. Wilkinson, A. Elbrecht, J.D. Hermes, J.M. Schaeffer, R.G. Smith, and D.E. Moller, Nuclear receptors have distinct affinities for coactivators: Characterization by fluorescence resonance energy transfer. Mol Endocrinol, 1998. **12**(10): p. 1594-1604.

67. Yang, W., C. Rachez, and L.P. Freedman, Discrete roles for peroxisome proliferator-activated receptor gamma and retinoid x receptor in recruiting nuclear receptor coactivators. Mol Cell Biol, 2000. **20**(21): p. 8008-80017.

68. Nettles, K.W. and G.L. Greene, Ligand control of coregulator recruitment to nuclear receptors. Annu Rev Physiol, 2005. **67**: p. 309-333.

69. Schoff, P.K. and G.T. Ankley, Effects of methoprene, its metabolites, and breakdown products on retinoid-activated pathways in transfected cell lines. Environmental Toxicology and Chemistry, 2004. **23**(5): p. 1305-1310.

70. Harmon, M.A., M.F. Boehm, R.A. Heyman, and D.J. Mangelsdorf, Activation of mammalian retinoid x receptors by the insect growth regulator methoprene. Proc Natl Acad Sci U S A, 1995. **92**(13): p. 6157-6160.

71. de Godoy, M.R. and K.S. Swanson, Companion animals symposium: Nutrigenomics: Using gene expression and molecular biology data to understand pet obesity. J Anim Sci, 2013. **91**(6): p. 2949-2964.

72. Zeliger, H.I., Lipophilic chemical exposure as a cause of cardiovascular disease. Interdiscip Toxicol, 2013. **6**(2): p. 55-62.

73. Wooten, K.J. and P.N. Smith, Canine toys and training devices as sources of exposure to phthalates and bisphenol a: Quantitation of chemicals in leachate and in vitro screening for endocrine activity. Chemosphere, 2013. **93**(10): p. 2245-2253.

74. Bellingham, M., N. Fiandanese, A. Byers, C. Cotinot, N.P. Evans, P. Pocar, M.R. Amezaga, R.G. Lea, K.D. Sinclair, S.M. Rhind, and P.A. Fowler, Effects of exposure to environmental chemicals during pregnancy on the development of the male and female reproductive axes. Reprod Domest Anim, 2012. **47 Suppl 4**: p. 15-22.

75. Takashima-Uebelhoer, B.B., L.G. Barber, S.E. Zagarins, E. Procter-Gray, A.L. Gollenberg, A.S. Moore, and E.R. Bertone-Johnson, Household chemical exposures and the risk of canine malignant lymphoma, a model for human non-hodgkin's lymphoma. Environmental Research, 2012. **112**: p. 171-176.

76. Severe, S., P. Marchand, I. Guiffard, F. Morio, A. Venisseau, B. Veyrand, B. Le Bizec, J.-P. Antignac, and J. Abadie, Pollutants in pet dogs: A model for environmental links to breast cancer. Springerplus, 2015. **4**.

77. Hayes, H.M., R.E. Tarone, K.P. Cantor, C.R. Jessen, D.M. McCurnin, and R.C. Richardson, Case-control study of canine malignant-lymphoma - positive association with dog owners use of 2,4-dichlorophenoxyacetic acid herbicides. Journal of the National Cancer Institute, 1991. **83**(17): p. 1226-1231.

78. Mason, E., Obesity in pet dogs. Veterinary Record, 1970. **86**(21): p. 612.

79. Deng, P. and K.S. Swanson, Companion animals symposium: Future aspects and perceptions of companion animal nutrition and sustainability12. J Anim Sci, 2015. **93**(3): p. 823-834.

80. Crane, S.W., Occurrence and management of obesity in companion animals. Journal of Small Animal Practice, 1991. **32**(6): p. 275-282.

Table 1. Identification and description of constructs used in all experiments.

Construct	Full Name	Description	Assays Used
PPARγ-ORF	pcDNA3.1-hPPARγ-(ORF)	Receptor subunit	PPARγ:RXRα complex activation and RXRα inhibition
RXRα-ORF	pcDNA3.1-hRXRα-(ORF)	Receptor subunit	PPARγ:RXRα complex activation and RXRα inhibition
SRC1	pcDNA3.1-hSRC1E	Coactivator	PPARγ:RXRα complex activation and RXRα inhibition
PPRE-tk-luc	PPRE X3-TK-luc	Firefly luciferase reporter gene	PPARγ:RXRα complex activation and RXRα inhibition
pRL-CMV	pRL-CMV	Provided *Renilla* luciferase	PPARγ:RXRα complex activation RXRα inhibition Individual subunit evaluation
PPARγ-gal4	pBIND-gal4-hPPARγ (DEF)	Gal4-fused receptor subunit	Individual subunit evaluation
RXRα-gal4	pBIND-gal4-hRXRα(DEF)	Gal4-fused receptor subunit	Individual subunit evaluation
pG5-luc	pG5-luc	Provided firefly luciferase	Individual subunit evaluation
mAmetrine-SRC1	pcDNA3.1-mAmetrine-hSRC1E	mAmetrine fused coactivator	Individual subunit evaluation BRET
PPARγ-EBFP2	pcDNA3.1-hPPARγ-EBFP2	EBFP2-fused receptor subunit	BRET
RXRα-Rluc2	pcDNA3.1-gal4-hRXRα(DEF)-Rluc2	Rluc2-fused receptor subunit	BRET
pcDNA3.1(-)	pcDNA3.1(-)	Empty vector	BRET

Figure 1. Chemical structures of the PPARγ agonist rosiglitazone and the IGRs pyriproxyfen, fenoxycarb, methoprene, and kinoprene.

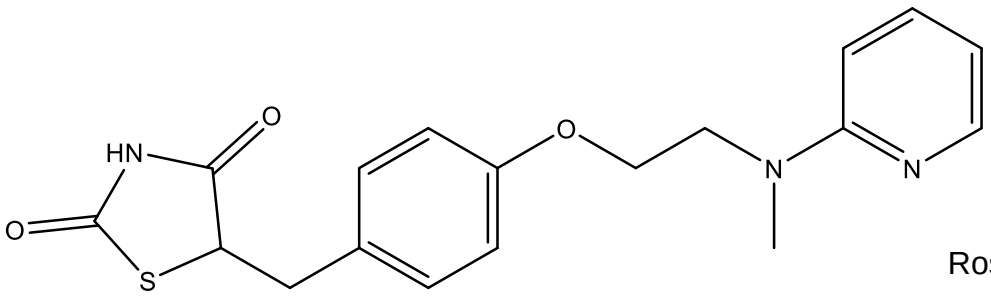

Rosiglitazone

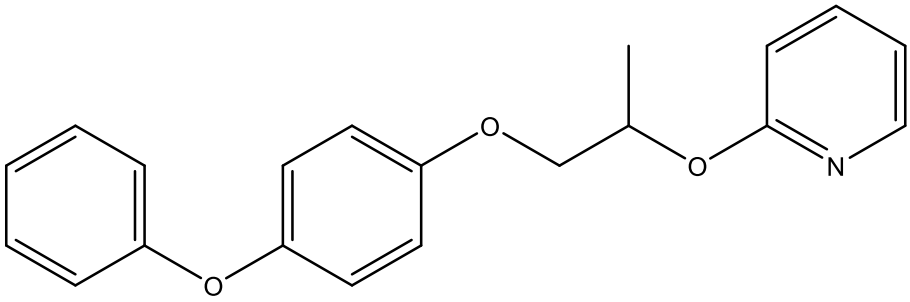

Pyriproxyfen

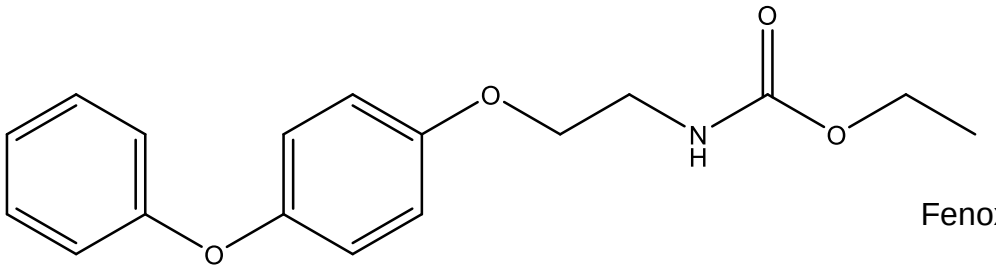

Fenoxycarb

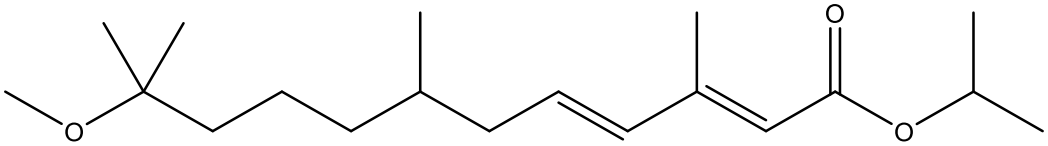

Methoprene

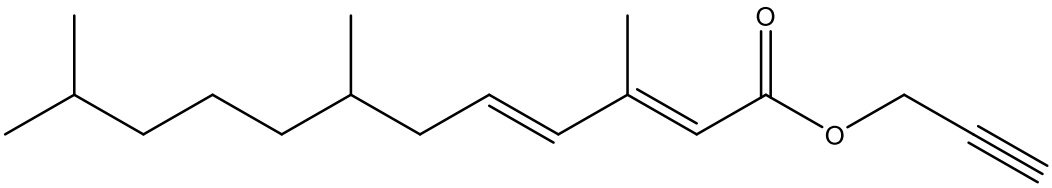

Kinoprene

Figure 2. Toxicity of pyriproxyfen (A), fenoxycarb (B), methoprene (C) and kinoprene (D) to HepG2 cells. Toxicity was indicated by increased uptake of fluorescent dye at 485 nm excitation/520 nm emission. Red circle denotes cellular fluorescence in the absence of ligand (control). Data are presented as means with error bars depicting standard deviations (n=3). An asterisk denotes a significant difference from the control ($p<0.05$, One-Way ANOVA, Tukey's Multiple Comparison Test).

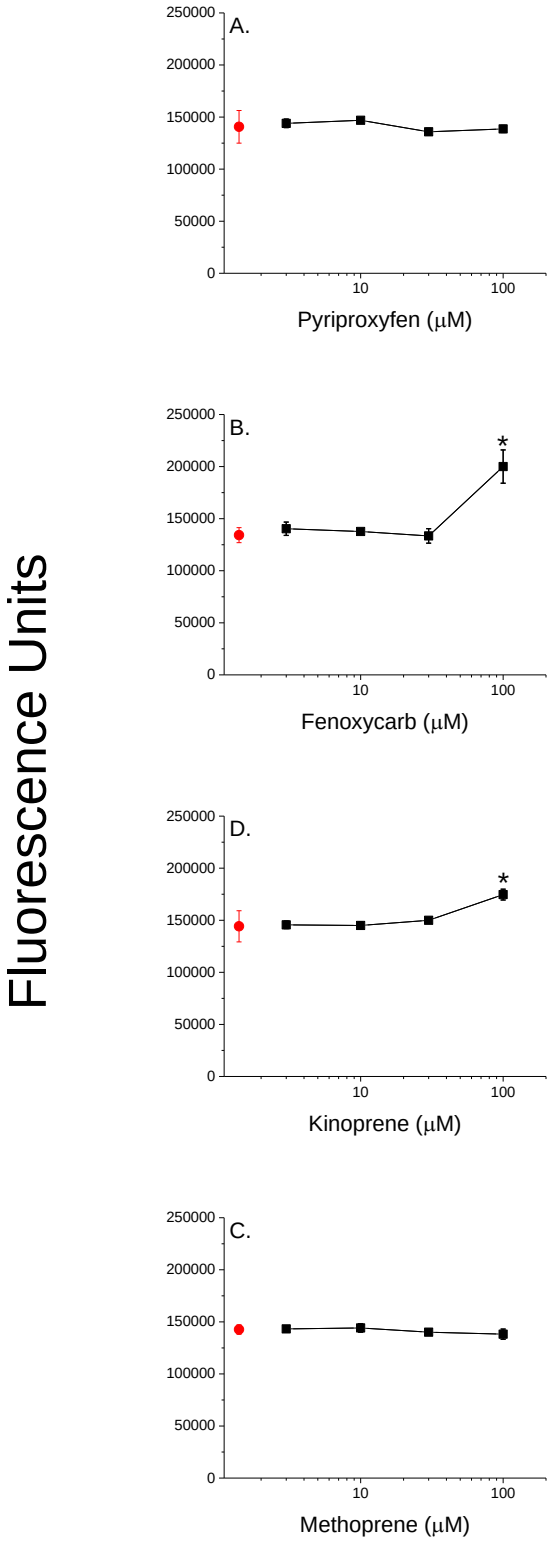
Fluorescence Units
A.
250000
200000
150000
100000
50000
0
10
100
Pyriproxyfen (μM)
B.
*
Fenoxycarb (μM)
D.
*
Kinoprene (μM)
C.
Methoprene (μM)

Figure 3. PPARγ:RXRα transactivation by IGRs as indicated by increased transcription of a PPRE-driven luciferase reporter gene after 24 (A-D) and 48 hour incubations (E-H). Data are presented as means with error bars depicting standard deviations (n=3). An asterisk denotes a significant difference from the control ($p<0.05$, One-Way ANOVA, Tukey's Multiple Comparison Test).

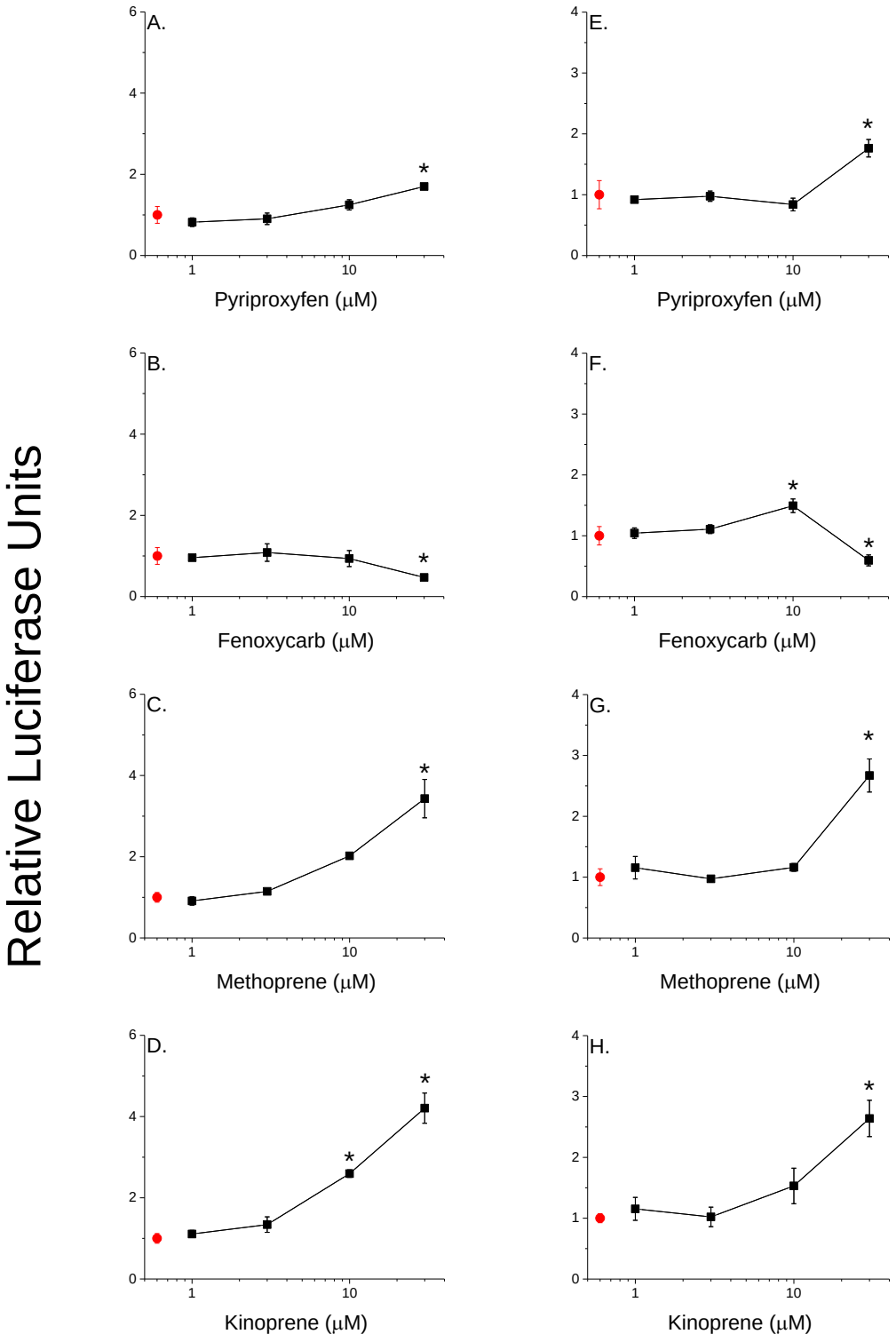
Relative Luciferase Units
A.
Pyriproxyfen (μM)
B.
Fenoxycarb (μM)
C.
Methoprene (μM)
D.
Kinoprene (μM)
E.
Pyriproxyfen (μM)
F.
Fenoxycarb (μM)
G.
Methoprene (μM)
H.
Kinoprene (μM)

Figure 4. Gal4-driven reporter gene transcription by the IGRs in HepG2 cells transfected with the individual PPARγ-gal4 subunit (A-D) and the RXRα-gal4 subunit (E-H). Red circle denotes the response in the absence of IGR (control). Data are presented as means with error bars depicting standard deviations (n=3). An asterisk denotes a significant difference from the control ($p<0.05$, One-Way ANOVA, Tukey's Multiple).

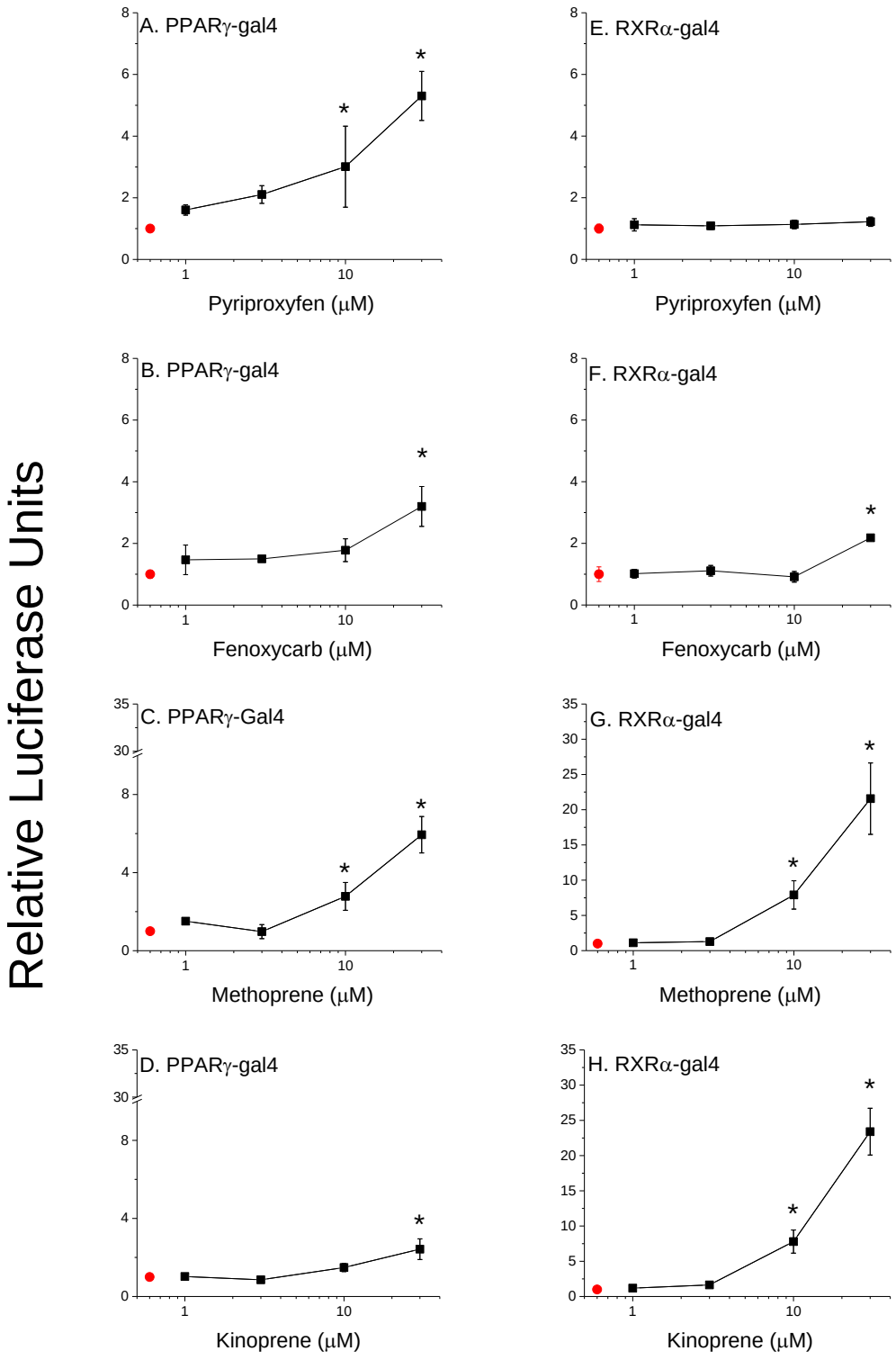
Relative Luciferase Units
A. PPARγ-gal4
Pyriproxyfen (μM)
E. RXRα-gal4
Pyriproxyfen (μM)
B. PPARγ-gal4
Fenoxycarb (μM)
F. RXRα-gal4
Fenoxycarb (μM)
C. PPARγ-Gal4
Methoprene (μM)
G. RXRα-gal4
Methoprene (μM)
D. PPARγ-gal4
Kinoprene (μM)
H. RXRα-gal4
Kinoprene (μM)

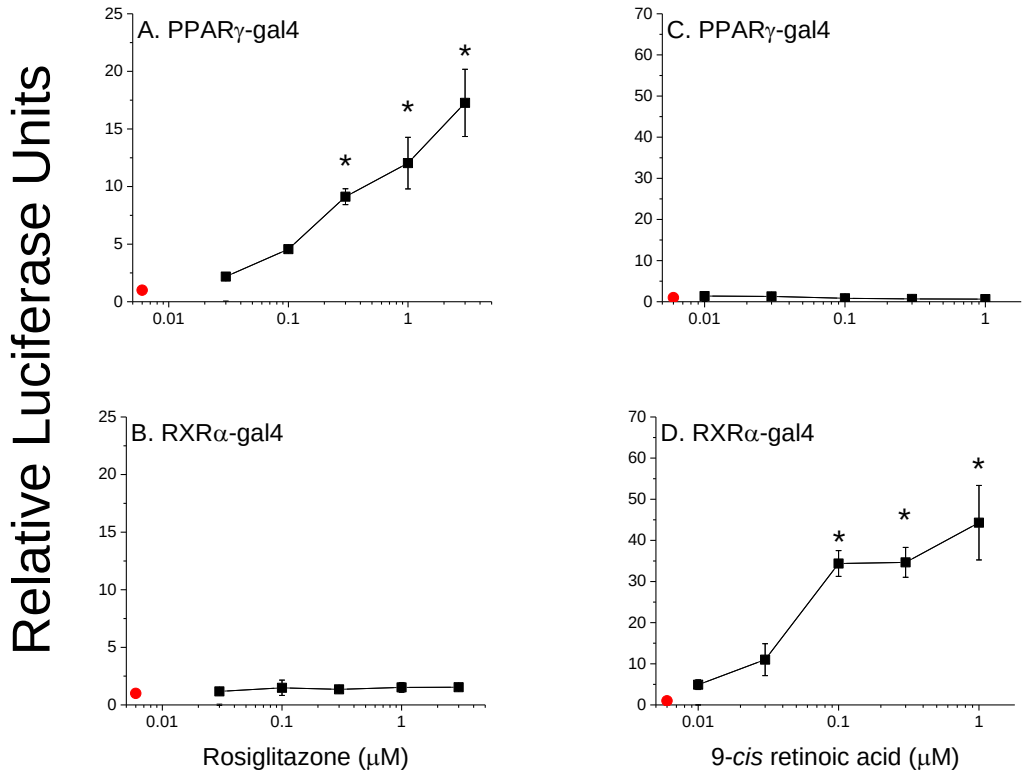

Figure 5. Gal4-driven luciferase transcription in response to the PPARγ agonist rosiglitazone (A-B) and the RXRα agonist 9-*cis* retinoic acid (C-D). HepG2 cells were transfected with the individual PPARγ-gal4 subunit and the RXRα-gal4 subunit. Red circle denotes the response in the absence of agonist (control). Data are presented as means with error bars depicting standard deviations (n=3). An asterisk denotes a significant difference from the control ($p<0.05$, One-Way ANOVA, Tukey's Multiple).

Figure 6. Inhibition of PPARγ:RXRα activity by UVI 3003 (1 μM) as indicated by decreased transcription of a PPRE-driven luciferase reporter gene in the presence and absence of rosiglitazone (1 μM; A), 9-*cis* retinoic acid (9-*cis* RA; 1 μM; B), and IGRs (30 μM; C-F). Data are presented as means with error bars depicting standard deviations (n=3). An asterisk denotes significant inhibition of receptor activity ($p<0.05$, One-Way ANOVA, Tukey's Multiple Comparison Test).

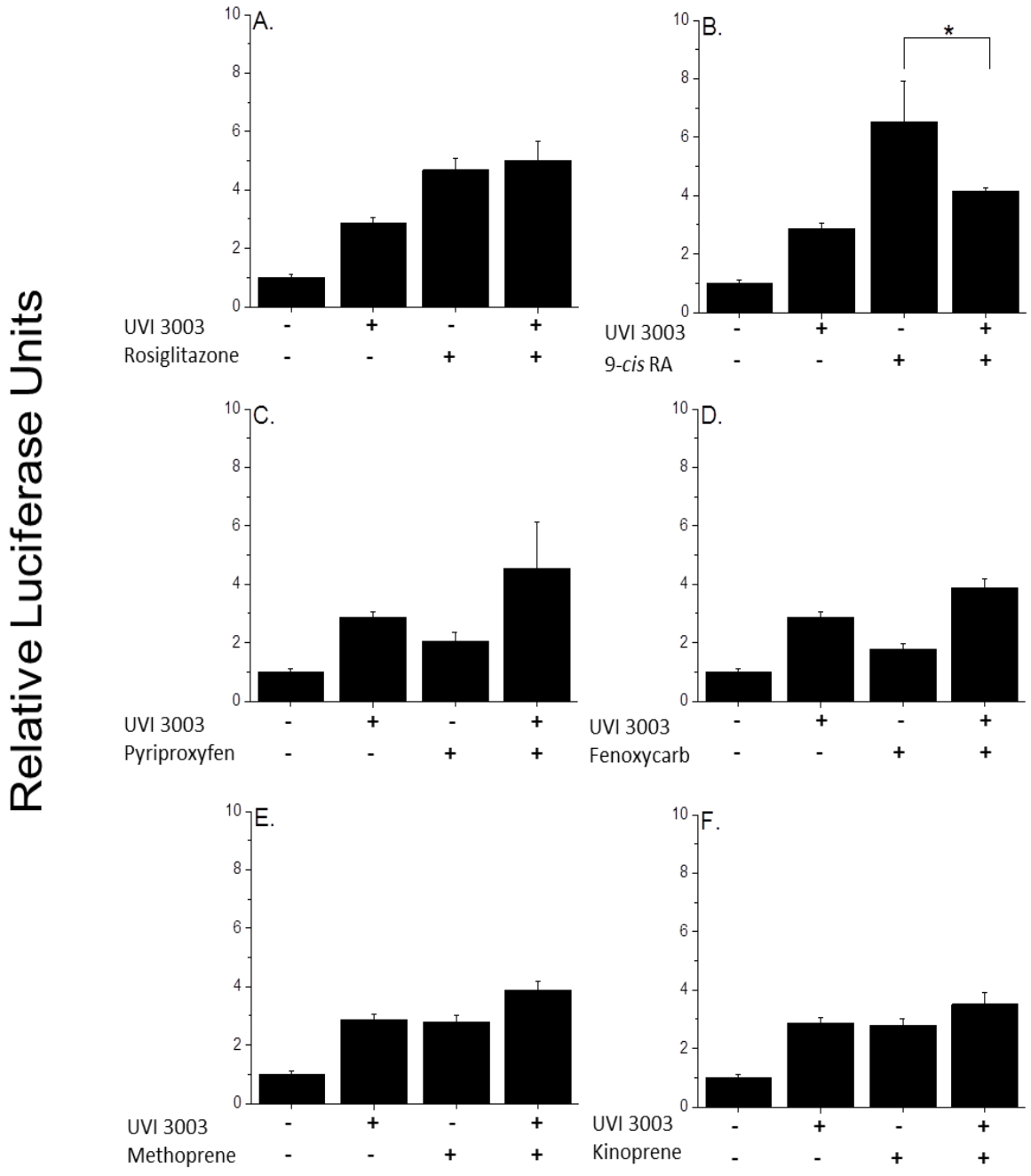
Relative Luciferase Units
A.
UVI 3003
Rosiglitazone
B.
UVI 3003
9-cis RA
*
C.
UVI 3003
Pyriproxyfen
D.
UVI 3003
Fenoxycarb
E.
UVI 3003
Methoprene
F.
UVI 3003
Kinoprene

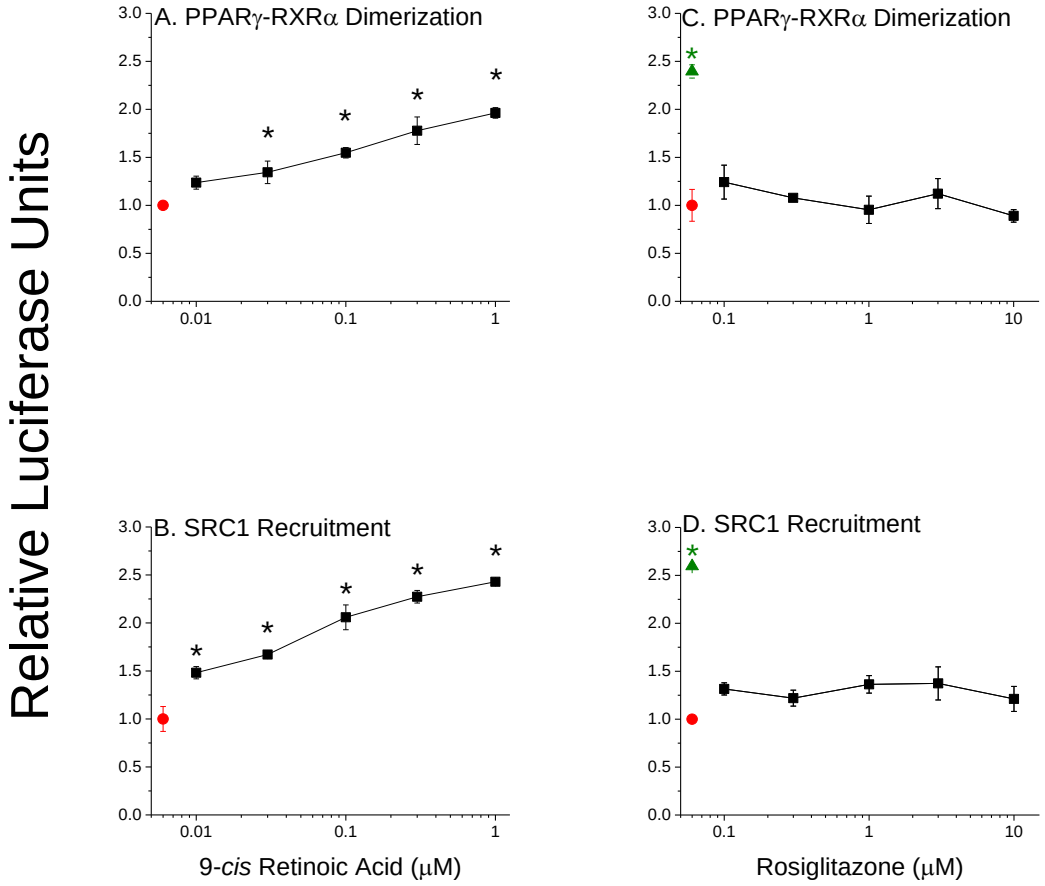

Figure 7. Assessment of PPARγ:RXRα receptor dimerization and SRC1 recruitment to the RXRα subunit by 9-*cis* retinoic acid (A-B) and rosiglitazone (C-D). Red circles denote the response in the absence of ligand (control). Green triangles denote stimulation by the positive control, 9-*cis* retinoic acid (1 μM). Data are presented as means with error bars depicting standard deviations (n=3). An asterisk denotes a significant difference from the control ($p<0.05$, One-Way ANOVA, Tukey's Multiple Comparison Test).

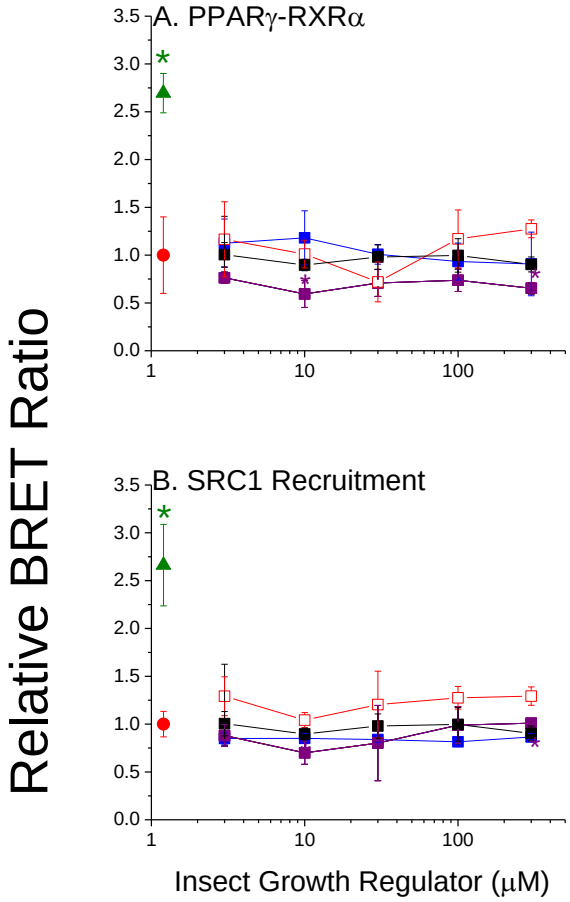

Figure 8. Assessment of PPARγ:RXRα dimerization (A) and the recruitment of SRC1 to the complex (B) by pyriproxyfen (open red square), fenoxycarb (black square), methoprene (purple square), and kinoprene (blue square). Red circles denote the response in the absence of ligand (control). Green triangles denote stimulation by the positive control, 9-*cis* retinoic acid (1 μM retinoic acid). Data are presented as means with error bars depicting standard deviations (n=3). An asterisk denotes a significant increase in dimerization from the control ($p<0.05$, One-Way ANOVA, Tukey's Multiple Comparison Test).

Figure 9. Lipid accumulation in 3T3-L1 cells following treatment with DMSO (control), rosiglitazone (2 μM; positive control), and the IGRs (30 μM) [A]. Images of 3T3-L1 differentiation and lipid accumulation at 100X (B) and 400X (C) magnification.

A.

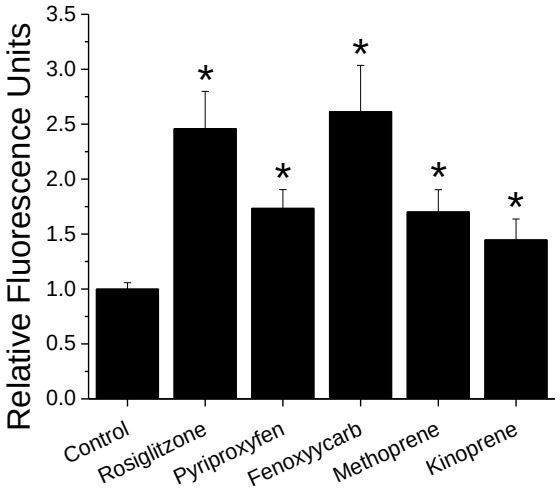
Relative Fluorescence Units
3.5
3.0
2.5
2.0
1.5
1.0
0.5
0.0
*
*
*
*
*
Control
Rosiglitzone
Pyriproxyfen
Fenoxycarb
Methoprene
Kinoprene

B.

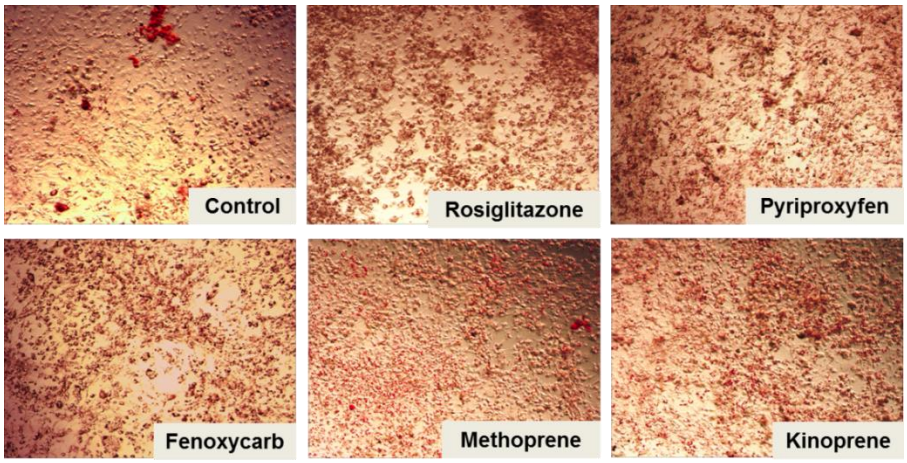
Control
Rosiglitazone
Pyriproxyfen
Fenoxycarb
Methoprene
Kinoprene

C.

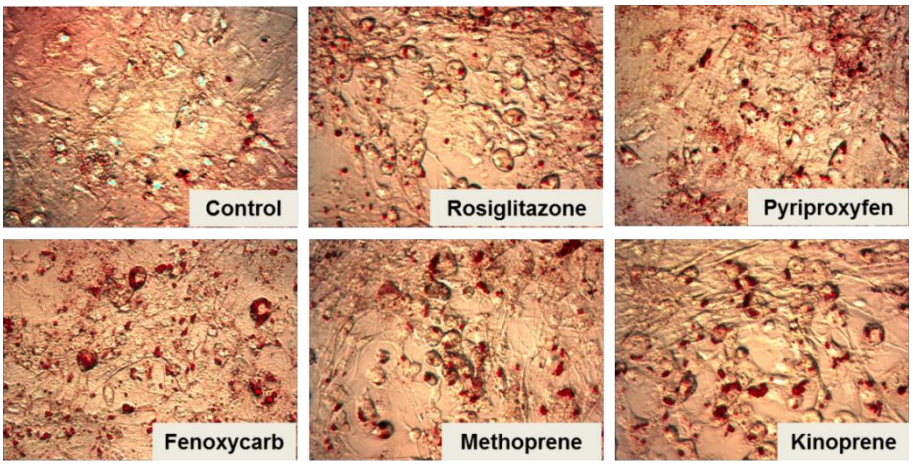
Control
Rosiglitazone
Pyriproxyfen
Fenoxycarb
Methoprene
Kinoprene

SUMMARY AND CONCLUSIONS

Endocrine toxicological studies often focus on the evaluation of environmental chemicals for their ability to interfere with estrogen, androgen, and thyroid hormone (EAT) signaling pathways due to their vital roles in regulating reproduction, growth, and developmental processes [1]. Non-EAT pathways including PPAR signaling pathways are susceptible to interference by environmental chemicals and disruption increases the risk for several conditions considered to be leading causes of death (e.g., heart disease, type II diabetes, stroke, and certain types of cancer) [1-3]. Clearly, non-EAT pathways must also be considered for toxicological evaluations. We demonstrated that some environmental chemicals can interact with the PPAR signaling network in a manner that could have profound implications for obesity and other symptoms of metabolic syndrome.

In Chapter 1, we investigated the effects of the organophosphate flame retardant, triphenyl phosphate, on the PPAR signaling network. Triphenyl phosphate inhibited the activity of the PPARα:RXRα receptor complex through interaction with both subunits (PPARα, RXRα). Triphenyl phosphate also stimulated the dissociation of the PPARα:RXRα heterodimer. Triphenyl phosphate activated the PPARγ:RXRα receptor complex and activation was specifically due to interaction with the PPARγ receptor subunit. PPARγ:RXRα is a master regulator of adipogenesis [4, 5]. Activation of this receptor complex by triphenyl phosphate raised the question: can triphenyl phosphate stimulate adipogenesis? We showed that triphenyl phosphate causes the differentiation of pre-adipocytes into adipocytes with commensurate lipid accumulation. Therefore, triphenyl phosphate inhibits the signaling pathway involved in fatty acid oxidation (PPARα signaling)

and activates the signaling pathway that promotes lipid accumulation (PPARγ signaling pathway). Together, these effects would lead to an adipogenic outcome.

Exposure to triphenyl phosphate can lead to developmental, reproductive, endocrine, cardiovascular, and neurological toxicities [6-9]. High levels of triphenyl phosphate have been detected in fish (e.g., 15 mg/kg), however, adverse effects resulting from human consumption of contaminated fish were not evident [10]. Triphenyl phosphate exposure also can occur dermally through the use of cosmetic products [10]. Triphenyl phosphate metabolite levels were significantly elevated in human urine hours after applying a finger nail polish containing 0.97% triphenyl phosphate by weight in comparison to those who did not apply nail polish [11]. Participants that underwent the nail polishing process, but painted latex gloves on their hands had insignificant triphenyl phosphate metabolite levels in their urine suggesting, the primary exposure route was dermal [11]. Additionally, long-term studies on most cosmetic products do not exist: thus, long-term exposure health risk implications for many cosmetic compounds are unknown [12]. Long-term exposure to triphenyl phosphate could increase the risk for metabolic disorders.

Ligand-binding is considered to stimulate dimerization of PPAR and RXR prior to transcriptional activation [13]. In Chapter 2, we hypothesized that dimerization may be used as an informative endpoint for the screening of chemicals reducing both time and costs of traditional screening assays (i.e., reporter gene transcription assays). We used BRET technology to investigate the utility of ligand-dependent receptor assembly as an endpoint for the use in the evaluation of chemicals for interaction with the PPARα:RXRα:SRC1 complex. Using known RXRα and PPARα agonists, we revealed that RXRα agonists stimulated

complex assembly and activated the assembled transcription factors. PPARα agonists had no effect on PPARα:RXRα:SRC1complex assembly, but activated existing receptor complexes. Additionally, we demonstrated that other organophosphate flame retardants exhibited similar effects as triphenyl phosphate (Chapter 1) on the PPARα signaling pathway. We screened a battery of organophosphate flame retardants and found that many of these compounds inhibited PPARα:RXRα receptor complex dimerization and activation. Results demonstrated that monitoring transcription factor assembly has the potential to discern agonist and antagonist activity, as well as, identify the specific subunit affected by the chemical in a time conservative manner.

Insecticides and their metabolites have been detected in both human plasma and urine. The presence of these chemicals can be due to recent exposure, cumulative exposure, or both [14]. A strong correlation exists between organochlorine insecticides and risk factors for metabolic syndrome [15]. With the exception of organochlorine compounds, limited data exists for insecticides with respect to metabolic syndrome related health conditions [15]. We aided in addressing this gap of information by evaluating the effects of another class of insecticides, insect growth regulators (IGRs). We found that the IGRs pyriproxyfen, fenoxycarb, methoprene, and kinoprene activated the PPARγ:RXRα receptor complex and the individual PPARγ receptor subunit (Chapter 3). Fenoxycarb, methoprene, and kinoprene also interacted with both the PPARγ and the RXRα subunits. However, activation of the PPARγ:RXRα receptor complex resulted specifically from interactions with the PPARγ receptor subunit. As PPARγ agonists, all of the IGRs promoted lipid accumulation and differentiation of pre-adipocytes into adipocytes.

IGRs are active ingredients in a variety of commercial products including topical flea/tick preventatives for companion pets. Topical preventatives are applied to protect both pets and their owners from pests; yet, we found that exposure could put these individuals at risk for metabolic disorders. However, modulation of PPARγ signaling by IGRs occurred only at high concentrations $\geq$ 10 μM, and IGR plasma levels resulting from normal usage could not be found for either pets or pet owners. Thus, it remains to be determined whether use of these compounds poses significant risk of metabolic syndrome. Nonetheless, this research revealed a class of chemicals with high exposure potential that can interact with the PPARγ signaling pathway in a manner that could contribute to increased adiposity.

Overall, the research presented identified environmental chemicals with the potential to stimulate adipogenesis through interaction with the PPAR signaling network. We addressed the hypothesis that environmental chemicals can interact with multiple components of the PPAR signaling network in a manner that may lead to adipogenesis. We found that some of these chemicals have the ability to simultaneously activate multiple components of the PPAR signaling network (i.e., inhibition of PPARα and activation of PPARγ by triphenyl phosphate), while others targeted multiple components (PPARγ, RXRα) specifically within the PPARγ signaling pathway to invoke adipogenesis (IGRs). In addition, we identified both PPARα inhibitors (organophosphate flame retardants) and PPARγ activators (IGRs) that significantly pose a risk to health due to their potential to co-exist in households with companion pets.

PPARα and PPARγ coordination are vital to lipid and glucose homeostasis. PPARα suppresses glucose utilization as an energy source, and stimulates fatty acid oxidation [16,

17]. PPARγ regulates the expression of genes that function in carbohydrate oxidation in the liver and other tissues, while enhancing lipid accumulation and storage in adipocytes [17]. Thus the simultaneous activation of PPARγ and the inhibition of PPARα would favor the utilization of glucose as an energy source while promoting lipid storage. Increased adiposity is a hallmark of both PPARα deficiency [18] and PPARγ activation [19] as well as, a symptom of metabolic syndrome. Information from this project supports the hypothesis that exposures to combinations of environmental chemicals could result in symptoms of metabolic syndrome.

References

1. Endocrine toxicology. 3rd ed. 2010, USA: CRC Press.
2. CDC. Adult obesity facts. 2015; Available from: http://www.cdc.gov/obesity/data/adult.html.
3. Desouza, C.V., L. Rentschler, and V. Fonseca, Peroxisome proliferator-activated receptors as stimulants of angiogenesis in cardiovascular disease and diabetes. Diabetes Metab Syndr Obes, 2009. **2**: p. 165-172.
4. Lee, J.E. and K. Ge, Transcriptional and epigenetic regulation of ppargamma expression during adipogenesis. Cell Biosci, 2014. **4**: p. 29.
5. Hamza, M., S. Pott, V.B. Vega, J.S. Thomsen, G. Kandhadayar, N. Patrick, N. Palanisamy, K.P. Chiu, C.L. Wei, and Y. Ruan, PPARg/RXR transcriptional circuitry governing adipocyte biology. Clinical Cancer Research, 2007. **13(**22 Supplement): p. C67-C67.
6. Meeker, J.D. and H.M. Stapleton, House dust concentrations of organophosphate flame retardants in relation to hormone levels and semen quality parameters. Environ Health Perspect, 2010. **118(**3): p. 318-323.
7. Liu, X., K. Ji, A. Jo, H.B. Moon, and K. Choi, Effects of TDCPP or TPP on gene transcriptions and hormones of hpg axis, and their consequences on reproduction in adult zebrafish (danio rerio). Aquat Toxicol, 2013. **134-135**: p. 104-11.
8. Du, Z., G. Wang, S. Gao, and Z. Wang, Aryl organophosphate flame retardants induced cardiotoxicity during zebrafish embryogenesis: By disturbing expression of the transcriptional regulators. Aquat Toxicol, 2015. **161**: p. 25-32.

9. Oliveri, A.N., J.M. Bailey, and E.D. Levin, Developmental exposure to organophosphate flame retardants causes behavioral effects in larval and adult zebrafish. Neurotoxicol Teratol, 2015. **52**(Pt B): p. 220-227.
10. Sundkvist, A.M., U. Olofsson, and P. Haglund, Organophosphorus flame retardants and plasticizers in marine and fresh water biota and in human milk. J Environ Monit, 2010. **12**(4): p. 943-951.
11. Mendelsohn, E., A. Hagopian, K. Hoffman, C.M. Butt, A. Lorenzo, J. Congleton, T.F. Webster, and H.M. Stapleton, Nail polish as a source of exposure to triphenyl phosphate. Environ Int, 2016. **86**: p. 45-51.
12. American cancer society. Available from: http://www.cancer.org/cancer/cancercauses/othercarcinogens/athome/cosmetics.
13. Desvergne, B. and W. Wahli, Peroxisome proliferator-activated receptors: Nuclear control of metabolism. Endocrine Reviews, 1999. **20**(5): p. 649-688.
14. CDC. Fourth national report on human exposure to environmental chemicals 2009; Available from: http://www.cdc.gov/exposurereport/pdf/fourthreport.pdf.
15. Ntp workshop: Role of envrionmental chemicals in the development of diabetes and obesity. 2011, Raleigh, NC: National Toxicology Program.
16. Berger, J. and D.E. Moller, The mechanisms of action of ppars. Ann. Rev. Med., 2002. **53**: p. 409-435.
17. Ferre, P., The biology of peroxisome proliferator-activated receptors. Diabetes, 2004. **3(Suppl. 1)**: p. S43-S50.

18. Guerre-Millo, M., C. Rouault, P. Poulain, J. Andre, V. Poitout, J.M. Peters, F.J. Gonzalez, J.-C. Fruchart, G. Reach, and B. Staels, PPAR-a-null mice are protected from high-fat diet-induced insulin resistance. Diabetes, 2001. **50**: p. 2809-2814.

19. Harrington, W.W., C.S. Britt, J.G. Wilson, M.O. Milliken, J.G. Binz, D.C. Lobe, W.R. Oliver, M.C. Lewis, and D.M. Ignar, The effect of pparalpha, ppardelta, ppargamma, and pparpan agonists on body weight, body mass, and serum lipid profiles in diet-induced obese akr/j mice. PPAR Res., 2007. http://dx.doi.org/10.1155/2007/97125.

APPENDIX

Appendix A: A Transgenerational Endocrine Signaling Pathway in Crustacea

Gerald A. LeBlanc[a], Ying H. Wang, Charisse N. Holmes, Gwijun Kwon, and Elizabeth K. Medlock
Department of Environmental and Molecular Toxicology
North Carolina State University
Raleigh, North Carolina, United States of America

Abstract

***Background*:** Environmental signals to maternal organisms can result in developmental alterations in progeny. One such example is environmental sex determination in Branchiopod crustaceans. We previously demonstrated that the hormone methyl farnesoate could orchestrate environmental sex determination in the early embryo to the male phenotype. Presently, we identify a transcription factor that is activated by methyl farnesoate and explore the extent and significance of this transgenerational signaling pathway.

***Methodology/Principal Findings*:** Several candidate transcription factors were cloned from the water flea *Daphnia pulex* and evaluated for activation by methyl farnesoate. One of the factors evaluated, the complex of two bHLH-PAS proteins, dappuMet and SRC, activated a reporter gene in response to methyl farnesoate. Several juvenoid compounds were definitively evaluated for their ability to activate this receptor complex (methyl farnesoate receptor, MfR) in vitro and stimulate male sex determination *in vivo*. Potency to activate the MfR correlated to potency to stimulate male sex determination of offspring (pyriproxyfen>methyl farnesoate>methoprene, kinoprene). Daphnids were exposed to concentrations of pyriproxyfen and physiologic responses determined over multiple generations. Survival, growth, and sex of maternal organisms were not affected by pyriproxyfen exposure. Sex ratio among offspring (generation 2) were increasingly skewed in favor of males with increasing pyriproxyfen concentration; while, the number of offspring per brood was progressively reduced. Female generation 2 daphnids were reared to reproductive maturity in the absence of pyriproxyfen. Sex ratios of offspring (generation 3)

were not affected in this pyriproxyfen lineage, however, the number of offspring per brood, again, was significantly reduced.

***Conclusions*:** Results reveal likely components to a hormone/receptor signaling pathway in a crustacean that orchestrates transgenerational modifications to important population metrics (sex ratios, fecundity of females). A model is provided that describes how these signaling processes can facilitate population sustainability under normal conditions or threaten sustainability when perturbed by environmental chemicals.

Keywords: methyl farnesoate, methoprene-tolerant gene, FISC, SRC, p160, environmental sex determination, daphnia, pyriproxyfen

Introduction

Hormones in the fetal environment regulate a variety of processes that orchestrate physiologic function in the resulting offspring. For example, intrauterine fetal position of mice, with respect to the sex of its adjacent litter mates and thus the hormonal environment of the fetus, influences later events such as the timing of puberty and sexual behavior [1]. Perturbations in the prenatal hormonal milieu can result in inter-individual variability in the expression of these programmed traits as well as disease [2]. Indeed, administration of hormones or hormone mimics to maternal rodents has resulted in the production of offspring with increased susceptibility to prostate cancer [3], mammary tumors [4], obesity [5], and glucose intolerance [5].

Changes in fetal programming due to alterations in the hormonal environment of the developing fetus, be it from maternal influences, *in utero* sibling influences, or maternal exposure to environmental chemicals and drugs, are generally considered to be caused by disruptions or alterations in hormonal regulation of epigenetic programming events. Various components of the epigenetic machinery are under the control of hormones and fetal exposure to hormones or their mimics have been shown to alter epigenetic modifications of several genes [6]. However, a precise understanding of the linkage between endocrinology and fetal programming is lacking.

Environmental sex determination provides a plausible phenomenon that could serve well to define the mechanistic linkages between endocrinology and fetal programming. Environmental sex determination is the ubiquitous process among metazoans whereby sex is determined, not by sex chromosomes allocated to the fetus by its parents, but by

environmental influences on the maternal organism or fetus. Environmental factors responsible for sex determination of offspring include temperature [7], nutrition [8], photoperiod [9], and population density [10]. Environmental sex determination serves to provide population sex ratios that will maximize sustainability of the population under incipient environmental conditions [11]. Generally, the environmental cue is considered to stimulate the release of a chemical signaling molecule (i.e., hormone) that orchestrates the sex programming of the neonate [12] . Despite the ubiquity with which environmental sex determination occurs, the process itself remains poorly understood.

Branchiopod crustaceans, such as *Daphnia* sp., are cyclic parthenogens that are subject to environmental sex determination [13]. Under suitable environmental conditions, daphnid populations consist largely of females that reproduce asexually. This clonal reproduction provides for the rapid expansion of the population. However, in response to specific environmental cues, that typically represent a limiting factor to unregulated population growth, the daphnids will produce male offspring. Male sex determination is under endocrine control. The sequiterpenoid hormone methyl farnesoate programs oocytes in late stages of maturation to develop into male offspring [14,15]. The males mate with sexually receptive females producing embryos that are more genetically diverse and less likely to carry gene mutations [16]. These embryos are typically in a diapause state and can develop once in a different time or space that is more conducive to parthenogenetic population expansion.

Daphnids can serve as an ideal model for the evaluation of transgenerational signaling owing to: a) environmental sex determination in this taxa is highly suitable to

mechanistically evaluate transgenerational signaling; b) populations can be readily reared and offspring sex can be controlled in the laboratory [14,17]; and c) the genome of a member of this taxa (*Daphnia pulex*) has been fully sequenced [18]. In the present study, we sought to identify the endocrine-related transcription factors that translate environmental signals received by the mother to sex determination of her offspring. Three transcription factors were characterized and evaluated for involvement in environmental sex determination. DappuPNR and dappuDSF are member of the NR2E group of nuclear receptors [19]. Members of this group of nuclear receptors are important in various aspects of neural development including sexual orientation sex-specific and reproductive behavior [20,21]. Thus, members of this group of transcription factors in daphnids were considered as candidates for contributing to environmental sex determination. The methoprene-tolerant (Met) protein is a member of the bHLH-PAS family of transcription factors and is a component of the juvenoid hormone signaling pathway in insects [22]. Consequently, we considered this protein to be a candidate for mediating the action of methyl farnesoate, the unepoxidated form of juvenile hormone III, in crustaceans. We also explored the significance of this transgenerational signaling pathway with respect to population sustainability parameters.

Results

Transcription factor cloning

The transcription factors dappuPNR, dappuDSF, and dappuMet were cloned from *D. pulex* using the deduced gene sequences derived from the published sequenced genome of

the organism (wFleaBase.org) [18,19]. Nucleotide sequences of the cloned genes (cDNAs) are presented in the Supporting Information (Figs. S1, S2, and S3). Deduced amino acid sequences for the gene products are provided in Figs 1, 2, and 3. The dappuPNR gene product was 548 amino acids in length and contained DNA-binding and ligand-binding sites characteristic of most other members of the nuclear receptor family. Its DNA-binding site was 89% identical and its ligand-binding site was 61% identical to those of PNR from *Drosophila melanogaster*. The dappuDSF gene product was 613 amino acids in length and also contained DNA-binding and ligand-binding sites. Its DNA-binding site was 90% identical and its ligand-binding site was 66% identical to those of DSF of *D. melanogaster*.

The Met cDNA was cloned from both *D. pulex* (dappuMet; Fig. S3) and *D. magna* (dapmagMet; Fig. S4) since *D. magna* was used for subsequent whole animal experiments and Met proved to be most relevant to these experiments. The sequenced dappuMet cDNA was highly similar to the sequence derived from wFleaBase. Overall, the two sequences were 97% identical with 100%, 91%, and 98% identity within the bHLH, PAS-A, and PAS-B domains, respectively. The major difference between the two sequences was an additional stretch of 10 nucleotides in the sequenced cDNA just 3' of the bHLH domain which may have been lost in the wFleaBase sequence due to an error in intro/exon designations. The sequenced dappuMet and dapmagMet cDNAs were also highly similar with 100%, 98%, and 88% identity in the bHLH, PAS-A, and PAS-B domains, respectively (Fig. 3). The bHLH domain is typically involved in protein dimerization and, in some cases, DNA binding [23]. The PAS domains are typically involved in dimerization to partner transcription factors or in binding, as a co-activator, to transcription factors, depending upon the specific function of

the bHLH-PAS protein [23]. No evidence of dappuMet paralogs was discerned during the cloning of the dappuMet cDNA.

The sequenced dappuMet was 64%, 36%, and 26% identical to the bHLH, PAS-A, and PAS-B domains of the *Drosophila melanogaster* Met, respectively (Fig. 3). In contrast, these domains were 62%, 24%, and 21% similar to the respective domains of the *D. melanogaster* Gce, a paralog of Met (Fig. 3). Taken together, the evidence supports the identification of the sequenced cDNAs from *D. pulex* and *D. magna* as being Met and not a Met paralog. Results also support the use of *D. magna* as a surrogate to *D. pulex* in subsequent whole animal experimentation.

Activation of the transcription factors by methyl farnesoate

Constructs of the transcription factors containing the Gal4 DNA binding domain were used in transcription reporter assays where luciferase was the reporter gene which contained GAL4 binding sites upstream of the transcription start site. In the initial screen, none of the transcription factors stimulated luciferase expression either alone or in the presence of 10 μM methyl farnesoate (Fig. 4). SRC is a bHLH-PAS protein that is known to associate with a number of nuclear receptor family of proteins, as well as, bHLH-PAS transcription factors [24]. We therefore, co-transfected insect SRC (previously identified as mosquito-FISC [25]) into the transfection reporter assays and evaluated methyl farnesoate responsiveness. SRC had no effect in reporter assays involving dappuPNR and dappuDSF (Fig. 4). However, dappuMet did activate gene transcription in response to methyl farnesoate when SRC was added to the assay (Fig. 4). Concentration-response analyses revealed that methyl farnesoate

activated the dappuMet –SRC complex, hereafter referred to as the methyl farnesoate receptor (MfR), with maximum activation of ~9-fold with a potency (EC_{50}) of 16 μM (Fig. 5A).

Three compounds that function as juvenile hormone mimics in insects were selected to determine whether these compounds also activated the MfR. Of the three compounds selected, only pyriproxyfen activated the MfR (Fig, 5B). Maximum activation of the complex was ~2/3 of that observed with methyl farnesoate though this compound appeared more potent with an estimated EC_{50} of 4.8 μM (Fig. 5B). Neither methoprene nor kinoprene activated the MfR at concentrations as high as 120 μM (Figs. 5C,D).

Male sex determination

We have shown that methyl farnesoate is a male sex determinant in daphnids [14]. Experiments next were performed to determine whether the relative potency of methyl farnesoate and the juvenile hormone mimics correlated to the relative potency of these compounds to activate the MfR. Both methyl farnesoate and pyriproxyfen stimulate male sex determination among offspring of exposed maternal organisms (Fig. 6 A,B) with pyriproxyfen being more potent. EC_{50} values for male offspring production were 34 nM and 0.22 nM for methyl farnesoate and pyriproxyfen, respectively. Neither, methoprene nor kinoprene stimulated male offspring production at the maternal exposure concentrations tested which were limited by toxicity (methoprene) or solubility (kinoprene) (Fig. 6 C,D). The potency ranking of the four compounds were comparable with respect to the activation of the MfR and male sex determination. Although, the magnitude of difference between

methyl farnesoate and pyriproxyfen was much greater for male sex determination as compared to activation of the MfR.

Transgenerational impacts on life history parameters

Having demonstrated that pyriproxyfen was most potent in activating the MfR we next evaluated whether elevated levels of the MfR ligand in the maternal organisms (generation 1) elicited responses specifically in offspring (generation 2) or next generation offspring (generation 3). Continuous exposure of first generation organisms to concentration of pyriproxyfen ranging from 0.084 to 0.62 nM had no discernible effect on longevity (Fig. 7A), growth (Fig. 7B) or molt frequency (Fig. 7C). All individuals exposed to pyriproxyfen, as well as controls, matured as reproductively competent females. However, male:female sex ratios of offspring (generation 2) increased with increasing concentration of pyriproxyfen and ranged from all female offspring at the exposure concentration of 0.084 nM pyriproxyfen to all male offspring at 0.56 nM pyriproxyfen (Fig. 7D). The magnitude of this effect was comparable to that observed in previous experiments (Fig. 6B) indicating that the effect of pyriproxyfen was not cumulative over the duration of exposure but rather reflected the magnitude of exposure as it occurred during a selected window of susceptibility of the prenatal second generation organisms. Further, the number of second generation individuals within a brood decreased with increasing concentration of pyriproxyfen (Fig. 7E) suggesting that pyriproxyfen decreased the number of oocytes recruited for maturation or increased the number of oocytes/embryos lost during the maturation process. Thus, pyriproxyfen had no discernible effect on parental organisms while modifying the development of neonates.

One female second generation neonate derived from each of ten first generation organisms exposed to 0.22 nM pyriproxyfen was isolated and reared to maturity in the absence of pyriproxyfen. These second generation female neonates all were derived from broods that contained both male and female offspring. Thus, even female offspring were likely exposed to a near sex-determining concentration of pyriproxyfen during prenatal development. Ten control neonates were similarly isolated and reared. There were no significant differences in survival and growth between the second generation pyriproxyfen-exposed lineage and the control daphnids (Fig. 8A, B). Furthermore, all offspring produced (third generation daphnids) in this experiment were female (Fig. 8C). However, consistent with reduced brood sizes observed among pyriproxyfen-exposed daphnids in the previous generation, broods of third generation organisms produced by the pyriproxyfen-exposed lineage were significantly smaller than broods produced by control daphnids (Fig. 8D).

Discussion

It has been recognized for decades that the hormone methyl farnesoate plays many important roles in crustacean development and reproduction [26]. Yet the receptor protein that mediates the activity of methyl farnesoate has remained an enigma. The close structural and function identity of methyl farnesoate to the insect hormone JHIII has led to speculation that these two hormones may function through some signaling pathway common to insects and crustaceans [27]. Ultraspiracle, the retinoid X receptor ortholog in *D. melanogaster*, was hypothesized to be the functional target of JHIII binding in this insect species [28]. However, we found no evidence to suggest that daphnid RXR is activated by methyl

farnesoate [29,30]. Although, methyl farnesoate did appear to bind to daphnid RXR resulting in synergistic activation of the daphnid ecdysteroid receptor complex (EcR:RXR) by 20-hydroxyecdysone [29]. Recently, we identified the nuclear receptors PNR and DSF within the *D. pulex* genome [19] and presently, we cloned the respective cDNAs. Both nuclear receptors were viewed as candidate methyl farnesoate receptors as members of this nuclear receptor group (NR2E) contribute to sexually dimorphic development in insects [31]. Neither receptor was activated by methyl farnesoate in the reporter gene assay.

We also cloned the methoprene tolerant (Met) gene ortholog from *D. pulex and D. magna*. This bHLH-PAS protein was recently shown to be a strong candidate as a JHIII-dependent transcription factor in mosquito [25]. Daphnid Met alone was unable to activate the reporter gene in the presence of methyl farnesoate. However, when co-transfected with SRC derived from mosquito [25], a functional methyl farnesoate-dependent activator of gene transcription was created. We refer to this receptor complex (Met-SRC) as the methyl farnesoate receptor (MfR). Efforts to clone and express the daphnid SRC are underway, but has proven challenging due to the large size of the gene (>7600 bp). Presently, it is not known whether SRC functions as a partner transcription factor to Met (i.e., contributes to DNA binding) or functions as a non-DNA binding coactivator. It is highly improbable that SRC was independently responsible for reporter gene activation since it did not possess the GAL4 DNA-binding domain. Furthermore, the presence of SRC in experiments involving PNR or DSF did not result in reporter gene activation. Previously, we demonstrated that methyl farnesoate is a male sex determinant in daphnids (*D. magna*) [14]. Subsequently, we and others have shown that methyl farnesoate functions as a sex determinant in other

Cladoceran species and some insecticidal juvenile hormone mimics are capable of mimicking this action of methyl farnesoate [15,17,32,33]. Having now identified a candidate MfR in daphnids, we evaluated whether the potency of putative ligands of the MfR correlated to their ability to stimulate male sex determination. The insecticide pyriproxyfen was a potent activator of the MfR and was extremely potent at stimulating male sex determination *in vivo*. Pyriproxyfen was approximately 3-times as potent as methyl farnesoate in activating the MfR in the mid-range of the concentration-response curve. However, the insecticide was approximately 150-times more potent in stimulating male sex determination. This increased potency *in vivo* may be due to differences in *in vivo*-relevant pharmacokinetic parameters such as uptake, distribution, metabolism, and elimination between the two ligands.

The JHIII mimics, methoprene and kinoprene, were unable to activate the MfR and also were inactive as male sex determinants *in vivo*. Methoprene was previously shown to have weak activity as a male sex determinant [34]. This subtle difference in response between studies may reflect strain differences in the MfR or differences in the manufacturers lots of methoprene used. Regardless, potent activators of the MfR (methyl farnesoate and pyriproxyfen) were shown to be potent male sex determinants *in vivo;* while, JHIII mimics that were inactive with the MfR also were unable to stimulate the production of male offspring *in vivo*. These observations support the hypothesis that MfR activation by methyl farnesoate is responsible for male sex determination in daphnids. Additional studies of MfR-ligand, MfR-protein, and MfR-DNA interactions are warranted to definitively establish this putative mechanistic linkage between MfR activation by methyl farnesoate and male-sex determination.

Experiments on the physiologic responses of daphnids to the potent MfR ligand pyriproxyfen demonstrated the profound multigenerational consequences of activation of this hormonal pathway. Though pyriproxyfen produced no discernible effects on the endpoints measured among parental (generation 1) organisms, these organisms produced progressively more male offspring (generation 2) with increasing exposure concentration of the hormone mimic. Further, female offspring (generation 2) derived from a pyriproxyfen-exposed lineage but whose only potential for exposure to pyriproxyfen was early in development produced fewer offspring (generation 3) than organisms derived from an unexposed lineage. These effects provide novel insight into the manner in which methyl farnesoate may regulate daphnid populations through multiple generations (Fig. 9). Under conditions of food abundance, daphnids reproduce asexually with maternal organisms producing large broods of all-female offspring. These offspring mature and continue the asexual reproductive cycle resulting in rapid population growth (Fig. 9, Phase 1). Ultimately, food resources are depleted and population density is very high (Fig. 9, Phase 2). These duel conditions cause an elevation in methyl farnesoate in maternal organisms resulting in activation of the MfR and the production of male offspring and a reduction in the rate of offspring production (Fig. 9, Phase 3). Population density declines, the population now has viable males, and through presently unidentified stimuli, females produce haploid eggs and become sexually receptive. The population density continues to decline due to the transgenerational suppression of fecundity by the original activation of the methyl farnesoate signaling pathway and fertilized diapause embryos (resting eggs) are introduced into the population (Fig. 9, Phase 4). The reduced density of feeding organisms allows for recovery of food resources, diapause eggs

hatch, and the asexual population growth cycle is restored (Fig. 9, Phase 5). A significant data gap in this hypothesis is the present lack of demonstration that methyl farnesoate levels are elevated in daphnids in response to food restriction and high population density (which are known to stimulate the production of male offspring in *D. magna* [10]).

Recently generated information on the molecular contributors to the sex determining pathway of Cladocera provides for assembly of a credible chain of events that link the initiating event (environmental signals) to the apical event (male sex determination) (Fig. 10). We had previously demonstrated that low food resources coupled with high population density are the initiating environmental signals for male sex determination in *D. magna* [10]. We also were the first to demonstrate that the crustacean hormone methyl farnesoate programs maturing oocytes to develop into males [14]. Presently, we show that the the Met:SRC complex (MfR) provides a functional target for mediating the activity of methyl farnesoate. The *transformer* gene (Tra*)* has been identified as the initial determinant of sex differentiation in several insect species [35]. The Tra gene has been identified in *D. magna* but its functionality in the sex-determining pathway is yet to be determined [36]. We propose that methyl farnesoate-activated MfR orchestrates a sex-specific modification to Tra that dictates downstream events leading to male or female differentiation. Essentially, we propose that the default sex in daphnids is female, but activated MfR triggers a "sex switch" that initiates a trajectory for Tra towards male sex differentiation. In insects, the *doublesex* gene (Dsx) is the target of Tra [37]. Dsx protein then orchestrates male or female sex differentiation [38]. In *D. magna*, Dsx expression during early embryogenesis also is responsible for male sex differentiation [39]. Thus, the sex switch may involve the induction

of doublesex expression by Tra. A major gap in this proposed pathway is the lack of functional characterization of Tra in Cladocerans.

Results of the present study not only help to elucidate the molecular signaling pathway that links environmental stimuli to sex differentiation, but provide insight into how environmental chemicals can disrupt such signaling pathways resulting in profound transgenerational consequences. Here, we demonstrate that exposure of maternal daphnids to extremely low (parts per trillion) concentrations of an insecticide could dramatically alter sex ratios in the subsequent generation and compromise fecundity of reproductively competent females for at least two generations. Short term reductions in population size of this important food source for juvenile fishes would likely occur under this scenario. Although, long-term consequences are questionable due to the ability of daphnid populations to rapidly recover [40]. None the less, the scenario described herein provides a model that depicts why concern exists for the presence of endocrine disrupting chemicals in the environment. 1) The model chemical targeted a specific receptor with high potency resulting in the capacity to elicit toxicity at very low exposure levels. 2) Processes that are critical to population sustainability were disrupted as a consequence of the initial chemical:target interaction. 3) Adverse consequences of the initial exposure event persisted into subsequent unexposed generations. The identification of such pathways and the characterization of their susceptibility to disruption by environmental chemicals can significantly refine the hazard risk characterization process.

Materials and Methods

Daphnids

Transcription factors were cloned from tissues of *D. pulex* (clone NP6 [15]) since we had previously identified and annotated several transcription factors from this species [19]. Life cycle experiments were performed with *D. magna* (clone NCSU1 [15]) due to the greater fecundity associated with this species. Animals were cultured and used in experiments under rearing conditions described previously [30]. Cultured daphnids were raised in media reconstituted from deionized water [41]. *D. pulex* were maintained at a density of 20 daphnids in 40 ml of media and were fed once daily with 1.4 X 10^7 cells of algae (*Pseudokirchneriella subcapitata*) and 0.4 mg (dry weight) Tetrafin^{TM} fish food suspension prepared as described previously [42]. *D. magna* were reared at a density of 40 daphnids in l liter of media and were fed twice daily with 1.4x10^8 cells of *P. subcapitata* and 4 mg dry weight of fish food suspension. Media was changed 3 times per week. Cultured daphnids were kept in incubators maintained at 20°C with a 16/8 hour light/dark cycle.

Transcription factor cloning

The SV Total RNA Isolation System (Promega) was used to isolate RNA from female *D. pulex* . Oligonucleotide primers were designed to cover the open reading frame of dappuMet, dappuPNR and dappuDSF based on wFleaBase: the Daphnia Genome Database (http://wfleabase.org/). Primer sequences used to amplify the respective cDNAs are provided in Table 1. Amplification of the dappuMet sequence was performed with an iCycler Thermal Cycler (Bio-Rad, Hercules, CA) using 0.25 U Phusion Hot Start DNA Polymerase

(New England Biolabs, Ipswich, MA), 5 μl of 5× Phusion GC Buffer, 0.75 μl DMSO, 200 μM dNTP, 0.5 μM primers, 100 ng template cDNA for a total amount of 25 μl. PCR conditions consisted of hot start at 98°C for 30 sec, followed by 40 cycles with each cycle consisting of 10 sec at 98°C, 30 sec at 58°C, and 45 sec at 72°C. Amplification of dappuPNR and dappuDSF were similarly performed but with 2X PCR Mastermix (Promega) at 94°C for 2 min, followed by 40 cycles with each cycle consisting of 30 sec at 94°C, 30 sec at 54.5°C, and 2 min at 72°C. The amplified DNA fragments were cloned into the pCR 4-TOPO vector (Invitrogen, Carlsbad, CA) following the manufacture's protocol. Plasmid DNA was sequenced by Eurofins MWG Operon (Huntsville, AL). The Met gene from *D. magna* also was cloned (dapmagMet) using procedures as described for dappuMet.

Luciferase reporter gene assays

Chimeric constructs consisting of the transcription factor and a Gal4 DNA binding domain were prepared for use in luciferase-based transcription reporter assays. DNA encoding the 489 nucleotides of the Gal4 DNA binding domain within the pBIND vector (Promega) was amplified using the oligonucleotide primers described in Table 1. The amplified DNA fragments were digested with SpeI and BstBI and cloned into the PMTB vector (Invitrogen). This construct was designated the PMT-Gal4 vector. DNA encompassing the DEF domain of dappuPNR and dappuDSF and the PAS domains of dappuMet were amplified using oligonucleotide primers depicted in Table 1. Amplified sequences are underlined in the transcription factor nucleotide sequences provided in the Supplementary Information (Figs. S1, S2, and S3). The PCR products were digested with the appropriate

enzymes (dappuMet: EcoRI and MluI; dappuDSF and dappuPNR: EcoRI and BstBI) and cloned into the PMT-Gal4 vector. Vector containing the SRC gene (pAC 5.1/V5-His A-FISC), isolated from mosquito (*Aedes aegypti*), was a generous gift from Dr Jinsong Zhu, Department of Biochemistry, Virginia Polytechnic Institute and State University, Blacksburg, VA. The reporter gene vector used in the assay (pGL5-Luc, Promega) contained the luciferase gene with five upstream GAL4 binding sites. The pPAC-β-gal vector, containing the β-galactosidase gene, served as a control for transfection efficiency and was a kind contribution from Dr. Robert Tjian (University of California, Berkeley).

Reporter gene assays were performed in *Drosophila* Schneider (S2) cells (Invitrogen). *Drosophila* S2 cells were grown in Schneider's medium (Gibco, Carlsbad, CA, USA), containing 10% heat inactivated fetal bovine serum (Gibco), 50 units/ml penicillin G (Fisher Scientific, Pittsburgh, PA), 50 μg/ml streptomycin sulfate (Fisher Scientific) and incubated at 23°C under ambient air atmosphere. Cells were seeded at a density of 3×10^6 in a 35 mm plate and transfected 16-23 hours after plating when the cells were at 50-70% confluence. Transfections were performed by calcium phosphate DNA precipitation with the relevant plasmids. Following transfection, cells were washed and transcription induced with the addition of $CuSO_4$ at a final concentration of 500 μM for 24 hours. Transfected cells were treated with the chemicals for 24 hours with Ex-cellTM 420 insect serum-free medium with L-glutamine (SAFC Biosciences, Sigma, St. Louis, MO) and harvested for luciferase and β-galactosidase determinations. Luciferase activities were measured using the luciferase Assay System (Promega), and normalized to β-galactosidase activities which were measured by the

β-galactosidase Enzyme Assay System with Reporter Lysis Buffer (Promega), according to the manufacturer's recommendation. Each experiment was repeated at least three times.

Compounds evaluated in the transcription reporter assays were: methyl farnesoate (95%, Echelon Biosciences Inc., Salt Lake City, Utah), pyriproxyfen (99.5%, Chem Service, West Chester, PA), methoprene (99%, Chem Service) and kinoprene (96%, Chem Service). Chemicals were dissolved in DMSO for reporter assays at a final assay concentration of 0.050%, v/v.

Male sex determination

The potency of several juvenoid analogs in stimulating male sex determination of daphnids was determined generally as described previously [34]. Compounds used were the same as used in the transcription reporter assays. All test compounds were dissolved in ethanol with a final ethanol concentration in treatments and controls of 0.050%, v/v. Female daphnids, carrying embryos in their brood chambers, were selected from the cultures and placed individually in 50-ml beakers containing 40 ml media and the desired concentration of juvenoid analog. Test solutions were changed daily and daphnids were observed daily for the release of broods of offspring. Food was provided to each beaker as $7X10^6$ cells of algae (*P. subcapitata)* and 0.20 mg (dry wt) of fish food homogenate [42] daily. Treatments were replicated 10-times (ie., one animal per beaker, 10 beakers per treatment). Assays were terminated when all maternal daphnids in the experiment had released their second brood of offspring.

The number of offspring present in the second brood released by each maternal daphnid was quantified and sex of individual daphnids within that brood was determined. Sex of individual offspring was established microscopically with males being discerned from females by the longer first antennae [14]. Daphnids typically produce only female offspring under these culture and assay conditions in the absence of juvenoid compound.

Life cycle assessment

Daphnids (*D. magna*) were exposed to concentrations of pyriproxyfen over their life cycle to test the hypothesis that maternal exposure to this methyl farnesoate mimic causes transgenerational effects. Individual female daphnids were exposed to a series of tightly spaced dilutions of pyriproxyfen for 21 days during which time effects on parental survival, growth, and molt cycle duration was evaluated. In addition, effects of pyriproxyfen on brood size and sex ratio of offspring was determined. Results were compared to those derived from 10 control organisms that were exposed only to the solvent used to deliver pyriproxyfen (ethanol, 0.020%, v/v). Animals were exposed individually in 50 ml beakers containing 40 ml of media. Solutions were exchanged every 2-3 days. Test beakers were provided $3.5X10^6$ cells of algae (*P. subcapitata)* and 0.10 mg (dry wt) of fish food homogenate [42] twice daily for daphnnids <7 days old and twice these amounts, for animals >7 days old. Experiments were maintained in incubators at 20^oC and a light:dark photoperiod of 16:8 hr. This experimental design has been described in detail previously [43].

Experimental animals were examined daily for survival, ecdysis, and offspring production. Exuvia and offspring were removed from the beakers when observed and sex of

individual offspring was determined microscopically based upon the length of the first antennae [14]. At 21 days exposure, length of individual parental organisms was determined as the distance from the top of the helmet to the base of the shell spine.

One female offspring derived from a mixed (males and females) brood from each of 10 maternal daphnids exposed to 0.22 nM pyriproxyfen were raised to reproductive maturity in the absence of pyriproxyfen. Ten offspring from unexposed daphnids were similarly isolated and raised to reproductive maturity. Survival and length of these organisms, size of their first brood of offspring and sex of individuals within the first brood produced by these organisms were determined as additional indicators of transgenerational effects of pyriproxyfen.

Statistics and modeling

Significant differences between treatment and controls were evaluated using Student's t test at p=0.05. All concentration-response curves were generated using the logistic equation. Statistics and curve generation were performed using Origin software (OriginLab Corp., Northampton, MA). The amino acid sequences were deduced from the nucleotide sequences using ExPASy software (http://www.expasy.org/). Amino acid sequence alignments were performed using ClustalW (http://www.genome.jp/tools/clustalw/.

ACKNOWLEDGEMENTS

The authors acknowledge the assistance of David Anick and Hong Li in the performance of some experiments.

References

1. vom Saal FS (1989) Sexual differentiation in litter-bearing mammals: influence of sex of adjacent fetuses in utero. J Anim Sci 67: 1824-1840.

2. Morgan PC, Bale TL (2011) Early prenatal stress epigenetically programs dysmasculinization in second-generation offspring via the paternal lineage. J Neurosci 31: 11748-11755.

3. Ho SM, Tang WY, Belmonte de Frausto J, Prins GS (2006) Developmental exposure to estradiol and bisphenol A increases susceptibility to prostate carcinogenesis and epigenetically regulates phosphodiesterase type 4 variant 4. Cancer Res 66: 5623-5632.

4. Betancourt AM, Eltoum IA, Desmond RA, russo J, Lamartiniere CA (2010) In utero exposure to bisphenol A shifts the window of susceptibility for mammary carcinogenesis in the rat. Environ Health Perspect 118: 1614-1619.

5. Wei J, Lin Y, Li Y, Ying C, Chen J, et al. (2011) Perinatal exposure to bisphenol A at reference dose predisposes offspring to metabolic syndrome in adult rats on a high-fat diet. Endocrinology 152: 3049-3061.

6. Zhang X, Ho S-M (2011) Epigenetics meets endocrinology. J Mol Endocrin 46: R11-R32.

7. Janzen FJ, Phillips PC (2006) Exploring the evolution of environmental sex determination, especially in reptiles. J Evol Biol 19: 1775-1784.

8. Warner DA, Lovern MB, Shine R (2007) Maternal nutrition affects reproductive output and sex allocation in a lizard with environmental sex determination. Proc Biol Sci 274: 883-890.

9. Korpelainen H (1990) Sex ratios and conditions required for environmental sex determination in animals. Biol Rev 65: 147-184.

10. Olmstead AW, LeBlanc GA (2001) Temporal and quantitative changes in sexual reproductive cycling of the cladoceran *Daphnia magna* by a juvenile hormone analog. J Exp Zool 290: 148-155.

11. Bull JJ (1981) Evolution of environmental sex determination from genotypic sex determination. Heredity 47: 173-184.

12. Bowden RM, Ewert MA, Nelson CE (2000) Environmental sex determination in a reptile varies seasonally and with yolk hormones. Proc Biol Sci 267: 1745-1749.

13. Hebert PDN (1978) The population biology of *Daphnia* (Crustacea, Daphnidae). Biol Rev 53: 387-426.

14. Olmstead AW, LeBlanc GA (2002) The juvenoid hormone methyl farnesoate is a sex determinant in the crustacean *Daphnia magna*. J Exp Zool 293: 736-739.

15. Rider CV, Gorr TA, Olmstead AW, Wasilak BA, LeBlanc GA (2005) Stress Signaling: Co-regulation of hemoglobin and male sex determination through a terpenoid signaling pathway in a crustacean. J Exp Biol 208: 15-23.

16. Paland S, Lynch M (2006) Transitions to asexuality result in excess amino acid substitutions. Science 311: 990-992.

17. Olmstead AW, LeBlanc GA (2003) Insecticidal juvenile hormone analogs stimulate the production of male offspring in the crustacean *Daphnia magna*. Environ Health Perspect 111: 919-924.

18. Colbourne JK, Pfrender ME, Gilbert D, Thomas WK, al. e (2011) The ecoresponsive genome of *Daphnia pulex*. Science 331: 555-561.

19. Thomson SA, Baldwin WS, Wang YH, Kwon G, LeBlanc GA (2009) Annotation, phylogenetics, and expression of the nuclear receptors in *Daphnia pulex*. BMC Genomics 10: 500.

20. Finley KD, Edeen PT, Taylor BJ, Gross EA, Ghbeish N, et al. (1998) Dissatisfaction encodes a tailless-like nuclear receptor expressed in a subset of CNS neurons controlling *Drosophila* sexual behavior. Neuron 21: 1363-1374.

21. O'Kane CJ, Asztalos Z (1999) Sexual behaviour: courting dissatisfaction. Curr Biol 9: R289-292.

22. Wilson TG, Fabian J (1986) A *Drosophila melanogaster* mutant resistant to chemical analog of juvenile hormone. Dev Biol 118: 190-201.

23. Parch CL, Gardner KH (2010) Coactivator recruitment: A new role for PAS domains in transcriptional regulation by the bHLH-PAS family. J Cell Physiol 223: 553-557.

24. Xu J, Li Q (2003) Review of the *in vivo* functions of the p160 steroid receptor coactivator family. Mol Endocrin 17: 1681-1692.

25. Li M, Mead EA, Jhu J (2011) Heterodimer of two bHLH-PAS proteins mediates juvenile hormone-induced gene expression. Proc Nat Acad Sciences USA 108: 638-643.

26. LeBlanc GA, Cambell PM, den Besten P, Brown RP, Chang E, et al. (1999) The endocrinology of invertebrates. In: deFur PL, Crane M, Ingersoll C, Tattersfield L, editors. Endocrine Disruption in Invertebrates: Endocrinology, Testing, and Assessment. Pensacola, FL: SETAC Press. pp. 23-106.

27. Laufer H, Biggers WJ (2001) Unifying concepts learned from methyl farnesoate for invertebrate reproduction and post-embryonic development. Amer Zool 41: 442-457.

28. Jones G, Jones D, Teal P, Sapa A, Wozniak M (2006) The retinoid-X receptor ortholog, ultraspiracle, binds with nanomolar affinity to an endogenous morphogenetic ligand. FEBS J 273: 1-14.

29. Wang YH, LeBlanc GA (2009) Interactions of methyl farnesoate and related compounds with a crustacean retinoid X receptor. Mol Cell Endocrin 309: 109-116.

30. Wang YH, Kwon G, Li H, LeBlanc GA (2011) Tributyltin synergizes with 20-hydroxyecdysone to produce endocrine toxicity. Tox Sci 123: 71-79.

31. Laudet V, Gronemeyer H (2002) The Nuclear Receptor Factsbook. New York: Academic Press. 462 p.

32. Minelli A, Fusco G (2006) Water flea males from the netherworld. Trends Ecol Evol 21: 474-476.

33. Tatarazako N, Oda S, Watanabe H, Morita M, Iguchi T (2003) Juvenile hormone agonists affect the occurrence of male *Daphnia*. Chemosphere 53: 827-833.

34. Wang HY, Olmstead AW, Li H, LeBlanc GA (2005) The screening of chemicals for juvenoid-related endocrine activity using the water flea *Daphnia magna*. Aquatic Toxicol 74: 193-204.

35. Verhulst EC, van de Zande L, Beukeboom LW (2010) Insect sex determination: it all evolves around *transformer*. Gen Develop 20: 376-383.

36. Kato Y, Kobayashi K, Oda S, Tatarazako N, Watanabe H, et al. (2010) Sequence divergence and expression of a transformer gene in the branchiopod crustacean, *Daphnia magna*. Genomics 95: 160-165.

37. Hoshijima K, Inoue K, Higuchi I, Sakamoto H, Shimura Y (1991) Control of doublesex alternative splicing by transformer and transformer-2 in *Drosophila*. Science 252: 833-836.

38. Burtis KC, Baker BS (1989) Drosophila doublesex gene controls somatic sexual differentiation by producing alternatively spliced mRNAs encoding related sex-specific expression. Cell 24: 997-1010.

39. Kato Y, Kobayashi K, Watanabe H, Iguchi T (2011) Environmental sex determination in the branchiopod crustacean *Daphnia magna*: Deep conservation of a doublesex gene in the sex-determining pathway. PLoS Genetics 7: e100134. doi: 100110.101371/journal.pgen.1001345.

40. Barnthouse LW (2009) Quantifying population recovery rates for ecological risk assessment. Environ Toxicol Chem 23: 500-508.

41. Baldwin WS, LeBlanc GA (1994) Identification of multiple steroid hydroxylases in *Daphnia magna* and their modulation by xenobiotics. Environ Toxicol Chem 13: 1013-1021.

42. Olmstead AW, LeBlanc GA (2007) The environmental-endocrine basis of gynandromorphism in a crustacean. Int J Biol Science 3: 77-84.

43. Olmstead AW, LeBlanc GA (2001) Low exposure concentration effects of methoprene on endocrine-regulated processes in the crustacean *Daphnia magna*. Toxicol Sciences 62: 268-273.

Table 1. Oligonucleotide primers used in the PCR amplification of various transcription factors. Bold denotes added restriction sites and italics denote spacer nucleotides added to facilitate proper cutting of the sequence. Some primers used in the reporter assay constructs were situated upstream or downstream of the sequence targeted for amplification.

Use	Gene	Primer S equence
cDNA cloning	dappuPNR	forward: 5'-AGTATCCCAACGGAGTGACG-3'
		reverse: 5'-TACTGAGGATCCCGGGTCA-3'
cDNA cloning	dappuDSF	forward: 5'-CATCGTCTCCCCTCCTTGTA-3'
		reverse: 5'-GGGGGAAAGGAAATCTCATC-3'
cDNA cloning	dappu & dapmag Met	forward: 5'-CCTTACGGAAAGCATCTTTAGTG-3'
		reverse: 5'-CGTATGAATTAAAACAGCTTATTAGAAGTC-3'
Reporter Assay	GAL4	forward: 5'-TATTACTAGTGGCATGAAGCTACTGTCTTCTATCGAACAAG-3'
		reverse: 5'-AATTTTCGAATCTAGATGATATCAACGCGTCAAGTCGAC-3'
Reporter Assay	dappuPNR	forward: 5'-TACTATGAATTCCGACCGGAAATTCTGGCCGAA-3'
		reverse: 5'-TACTATTTCGAATTAATTTTTGTACATATCGCAGAG-3'
Reporter Assay	dappuDSF	forward: 5'-CAACGAATTCAACAGCGTCCATCACCATTTC-3'
		reverse: 5'-CTCTTTCGAACATCGATGAAACCAAACCAA-3'
Reporter Assay	dappuMet	forward: 5'-TACTATGAATTCATACATCAGAATGTGGATTTACGGGT-3'
		reverse: 5'-TACTATACGCGTTCACGGACTACTAGTTCCAG-3'

```
D. pulex      ------------------------------------------MGVPSRP---------V 8
D. melanogaster MNKEENSSETRPSSQELHSPQRHCYTPPPAPMHGQAPPPTSTGVAPPTQPPPPHPAAPNV 60

D. pulex        ENN--------------------------------GASSKNAIPG----LTCLVCGDSSSG 33
D. melanogaster PNGRLLSWNHSAAAAAAAAAAQAAANSMNHSSAAEGSSMTRIKGQNLGLICVVCGDTSSG 120

                                DBD
D. pulex        KHYGILACNGCSGFFKRSVRRRLIYRCQAGSGHCVIDKAHRNQCQACRLKKCLQMGMNKD 93
D. melanogaster KHYGILACNGCSGFFKRSVRRKLIYRCQAGTGRCVVDKAHRNQCQACRLKKCLQMGMNKD 180

D. pulex        AVQNERQPRNSATLRPEILAEMDHERIIREAAAAVGAFGPPVSLAMG-LASAAAHAHYVN 152
D. melanogaster AVQNERQPRNTATIRPETLREMEHGRALREAAVAVGVFGPPVLLSPPCYGSGLLPPPSLG 240

D. pulex        GMVGGRGDGHHYPAAALHAAAAAAAAAASSAAAAQRAEIEREEIDRDRDWLTCPSYKGTS 212
D. melanogaster SLPTGRLLHHNHLTSSMQLAANHMGAGSFPMFNAAGVHHSPKEKAYG-------MEMATS 293

D. pulex        SGEGERTPSAVEDSPSPSAPPPRKLARIEGAFHQHFGVNQFRRSPSPQHIQQQSIPPPLP 272
D. melanogaster GNVSHSTNSSSNHSIDPSSPAPENAKEIN----------------------------IA 324

D. pulex        SSSLLSISHSQPPPLTPVVPGPMPPLSSIVSSGSAGWYQNENQQQHKQQQQQQQQTSTAT 332
D. melanogaster GGSVSSVSSS-----SPTMENDNDDDSIDVTNDNE-----EPHAVSRSDSSFIMPQFMSP 374

D. pulex        FLSTFQPQDNIYETAARLLFMAVKWAKSLPSFAGLPFRDQVILLEESWSELFLICAIQFC 392
D. melanogaster NLYTHQ-HETVYETSARLLFMAVKWAKNLPSFARLSFRDQVILLEESWSELFLLNAIQWC 433

                                LBL
D. pulex        LPMDNN--PLFSLAHFNQPHSATLGCGNGGGNNGGTNNKNSQQTGTDLRFLAELVTRFRV 450
D. melanogaster IPLDPTGCALFSVAEH---------CNNLENNANGDTCITKEELAADVRTLHEIFCKYKA 484

D. pulex        VAVDPAEFACLKAIILFKSETRGLKDPIQVENLQDQAQVMLNQHIRNQQPQRPARFGRLL 510
D. melanogaster VLVDPAEFACLKAIVLFRPETRGLKDPAQIENLQDQAHVMLSQHTKTQFTAQIARFGRLL 544

D. pulex        LTLPLLRHVTAYRLEQLYFRHTIGSTPMEKVLCDMYKN- 548
D. melanogaster LMLPLLRMISSHKIESIYFQRTIGNTPMEKVLCDMYKN- 582
```

Figure 1. Amino acid sequence of *D. pulex* PNR deduced from the nucleotide sequence of dappuPNR (Fig. S1)and aligned to PNR from *D. melanogaster*. The *D. melanogaster* sequence was deduced from the nucleotide sequence provided in GeneBank (accession # NP_611032.2). The DNA-binding domain (DBD) and the ligand-binding domain (LBD) are indicated. Common amino acids between the two sequences are shaded.

Figure 2. Amino acid sequence of *D. pulex* DSF deduced from the nucleotide sequence of dappuDSF (Fig. S2) and aligned to DSF from *D. melanogaster*. The *D. melanogaster* sequence was deduced from the nucleotide sequence at Gene Bank (accession number AAD05225.1). The DNA-binding domain (DBD) and the ligand-binding domain (LBD) are indicated. Common amino acids between the two sequences are shaded.

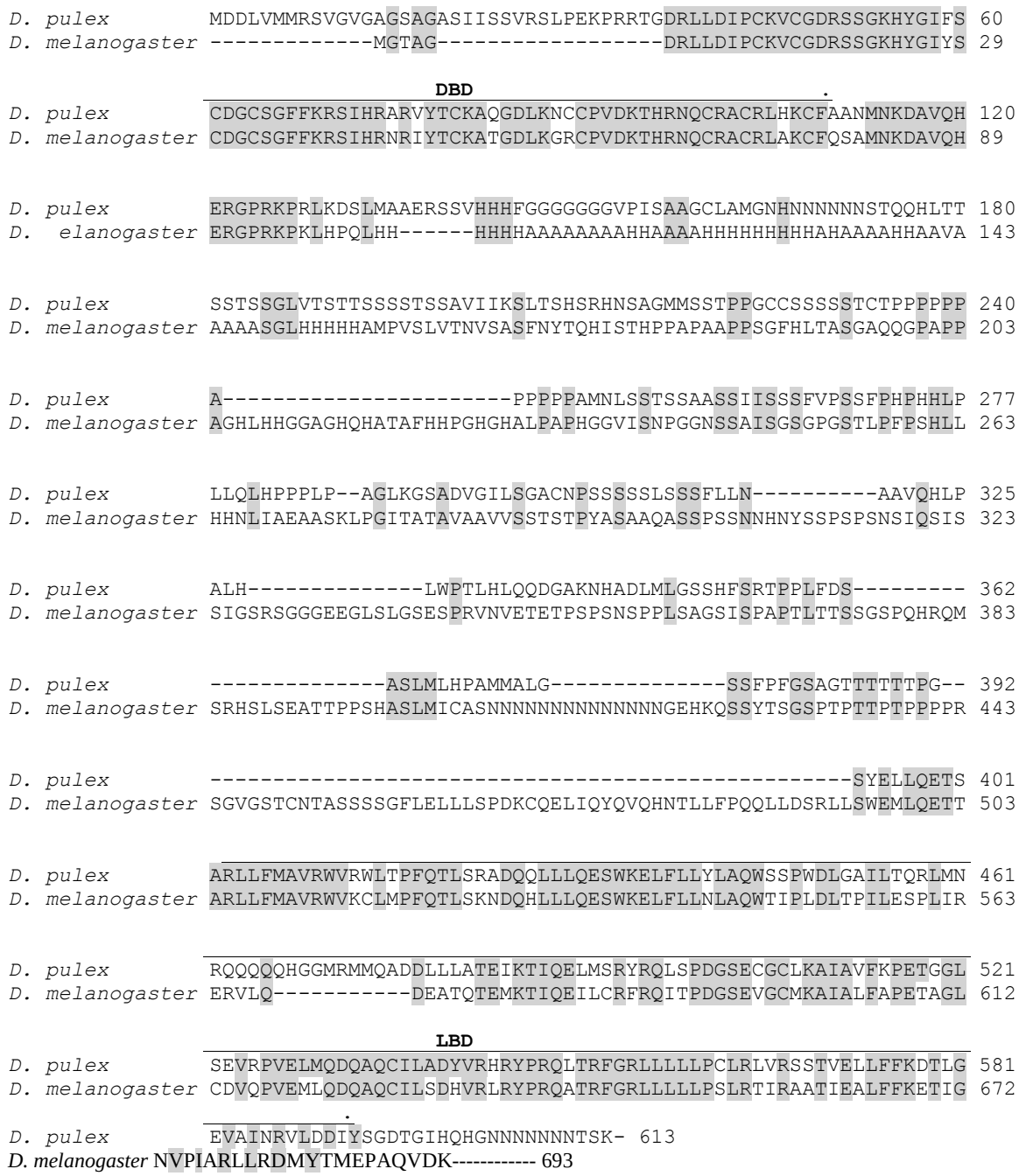
D. pulex MDDLVMMRSVGVGAGSAGASIISSVRSLPEKPRRTGDRLLDIPCKVCGDRSSGKHYGIFS 60
D. melanogaster ----------MGTAG----------DRLLDIPCKVCGDRSSGKHYGIYS 29
DBD
D. pulex CDGCSGFFKRSIHRARVYTCKAQGDLKNCCPVDKTHRNQCRACRLHKCFAANMNKDAVQH 120
D. melanogaster CDGCSGFFKRSIHRNRIYTCKATGDLKGRCPVDKTHRNQCRACRLAKCFQSAMNKDAVQH 89
D. pulex ERGPRKPRLKDSLMAAERSSVHHHFGGGGGGGVPISAAGCLAMGNHNNNNNNSTQQHLTT 180
D. elanogaster ERGPRKPKLHPQLHH------HHHHAAAAAAAAHHAAAHHHHHHHHHAHAAAAHHAAVA 143
D. pulex SSTSSGLVTSTTSSSSTSSAVIIKSLTSHSRHNSAGMMSSTPPGCCSSSSSTCTPPPPPP 240
D. melanogaster AAAASGLHHHHHAMPVSLVTNVSASFNYTQHISTHPPAPAAPPSGFHLTASGAQQGPAPP 203
D. pulex A----------PPPPPAMNLSSTSSAASSIISSSFVPSSFPHPHHLP 277
D. melanogaster AGHLHHGGAGHQHATAFHHPGHGHALPAPHGGVISNPGGNSSAISGSGPGSTLPFPSHLL 263
D. pulex LLQLHPPPLP--AGLKGSADVGILSGACNPSSSSSLSSSFLLN----------AAVQHLP 325
D. melanogaster HHNLIAEAASKLPGITATAVAAVVSSTSTPYASAAQASSPSSNNHNYSSPSPSNSIQSIS 323
D. pulex ALH--------------LWPTLHLQQDGAKNHADLMLGSSHFSRTPPLFDS--------- 362
D. melanogaster SIGSRSGGGEEGLSLGSESPRVNVETETPSPSNSPPLSAGSISPAPTLTTSSGSPQHRQM 383
D. pulex --------------ASLMLHPAMMALG--------------SSFPFGSAGTTTTTTPG-- 392
D. melanogaster SRHSLSEATTPPSHASLMICASNNNNNNNNNNNNNNGEHKQSSYTSGSPTPTTPTPPPPR 443
D. pulex ----------SYELLQETS 401
D. melanogaster SGVGSTCNTASSSSGFLELLLSPDKCQELIQYQVQHNTLLFPQQLLDSRLLSWEMLQETT 503
D. pulex ARLLFMAVRWVRWLTPFQTLSRADQQLLLQESWKELFLLYLAQWSSPWDLGAILTQRLMN 461
D. melanogaster ARLLFMAVRWVKCLMPFQTLSKNDQHLLLQESWKELFLLNLAQWTIPLDLTPILESPLIR 563
D. pulex RQQQQQHGGMRMMQADDLLLATEIKTIQELMSRYRQLSPDGSECGCLKAIAVFKPETGGL 521
D. melanogaster ERVLQ-----------DEATQTEMKTIQEILCRFRQITPDGSEVGCMKAIALFAPETAGL 612
LBD
D. pulex SEVRPVELMQDQAQCILADYVRHRYPRQLTRFGRLLLLLPCLRLVRSSTVELLFFKDTLG 581
D. melanogaster CDVQPVEMLQDQAQCILSDHVRLRYPRQATRFGRLLLLLPSLRTIRAATIEALFFKETIG 672
D. pulex EVAINRVLDDIYSGDTGIHQHGNNNNNNNTSK- 613
D. melanogaster NVPIARLLRDMYTMEPAQVDK---------- 693

Figure 3. Aligned amino acid sequences of *D. magna* and *D. pulex* Met deduced from the nucleotide sequences of dapmagMet and dappuMet (Figs. S3 and S4, respectively) and aligned to Met and Gce from *D. melanogaster*. The *D. melanogaster* sequences were deduced from the nucleotide sequence at GeneBank (accession numbers NM_078571 and NP_001259566.1). The bHLH and PAS domains (A and B) are indicated. Identical amino acids are indicated by the same shading.

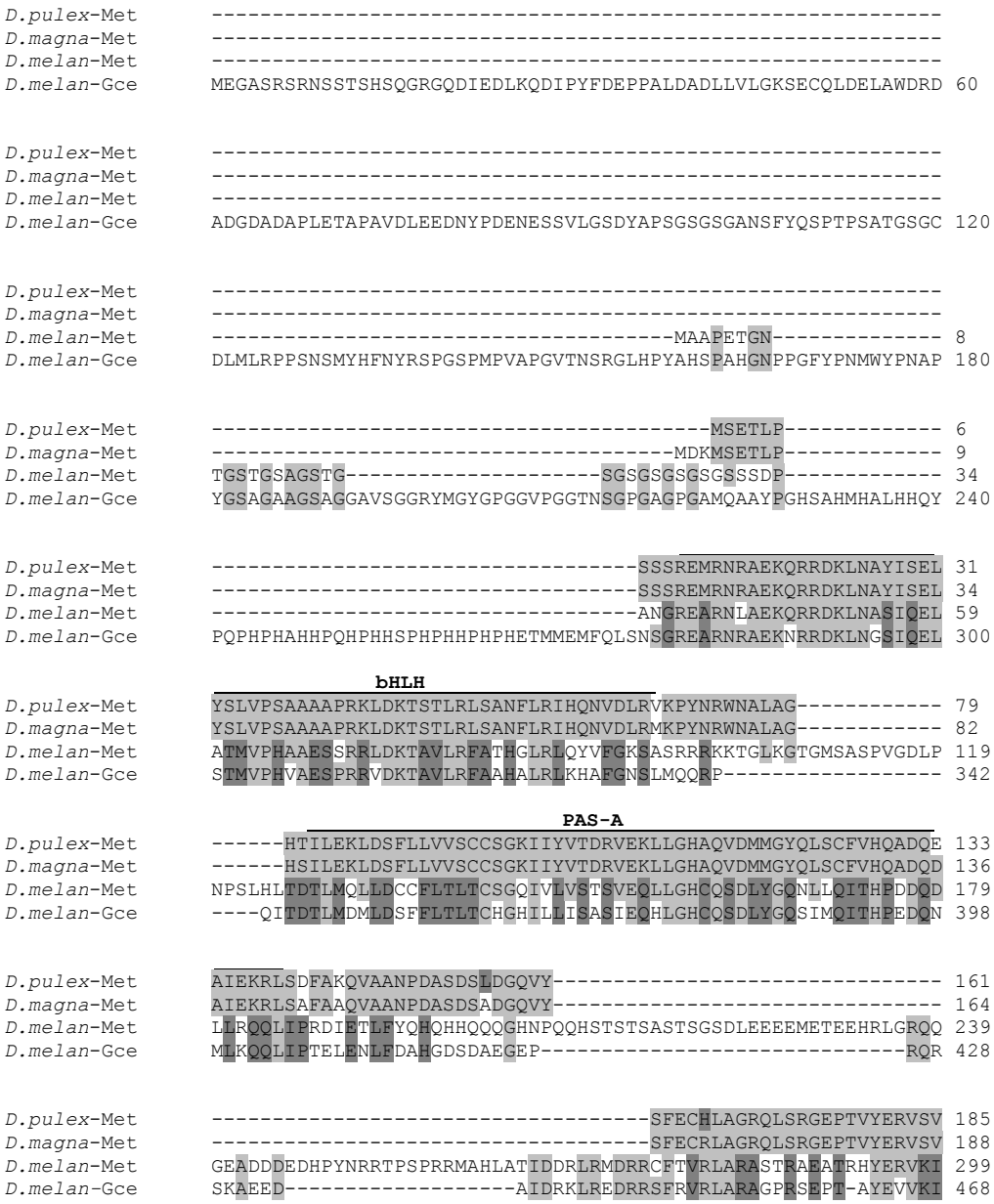
D.pulex-Met
D.magna-Met
D.melan-Met
D.melan-Gce
bHLH
PAS-A

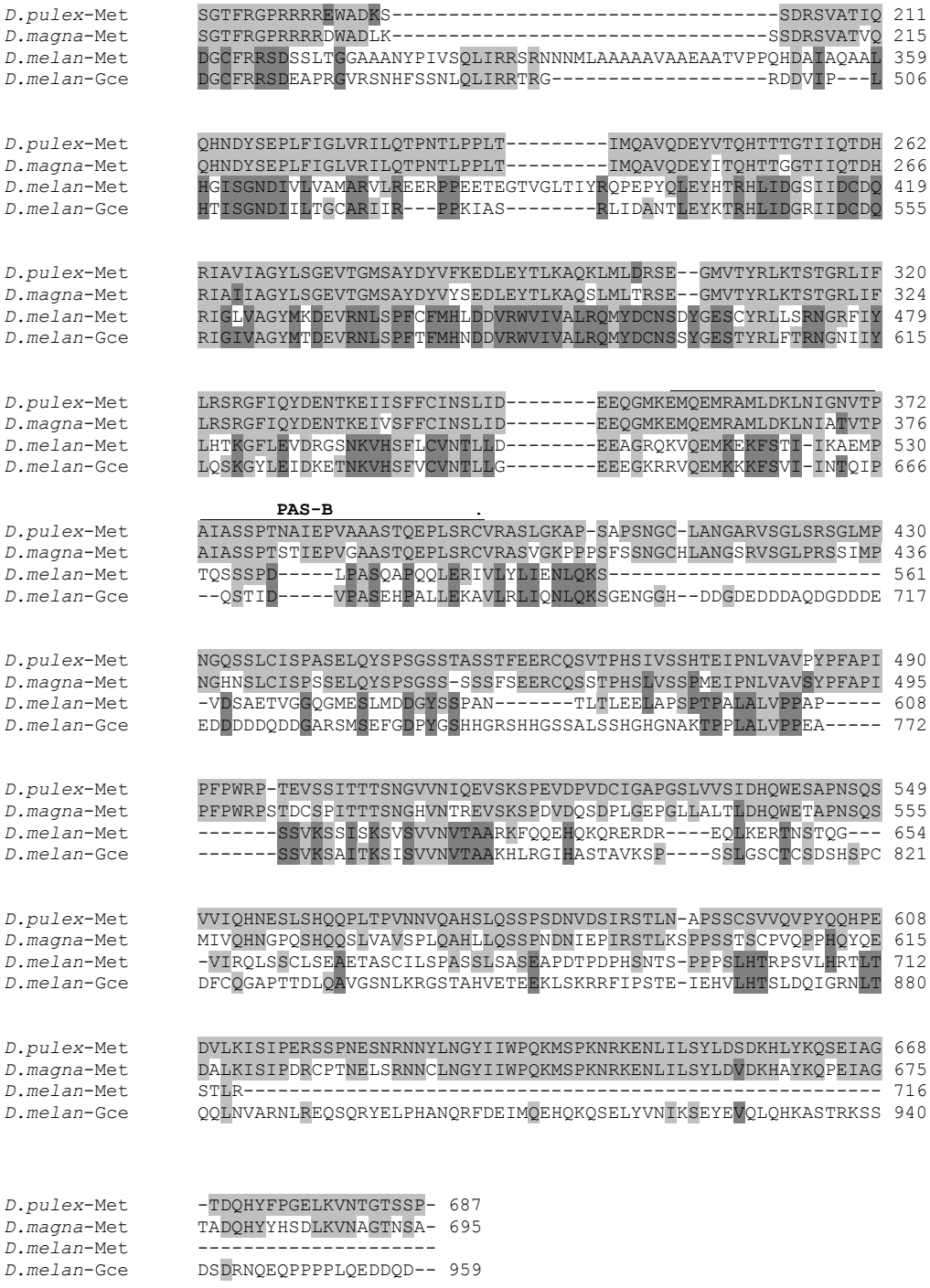
D.pulex-Met SGTFRGPRRRREWADKS---------- SDRSVATIQ 211
D.magna-Met SGTFRGPRRRRDWADLK---------- SSDRSVATVQ 215
D.melan-Met DGCFRRSDSSLTGGAAANYPIVSQLIRRSRNNNMLAAAAAVAAEAATVPPQHDAIAQAAL 359
D.melan-Met DGCFRRSDEAPRGVRSNHFSSNLQLIRRTRG---------- RDDVIP---L 506
D.pulex-Met QHNDYSEPLFIGLVRILQTPNTLPPLT---------IMQAVQDEYVTQHTTTGTIIQTDH 262
D.magna-Met QHNDYSEPLFIGLVRILQTPNTLPPLT---------IMQAVQDEYITQHTTGGTIIQTDH 266
D.melan-Met HGISGNDIVLVAMARVLREERPPEETEGTVGLTIYRQPEPYQLEYHTRHLIDGSIIDCDQ 419
D.melan-Met HTISGNDIILTGCARIIR---PPKIAS--------RLIDANTLEYKTRHLIDGRIIDCDQ 555
D.pulex-Met RIAVIAGYLSGEVTGMSAYDYVFKEDLEYTLKAQKLMLDRSE--GMVTYRLKTSTGRLIF 320
D.magna-Met RIAIIAGYLSGEVTGMSAYDYVYSEDLEYTLKAQSLMLTRSE--GMVTYRLKTSTGRLIF 324
D.melan-Met RIGLVAGYMKDEVRNLSPFCFMHLDDVRWVIVALRQMYDCNSDYGESCYRLLSRNGRFIY 479
D.melan-Met RIGIVAGYMTDEVRNLSPFTFMHNDDVRWVIVALRQMYDCNSSYGESTYRLFTRNGNIIY 615
D.pulex-Met LRSRGFIQYDENTKEIISFFCINSLID--------EEQGMKEMQEMRAMLDKLNIGNVTP 372
D.magna-Met LRSRGFIQYDENTKEIVSFFCINSLID--------EEQGMKEMQEMRAMLDKLNIATVTP 376
D.melan-Met LHTKGFLEVDRGSNKVHSFLCVNTLLD--------EEAGRQKVQEMKEKFSTI-IKAEMP 530
D.melan-Met LQSKGYLEIDKETNKVHSFVCVNTLLG--------EEEGKRRVQEMKKKFSVI-INTQIP 666
PAS-B
D.pulex-Met AIASSPTNAIEPVAAASTQEPLSRCVRASLGKAP-SAPSNGC-LANGARVSGLSRSGLMP 430
D.magna-Met AIASSPTSTIEPVGAASTQEPLSRCVRASVGKPPPSFSSNGCHLANGSRVSGLPRSSIMP 436
D.melan-Met TQSSSPD-----LPASQAPQQLERIVLYLIENLQKS---------- 561
D.melan-Met --QSTID-----VPASEHPALLEKAVLRLIQNLQKSGENGGH--DDGDEDDDAQDGDDDE 717
D.pulex-Met NGQSSLCISPASELQYSPSGSSTASSTFEERCQSVTPHSIVSSHTEIPNLVAVPYPFAPI 490
D.magna-Met NGHNSLCISPSSELQYSPSGSS-SSSFSEERCQSSTPHSLVSSPMEIPNLVAVSYPFAPI 495
D.melan-Met -VDSAETVGGQGMESLMDDGYSSPAN-------TLTLEELAPSPTPALALVPPAP----- 608
D.melan-Met EDDDDDQDDGARSMSEFGDPYGSHHGRSHHGSSALSSHGHGNAKTPPLALVPPEA----- 772
D.pulex-Met PFPWRP-TEVSSITTTSNGVVNIQEVSKSPEVDPVDCIGAPGSLVVSIDHQWESAPNSQS 549
D.magna-Met PFPWRPSTDCSPITTTSNGHVNTREVSKSPDVDQSDPLGEPGLLALTLDHQWETAPNSQS 555
D.melan-Met -------SSVKSSISKSVSVVNVTAARKFQQEHQKQRERDR----EQLKERTNSTQG--- 654
D.melan-Met -------SSVKSAITKSISVVNVTAAKHLRGIHASTAVKSP----SSLGSCICSDSHSPC 821
D.pulex-Met VVIQHNESLSHQQPLTPVNNVQAHSLQSSPSDNVDSIRSTLN-APSSCSVVQVPYQQHPE 608
D.magna-Met MIVQHNGPQSHQQSLVAVSPLQAHLLQSSPNDNIEPIRSTLKSPPSSTSCPVQPPHQYQE 615
D.melan-Met -VIRQLSSCLSEAETASCILSPASSLSASEAPDTPDPHSNTS-PPPSLHTRPSVLHRTLT 712
D.melan-Met DFCQGAPTTDLQAVGSNLKRGSTAHVETEEKLSKRRFIPSTE-IEHVLHTSLDQIGRNLT 880
D.pulex-Met DVLKISIPERSSPNESNRNNYLNGYIIWPQKMSPKNRKENLILSYLDSDKHLYKQSEIAG 668
D.magna-Met DALKISIPDRCPTNELSRNNCLNGYIIWPQKMSPKNRKENLILSYLDVDKHAYKQPEIAG 675
D.melan-Met STLR---------- 716
D.melan-Met QQLNVARNLREQSQRYELPHANQRFDEIMQEHQKQSELYVNIKSEYEVQLQHKASTRKSS 940
D.pulex-Met -TDQHYFPGELKVNTGTSSP- 687
D.magna-Met TADQHYYHSDLKVNAGTNSA- 695
D.melan-Met ----------
D.melan-Met DSDRNQEQPPPPLQEDDQD-- 959

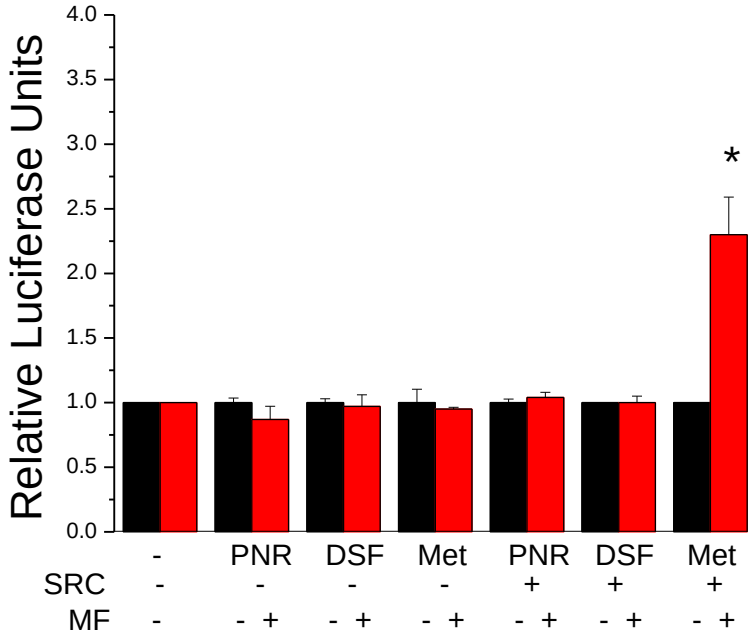

Figure 4. Activation of a GAL4-driven luciferase reporter gene by dappuPNR-GAL4, dappuDSF-GAL4, and dappuMet-GAL4 in the presence and absence of SRC (1 μg plasmid DNA transfected) and methyl farnesoate (MF, 10 μM). An asterisk denotes a significant difference ($p<0.05$) from the respective assay performed in the absence of MF. All data are represented by the mean and standard deviation of three replicate assays.

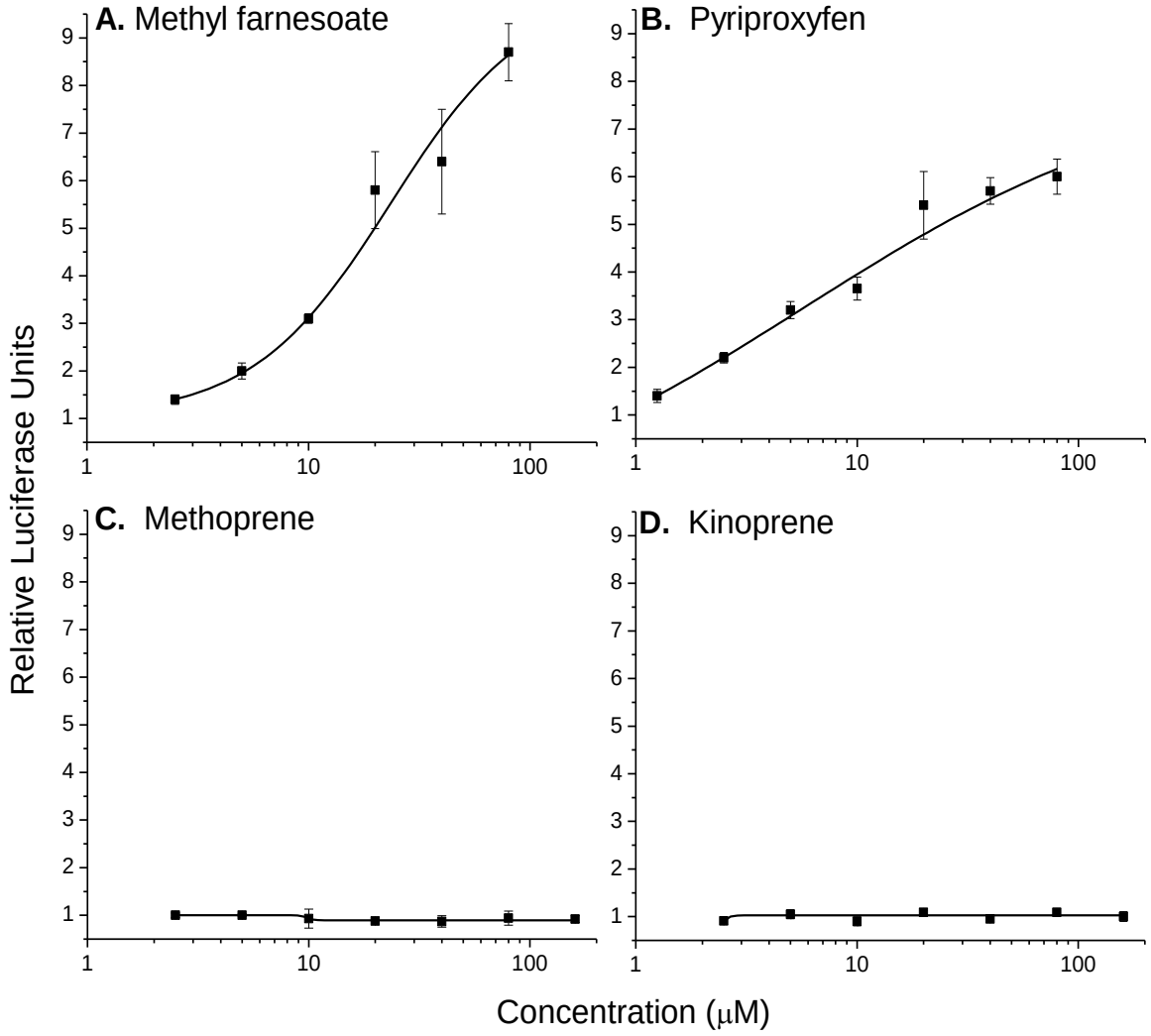

Figure 5. Activation of a GAL4-driven luciferase reporter gene by the dappuMfR (Met-GAL4:SRC) by different concentrations of putative ligands. Data represents the mean (data point) and standard deviation (error bars) of three replicate assays.

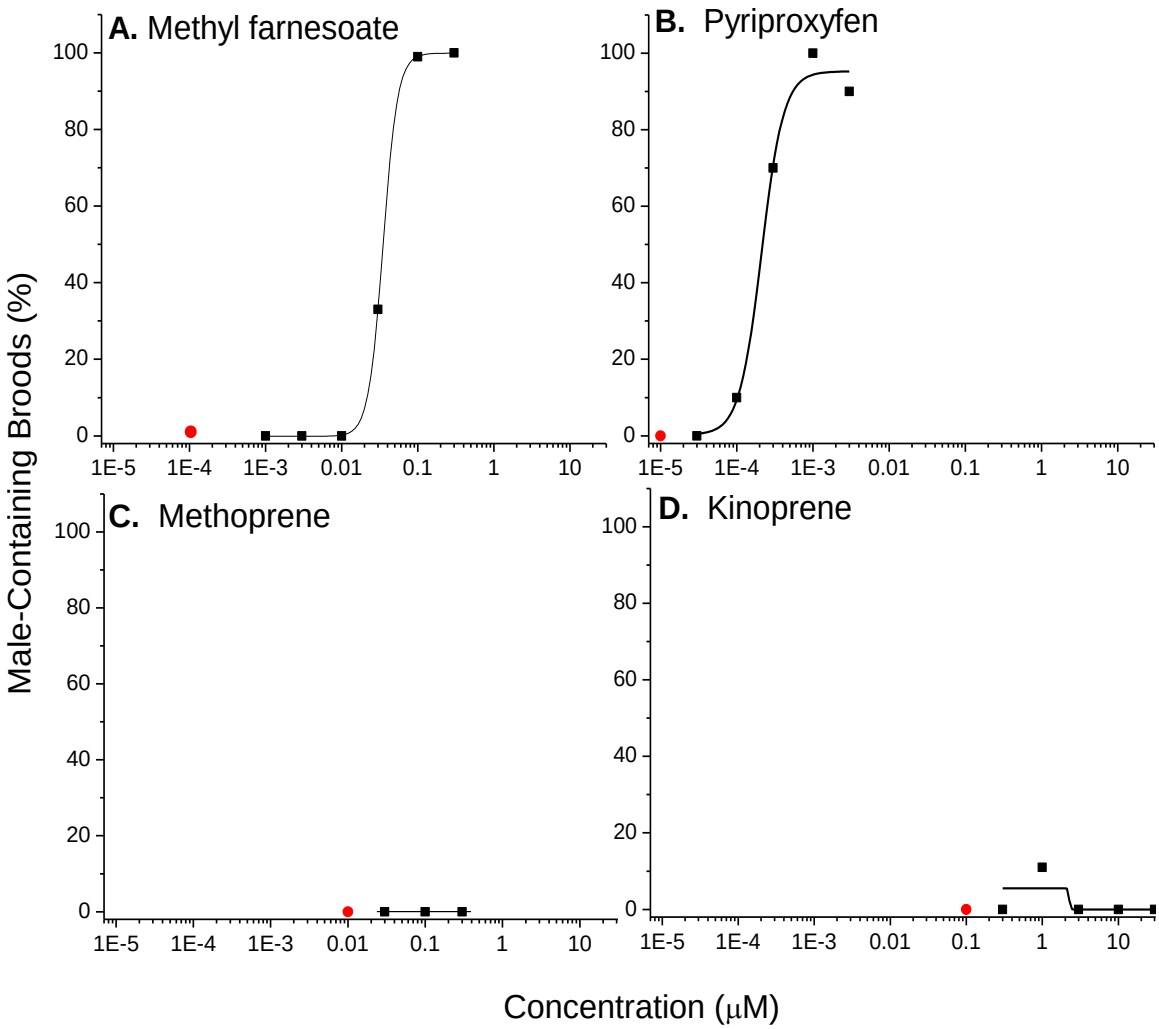

Figure 6. Percentage maternal daphnids (*D. magna*; n=10) that produced male-containing broods following exposure to putative MfR ligands. Red dots denote the percentage male-containing broods among 10 daphnids that were not exposed to ligands (negative control).

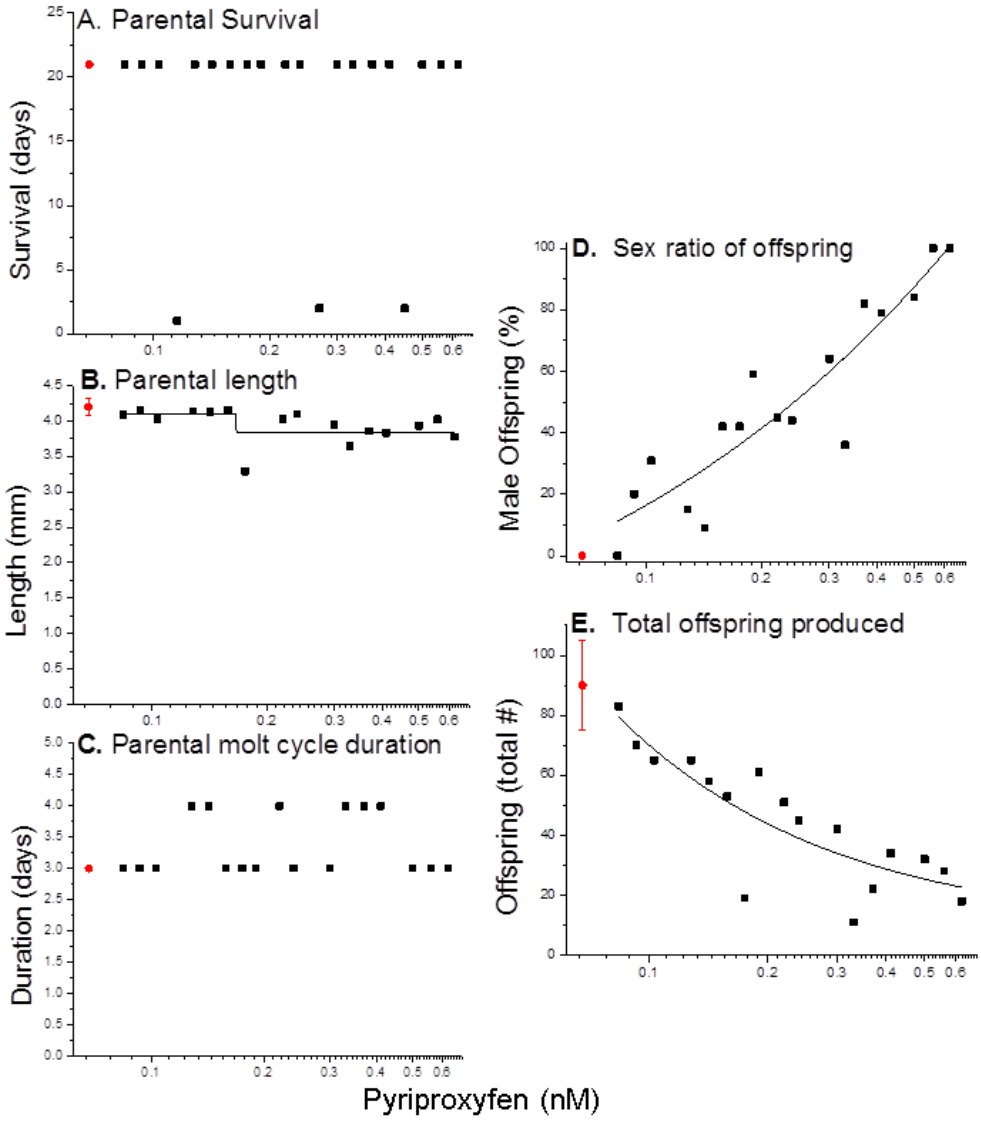

Figure 7. Physiological responses of daphnids (*D. magna*) exposed to concentrations of the MfR ligand pyriproxyfen through their life cycle. Each black data point represents the response of a single daphnid. Red dots depict the performance (mean ± standard deviation) of ten unexposed daphnids.

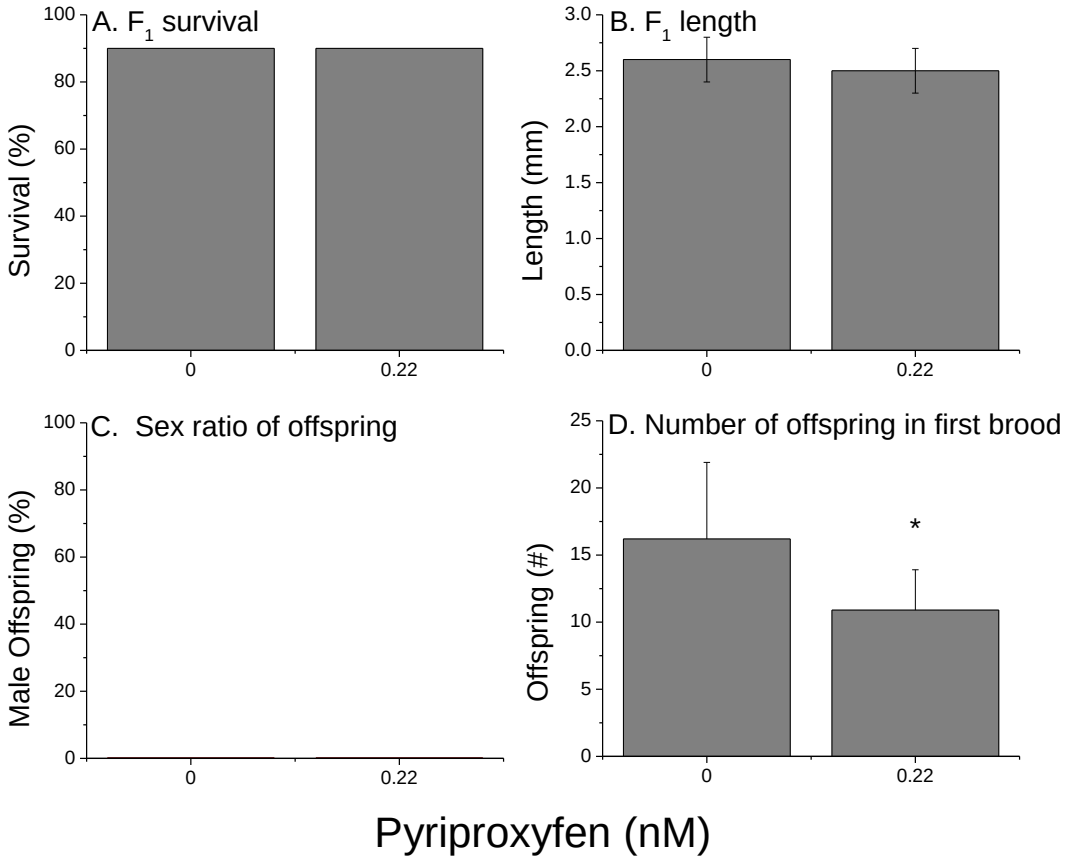

Figure 8. Physiologic performance of daphnids (*D. magna*), produced by maternal organisms that were exposed to either 0.00 or 0.22 nM pyriproxyfen. These offspring were reared in the absence of pyriproxyfen. Data represent the mean and standard deviation (where appropriate) of ten individuals. An asterisk denotes a significant ($p<0.05$) difference between the treatments.

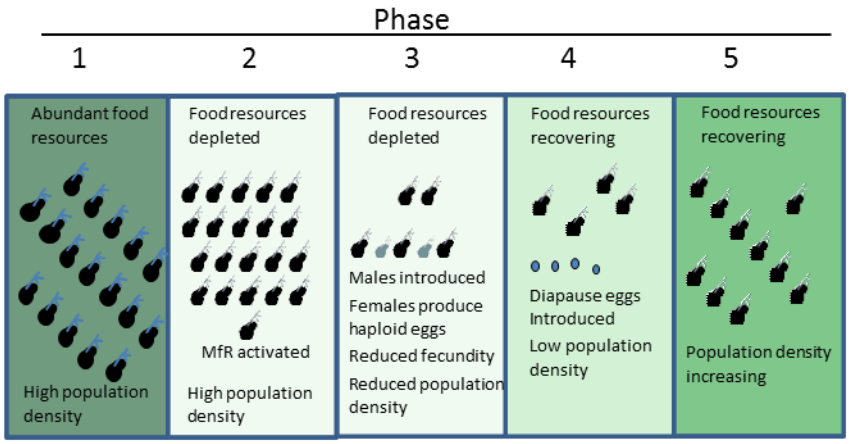

Figure 9. Proposed transgenerational population consequences of activation of the MfR resulting from depleted food resources and high population density.

Figure 10. Proposed mechanistic linkage whereby environmental signals receive by material organisms results is sex determination of next generation individuals.

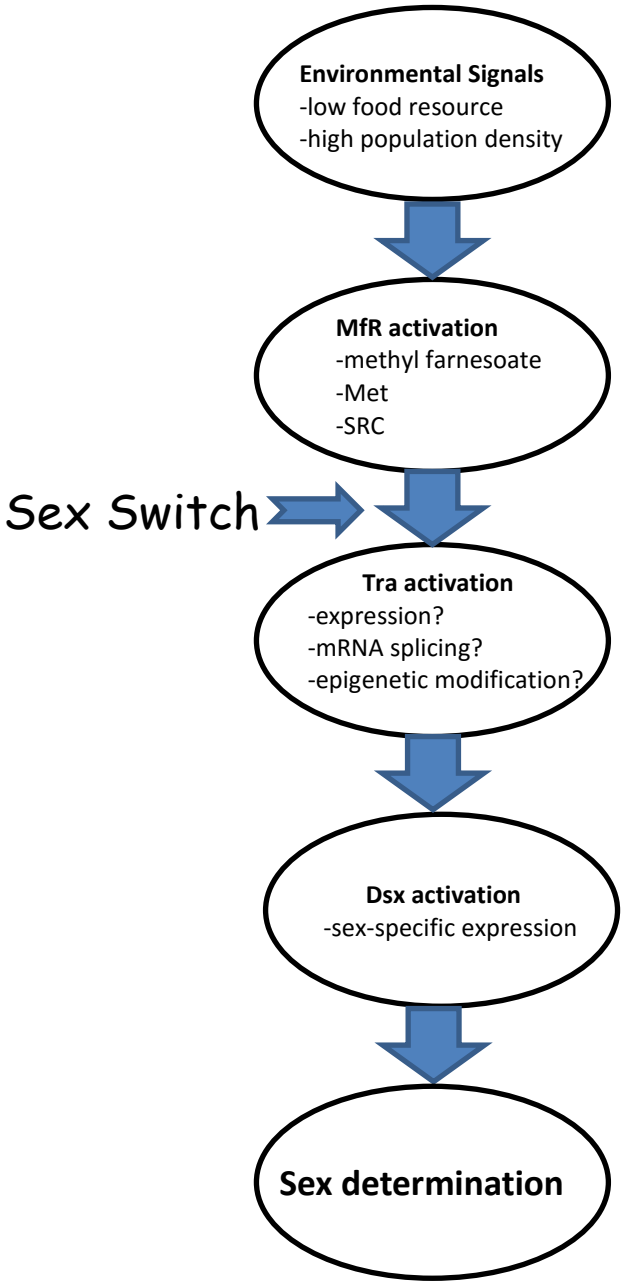
Environmental Signals
-low food resource
-high population density
MfR activation
-methyl farnesoate
-Met
-SRC
Sex Switch
Tra activation
-expression?
-mRNA splicing?
-epigenetic modification?
Dsx activation
-sex-specific expression
Sex determination

Supplementary information

```
   1 ATGGGAGTTC CGTCCAGGCC GGTCGAGAAC AATGGAGCCA GCAGTAAGAA TGCCATTCCC
  61 GGATTGACTT GTCTCGTCTG CGGCGATTCC AGCTCAGGAA AACATTACGG CATTTTAGCT
 121 TGCAATGGAT GCAGCGGATT TTTCAAGCGG AGCGTTCGTC GCCGGCTCAT CTACAGGTGT
 181 CAAGCTGGTA GCGGCCATTG TGTTATTGAC AAAGCGCATC GCAACCAGTG CCAGGCATGT
 241 CGCCTGAAAA AATGTCTACA AATGGGAATG AACAAAGACG CTGTTCAAAA CGAACGTCAG
 301 CCCCGTAACA GCGCCACTCT TCGACCGGAA ATTCTGGCCG AAATGGATCA CGAGAGGATC
 361 ATTCGAGAAG CTGCCGCAGC TGTCGGAGCT TTCGGGCCTC CGGTTTCGCT GGCCATGGGT
 421 CTTGCCTCGG CCGCTGCTCA TGCGCATTAT GTCAACGGGA TGGTTGGTGG ACGAGGAGAT
 481 GGACATCATT ATCCAGCTGC AGCTTTACAC GCCGCCGCTG CCGCTGCTGC CGCCGCAGCC
 541 TCTTCAGCAG CAGCGGCTCA ACGTGCCGAG ATTGAACGAG AAGAAATTGA CCGTGACCGA
 601 GATTGGTTGA CTTGTCCCTC CTACAAAGGT ACTTCGTCGG GAGAAGGTGA ACGAACTCCT
 661 AGCGCCGTTG AAGACAGCCC ATCCCCTTCC GCCCCTCCGC CCAGGAAATT GGCTCGCATT
 721 GAGGGAGCAT TTCATCAGCA TTTCGGCGTC AATCAGTTTC GTCGATCGCC GTCACCTCAG
 781 CACATCCAAC AACAATCCAT TCCTCCTCCC CTGCCATCAT CATCCCTTCT TTCCATCTCA
 841 CACTCACAAC CACCGCCTCT TACCCCGGTT GTTCCAGGCC CAATGCCGCC CCTCTCTTCG
 901 ATTGTTTCCA GCGGCAGCGC TGGATGGTAT CAGAACGAAA ATCAGCAGCA ACACAAGCAG
 961 CAACAACAAC AACAACAACA AACATCTACT GCAACATTCC TCTCCACTTT CCAACCGCAG
1021 GACAATATTT ATGAAACAGC GGCACGCTTG CTCTTCATGG CTGTCAAGTG GGCTAAAAGT
1081 TTGCCCTCTT TTGCTGGACT ACCTTTCCGC GATCAGGTCA TTCTACTGGA AGAATCGTGG
1141 AGCGAATTAT TCCTCATCTG CGCAATACAG TTCTGTTTAC CAATGGACAA CAATCCGCTG
1201 TTTTCGCTGG CCCACTTCAA CCAGCCACAC TCGGCAACTT TAGGCTGTGG CAATGGCGGT
1261 GGAAATAACG GAGGAACCAA CAACAAAAAT TCACAGCAAA CTGGGACTGA TTTGCGCTTT
1321 CTGGCGGAGC TAGTTACGCG TTTCCGCGTG GTCGCTGTTG ATCCAGCTGA ATTTGCATGC
1381 CTCAAGGCTA TCATCCTATT CAAGTCAGAA ACCCGTGGAC TGAAGGATCC AATACAGGTT
1441 GAGAATCTAC AGGATCAGGC GCAAGTGATG CTAAATCAAC ACATCCGCAA TCAGCAACCG
1501 CAGCGGCCTG CTCGTTTCGG TCGACTTCTT CTAACACTTC CTCTGCTTCG TCACGTTACA
1561 GCTTACCGAT TGGAACAGTT GTATTTTCGC CACACCATCG GCTCCACTCC CATGGAAAAG
1621 GTTCTCTGCG ATATGTACAA AAATTAA
```

Figure S1. Open reading frame nucleotide sequence of the of the dappuPNR cDNA.

Underlined sequence denotes the portion that was used in the transcription reporter assays.

```
   1 ATGGACGACT TGGTGATGAT GAGGTCAGTT GGCGTAGGAG CCGGAAGCGC CGGAGCTTCA
  61 ATTATTTCCA GCGTCAGATC GTTACCAGAA AAACCACGGC GAACAGGTGA CCGATTATTG
 121 GATATTCCGT GCAAAGTTTG CGGCGATCGC AGTTCAGGCA AACATTACGG CATCTTCAGT
 181 TGCGATGGTT GTTCGGGATT CTTCAAGCGC AGCATCCATC GAGCCCGGGT CTACACTTGC
 241 AAGGCCCAGG GCGACCTGAA AAATTGCTGC CCAGTCGACA AGACTCACCG CAATCAATGC
 301 CGAGCTTGTC GCCTCCACAA ATGCTTCGCA GCCAACATGA ACAAAGATGC AGTTCAACAC
 361 GAACGGGGTC CTCGTAAACC GCGTTTGAAA GATTCGCTGA TGGCCGCCGA GCGATCCAGC
 421 GTCCATCACC ATTTCGGCGG TGGCGGCGGC GGCGGTGTTC CCATATCGGC GGCCGGCTGC
 481 CTAGCCATGG GCAACCACAA CAACAACAAC AACAACAGTA CTCAACAGCA TTTAACGACT
 541 TCCTCGACTT CATCAGGACT GGTCACTAGC ACGACGAGCA GCAGCAGCAC TAGCTCGGCC
 601 GTCATCATCA AATCGCTAAC GTCTCATTCG CGCCATAATA GCGCCGGAAT GATGTCGTCA
 661 ACTCCGCCCG GATGCTGTTC GTCTTCTTCG TCGACTTGCA CTCCGCCGCC TCCGCCGCCA
 721 GCACCGCCTC CTCCGCCGGC CATGAATCTC TCGTCGACGT CCAGCGCGGC TTCGTCCATC
 781 ATTTCCAGTT CGTTCGTCCC GTCGTCCTTT CCGCATCCGC ATCATTTACC TTTGCTGCAA
 841 TTGCATCCAC CTCCGCTTCC GGCCGGTCTC AAAGGATCTG CGGACGTCGG GATCTTGTCG
 901 GGCGCTTGCA ATCCTTCGTC GTCGTCCTCT CTGTCCAGCT CCTTTCTACT CAACGCGGCC
 961 GTTCAACACC TTCCGGCGCT CCATCTTTGG CCGACGCTCC ACTTGCAACA GGACGGCGCC
1021 AAAAATCACG CCGATTTGAT GCTGGGTTCC AGCCATTTTA GCCGGACGCC GCCCTTGTTC
1081 GACTCGGCCA GCTTGATGCT CCATCCAGCC ATGATGGCTC TGGGAAGTTC TTTCCCATTC
1141 GGAAGCGCTG GCACAACAAC AACAACAACA CCCGGCTCCT ACGAGCTTCT CCAAGAAACT
1201 TCGGCCAGGC TTTTGTTTAT GGCGGTTCGT TGGGTTCGTT GGCTGACGCC GTTCCAGACT
1261 CTGTCGAGAG CCGATCAGCA ACTCCTCCTC CAAGAATCTT GGAAGGAGCT TTTCCTTCTC
1321 TATCTGGCCC AGTGGTCATC GCCCTGGGAC TTGGGAGCGA TTTTGACTCA GCGGTTGATG
1381 AACCGCCAGC AACAGCAACA GCACGGCGGA ATGCGGATGA TGCAGGCCGA CGATCTCCTG
1441 CTAGCGACGG AAATCAAAAC GATTCAGGAA TTGATGAGCA GGTACAGGCA ACTTTCTCCC
1501 GACGGAAGTG AATGCGGTTG CCTCAAAGCG ATCGCTGTTT TCAAACCAGA AACGGGAGGA
1561 TTGTCCGAGG TCCGGCCAGT TGAATTGATG CAAGATCAAG CCCAGTGTAT TTTGGCTGAC
1621 TACGTACGCC ATCGGTATCC GAGACAATTG ACACGATTCG GTCGGCTGTT GCTTCTTTTA
1681 CCTTGTCTCC GGCTAGTCCG TTCGTCCACC GTCGAGCTGC TCTTCTTCAA GGACACACTG
1741 GGTGAAGTGG CCATTAACCG CGTCCTGGAC GACATTTATT CAGGTGACAC TGGCATTCAC
1801 CAACACGGAA ACAACAACAA CAACAACAAC ACTAGCAAAT AA
```

Figure S2. Open reading frame nucleotide sequence of the of the dappuDSF cDNA.

Underlined sequence denotes that which was used in transcription reporter assays.

```
   1 ATGAGTGAAA CATTACCAAG TTCGAGCCGG GAGATGCGGA ATCGGGCGGA AAAGCAGCGG
  61 CGTGACAAGC TCAATGCCTA CATCTCGGAG CTTTATAGTC TGGTTCCGTC AGCGGCGGCC
 121 GCCCCTAGGA AACTGGACAA GACCAGCACG CTCCGTCTCT CGGCCAATTT CTTACGAATA
 181 CATCAGAATG TGGATTTACG GGTCAAACCA TACAACCGAT GGAACGCTCT TGCTGGTCAT
 241 ACAATCTTGG AGAAATTGGA TTCCTTCTTG CTCGTCGTTT CTTGCTGTTC TGGAAAGATC
 301 ATCTACGTGA CGGATCGAGT GGAGAAATTG CTCGGTCATG CGCAGGTTGA TATGATGGGC
 361 TACCAGTTGT CCTGTTTTGT TCACCAGGCA GACCAAGAAG CAATCGAAAA GCGGTTAAGT
 421 GATTTCGCCA AACAAGTGGC TGCCAATCCG GATGCTTCAG ATTCTCTAGA TGGCCAAGTT
 481 TACTCGTTCG AATGTCATCT GGCCGGACGA CAGCTGAGTC GGGGCGAGCC GACCGTCTAC
 541 GAGCGTGTCA GCGTCTCGGG CACTTTCCGA GGTCCCCGTC GAAGACGCGA ATGGGCTGAC
 601 AAAAGTAGTG ATAGATCTGT GGCAACTATT CAACAACACA ACGACTACAG CGAGCCTCTT
 661 TTTATCGGCT TGGTGCGCAT TCTTCAAACC CCCAACACAT TACCTCCCTT GACCATCATG
 721 CAAGCTGTTC AGGACGAATA TGTTACTCAG CACACAACCA CTGGCACCAT TATCCAAACG
 781 GATCACCGCA TCGCCGTCAT TGCCGGATAC CTGAGCGGCG AGGTGACGGG CATGTCTGCC
 841 TATGATTATG TTTTCAAAGA AGATTTGGAG TACACTCTCA AAGCTCAAAA GCTGATGTTG
 901 GATCGAAGCG AGGGAATGGT GACCTATCGG CTCAAAACCA GTACGGGTCG TTTGATCTTC
 961 CTCCGATCGC GGGGTTTCAT CCAGTACGAT GAGAACACCA AAGAAATTAT CAGCTTCTTC
1021 TGCATCAACT CACTCATCGA CGAAGAACAA GGTATGAAGG AGATGCAGGA AATGAGAGCC
1081 ATGCTGGATA AACTTAACAT AGGAAATGTT ACACCGGCGA TCGCGTCATC ACCAACCAAT
1141 GCGATCGAAC CGGTTGCAGC AGCTTCTACT CAAGAACCAC TTTCTCGCTG TGTTCGGGCA
1201 TCCTTGGGCA AAGCGCCTTC CGCGCCGTCT AATGGCTGCC TTGCGAACGG GGCTAGGGTC
1261 TCTGGTCTTT CGAGATCCGG TCTCATGCCC AATGGACAGT CCAGTTTGTG TATTTCACCC
1321 GCCTCTGAAC TTCAGTACTC TCCATCGGGA TCGTCAACGG CCTCGTCTAC TTTTGAAGAG
1381 CGTTGCCAGT CTGTCACTCC TCATTCGATT GTATCATCTC ACACGGAAAT TCCTAATTTA
1441 GTTGCTGTCC CATACCCATT TGCACCCATA CCTTTCCCAT GGCGACCAAC AGAAGTGTCA
1501 TCGATCACGA CGACATCTAA CGGCGTCGTC AACATTCAAG AAGTCAGCAA ATCTCCAGAA
1561 GTGGATCCAG TCGATTGTAT TGGCGCACCG GGATCGCTGG TGGTTTCAAT TGATCATCAA
1621 TGGGAATCGG CTCCTAATAG TCAGAGCGTC GTCATACAGC ATAACGAATC ACTCAGTCAT
1681 CAGCAGCCCT TGACACCTGT GAATAATGTG CAAGCTCATT CACTTCAGTC ATCACCAAGT
1741 GATAATGTAG ATTCAATTCG CTCTACGCTG AATGCGCCGT CCTCCTGTTC GGTTGTTCAA
1801 GTTCCCTACC AACAGCATCC AGAGGATGTT CTGAAAATCT CTATTCCGGA ACGTAGCTCA
1861 CCCAACGAAT CGAATAGAAA CAACTATCTC AACGGATACA TCATTTGGCC TCAGAAGATG
1921 TCCCCCAAAA ATCGAAAGGA GAATTTAATA CTGTCCTACT TGGACTCGGA CAAGCATTTG
1981 TACAAACAGT CGGAGATCGC CGGAACGGAC CAACATTATT TTCCTGGTGA ATTGAAAGTG
2041 AACACTGGAA CTAGTAGTCC GTGA
```

Figure S3. Open reading frame nucleotide sequence of the of the dappuMet cDNA.

Underlined sequence denotes that which was used in transcription reporter assays.

```
   1 ATGGACAAAA TGAGCGAGAC ATTACCAAGT TCGAGCAGGG AGATGCGGAA TCGTGCGGAG
  61 AAGCAACGAC GTGACAAGCT CAATGCCTAC ATTTCGGAGC TTTATAGTCT CGTTCCGTCA
 121 GCGGCTGCCG CCCCTAGGAA GCTGGACAAG ACGAGCACGC TCCGTCTTTC GGCAAATTTT
 181 TTGCGCATCC ATCAAAATGT GGATCTTCGA ATGAAGCCGT ACAACCGATG GAATGCTTTA
 241 GCTGGTCATT CAATCTTAGA GAAATTGGAC TCCTTTTTGC TTGTCGTCTC GTGCTGCTCT
 301 GGCAAGATCA TCTACGTCAC GGATCGAGTG GAGAAATTGC TCGGACATGC GCAGGTCGAT
 361 ATGATGGGCT ACCAGTTATC CTGTTTTGTC CACCAGGCAG ATCAAGATGC AATTGAAAAA
 421 CGACTCAGTG CTTTTGCTGC GCAAGTGGCT GCTAATCCAG ATGCTTCAGA TTCTGCTGAT
 481 GGACAAGTCT ATTCATTCGA ATGTCGCCTA GCCGGACGCC AACTCAGTCG GGGCGAACCG
 541 ACCGTCTATG AACGGGTCAG TGTCTCAGGG ACTTTTCGAG GCCCTCGGAG AAGACGTGAC
 601 TGGGCTGATC TCAAAAGCAG TGATAGATCT GTGGCAACTG TTCAACAACA CAACGACTAC
 661 AGCGAGCCGC TTTTTATTGG CTTGGTGCGC ATTTTACAAA CACCCAACAC CTTACCTCCA
 721 TTGACGATCA TGCAAGCTGT TCAGGACGAG TATATCACTC AGCACACAAC CGGTGGCACC
 781 ATTATACAAA CCGATCATCG CATCGCCATC ATTGCTGGTT ATCTGAGTGG CGAGGTGACG
 841 GGCATGTCAG CATACGATTA TGTTTATAGC GAAGATTTGG AGTACACTCT CAAAGCTCAA
 901 AGCCTCATGT TAACTCGGAG TGAAGGAATG GTGACTTATC GCCTAAAAAC CAGTACGGGT
 961 CGTTTGATTT TCCTTCGATC AAGAGGTTTC ATCCAATACG ATGAAAACAC GAAGGAAATT
1021 GTCAGCTTTT TCTGCATCAA TTCACTCATC GACGAAGAGC AAGGAATGAA GGAAATGCAG
1081 GAAATGCGGG CCATGTTAGA CAAACTTAAC ATTGCAACTG TTACGCCAGC GATAGCGTCA
1141 TCGCCAACGA GCACGATTGA ACCAGTTGGA GCAGCTTCTA CTCAAGAGCC ACTTTCTCGT
1201 TGTGTTCGGG CGTCAGTGGG GAAACCACCG CCTTCTTTTT CTTCTAATGG CTGCCACCTT
1261 GCGAATGGGT CTAGGGTCTC GGGCCTGCCT AGATCCAGTA TTATGCCCAA CGGACATAAC
1321 AGTTTATGCA TTTCACCCTC CTCTGAACTT CAGTACTCCC CTTCAGGATC GTCTTCGTCT
1381 TCTTTCAGTG AAGAACGTTG CCAATCTTCT ACACCGCATT CGCTCGTGTC ATCTCCCATG
1441 GAAATTCCTA ATTTAGTTGC TGTTTCCTAC CCATTTGCAC CCATACCTTT CCCATGGCGA
1501 CCATCGACAG ACTGTTCTCC GATCACCACG ACATCTAACG GTCACGTTAA CACTAGAGAA
1561 GTTAGCAAAT CCCCCGATGT CGATCAGAGC GATCCTCTTG GTGAACCAGG ATTGCTGGCT
1621 CTTACGCTGG ATCATCAATG GGAAACGGCT CCCAATAGTC AGAGCATGAT CGTCCAGCAC
1681 AATGGGCCAC AAAGTCATCA GCAGTCCTTG GTAGCCGTCA GTCCCCTTCA AGCTCATTTG
1741 CTTCAGTCAT CGCCAAACGA TAACATAGAA CCGATTCGGT CCACCCTGAA ATCGCCGCCA
1801 TCGTCCACCA GCTGTCCCGT TCAACCTCCC CACCAATATC AGGAAGATGC TCTGAAAATC
1861 TCGATTCCCG ATCGTTGTCC GACGAATGAA CTGAGTCGAA ACAACTGTCT CAACGGCTAC
1921 ATCATTTGGC CTCAAAAGAT GTCGCCCAAA AATCGAAAGG AGAATCTTAT ATTGTCGTAC
1981 TTGGACGTCG ACAAGCATGC CTACAAACAG CCAGAGATTG CCGGAACTGC TGACCAGCAC
2041 TACTATCATA GTGATTTAAA AGTGAATGCT GGAACCAACA GTGCATAG
```

Figure S4. Open reading frame nucleotide sequence of the of the dapmagMet cDNA.